



**PRESSURE-CONTROLLED ATOMIZATION PROCESS (PCAP)
FOR DIMENSIONAL RESTORATION OF AVIATION PARTS
PART 2**

John C. Tierney, Ronald J. Glovan, Ying-Ming Lee

**MSE, Inc.
Post Box 4078
Butte MT 59702**

**ENVIRONICS DIRECTORATE
139 Barnes Drive, Suite 2
Tyndall AFB FL 32403-5323**

July 1996

Final Technical Report for Period August 1990 - May 1995

Approved for public release; distribution unlimited.

19961108 049

**AIR FORCE MATERIEL COMMAND
TYNDALL AIR FORCE BASE, FLORIDA 32403-5323**

DTIC QUALITY INSPECTED 1

**ARMSTRONG
LABORATORY**

NOTICES


This report was prepared as an account of work sponsored by an agency of the United States Government. Neither the United States Government nor any agency thereof, nor any employees, nor any of their contractors, subcontractors, or their employees, make any warranty, expressed or implied, or assume any legal liability or responsibility for the accuracy, completeness, or usefulness of any privately owned rights. Reference herein to any specific commercial products, process, or service by trade name, trademark, manufacturer, or otherwise, does not necessarily constitute or imply its endorsement, recommendation, or favoring by the United States Government or any agency, contractor, or subcontractor thereof. The views and opinions of the authors expressed herein do not necessarily state or reflect those of the United States Government or any agency, contractor, or subcontractor thereof.


When Government drawings, specifications, or other data are used for any purpose other than in connection with a definitely Government-related procurement, the United States Government incurs no responsibility or any obligation whatsoever. The fact that the Government may have formulated or in any way supplied the said drawings, specifications, or other data, is not to be regarded by implication, or otherwise in any manner construed, as licensing the holder or any other person or corporation; or as conveying any rights or permission to manufacture, use, or sell any patented invention that may in any way be related thereto.

This technical report has been reviewed by the Public Affairs Office (PA) and is releasable to the National Technical Information Service, where it will be available to the general public, including foreign nationals.

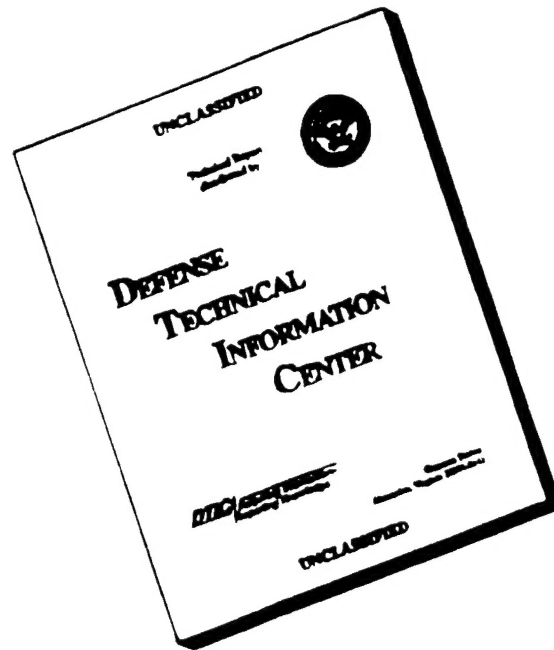
This report has been reviewed and is approved for publication.

FOR THE COMMANDER:


RAY A SMITH, 1Lt, USAF, BSC
Project Manager


ALLAN M. WEINER, Lt Col, USAF
Chief, Environmental Compliance Division

DISCLAIMER NOTICE



**THIS DOCUMENT IS BEST
QUALITY AVAILABLE. THE
COPY FURNISHED TO DTIC
CONTAINED A SIGNIFICANT
NUMBER OF PAGES WHICH DO
NOT REPRODUCE LEGIBLY.**

| | | | | | |
|--|----------------------------------|-----------------------------------|---|---|---|
| 1. Report Date (dd-mm-yy) July 1996 | | 2. Report Type Final | | 3. Dates covered (from... to) Aug 1990 - May 1995 | |
| 4. Title & subtitle Pressure-Controlled Atomization Process (PCAP) for Dimensional Restoration of Aviation Parts (Part 2 of 2, Pages 213-393) | | | | 5a. Contract or Grant # DE-AC22-88ID12735 | |
| | | | | 5b. Program Element # 63723 | |
| 6. Author(s) John C. Tierney, Ronald J. Glovan, and Ying-Ming Lee | | | | 5c. Project # 2103 | |
| | | | | 5d. Task # 71 | |
| | | | | 5e. Work Unit # 22 | |
| 7. Performing Organization Name & Address MSE, Inc P. O. Box 4078 Butte MT 59702 | | | | 8. Performing Organization Report # | |
| 9. Sponsoring/Monitoring Agency Name & Address AL/EQS-OL (Lt Smith) 139 Barnes Drive, Suite 2 Tyndall AFB FL 32403-5323 | | | | 10. Monitor Acronym | |
| | | | | 11. Monitor Report # AL/EQ-TR-1995-0029 | |
| 12. Distribution/Availability Statement Approved for Public Release/Distribution Unlimited | | | | | |
| 13. Supplementary Notes Availability of this report is specified on the reverse of the front cover. | | | | | |
| 14. Abstract The Pressure-Controlled Atomization Process (PCAP) is a new thermal spray process in which a liquid metal is atomized in a supersonic nozzle, which also directs the spray to a suitable substrate. The Spray Casting Project was jointly sponsored by the United States Air Force, Armstrong Laboratory Envirionics Directorate at Tyndall AFB, and the United States Department of Energy, Office of Technology Development (DOE-OTD) under the U. S. Air Force - DOE Memorandum of Understanding (MOU). The Air Force application uses the Pressure Controlled Atomization Process (PCAP) to thermally spray metallic replacement coatings for electroplated hard chromium. The report presents a history of PCAP as it relates to the development of the process, the development of the hardware to support the process development, and the testing that was conducted to understand the process and generate engineering data to support the replacement hard chromium electroplating with PCAP sprayed coating. | | | | | |
| 15. Subject Terms Thermal spraying of metals, hard chromium replacement. | | | | | |
| Security Classification of | | | 19. Limitation of Abstract Unlimited | 20. # of Pages 183 | 21. Responsible Person (Name and Telephone #) 1Lt Ray A. Smith (904)283-6462 |
| 16. Report Unclassified | 17. Abstract Unclassified | 18. This Page Unclassified | | | |

DTIC QUALITY INSPECTED 1

APPENDIX C
SPRAY CASTING PROJECT
WRIGHT LABORATORY TEST SERIES REPORT

SPRAY CASTING PROJECT

**WRIGHT LABORATORIES
TEST SERIES REPORT**

Prepared by

Materials Directorate
Systems Support Division, WL/MLS
2179 12th Street, Suite 1
Wright-Patterson AFB, OH 45433-7718

Prepared for

U.S. Department of Energy
Under Contract DE-AC22-88ID12735

CONTENTS

| | Page |
|-----------------------|------|
| 1. INTRODUCTION | 1 |
| APPENDIX A | A-1 |
| APPENDIX B | B-1 |

1. INTRODUCTION

Phase III of the Spray Casting Project is being conducted by MSE, Inc., at its Spray Casting Facility in Butte, Montana. The primary purpose of Phase III work is qualifying the spray casting process to meet Air Force standards and then designing, fabricating, and testing pilot spray casting equipment that will be used at an Air Force Logistics and Service Center. The qualification process consists of three separate test series: the MSE Test Series, the Boeing Test Series, and the Wright Laboratories Test Series; a separate report will be prepared for each of these series.

The Wright Laboratories Test Series used the experience of the Air Force to evaluate sprayed coatings that were produced by MSE. This test series was the final analysis and determination after the intermediate set of engineering tests conducted by the Boeing Defense and Space Group in Kent, Washington. This final analysis consisted of an evaluation of mechanical properties and coating quality of spray casted metals.

The complete text of the final two Air Force reports, *Evaluation Report--Evaluation of Spray Casted Materials*, and *Evaluation Report--Spray Casting Evaluation* are included in Appendices A and B, respectively.

APPENDIX A

Evaluation Report--Evaluation of Spray Casted Materials

MATERIALS DIRECTORATE
SYSTEMS SUPPORT DIVISION, WL/MLS
2179 Twelfth St Ste 1
WRIGHT PATTERSON AFB, OH 45433-7718

EVALUATION REPORT

EVALUATION OF SPRAY CASTED MATERIALS

| | |
|---------------------------|--------------------------------|
| REPORT NO: MLS 93-78 | DATE: 20 AUGUST 1993 |
| PROJECT NR: 24180703 | TYPE EVAL: Mechanical Property |
| MANUFACTURER: MSE/EG&G | SPEC NO: N/A |
| REQUESTED BY: TYNDALL AFB | ITEM SERIAL NO: N/A |

DISTRIBUTION STATEMENT C: Distribution is limited to U.S. Government agencies and their contractors: test and evaluation/Aug 93.. Other requests for this document must be referred to WL/MLSE, Wright Patterson AFB OH 45433-7718.

DESTRUCTION NOTICE: Destroy by any method that will prevent disclosure or reconstruction of the document.

I. PURPOSE

Evaluation of mechanical properties and coating quality of spray casted metals.

II. BACKGROUND

The System Support Division (MLSE and MLSA) was asked to evaluate metal samples that had been coated with Versalloy. The coating was applied using a newly developed method called Spray Casting which MSE Inc. was contacted by Tyndall AFB to develop, design and fabricate. This spray casting process, as a replacement for chromium electroplating, reduces the generation of hazardous wastes associated with chromium.

III. MATERIALS AND PROCEDURES

Flat axial fatigue specimens were machined from 4130 steel, titanium 6-4 and 304 stainless steel. The spray casting was applied to fifteen 4130 steel fatigue specimens, fifteen titanium 6-4 fatigue specimens and fifteen 304 stainless steel fatigue specimens. Ten additional 4130 steel fatigue specimens were machined and no coating was applied.

Residual Stress measurement tests were performed on the spray casted 4130 steel.

Corrosion, hardness, coating thickness and quality of the coating information are contained in the attached evaluation report MLS-93-59.

IV. RESULTS AND DISCUSSION

The fatigue data for the 4130 steel uncoated, chrome coated and Versalloy coated are shown in Tables 1 thru 3 and in Figure 1. A number of fatigue samples broke in the grips and this data was not recorded. The radius in the specimen was thought to be too sharp and some specimens were remachined. The spray casted 4130 steel (Versalloy coating) had significantly better fatigue properties than the chrome coated 4130 steel. Only a few samples of uncoated 4130 steel were valid, however the four samples showed better fatigue properties compared to the chrome coated 4130 steel samples at high stress levels. None of the chrome or spray casted 4130 steel fatigue specimen's coating cracked until failure.

Fatigue results for the spray casted 304 stainless steel are shown in Table 4 and Figure 2. The spray casted coating cracked after a minimum number of cycles on all the samples at a stress of 50.4 Ksi and greater (Figure 3). Unfortunately no chrome plated 304 stainless steel fatigue data were available for comparison.

The spray casted titanium 6-4 fatigue results are shown in Table 5 and Figure 4. The spray cast coating did not crack on any of the samples until failure. No chrome plated titanium 6-4 fatigue data were available for comparison.

Residual Stress measurements of the Versalloy coating on the 4130 steel produced a steep, positive residual strain gradient that leveled off at the 0.008 inch depth, which corresponds to the coating thickness. The readings were too high to make sense, which suggests a lower modulus than the base steel. A matrix of two materials with varying moduli is not easy to analyze. A significant tensile residual stress exists in the coating layer, but actual residual stress numbers are not available.

Corrosion, hardness, coating thickness, and quality of the coating results are contained in the attached evaluation report MLS-93-59.

V. CONCLUSIONS

1. Spray casted 4130 steel has significantly better axial fatigue properties compared to chrome coated 4130 steel.

Conclusions 2 thru 4 from Evaluation Report MLS-93-59.

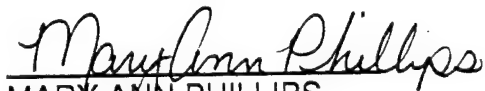
2. The samples performed poorly in the corrosion test. The B117 test is often used to evaluate the corrosion performance of plating. The short period of time before the onset of severe visual corrosion is of concern for application where corrosion resistance is desirable.

3. The hardness traverse performed on several samples indicate that there is no detectable material degradation due to the thermal loads induced during coating.

4. The metallography indicates that coating thickness varies widely and porosity and cracking were evident. These findings support those of the corrosion testing.

PREPARED BY:

COORDINATION:



MARY ANN PHILLIPS
Engineering and Design Data Section
Materials Engineering Branch
Systems Support Division
Material Directorate



CLAYTON L HARMSWORTH, Tech Area Manager
Engineering & Design Data Section
Materials Engineering Branch
Systems Support Division
Materials Directorate

PUBLICATION REVIEW

This report has been reviewed and is approved.



THEODORE J. REINHART
Materials Engineering Branch
Systems Support Division
Materials Directorate

DISTRIBUTION:

WL/MLSE (Mary Ann Phillips)
MLSA (Carolyn Westmark)
MLSA (Larry Perkins)

1 Atch

1. MLS-93-59 Evaluation Report

Lt Phil Brown
AL/EQS-OL
139 Barnes Dr Suite 2
Tyndall AFB Florida 32403-5323 (2 copies)

Ron Glovan
MSE Corporation
CDIF Industrial Park
Butte MT 59701 (2 copies)

TABLE 1

4130 STEEL AXIAL FATIGUE RESULTS

(Kt+1.0, R=0.1, Freq+10-20 Hz, 75°F and Long Orientation)

| SPECIMEN ID | MAXIMUM STRESS (Ksi) | CYCLES |
|----------------|-------------------------|------------|
| 4130-P8 | 100 | 2,299,139* |
| 4130-P11 | 105 | 53,006** |
| 4130-P14 | 105 | 89,265** |
| 4130-P9 | 110 | 60,887 |
| 4130-P13 | 110 | 73,319 |
| 4130-P12 | 115 | 51,555 |
| 4130-P7 | 120 | 80,578** |
| 4130-P6 | 125 | 60,611 |

* Specimen invalid (broke in grip)

** Specimen broke in transition area

TABLE 2
CHROME PLATED 4130 STEEL AXIAL FATIGUE RESULTS
(Kt=1.0, R=0.1, Freq=10-20 Hz, 75°F and Long Orientation)

| SPECIMEN ID | MAXIMUM STRESS (Ksi) | CYCLES |
|----------------|-------------------------|-------------|
| 4130-CHR11 | 45 | 10,000,000* |
| 4130-CHR12 | 54 | 180,438 |
| 4130-CHR10 | 54 | 139,112 |
| 4130-CHR9 | 63 | 238,519 |
| 4130-CHR15 | 63 | 125,038 |
| 4130-CHR14 | 72 | 161,869 |
| 4130-CHR8 | 72 | 144,050 |
| 4130-CHR13 | 81 | 103,698 |
| 4130-CHR7 | 81 | 85,049 |
| 4130-CHR6 | 90 | 61,973 |
| 4130-CHR5 | 90 | 38,717 |
| 4130-CHR4 | 99 | 43,307 |
| 4130-CHR3 | 108 | 40,305 |
| 4130-CHR2 | 117 | 31,458 |
| 4130-CHR1 | 126 | 35,153 |

* Specimen did not fail

TABLE 3
 SPRAY CASTED 4130 STEEL AXIAL FATIGUE RESULTS
 (Kt=1.0, R=0.1, Freq=10-20 Hz, 75°F and Long Orientation)

| SPECIMEN ID | MAXIMUM STRESS (Ksi) | CYCLES | COMMENT |
|----------------|-------------------------|--------------|------------|
| 4130-12 | 90 | 2,085,681* | |
| 4130-13 | 90 | 10,000,000** | |
| 4130-15 | 99 | 4,752,722 | |
| 4130-14 | 117 | 91,982 | |
| 4130-11 | 126 | 70,400 | |
| 4130MOD-5 | 108 | 10,000,000** | Remachined |
| 4130MOD-15 | 111.6 | 169,407 | Remachined |
| 4130MOD-13 | 111.6 | 248,341 | Remachined |
| 4130MOD-8 | 112.5 | 193,141 | Remachined |
| 4130MOD-4 | 117 | 76,135 | Remachined |
| 4130MOD-6 | 117 | 140,841 | Remachined |
| 4130MOD-12 | 117 | 155,881*** | Remachined |
| 4130MOD-11 | 126 | 107,211 | Remachined |
| 4130MOD-1 | 126 | 109,522*** | Remachined |
| 4130MOD-2 | 135 | 84,981 | Remachined |

* Broke in grip

** Specimen did not fail

*** Broke out side of coating

TABLE 4
 SPRAY CASTED 304 STAINLESS STEEL AXIAL FATIGUE RESULTS
 (Kt=1.0, R=0.1, Freq=20 Hz, 75°F and Long Orientation)

| SPECIMEN ID | MAXIMUM STRESS (Ksi) | CYCLES | COMMENT |
|----------------|-------------------------|-------------|--|
| SS-3 | 42.0 | 10,000,000* | |
| SS-13 | 42.0 | 10,000,000* | |
| SS-8 | 46.2 | 534,560 | |
| SS-9 | 46.2 | 977,508 | |
| SS-12 | 46.2 | 2,826,483 | |
| SS-5 | 50.4 | 143,313 | 4000 cycles coating cracks on front face |
| SS-2 | 50.4 | 182,631 | 7000 cycles coating cracks on front face |
| SS-11 | 54.6 | 122,023 | 200-300 cycles coating cracks both sides |
| SS-1 | 58.8 | 74,088 | 3000 cycles coating cracks both sides |
| SS-4 | 58.8 | 84,505 | 500-1000 cycles coating cracks both sides |
| SS-10 | 63.0 | 64,819 | 200-300 cycles coating cracks both sides |
| SS-6 | 67.2 | 42,587 | 300-400 cycles coating cracks both sides |
| SS-7 | 67.2 | 47,048 | 200-300 cycles coating cracks both sides |

*Specimen did not fail

TABLE 5
 SPRAY CASTED TITANIUM 6-4 AXIAL FATIGUE RESULTS
 (Kt=1.0, R=0.1, Freq=20 Hz, 75°F and Long Orientation)

| SPECIMEN ID | MAXIMUM STRESS (Ksi) | CYCLES |
|----------------|-------------------------|--------------|
| TIT-8 | 69.0 | 10,000,000* |
| TIT-9 | 75.9 | 10,000,000** |
| TIT-10 | 82.8 | 158,840 |
| TIT-7 | 82.8 | 524,058 |
| TIT-11 | 89.6 | 97,043 |
| TIT-14 | 89.6 | 263,558 |
| TIT-1 | 89.6 | 942,873** |
| TIT-5 | 96.6 | 173,674 |
| TIT-6 | 96.6 | 227,253 |
| TIT-12 | 103.5 | 160,065 |
| TIT-2 | 103.5 | 175,557 |
| TIT-4 | 110.4 | 85,091 |
| TIT-13 | 110.4 | 103,408 |
| TIT-3 | 117.3 | 47,326 |

* Specimen did not fail

**Specimen broke in grip

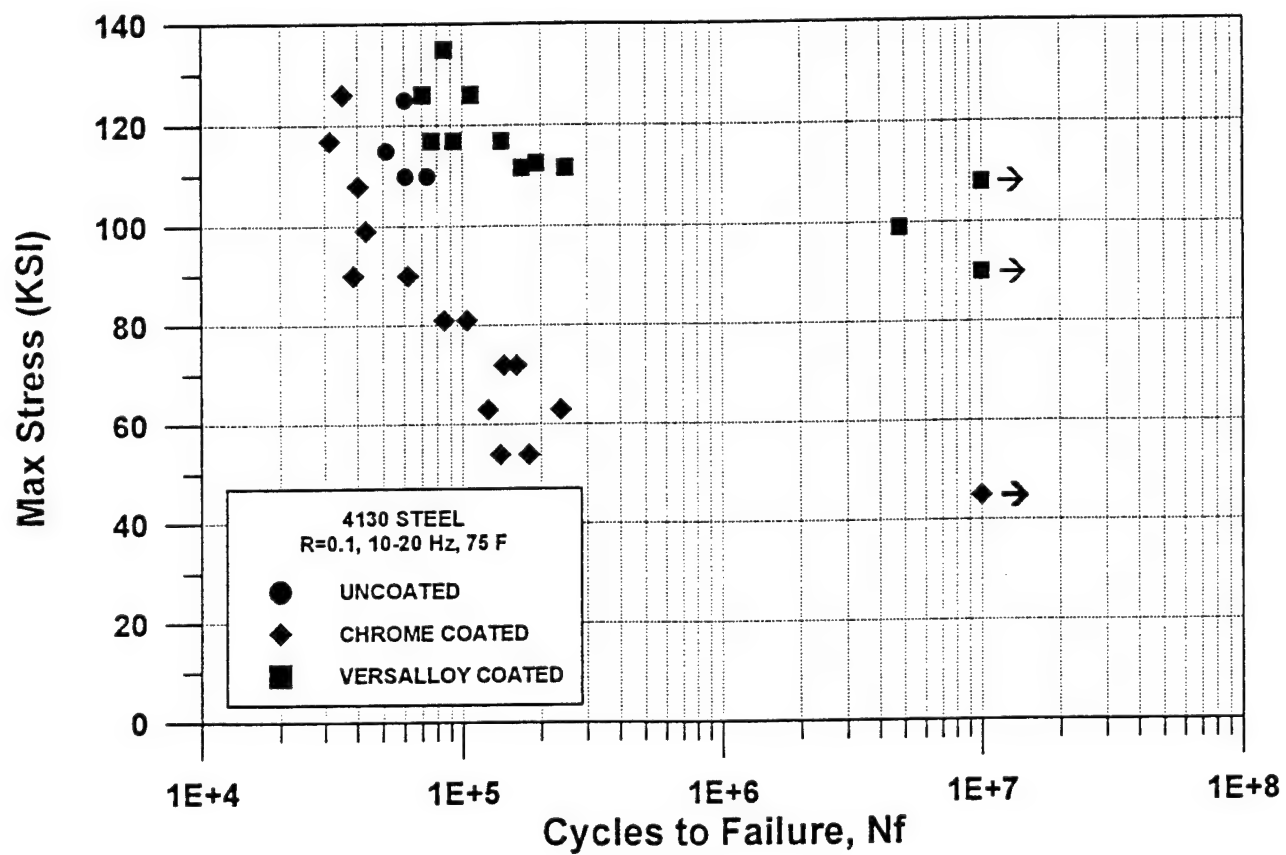


FIGURE F1. Axial Fatigue Data for 4130 steel uncoated, chrome coated and versalloy coated. ($K_t=1.0$).

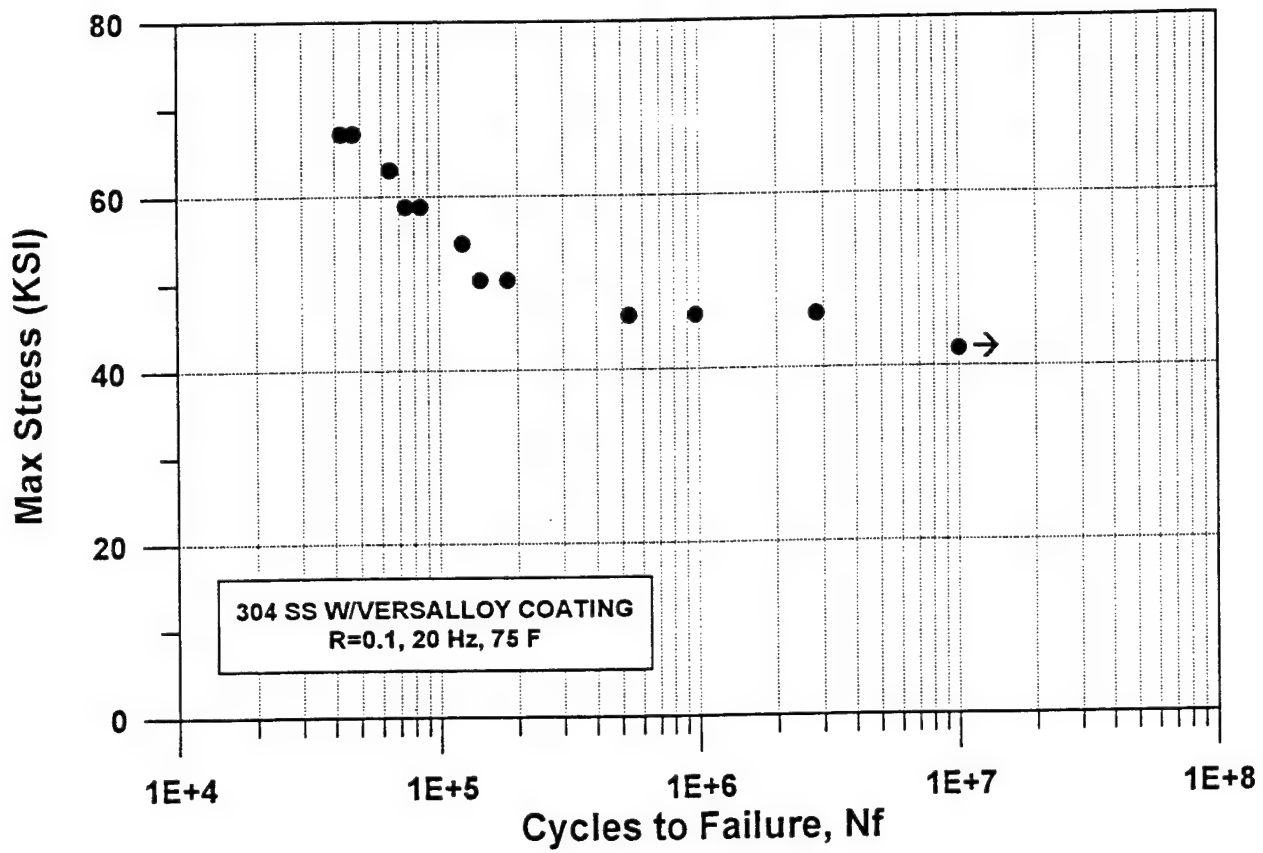


FIGURE F2. Axial Fatigue Data for 304 Stainless Steel with versalloy coating. ($K_t=1.0$).



FIGURE F3. Spray Casted 304 Stainless Steel Coating Cracking after Minimum Number of Cycles, (Specimen SS-1).

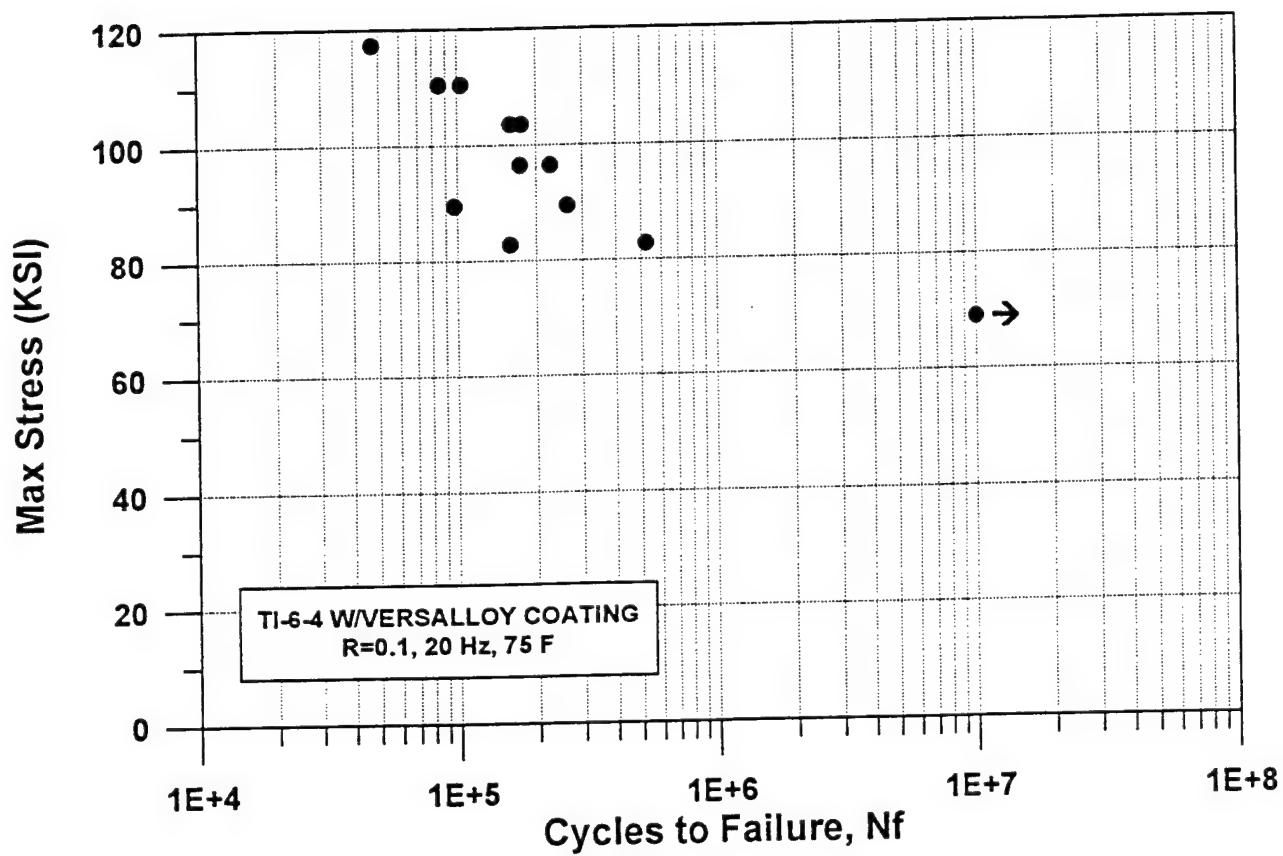


FIGURE F4. Axial Fatigue Data for Titanium 6-4 with versalloy coating. ($K_t=1.0$).

APPENDIX B

Evaluation Report--Spray Casting Evaluation

MATERIALS DIRECTORATE
SYSTEMS SUPPORT DIVISION, WL/MLS
2179 TWELFTH ST STE 1
WRIGHT-PATTERSON AFB OH 45433-7718

EVALUATION REPORT

SPRAY CASTING EVALUATION

REPORT NO: 93-59

DATE: 27 JULY 1993

PROJECT NO: ASC08613

TYPE EVAL: MATERIALS EVALUATION

SUBMITTED BY: WL/MLSE
Ms MaryAnn Phillips

DISTRIBUTION STATEMENT C: Distribution limited to U.S. Government agencies and their contractors: test and evaluation/27 July 1993. Other requests for this document shall be referred to WL/MLSA, Wright-Patterson AFB OH 45433-7718.

DESTRUCTION NOTICE: Destroy by any method that will prevent disclosure or reconstruction of the document.

I. PURPOSE: The purpose of this evaluation is to determine the quality of the coating.

II. FACTUAL DATA:

1. MLSA was asked to evaluate samples produced by Spray Casting Inc. Spray Casting Inc. has developed a new method to apply metallic coatings to substrates. Tests were conducted to determine corrosion resistance, hardness changes from the heat of spray and metallography of the coating/base metal interface. The samples consisted of rectangular specimens of 4130 steel sprayed with a metallic coating. Coating thicknesses were measured using a Quantix 1500 coating thickness measuring instrument. The thickness measurements are shown in Table 1.

2. The corrosion samples were edged with wax to prevent attack at the coating/base metal interface. The samples prior to testing are shown in Figures 1 and 2. The samples were exposed in a salt fog chamber to the requirements of ASTM B117. The test was stopped after 67 hours due to excessive corrosion of the samples. The samples after exposure are shown in Figures 3 and 4.

3. The hardness samples were sectioned and mounted using standard metallographic procedures. A Zeiss micro hardness tester was used to determine the hardness across the bond line. As shown in Figure 5, there is a significant hardness difference between the coating and the base metal (Rc 48 vs Rb 78). However, no significant change in base metal hardness could be detected due to the spray process.

4. As shown in Figure 6, the coating exhibited a variation in thickness of 50% in some localized areas. Cracking and porosity was evident in some samples as shown in Figure 7. While separation appears to have occurred at the bond line, no evidence of debonding could be detected on the bulk samples. The apparent separation could be due to

preferential attack of the etchant.

III. CONCLUSIONS:

1. The samples performed poorly in the corrosion test. The B117 test is often used to evaluate the corrosion performance of plating. The short period of time before the onset of severe visual corrosion is of concern for application where corrosion resistance is desirable.

2. The hardness traverse performed on several samples indicate that there is no detectable material degradation due to the thermal loads induced during coating.

3. The metallography indicates that coating thickness varies widely and porosity and cracking were evident. These findings support those of the corrosion testing.

IV. ACKNOWLEDGMENT: The effort of Mr. Andy Logue, UDRI, and Mr. Dan Laufersweiler, UTC, were critical to the completeness of this report.

PREPARED BY

Larry Perkins

LARRY PERKINS
Corrosion Control & Nondestructive
Evaluation Section
Materials Integrity Branch
Systems Support Division
Materials Directorate

COORDINATION

Grover L. Hardy

GROVER L. HARDY, Acting TAM
Corrosion Control & Nondestructive
Evaluation Section
Materials Integrity Branch
Systems Support Division
Materials Directorate

PUBLICATION REVIEW

This report has been reviewed and is approved.

Ronald H. Williams

RONALD H. WILLIAMS
Materials Integrity Branch
Systems Support Division
Materials Directorate

TABLE 1
Coating Thickness*

| sample | average | high | low | Std Div |
|--------|---------|------|-----|---------|
| 1 | 8.4 | 10 | 7 | 0.8 |
| 2 | 7.6 | 8.5 | 7 | 0.4 |
| 3 | 8.5 | 9 | 8 | 0.5 |
| 4 | 7.5 | 8 | 6.5 | 0.5 |
| 5 | 8.5 | 10 | 7 | 0.8 |
| 6 | 7.3 | 8 | 6.6 | 0.5 |
| 7 | 8.2 | 9 | 7.5 | 0.5 |
| 8 | 7.2 | 8 | 6.5 | 0.4 |

* Average of several measurements; all measurements in Mils

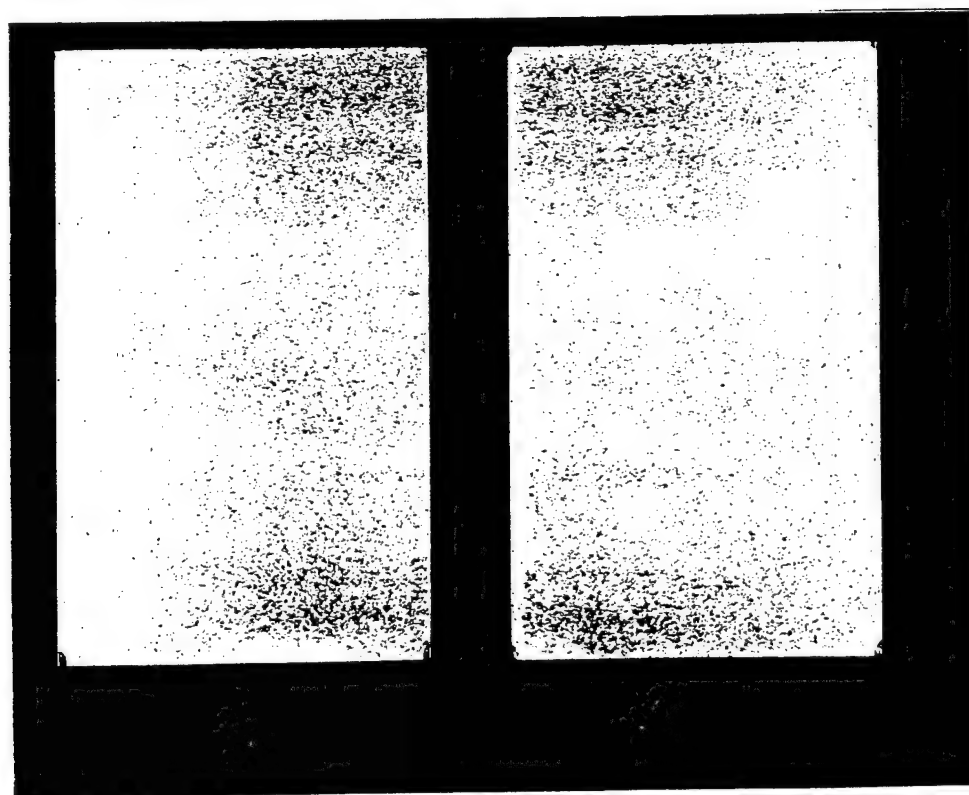
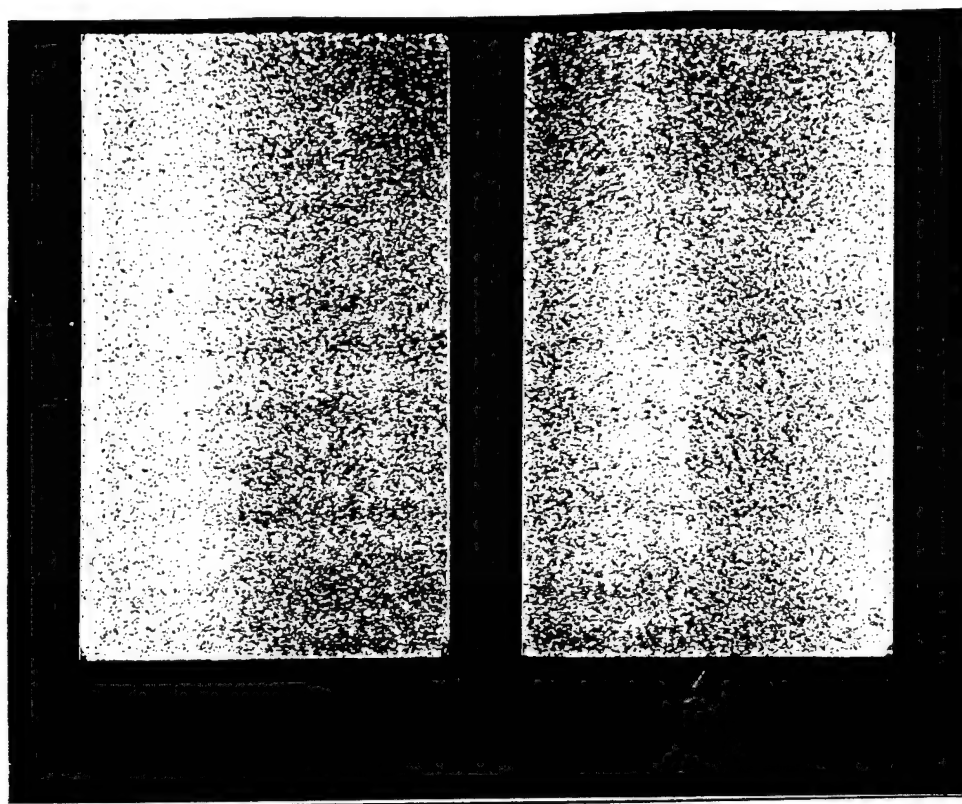


Figure 1. Samples prior to corrosion testing.

Mag. 0.7x

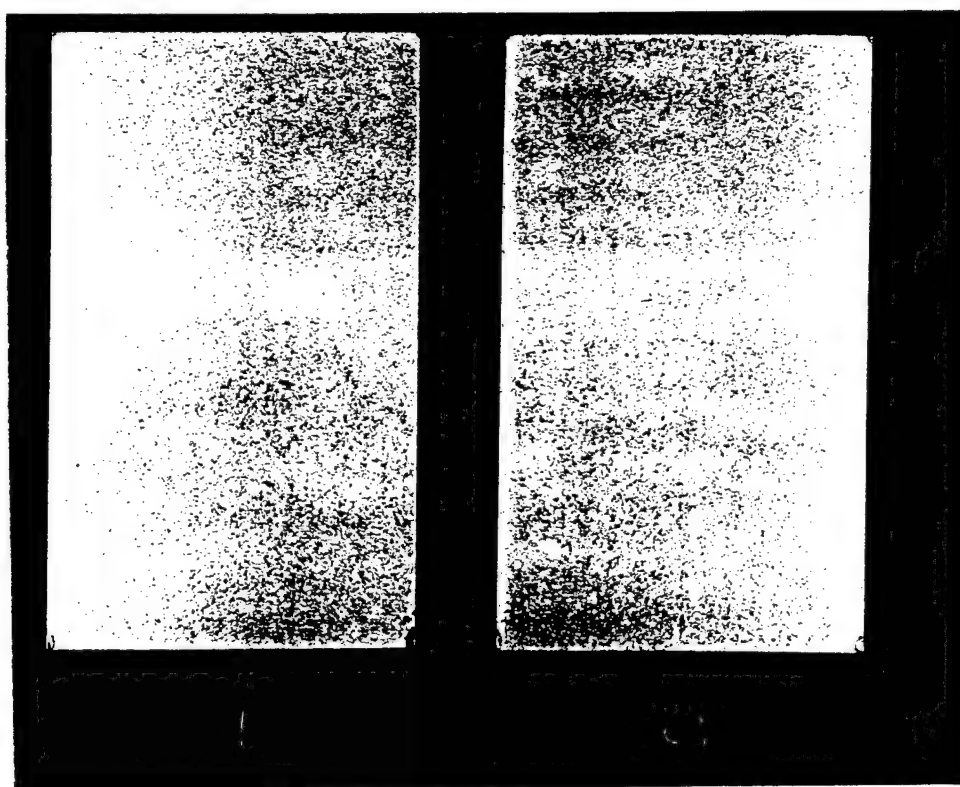
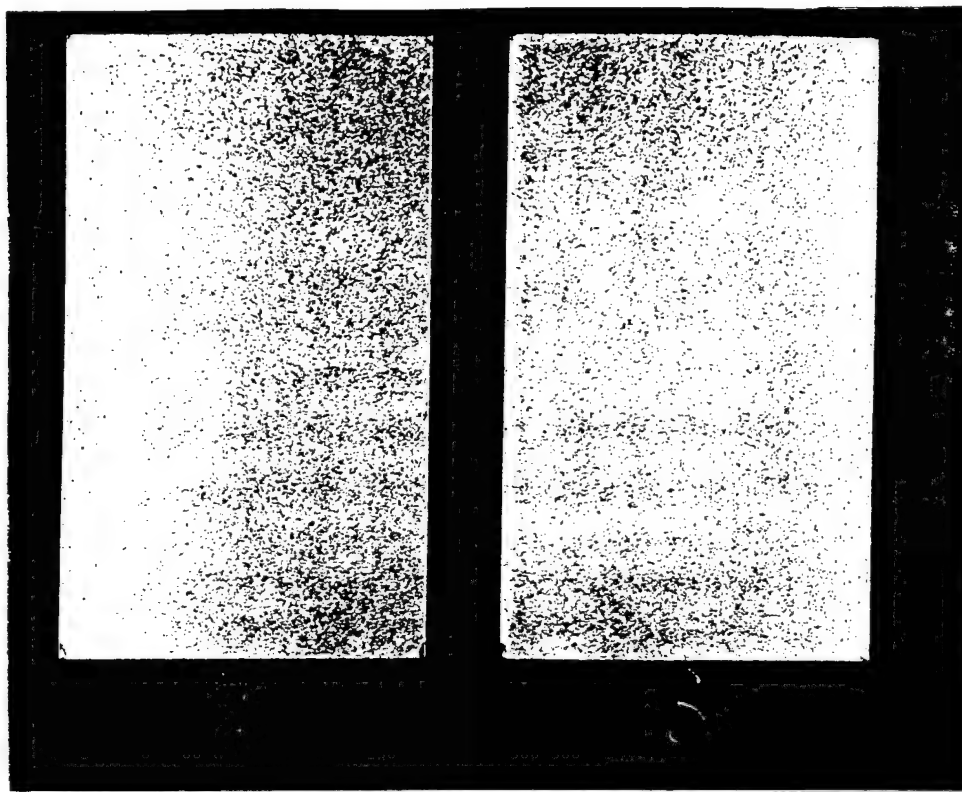


Figure 2. Samples prior to corrosion testing.

Mag. 0.7x

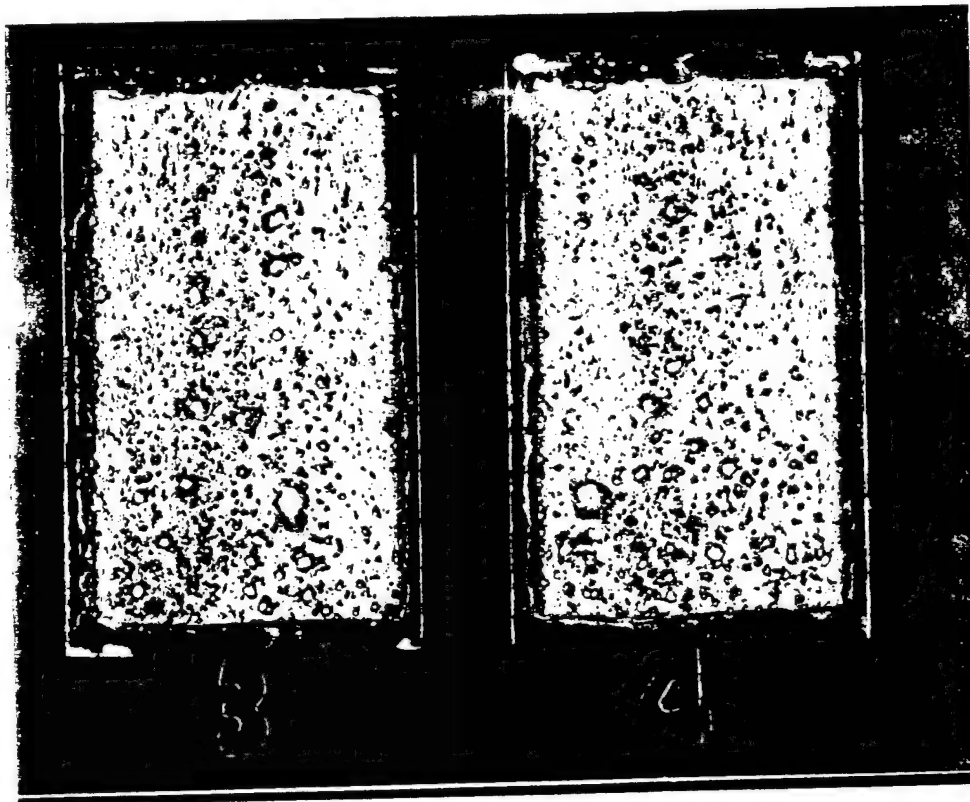
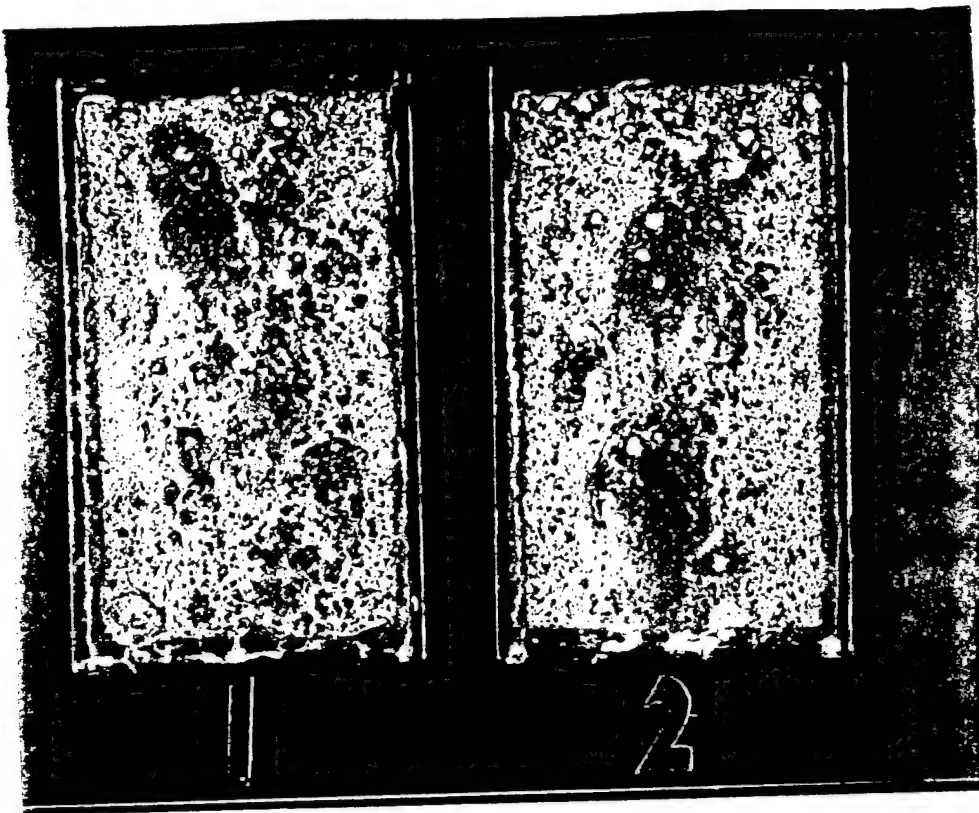


Figure 3. Samples after corrosion testing.

Mag. 0.7x

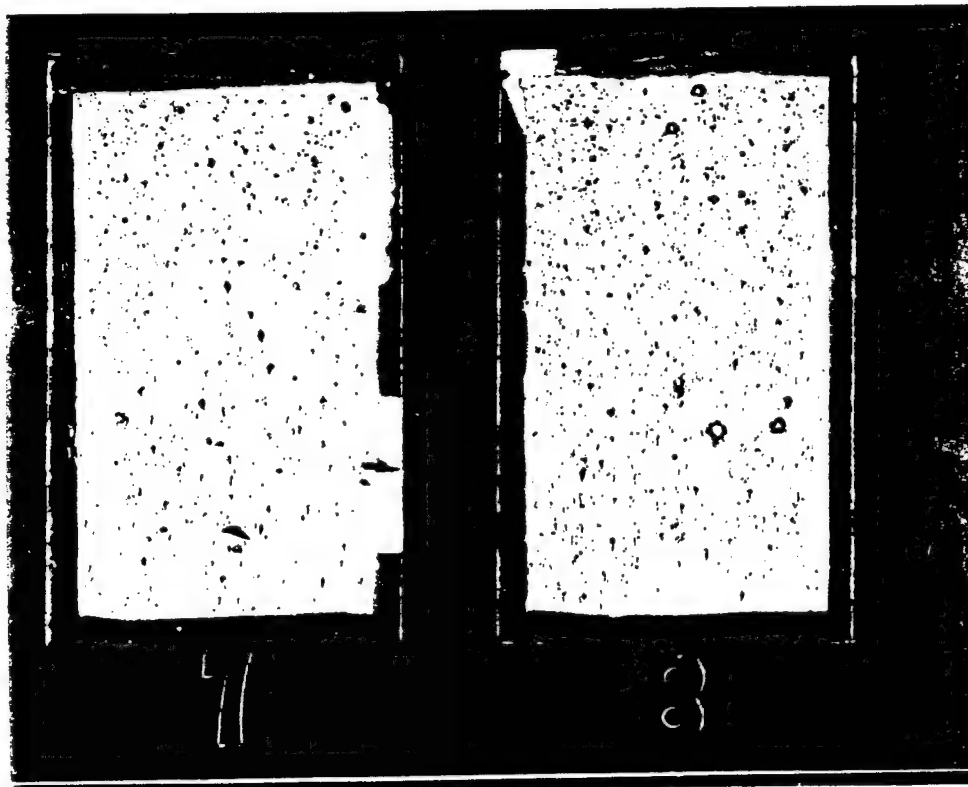
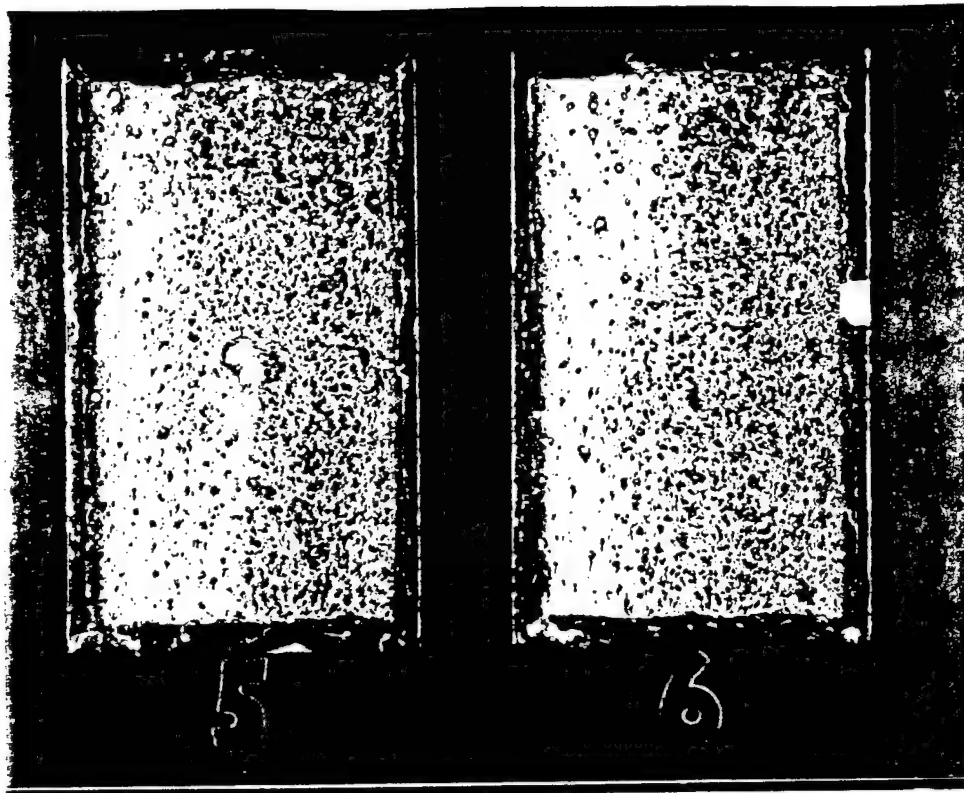


Figure 4. Samples after corrosion testing.

Mag 0.7x

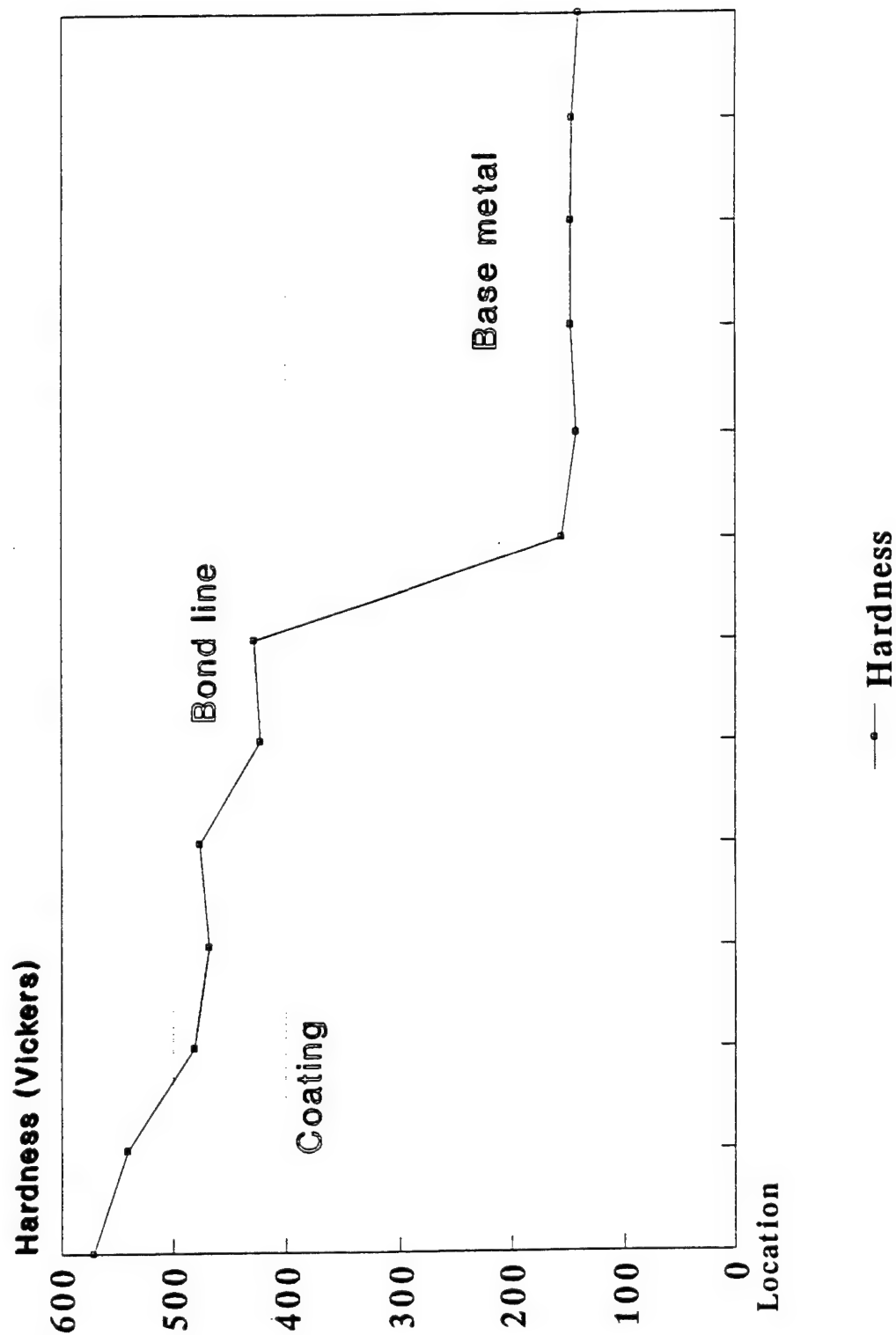


Figure 5. Hardness traverse.

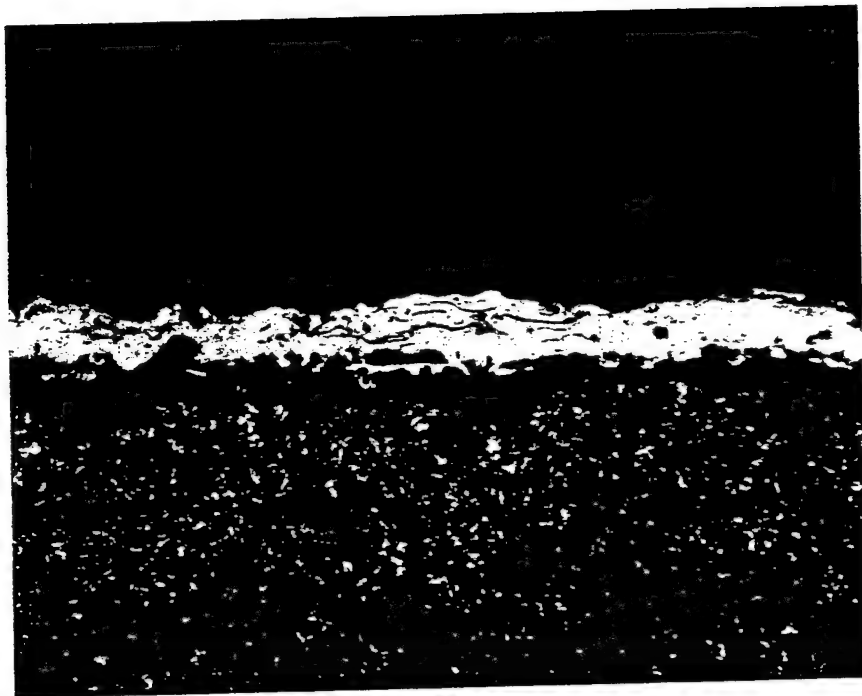


Figure 6. Coating thickness variation.
Mag. 100x

Etchant Nital

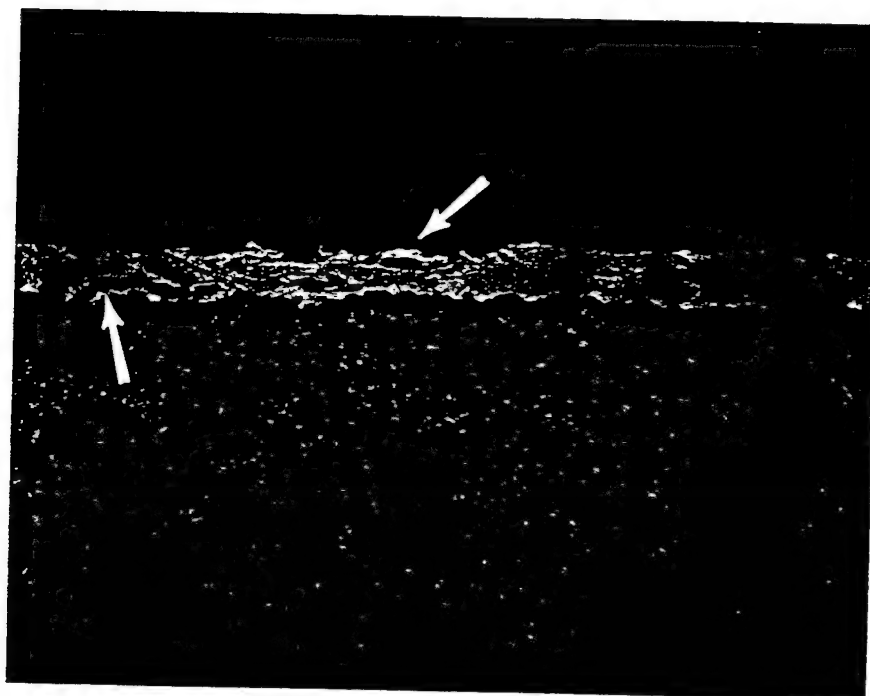


Figure 7. Coating porosity and cracking (arrows).
Mag 100x

Etchant Nital

APPENDIX D
SPRAY CASTING PROJECT
WEAR- AND CORROSION-INTEGRATED TEST SERIES

**SPRAY CASTING PROJECT
WEAR AND CORROSION
INTEGRATED TEST SERIES**

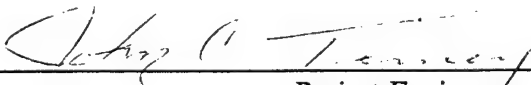
Prepared by

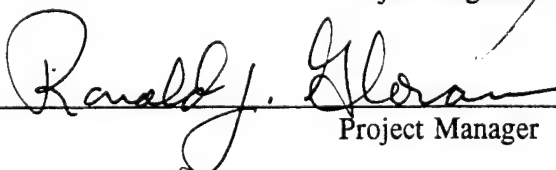
MSE, Inc.
P.O. Box 4078
Butte, Montana 59702

Prepared for

U.S. Department of Energy
Under Contract DE-AC22-88ID12735

REVIEWS AND APPROVALS:

Prepared by: 
Project Engineer

Reviewed by: 
Project Manager

Approved by: 
Program Manager

CONTENTS

| | Page |
|--|------|
| 1. INTRODUCTION | 1 |
| 2. HARDWARE DEVELOPMENT | 2 |
| 2.1 Gas Heating System | 2 |
| 2.2 Metal Feed System | 2 |
| 2.3 Spray Chamber, Tundish Pressure Control, and Filter System | 6 |
| 2.4 Nozzle/Tundish Heating System | 8 |
| 2.5 Six-Axis Robotic Arm | 8 |
| 2.6 Two-Piece Nozzle | 9 |
| 3. COMPUTER MODELING | 12 |
| 4. EXPERIMENTAL DESIGN | 14 |
| 4.1 Phase I: Preliminary Test | 15 |
| 4.1.1 Experimental Description | 15 |
| 4.1.2 Experimental Procedure | 16 |
| 4.2 Phase II: Completely Random Design | 16 |
| 4.2.1 Experimental Description | 16 |
| 4.2.2 Experimental Procedure | 17 |
| 4.3 Phase III: Central Composite Design | 17 |
| 4.3.1 Experimental Description | 17 |
| 4.3.2 Experimental Procedure | 18 |
| 4.4 Phase IV: Validation Testing | 20 |
| 4.4.1 Experimental Description | 20 |
| 4.4.2 Experimental Procedure | 20 |
| 5. RESULTS | 21 |
| 5.1 Phase I: Preliminary Test | 21 |
| 5.1.1 Deposit Profiles | 21 |
| 5.2 Phase II: Completely Random Design | 21 |
| 5.2.1 ASTM B117 Salt Fog Corrosion Data | 21 |
| 5.2.2 Taber Abraser Wear Data | 26 |
| 5.2.3 Vickers Microhardness and Percent Porosity Data | 26 |
| 5.2.4 Statistical Analysis | 27 |
| 5.3 Phase III: Central Composite Design | 28 |
| 5.3.1 ASTM B117 Salt Fog Corrosion Data | 28 |
| 5.3.2 Taber Abraser Wear Data | 28 |
| 5.3.3 Vickers Microhardness and Percent Porosity Data | 31 |
| 5.3.4 Statistical Analysis | 31 |

CONTENTS (Cont'd)

| | Page |
|---|------|
| 5.4 Phase IV: Validation Testing | 33 |
| 5.4.1 ASTM B117 Salt Fog Corrosion Data | 33 |
| 5.4.2 Taber Abraser Wear Data | 40 |
| 5.4.3 Vickers Microhardness and Percent Porosity Data | 41 |
| 5.4.4 Statistical Analysis | 42 |
| 6. CONCLUSIONS | 43 |
| 6.1 Phase I: Preliminary Test | 43 |
| 6.2 Phase II: Completely Random Design | 43 |
| 6.3 Phase III: Central Composite Design | 43 |
| 6.4 Phase IV: Validation Testing | 43 |
| 7. RECOMMENDATIONS | 45 |
| APPENDIX A Spray Deposit Profile Data Sheets | |
| APPENDIX B Phase II Corrosion Test Results | |
| APPENDIX C Phase II Taber Abraser Wear Test Results | |
| APPENDIX D Phase II Metallurgical Coupon Microstructures | |
| APPENDIX E Phase III Corrosion Test Results | |
| APPENDIX F Phase III Taber Abraser Wear Test Results | |
| APPENDIX G Phase III Metallurgical Coupon Microstructures | |
| APPENDIX H Predicted Response and Standard Error Contour Plots for Phase III Test Results | |
| APPENDIX I Phase IV Corrosion Test Results | |
| APPENDIX J Phase IV Taber Abraser Wear Test Results | |
| APPENDIX K Phase IV Metallurgical Coupon Microstructures | |

FIGURES

| | Page |
|--|------|
| 1. Cross-Sectional View of MSE-Designed Gas Heating System. | 3 |
| 2. Twin-Wire Arc System in Test Stand. | 4 |
| 3. Twin-Wire Arc Connection in Spray Chamber. | 5 |
| 4. Overall View of Spray Casting Equipment. | 6 |
| 5. Opposite Side View of Spray Casting Equipment. | 6 |
| 6. Serpentine Graphite Heating Element Around Nozzle/Tundish Assembly. | 8 |
| 7. Pilot-Scale Serpentine Heating Element, Spray Nozzle, and Power Leads | 9 |
| 8. Pilot-Scale Two-Piece Nozzle. | 11 |
| 9. Modeling Results for Particle Velocities from Two-Piece Nozzle. | 12 |
| 10. Modeling Results for Particle Temperatures from Two-Piece Nozzle. | 13 |
| 11. Wear and Corrosion Spray Fixture Mounted on Robotic Arm. | 15 |
| 12. Plot of Spray Distribution at 4.3 Inches. | 22 |
| 13. Plot of Spray Distribution at 5 Inches | 22 |
| 14. Plot of Spray Distribution at 6 Inches | 23 |
| 15. Plot of Spray Distribution at 7 Inches | 23 |
| 16. Plot of Spray Distribution at 7.7 Inches | 24 |
| 17. Salt Fog Corrosion Testing System. | 24 |
| 18. Phase II Corrosion Coupons in the Salt Fog Chamber | 25 |
| 19. Phase II Taber Abraser Test Results. | 26 |
| 20. Phase III Corrosion Coupons in the Salt Fog Chamber | 30 |
| 21. Phase III Taber Abraser Test Results | 30 |
| 22. Normal Probability Plot for the Porosity Model. | 34 |
| 23. Residual Plot for the Porosity Model. | 34 |
| 24. Normal Probability Plot for the Corrosion Model. | 35 |
| 25. Residual Plot for the Corrosion Model | 35 |
| 26. Normal Probability Plot for the Wear-1 Model | 36 |
| 27. Residual Plot for the Wear-1 Model | 36 |
| 28. Normal Probability Plot for the Wear-2 Model | 37 |
| 29. Residual Plot for the Wear-2 Model | 37 |
| 30. Normal Probability Plot for the Microhardness Model | 38 |
| 31. Residual Plot for the Microhardness Model | 38 |
| 32. Contour Plot of Predicted Response for Taber Wear Index Wear-2 Model with Contour plot of Predicted Standard Error Overlaid | 39 |
| 33. Phase IV Corrosion Coupons in Salt Fog Chamber | 40 |
| 34. Phase IV Taber Abraser Results | 41 |

TABLES

| | |
|--|----|
| 1. Phase II Spray Patterns | 17 |
| 2. Phase III Variable System Operating Parameters | 19 |
| 3. Phase I Standard Deviation for Each Standoff Distance | 21 |
| 4. Phase II Corrosion Protection Rating Assigned to Samples | 25 |
| 5. Phase II Vickers Microhardness and Percent Porosity Data | 27 |
| 6. Phase III Corrosion Protection Rating Assigned to Samples | 29 |
| 7. Phase III Vickers Microhardness and Percent Porosity Data | 32 |
| 8. Phase IV Corrosion Protection Rating Assigned to Samples | 40 |
| 9. Phase IV Vickers Microhardness and Percent Porosity Data | 41 |

1. INTRODUCTION

Phase III of the Air Force Spray Casting Project was conducted by MSE, Inc., at its Spray Casting Facility in Butte, Montana. The primary purpose of Phase III work has been to qualify the Pressure Controlled Atomization Process (PCAP) to Air Force standards as a means of replacing hard chromium electroplating as a refurbishment technique for the dimensional restoration of Air Force parts. Up to this point, the qualification process has been broken down into three separate test series: the MSE Test Series, the Boeing Test Series, and the Wright Laboratory Test Series. A separate report has been issued for each test series.

The Wear and Corrosion Integrated (WIT) Test Series was conducted in response to concerns expressed by the Air Force with regard to the wear and corrosion performance of PCAP sprayed VERSAlloy 50 coupons that were tested during the Wright Laboratory Test Series.

To evaluate the effects of PCAP primary process variables on the wear and corrosion performance of VERSAlloy 50 sprayed test coupons, a four-phase designed experiment was conducted. The experiment also evaluated microhardness and porosity of the coating. In addition to the designed experiment and associated testing, a major effort was made to upgrade the spray hardware into a developmental pilot-scale spray system.

2. HARDWARE DEVELOPMENT

Before conducting the WIT Test Series, the MSE modified Phase II hardware was upgraded into a developmental pilot-scale system. This system was designed, fabricated, and integrated for operation by one technician. The new hardware included a vacuum/pressure chamber, an electric twin-wire arc liquid metal supply system, a two-piece nozzle, an inert gas heating system capable of 1800 °C, a six-axis robotic arm to manipulate substrates into the spray plume, and a nozzle/tundish heating system. Portions of this hardware were developed during the Boeing and Wright Laboratory Test Series but were not installed into the system until the Wright Laboratory Test Series had been completed.

2.1 GAS HEATING SYSTEM

The gas heating system used for the Boeing and Wright Laboratory Test Series was designed and fabricated by the American Furnace Company (AFC) of Knoxville, Tennessee. Although the AFC gas heating system allowed higher melting point materials to be sprayed, maximum output temperature was measured at 1150 °C. Therefore, MSE designed a new heating system capable of reaching output gas temperatures exceeding 1800 °C. The new system utilized the water-cooled pressure vessel designed by AFC, as well as the control instrumentation, power transformer, and safety systems supplied with the original unit.

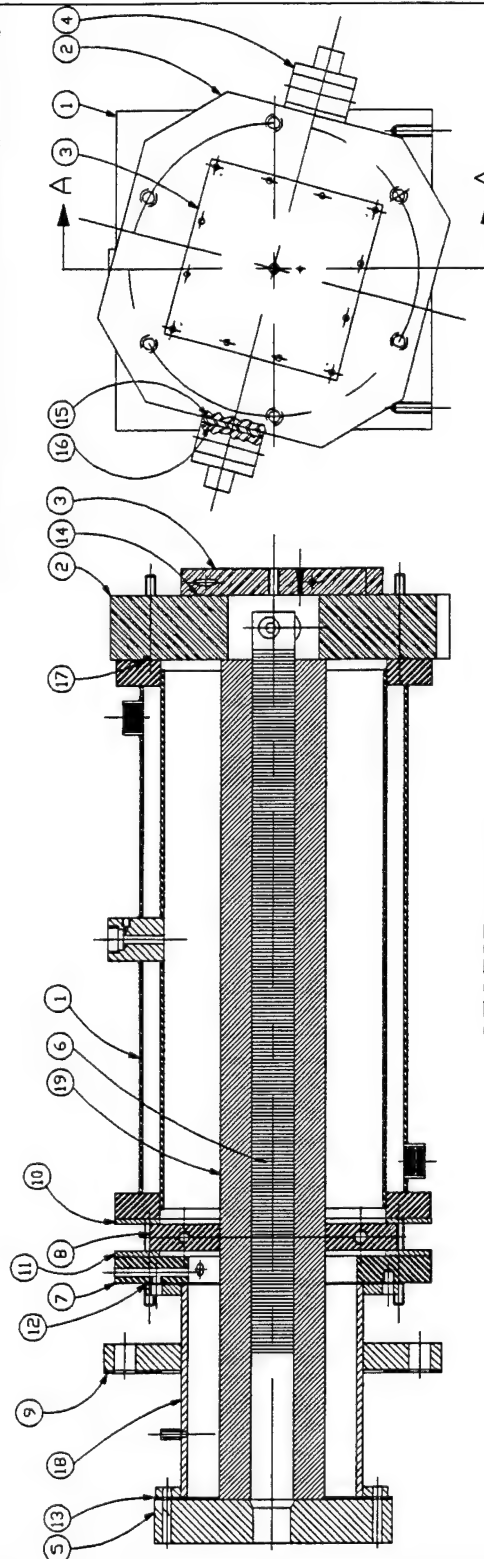
The new design incorporates a graphite hair-pin heating element inserted in a rigid felt graphite tube lined with CALGRAPH flexible graphite material. The hair-pin heating element and tube form an annulus that provides a large surface area and places the hottest portion of the element at the exit of the gas heating vessel, which is the entrance to the nozzle. Clearance between the graphite hair-pin heating element and the rigid felt graphite tube provides a close tolerance annulus that develops turbulent gas flow. The turbulent flow conditions from the high gas velocity produces a nominal heat transfer efficiency of 90% (efficiency of the system varies depending on gas type and inlet gas mass flow). The new system was tested and exit gas temperatures of 1700 °C for argon and 1800 °C for nitrogen were measured with a type "C" open-tipped thermocouple. The maximum exit gas temperature of the system has not been tested. Figure 1 shows a cross-section view of the MSE gas heating system.

2.2 METAL FEED SYSTEM

The idea for a continuous molten metal feed system was presented in a conceptual design at the Idaho National Engineering Laboratory (INEL) on June 26, 1991. The idea was to use an electric twin-wire arc system to supply molten metal to a pressurized tundish. Since the twin-wire arc ram (spray gun) and associated controls and power supplies were available from a commercial vendor, a spray system from Hobart/TAFA was ordered. Additionally, the system was to be used to compare the PCAP to a commercial process for testing during the MSE Test Series.

The system was initially installed in a test setup stand as shown in Figure 2. As shown, the system is a modular design with remote control console, a power supply, a wire drive motor/control, a spray gun with a 4-inch-diameter straight extension ram, a lead screw/DC gear motor system for positioning the ram, and a 4-inch gate valve.

| ITEM | PART NO. | DESCRIPTION | QTY. |
|------|------------------|-------------------------------------|------|
| 1 | DD5-20ME-011 MOD | GAS HEATER VESSEL | 1 |
| 2 | DD5-20ME-012 MOD | GAS HEATER END PLATE | 1 |
| 3 | DD5-20ME-013 MOD | GAS HEATER WATER COOLED COVER PLATE | 1 |
| 4 | DD5-20ME-014 MOD | GAS HEATER POWER LEAD | 2 |
| 5 | DD5-20ME-015 MOD | GAS HEATER GRAPHITE END PLATE | 1 |
| 6 | DD5-20ME-016 MOD | GAS HEATER ELEMENT | 1 |
| 7 | DD5-20ME-017 MOD | GAS HEATER OUTLET FLANGE | 1 |
| 8 | DD5-20ME-018 MOD | GAS HEATER COOLING FLANGE | 1 |
| 9 | DD5-20ME-019 MOD | GAS HEATER SEAL | 1 |
| 10 | DD5-20ME-019 MOD | GAS HEATER SEAL | 1 |
| 11 | DD5-20ME-019 MOD | GAS HEATER SEAL | 1 |
| 12 | DD5-20ME-019 MOD | GAS HEATER SEAL | 1 |
| 13 | DD5-20ME-019 MOD | GAS HEATER SEAL | 1 |
| 14 | DD5-20ME-019 MOD | GAS HEATER SEAL | 1 |
| 15 | DD5-20ME-019 MOD | GAS HEATER SEAL | 1 |
| 16 | DD5-20ME-019 MOD | GAS HEATER SEAL | 1 |
| 17 | DD5-20ME-019 MOD | GAS HEATER SEAL | 1 |
| 18 | DD5-20ME-020 MOD | GAS HEATER EXTENSION | 1 |
| 19 | DD5-20ME-021 MOD | GAS HEATER ELEMENT INSULATOR | 1 |



SECTION A-A
GAS HEATER ASSEMBLY

MSE Inc.
ACAD#: A95R0816
REV: - DATE: 8/22/95
DRAFTER: SEL

Figure 1. Cross-sectional view of MSE-designed gas heating system.

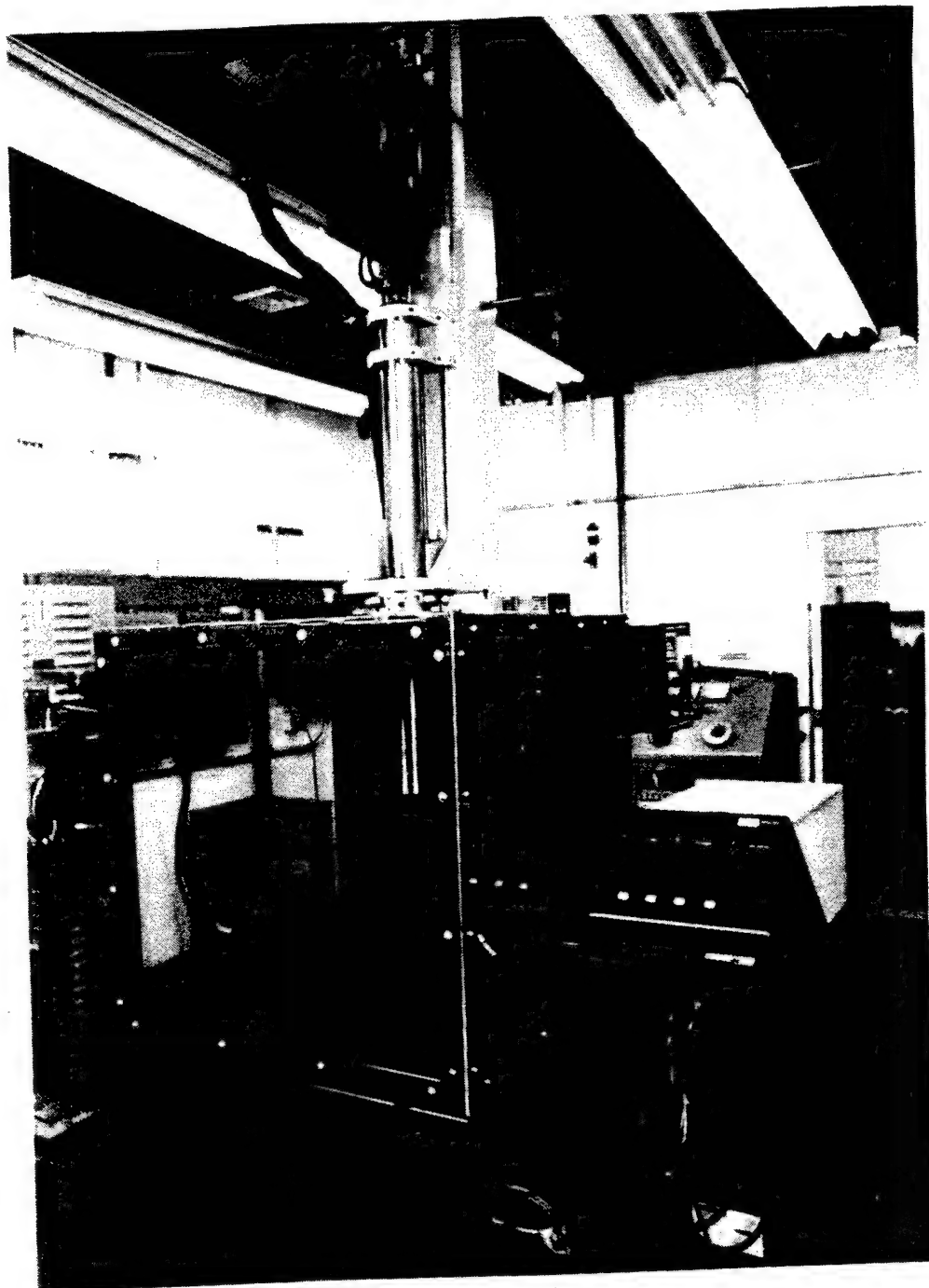


Figure 2. Twin-wire arc system in test stand.

The twin-wire arc was tested for operation without atomizing gas flow to carry molten metal away from the electric arc, and the results indicated that the system would operate without gas flow in the ram. The system was then installed on the Advanced Vacuum Systems vacuum/pressure spray chamber.

Before using the twin-wire system, a water cooled connection was designed to allow the ram of the twin-wire arc to connect with the heated nozzle. The connection is designed with an O-ring receptacle that allows the ram to be pressurized to control the spray deposition rate and to direct molten material into the tundish. The twin-wire arc connection is shown in Figure 3.

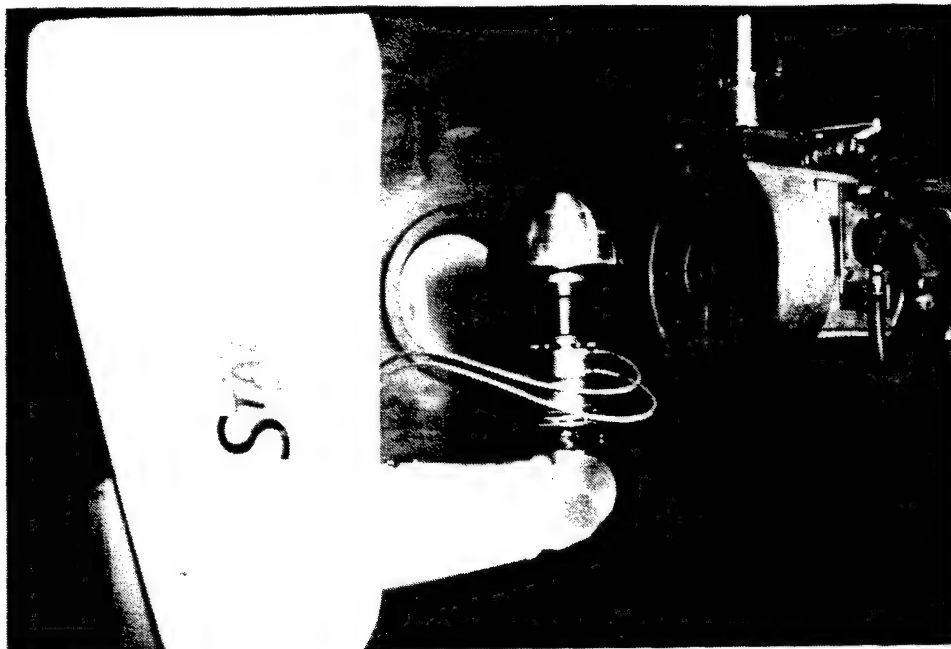


Figure 3. Twin-wire arc connection in spray chamber.

Normal operation of the system is to extract the ram from the spray chamber and to close the 4-inch gate valve. The ram is then purged with argon, and the spray chamber vacuum pumping system is started. When the spray chamber has been evacuated and backfilled with argon, the gate valve is opened and the purged ram is lowered into the O-ring receptacle of the twin-wire arc connection.

The twin-wire arc system was tested on May 4, 1994. Parameters for wire speed, amperage, and DC voltage settings were recorded. After extended testing of the twin-wire arc system, the plastic tip of the ram (next to the arc) deteriorated. MSE modified the twin-wire arc with copper, boron nitride insulators, and G10 epoxy glass so that the existing water cooling passages provided enough heat transfer to cool the tip of the unit. Testing of the system resumed June 9, 1994. The MSE-modified system supplied molten material to the tundish and performed as expected. Parameters for wire speed, amperage, and DC voltage settings were again recorded; however, after several refills, the nozzle would plug and the spray test would terminate. Post test investigations showed that vaporized copper was causing slagging problems in the tundish that eventually plugged the liquid orifice in the spray nozzle.

To resolve this problem, MSE scientists decided to feed wire directly into the molten pool of metal in the tundish. The internal components of the twin-wire arc were removed and a single tube was inserted into the 4-inch-diameter ram to guide wire into the tundish. Initial testing at the Spray Casting Facility showed that the nozzle/tundish heating system can handle the additional load to melt wire for a continuous feed system.

Additional testing of the direct wire feed system is required and a means for accurately measuring the level of the liquid metal also needs to be developed before the metal feed system is functional.

2.3 SPRAY CHAMBER, TUNDISH PRESSURE CONTROL, AND FILTER SYSTEM

A new spray chamber with industrial controls and a particulate filter were installed in the Spray Casting Facility as part of the work for the pilot-scale system. The new spray chamber consists of a horizontal ASME-stamped and registered pressure vessel, a three-stage mechanical booster vacuum pumping system, a control console, and a particulate exhaust filter. The new equipment in the Spray Casting Facility is shown in Figures 4 and 5.

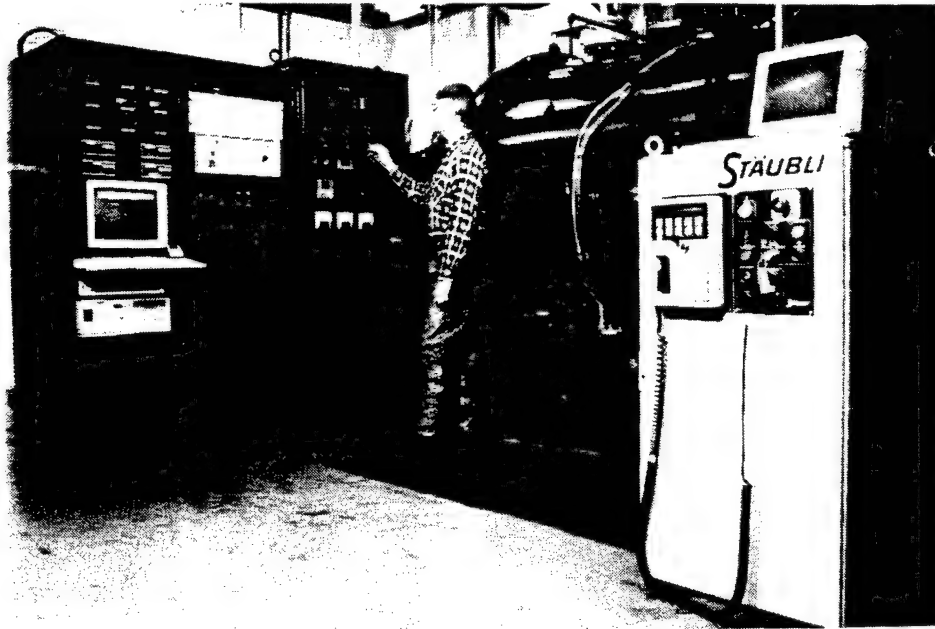


Figure 4. Overall view of spray casting equipment.

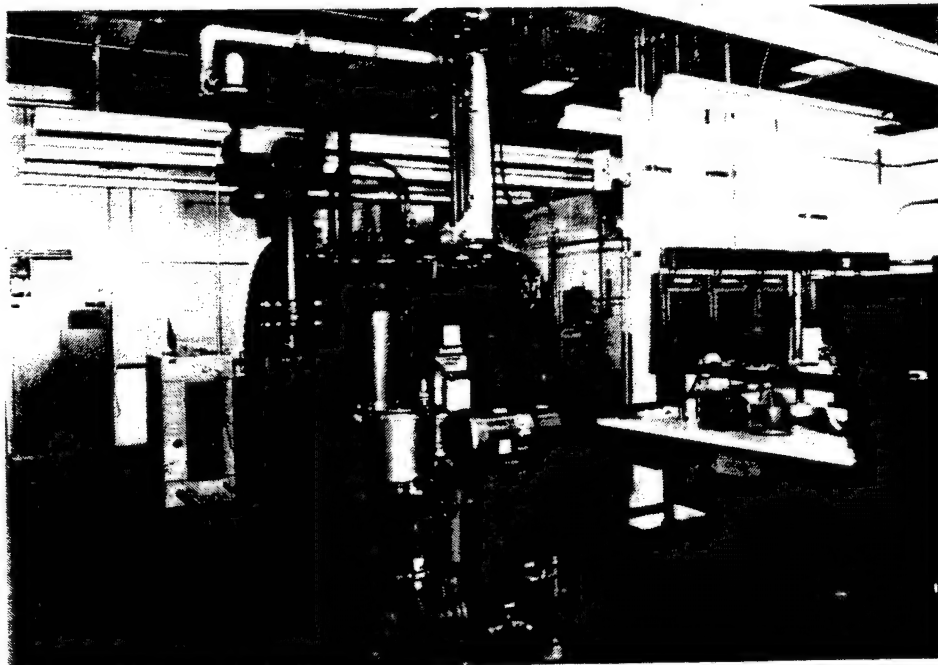


Figure 5. Opposite side view of spray casting equipment.

The system is designed to operate at a working pressure of 4379 Torr or at a vacuum of 0.001 Torr. The vessel is 60 inches in diameter by 72 inches long and was manufactured by Advanced Vacuum Systems. The chamber was fabricated from mild steel and has two 12-inch-diameter tempered glass observation ports. Access to the interior of the chamber is provided by two 24-inch-diameter doors with quick release latches. The mechanical booster vacuum pumping system, manufactured by the Kinney Vacuum Company, consists of a 150 cfm mechanical roughing pump, a 250 cfm first-stage vacuum blower, and a 850 cfm second-stage vacuum blower. The system is designed to take the atmosphere in the chamber to 0.001 Torr in 20 minutes. Pressure in the vessel is measured with a high accuracy (0.8% of reading) dual capacitance manometer system manufactured by MKS Instruments, Inc. The system automatically changes to the reading sensor and permits continuous display of pressure from atmospheric to 0.001 Torr.

Controls for the PCAP and all fuses, contactors, step down isolation transformers, breakers, switches, and indicating lights for the vessel vacuum pumping system are mounted in a NEMA 12 control console.

Overspray from the PCAP is filtered through a 0.02 micron filter manufactured by ZANDER Filter Systems, Inc. The filter is encased in an ASME-stamped and registered pressure vessel and has a capacity to handle 1445 scfm of air at 100 psi.

Typical operation of the system is described as follows. External valves on the spray chamber are closed and the 150 cfm mechanical roughing pump is activated. At 200 Torr, a pressure switch activates the 250 cfm first-stage vacuum blower, and at 50 Torr, a second pressure switch activates the 850 cfm second-stage vacuum blower. With all three pumps running simultaneously, an ultimate pressure of 0.001 Torr is achieved in 20 minutes. The vacuum pumping system is then turned off and the vessel is backfilled with argon until the pressure in the chamber returns to 760 Torr. All external valves on the vessel are opened, and the process is ready for operation. At this time, the PCAP has not been used with a pressurized atmosphere.

An industrial process controller to regulate the pressure in the tundish was also installed after completing the Wright Laboratory Test Series. The automatic pressure controller is a self-contained PID module manufactured by MKS Instruments, Inc. Pressure feedback information to the controller is provided from a capacitance manometer sensor, and a linear proportioning electromagnetic valve is used to control tundish pressure. The controller can also be programmed with a 0- to 5-volt analog external set-point signal. Circuitry for the external analog signal was designed, fabricated, and installed by MSE personnel to provide a method for automating the on/off action of the spray process.

Installation of the spray chamber, tundish pressure control, and filter systems was completed April 1, 1993. The first spray test with the pilot-scale system was conducted April 2, 1993. Measurements from spray tests indicate that oxygen concentration in the spray chamber after vacuum pumping and argon backfilling measured between 0.01 and 0.2%. Measurements were taken with a Rosemount, Model 755R, oxygen analyzer.

During testing, particulate overspray accumulated on the interior of the spray chamber with only a small percentage of the solidified particles making it to the 0.02 micron ZANDER filter. The chamber was not designed to keep the metal particulate entrained in the off-gas stream, where it would be captured by the filter. The overspray accumulated in the chamber was removed with a standard vacuum cleaner.

2.4 NOZZLE/TUNDISH HEATING SYSTEM

The nozzle/tundish heating system was first developed to replace induction heating coils used in the Phase I and II equipment operated at the INEL. The first system designed by MSE was used for the Boeing and the Wright Laboratory Test Series. The system consisted of a serpentine graphite resistance element that enclosed the nozzle and tundish. Figure 6 shows the serpentine element around a nozzle and tundish. Electrical power to the heating assembly is supplied by a silicon-controlled rectifier (SCR)/transformer system. A 4-20 mA signal from an Eurotherm temperature controller regulates the SCR output to the primary feed of a 240-volt, 60-Hz, 12-kVA transformer. Electrical connections from the transformer to the element are through 350-MCM copper-braided, water-cooled flex cables.

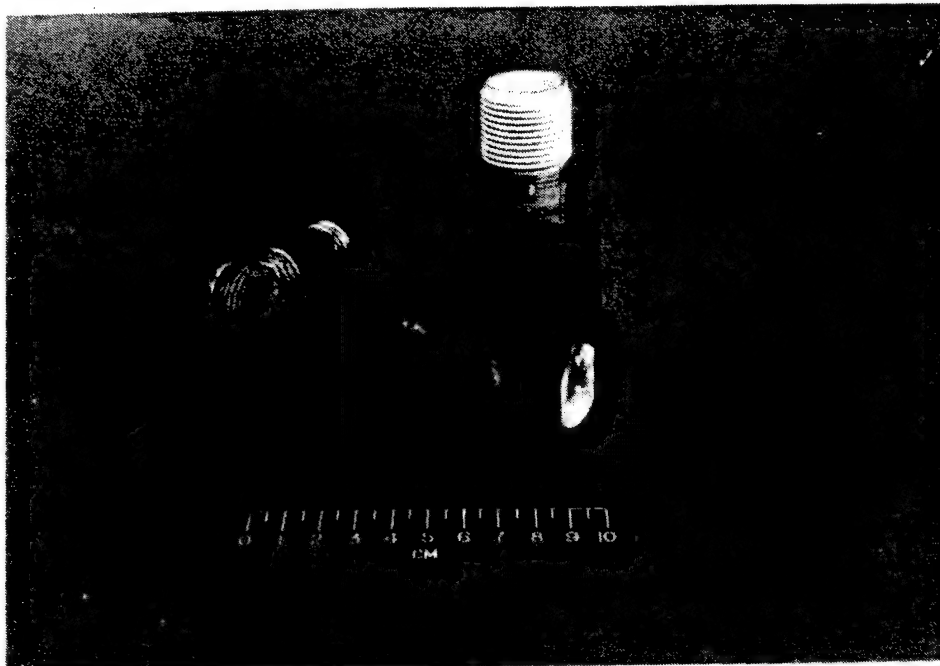


Figure 6. Serpentine graphite heating element around nozzle/tundish assembly.

The system was redesigned for the pilot-scale unit. The new nozzle/tundish heating system included new power connections that were anchored to the twin-wire arc housing, new rigid felt graphite insulation around the serpentine element, and a larger graphite element. Figure 7 shows the new nozzle/tundish heating power connections and graphite element.

The heating system was tested, and 120-gram loads of VERSAlloy 50 were melted and sprayed. Nozzle and tundish temperatures were measured with type "C" open-tipped thermocouples. The system heated uniformly to 1700 °C. The maximum temperature of the system has not been tested.

2.5 SIX-AXIS ROBOTIC ARM

To support the DOE-OTD portion of the project, a robotic arm was required to articulate substrates with complex geometries into the spray plume. The arm replaced the X-Y translation device installed in Phase II equipment for the MSE, Boeing, and Wright Laboratory Test Series. The robotic arm

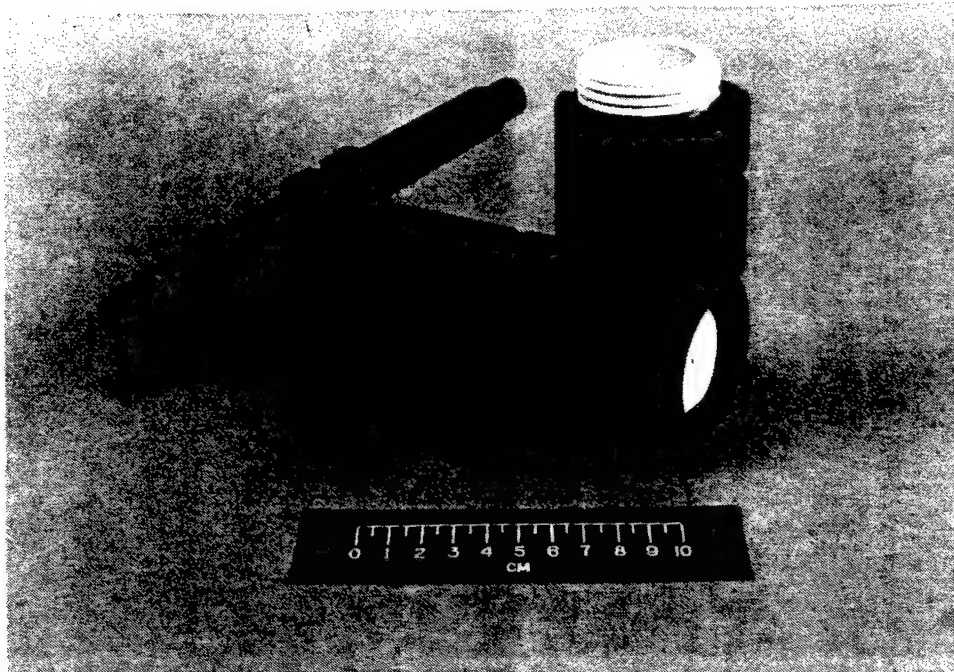


Figure 7. Pilot-scale serpentine heating element, spray nozzle, and power leads.

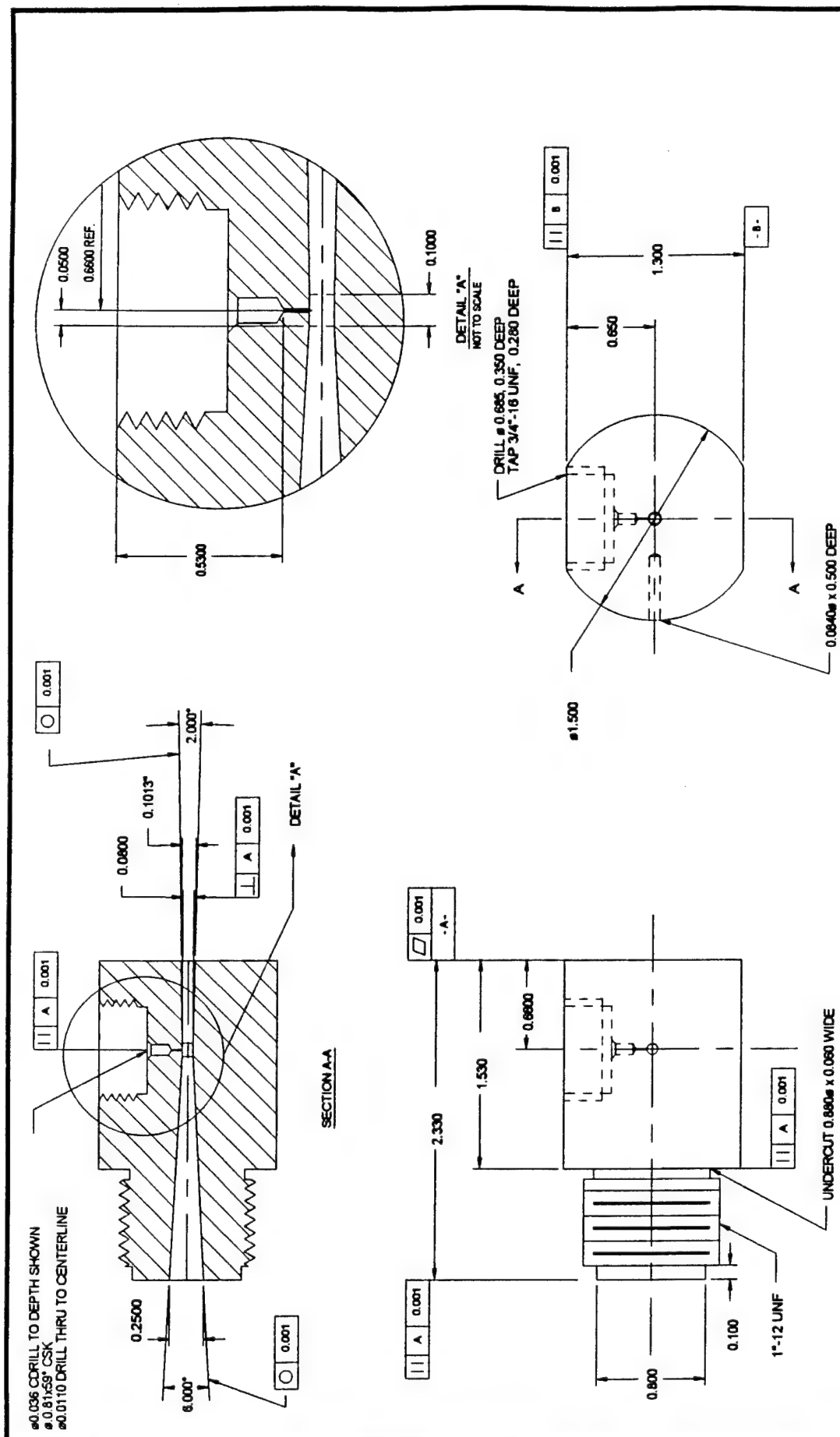
selected for manipulating substrates was a Staubli-Unimation, six-axis RX 90 model. The RX 90 is capable of high speed translation and its motion is repeatable within ± 0.00078 inches. The arm can lift a maximum payload of 9 Kg and is well suited for complex motion. The arm utilizes the latest technologies for performance, reliability, and maintainability. Specifically, AC brushless motors, absolute resolvers and modular, integrated reducer/bearing assemblies called "J.C.S." modules.

The arm installation was completed February 11, 1994, and the first spray test with the arm was conducted on March 17, 1994. A robotic arm is not required for spraying Air Force parts. Air Force parts are typically cylindrical and can be manipulated with a turntable mounted on an X-Y translation system.

2.6 TWO-PIECE NOZZLE

Nozzles for the MSE, Boeing, and Wright Laboratory Test Series were fabricated from hexagonal boron nitride. Boron nitride is soft, easy to machine material that is resistant to chemical attack by liquid VERSAlloy 50; however, the boron nitride experienced erosion during spray testing. MSE set out to design a two-piece nozzle that could be manufactured from ceramic materials and be easily replaced in the spray system. Additionally, internal geometry for the new nozzle was determined by using the quasi-one dimensional computer code to model different nozzle dimensions. The nozzle was designed for increased particle spray velocity. Higher particle velocities were desired to increase adhesion strength of the coating and to increase the spray distance to the substrate. A larger tundish was also incorporated in the design of the new nozzle. The new nozzle has a circular cross-section and is nominally 2.33 inches long. The converging section is approximately 1.62 inches long and has a 6-degree angle of convergence. The throat is 0.080 inches in diameter and is 0.100 inches long. The diverging section is approximately 0.660 inches long and has a 2-degree angle of divergence. The liquid orifice of the nozzle is 0.011 inches in diameter. A drawing of the pilot-scale nozzle is

shown in Figure 8. Two-piece nozzles were fabricated from hexagonal boron nitride and tested in the spray system. The nozzle performed as expected. However, no nozzles have been fabricated from the candidate nozzle materials identified during the MSE Test Series.



| | | | |
|----------------|---|--|--|
| NOTES: | | 1) UNITS IN INCHES UNLESS OTHERWISE NOTED 2) SURFACE FINISH TO BE 36 RMS UNLESS OTHERWISE NOTED. 3) SOME ITEMS NOT SHOWN IN ALL VIEWS FOR CLARITY. | |
| D05-20ME-007 | TWIN WIRE ARC TWO PIECE NOZZLE SUB-ASSEMBLY | | |
| DRAWING NUMBER | DESCRIPTION | | |
| REFERENCES | | | |

3. COMPUTER MODELING

Studies were performed with the Phase I quasi-one-dimensional model to estimate nozzle geometry effects on particle velocity and temperature. The modeling simulated flow conditions during spraying with a 6-degree inlet angle and 2-degree exit angle nozzle. Sixteen computer runs were performed and the following conditions were used for the simulation:

| | |
|------------------------------|---|
| Inlet pressure: | 60 psia; |
| Tundish pressure: | iterated to be 1 psi higher than the throat pressure; |
| Nozzle temperature: | 1300 °C; |
| Inlet gas temperature: | 1300 °C; |
| Sizes of the injection hole: | 0.011 inch; |
| Gas: | argon; and |
| Particle sizes: | 5, 10, 15, and 20 μm . |

Figures 9 and 10 summarize the particle velocities and particle temperatures for different particle sizes. The 5 μm particles solidified before they reached 2 inches from the nozzle exit, which limits the stand-off spray distance.

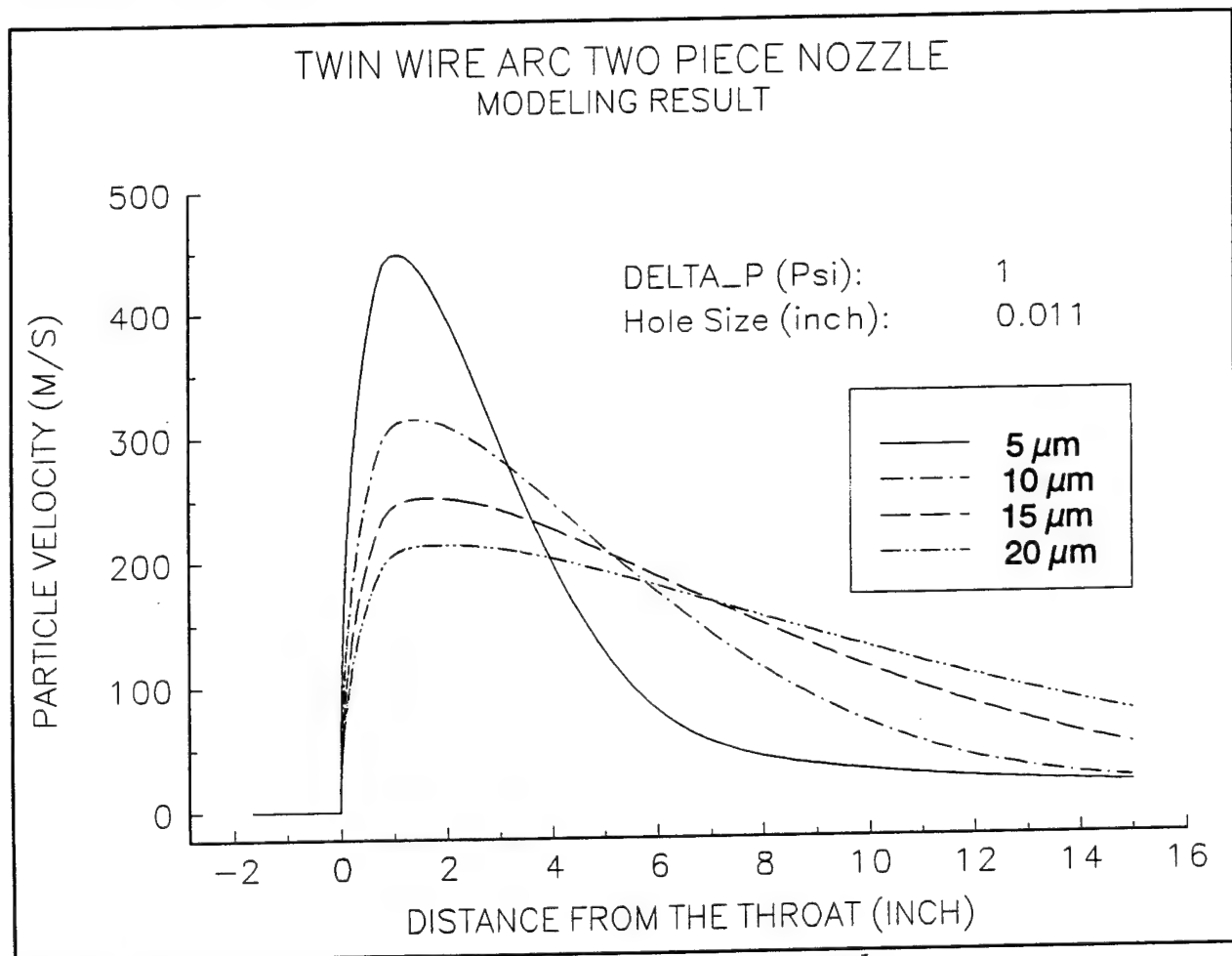


Figure 9. Modeling results for particle velocities from two-piece nozzle.

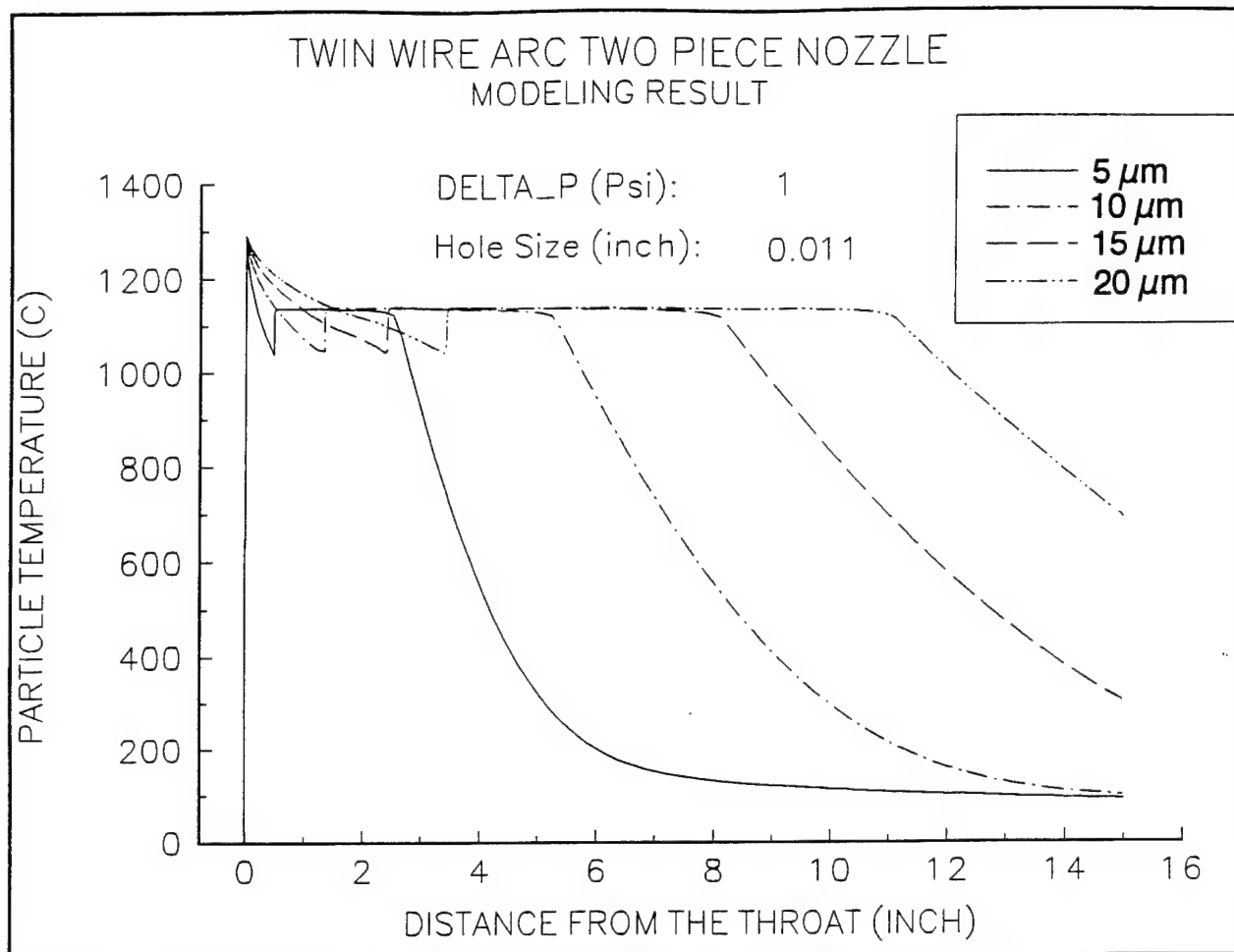


Figure 10. Modeling results for particle temperatures from two-piece nozzle.

4. EXPERIMENTAL DESIGN

The objective of this investigation was to improve the qualities of VERSAlloy 50 coatings applied by PCAP. Improvements in corrosion protection, wear resistance, microhardness, and porosity were sought. By varying several process control parameters and analyzing the sprayed coatings, tradeoffs between the responses were evaluated using statistical techniques. The testing required 35 runs and was divided into four phases:

- Phase I: Preliminary Test;
- Phase II: Completely Random Design;
- Phase III: Central Composite Design; and
- Phase IV: Validation Testing.

The Phase I preliminary testing phase was accomplished with a single spray test. A single plate of sheet steel was sprayed at five different spray distances. At each spray distance, the plate was cycled in place until a representative coating had been applied. The sprayed coating was then cross-sectioned and analyzed to characterize the profile of the spray plume at each of the five spray distances.

Phase II testing incorporated a completely random 8-run design to investigate the effects of four different spray patterns. The patterns employed the same basic motion used in Phase I, but differed in the amount of overlap between consecutive passes. The Phase II coatings were analyzed for corrosion protection, abrasive wear resistance, microhardness, and porosity. An "optimal" spray pattern, based on the Phase II analysis, was then chosen for Phases III and IV. Phase II also served as a primer for the post-spray testing that was performed at the Spray Casting Facility. The significance of several covariates was also analyzed during Phase II testing.

After completing Phases I and II, a 22-run central composite design was used in Phase III testing to explore three important parameters. The effects of spray standoff distance, nozzle inlet pressure, and nozzle-to-tundish pressure differential on spray coating characteristics were investigated. Statistical analysis of the coatings indicated which operating parameter settings offered the optimal coating for corrosion protection, abrasive wear resistance, microhardness, and porosity characteristics.

The final phase of the experimental design, Phase IV Validation Testing, was comprised of four validation spray tests. These tests verified that the operating parameters recommended in the Phase III analysis produced optimal coating characteristics.

For all four phases of testing, the coupons were prepared by degreasing with detergent, then acetone, which was followed by grit blasting. All grit blasting was accomplished by a single individual. Grit blasting parameters are shown below:

- distance: 4 inches;
- pressure: 60 psi;
- grit: Al_2O_3 ;
- size: 36 mesh; and
- blast angle: 45° .

System parameters held constant during testing, and the respective allowable operating tolerances are listed below:

- feedstock material: VERSAlloy 50;

- system gas: argon;
- nozzle material: boron nitride;
- tundish material: boron nitride;
- nozzle temperature: 1300 °C (+/- 10 °C);
- tundish temperature: 1300 °C (+/- 10 °C);
- gas temperature: 1300 °C (+/- 10 °C); and
- spray pattern: vertical passes.

For Phases II, III, and IV, all coupons were fabricated from AISI 4130 sheet steel that was 0.0625 inches thick. One 4- by 4-inch abrasion coupon, one 3- by 5-inch corrosion coupon, and one 1- by 5-inch microstructural coupon were placed on a shadow mask fixture (see Figure 11).

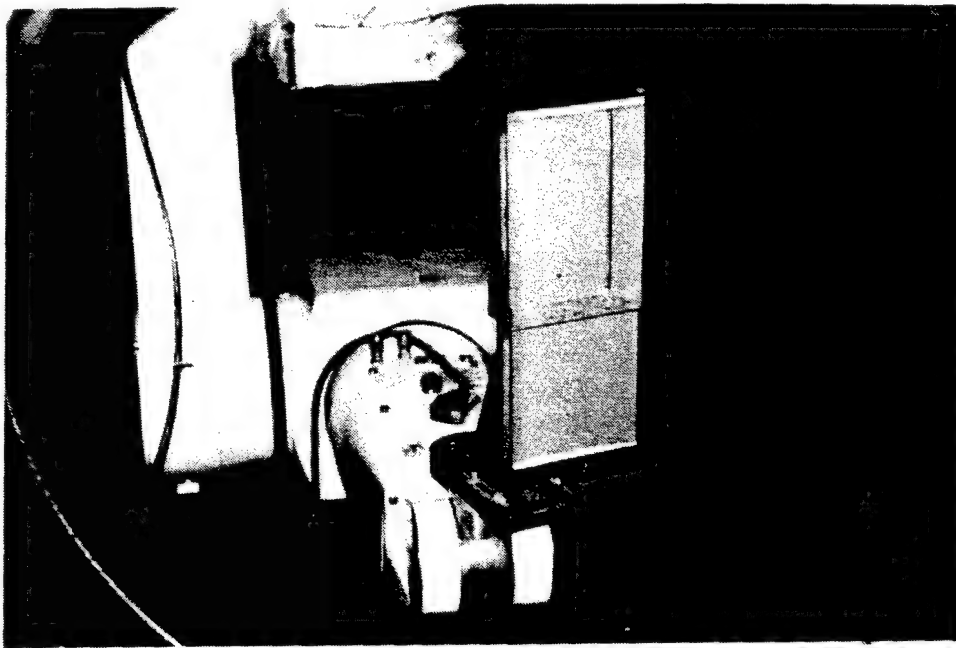


Figure 11. Wear and corrosion spray fixture mounted on robotic arm.

For Phases II, III, and IV, the following procedure was used to analyze the sprayed coupons. The abrasion coupon was tested at the MSE Spray Casting Facility with the Taber 5130 abraser per Federal Test Method Std. No. 141C, Method 6192.1. The corrosion coupon was tested at the Spray Casting Facility with the salt fog corrosion chamber per ASTM B 117-90. The microstructure coupon was sent to Tubal Cain Company, Inc., for microhardness and porosity measurements.

4.1 PHASE I: PRELIMINARY TEST

4.1.1 Experimental Description

This testing phase consisted of a single run. A 5- by 10-inch sheet of low carbon steel was sprayed at five different standoff distances. The standoff distance is the distance between the end of the nozzle

and the face of the substrate to be coated. At each distance, the plate was cycled in place a fixed number of times to obtain a representative coating profile.

Only one system parameter was varied during this phase, which was spray standoff distance. All other parameters remained constant for the test. The response variables for this phase were the cross-sectional heights of the five sprayed coatings.

The purpose of Phase I testing was to calculate a standard deviation for the profile of a sprayed deposit at each of the five standoff distances. The plate containing the five spray patterns was cross-sectioned, mounted and polished in metallurgical mounts, and photographed. The mounted profiles were analyzed with a Mitutoyo toolmakers microscope, which is accurate to ± 0.00005 inch. An algorithm to calculate the standard deviation of a distribution was performed for each of the five spray patterns. This yielded a standard deviation at each spray distance, which determined the overlap or track gap between consecutive spray passes. The calculated standard deviations were then used in Phase II, III, and IV testing.

4.1.2 Experimental Procedure

A single coupon was arranged and prepared for Phase I testing. One 1/8-inch-thick by 5-inch-wide by 10-inch-long, low carbon steel sheet was secured onto a test fixture on the six-axis robotic arm. Spray system operating parameters and allowable tolerances for the test were set as follows:

- operating pressure: 48 psig (± 0.5 psig); and
- pressure differential: 1 psig (± 0.01 psig).

Standoff distance was the only variable system operating parameter for Phase I testing. The standoff distance was set at 4.3; 5.0; 6.0; 7.0; and 7.7 inches.

4.2 PHASE II: COMPLETELY RANDOM DESIGN

4.2.1 Experimental Description

The effects of four different spray patterns were evaluated by performing a completely random eight-run design. The spray patterns used the same basic vertical motion of Phase I but differed in the amount of overlap between consecutive passes. The coatings in this phase were analyzed, and an optimal spray pattern was chosen for Phases III and IV. This phase also served as a primer for the corrosion and abrasion testing performed at the Spray Casting Facility. The significance of two covariates, atmospheric pressure and nozzle deterioration, were also examined.

Spray pattern was the only parameter varied during this phase. The patterns were based on the standard deviation (σ) for the middle level (6 inch) spray distance calculated during the Phase I analysis. The four patterns used track gaps (center to center distance between consecutive passes) of 0.5σ , 1σ , 2σ , and 3σ .

The response variables for this phase of testing included:

- corrosion resistance;

- abrasive wear resistance;
- Vickers microhardness; and
- porosity.

4.2.2 Experimental Procedure

For this test phase, three coupons were arranged, prepared, and sprayed for each spray test. All coupons were fabricated from AISI 4130 sheet steel that was 0.0625-inch thick. One abrasion coupon, one corrosion coupon, and one microstructural coupon were placed on a shadow mask fixture. Constant system operating parameters and allowable tolerances for the tests were set as follows:

- feedstock quantity: 120 g (+/- 1 g);
- nozzle design: TP2-HLM (S/N's BN07 and BN08);
- operating pressure: 48 psig (+/- .5 psig); and
- pressure differential: 0.5 psig (+/- .01 psig).

Four different spray patterns were used in this phase. The random run order is listed in Table 1.

Table 1. Phase II spray patterns.

| Random Order | Track Gap |
|--------------|------------|
| 1 | σ |
| 2 | $.5\sigma$ |
| 3 | 3σ |
| 4 | 2σ |
| 5 | σ |
| 6 | $.5\sigma$ |
| 7 | 3σ |
| 8 | 2σ |

4.3 PHASE III: CENTRAL COMPOSITE DESIGN

4.3.1 Experimental Description

A 22-run central composite design was used in this phase to investigate the effects of varying three system operating parameters, which were spray standoff distance, nozzle inlet pressure, and nozzle to tundish pressure differential. Five different levels of each of these parameters were investigated in this phase. Statistical analysis of the coatings indicated which operating parameter settings offered the

optimal coatings for superior corrosion protection, abrasive wear resistance, highest microhardness, and lowest porosity characteristics.

A central composite design was appropriate for this situation. With 10 degrees of freedom allocated to the quadratic equations and a maximum of 3 degrees of freedom allocated to covariates, a minimum of 8 degrees of freedom were available for the error estimate. Because the responses were presumed to exhibit nonlinear behavior with respect to the three parameters in question, a two-level factorial design would not have been adequate. A two-level factorial augmented with replications at the center point can detect the presence of curvature, but does not provide sufficient information for modelling purposes. A three-level factorial was a legitimate alternative, but was unnecessarily restrictive and required numerous runs. Since operating parameters can be controlled over a given range, the optimum level over the entire feasible range was sought after, rather than the best of three levels. Therefore, the central composite design which exploited this flexibility, provided more information than a standard factorial or fractional-factorial design.

The response variables for Phase III testing included:

- corrosion resistance;
- abrasive wear resistance;
- Vickers microhardness; and
- porosity.

The following procedure was followed after each of the 22 spray tests. When the chamber cooled, the coupons were removed. The abrasion coupons were tested at the Spray Casting Facility with the Taber 5130 abraser per Federal Test Method Std. No. 141C, Method 6192.1. The corrosion coupons were tested at the Spray Casting Facility with the salt fog corrosion chamber per ASTM B 117-90. The microstructure coupons were sent to Tubal Cain Company, Inc., for microhardness and porosity measurements.

With the aid of the statistical package SAS, the significance of the spray distance, operating pressure, and pressure differential were evaluated. Quadratic equations were obtained for each response, and contour plots were used to determine optimal parameter settings.

4.3.2 Experimental Procedure

For this test phase, three coupons fabricated from AISI 4130 sheet steel were arranged, prepared, and sprayed for each spray test. Spray system operating parameters and allowable tolerances for the tests were set as follows:

- feedstock quantity: 125 g, (+/- 1 g); and
- spray pattern: (1 σ) overlap/track gap.

Variable system operating parameters are listed in Table 2. Variable parameters are: spray distance; operating pressure; and pressure differential.

Table 2. Phase III variable system operating parameters.

| Random Order | Spray Distance Inches | Operating Pressure - psi | Differential Pressure - psi |
|--------------|--------------------------|-----------------------------|--------------------------------|
| 1 | 7.0 | 52.0 | 1.4 |
| 2 | 6.0 | 47.0 | 1.0 |
| 3 | 7.0 | 52.0 | 1.6 |
| 4 | 5.0 | 42.0 | 1.4 |
| 5 | 6.0 | 38.0 | 1.0 |
| 6 | 7.0 | 42.0 | 1.4 |
| 7 | 4.3 | 47.0 | 1.0 |
| 8 | 6.0 | 47.0 | 0.3 |
| 9 | 6.0 | 47.0 | 1.0 |
| 10 | 6.0 | 47.0 | 1.7 |
| 11 | 6.0 | 47.0 | 1.0 |
| 12 | 7.7 | 47.0 | 1.0 |
| 13 | 6.0 | 47.0 | 1.0 |
| 14 | 5.0 | 42.0 | 0.6 |
| 15 | 6.0 | 55.4 | 1.0 |
| 16 | 5.0 | 52.0 | 0.6 |
| 17 | 7.0 | 42.0 | 0.6 |
| 18 | 6.0 | 47.0 | 1.0 |
| 19 | 5.0 | 52.0 | 1.4 |
| 20 | 6.0 | 47.0 | 1.0 |
| 21 | 6.0 | 47.0 | 1.0 |
| 22 | 6.0 | 47.0 | 1.0 |

4.4 PHASE IV: VALIDATION TESTING

4.4.1 Experimental Description

The validation phase consisted of four spray tests. These tests verified that the operating parameters recommended from Phase III testing and analysis produced desired coating characteristics. The objective of validation testing was to predict coating characteristics based upon process operating parameters.

Process parameters were varied during this phase of testing to optimize wear and corrosion resistance for VERSAlloy 50 sprayed coatings on AISI 4130 steel sheet.

The response variables for Phase IV testing included:

- corrosion resistance;
- abrasive wear resistance;
- Vickers microhardness; and
- porosity.

The results of the Phase IV coating were compared with the predicted values derived from Phase III testing and analysis.

4.4.2 Experimental Procedure

For this test phase, three coupons fabricated from AISI 4130 sheet steel were arranged, prepared, and sprayed for each spray test. Spray system operating parameters and allowable tolerances for the tests were set as follows.

- feedstock quantity: 78 g (+/- 1 g);
- nozzle design: TP2-HLM (S/N's BN08 and BN09);
- operating pressure: 55 psig (+/- .5 psig); and
- spray distance: 5 inches (+/- .1 inch).

The only spray operating parameter varied was nozzle to tundish differential pressure. For maximum corrosion protection the pressure differential was set at 0.9 psig, and for maximum resistance to abrasive wear, the differential pressure was set at 1.60 psig.

5. RESULTS

5.1 PHASE I: PRELIMINARY TEST

5.1.1 Deposit Profiles

The sprayed deposit profile data sheets are in Appendix A, and plots of the data for the five different standoff distances are shown in Figures 12 through 16. The calculated standard deviation for each standoff distance is listed in Table 3.

Table 3. Phase I standard deviation for each standoff distance.

| Standoff Distance Inches | Standard Deviation σ - Inches |
|--------------------------|--------------------------------------|
| 4.3 | 0.16 |
| 5.0 | 0.18 |
| 6.0 | 0.22 |
| 7.0 | 0.25 |
| 7.7 | 0.28 |

The standard deviations were calculated using the following equation:

$$\sigma_y^2 = \sum (y_i - \mu)^2 * \left(\frac{z_i}{\sum z_i} \right)$$
$$\text{where } \mu = y_i * \left(\frac{z_i}{\sum z_i} \right)$$

and z_i is the height from the substrate surface to a point on the cross-sectioned profile; y_i is the corresponding position along the profile where z_i is measured.

5.2 PHASE II: COMPLETELY RANDOM DESIGN

5.2.1 ASTM B117 Salt Fog Corrosion Data

The Phase II corrosion coupons were tested in a salt fog corrosion chamber for 48 hours per ASTM B117-94, Standard Practice for Operating Salt Spray (Fog) Testing Apparatus. The 48-hour exposure was the same duration used in the Boeing Test Series and all phases of this test series, which allowed data from all tests to be compared. The salt fog corrosion testing system is shown in Figure 17.

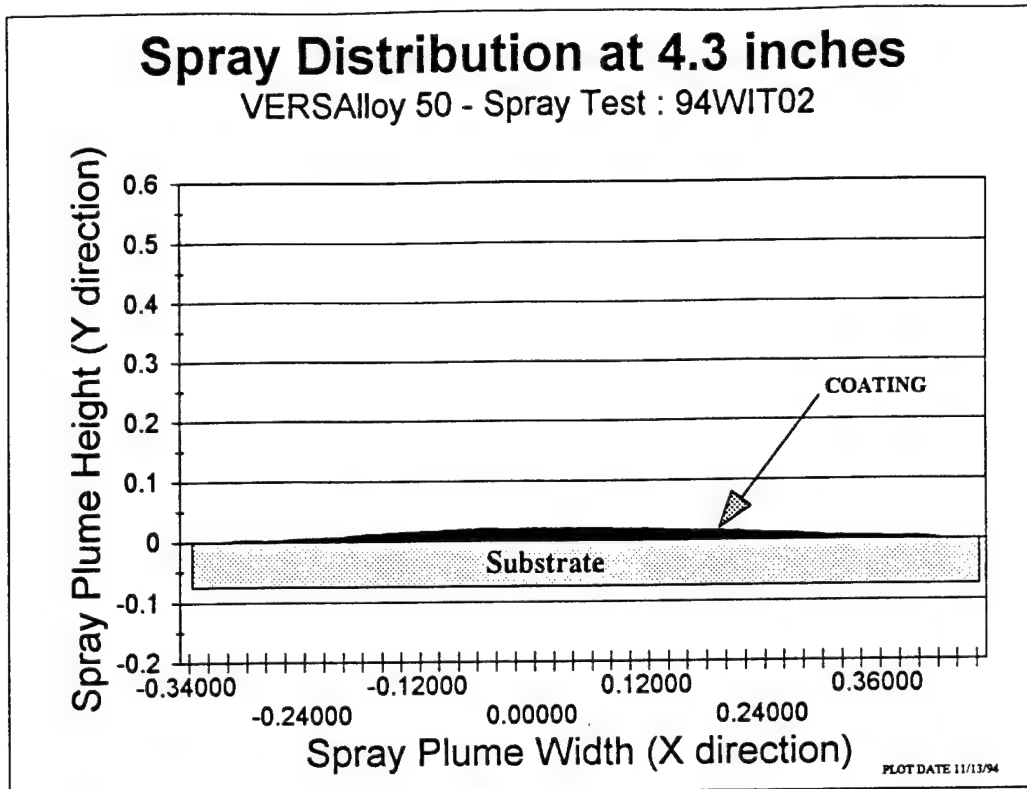


Figure 12. Plot of spray distribution at 4.3 inches.

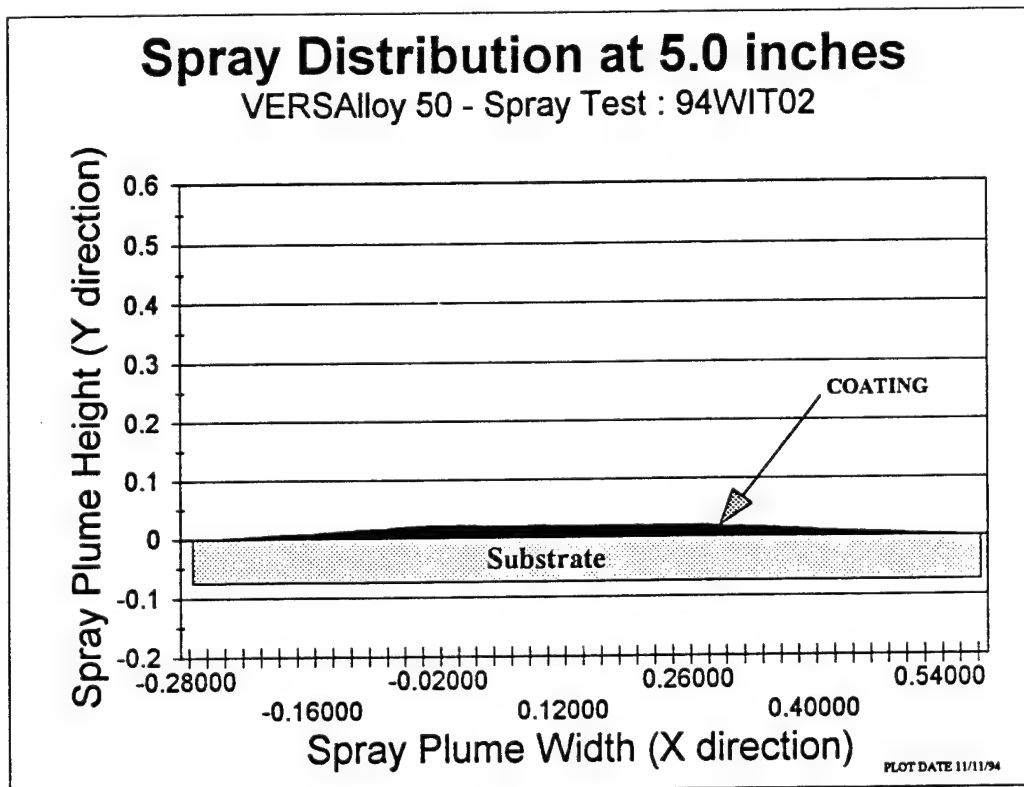


Figure 13. Plot of spray distribution at 5 inches.

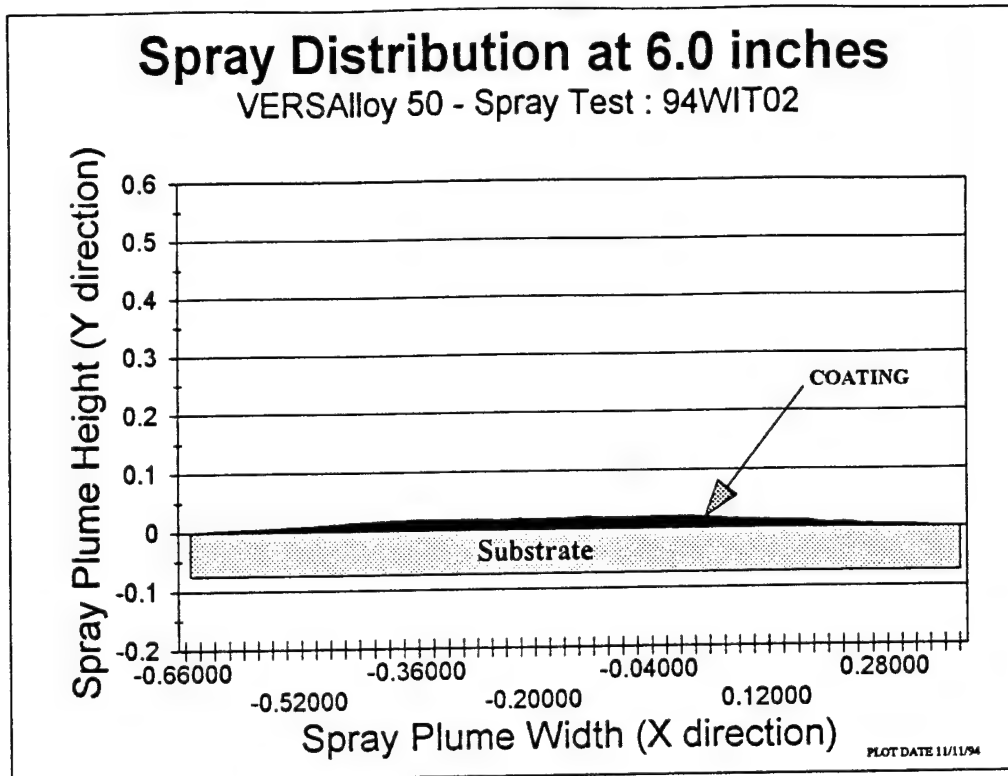


Figure 14. Plot of spray distribution at 6 inches.

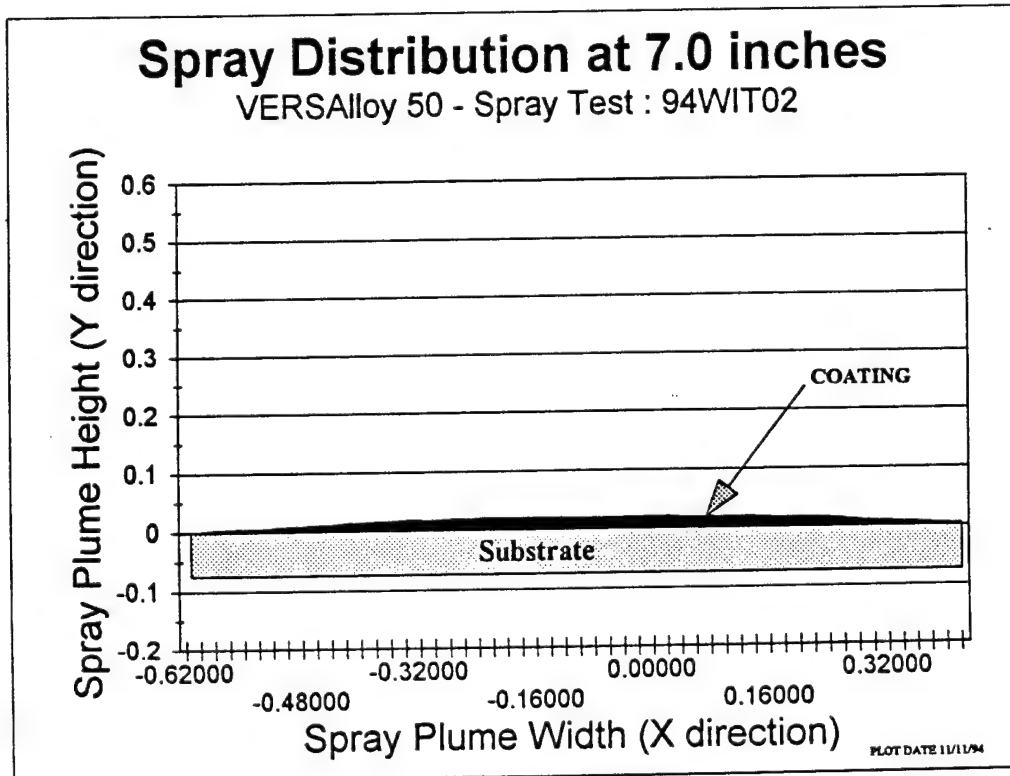


Figure 15. Plot of spray distribution at 7 inches.

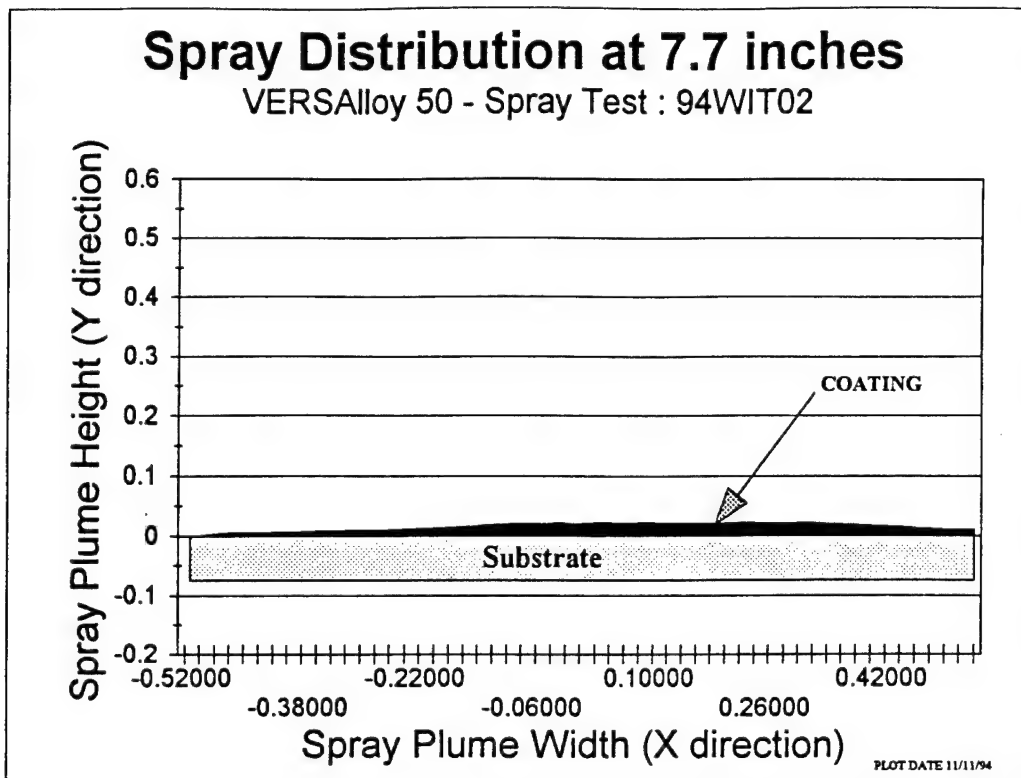


Figure 16. Plot of spray distribution at 7.7 inches.



Figure 17. Salt fog corrosion testing system.

Photographs of the exposed corrosion coupons are in Appendix B. Figure 18 shows the exposed Phase II coupons in the salt fog chamber. Table 4 lists the numerical corrosion protection rating assigned to the samples.

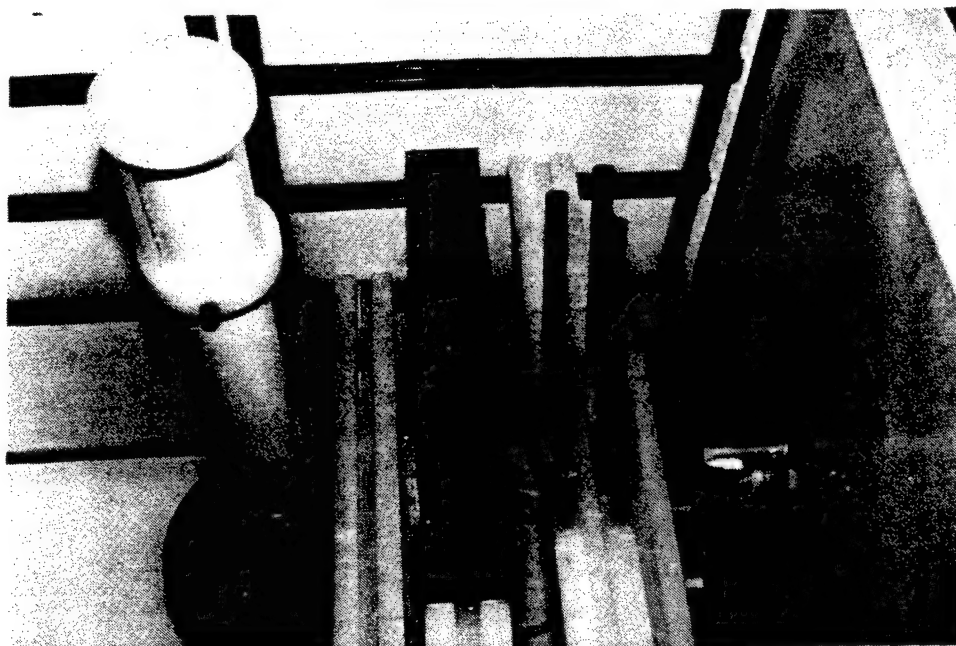


Figure 18. Phase II corrosion coupons in the salt fog chamber.

Table 4. Phase II corrosion protection rating assigned to samples.

| Spray Test Number | Corrosion Rating |
|-------------------|------------------|
| 95-WIT-007 | 1 |
| 95-WIT-008 | 5 |
| 95-WIT-009 | 1 |
| 95-WIT-010 | 4 |
| 95-WIT-011 | 5 |
| 95-WIT-012 | 5 |
| 95-WIT-013 | 1 |
| 95-WIT-014 | 4 |

5.2.2 Taber Abraser Wear Data

The sprayed abrasion coupons were tested with a Taber Model 5130 Abraser per Federal Test Method Std. No. 141C, Method 6192.1. The test duration was 10,000 revolutions with 1000 gram load and CS17 abrasive wheels. Because the surface roughness of the "as sprayed" coupons appeared to produce erroneous results, the abrasion coupons were first flat ground with a standard magnetic chuck flat grinding system, equipped with a 60 grit aluminum oxide grinding wheel. In addition to removing surface roughness, the flat grinding also produced a surface finish that was similar to that encountered on actual aviation parts that had been hard chromium plated and ground to a finished dimension. The summary for abrasion data is shown in Figure 19. Individual test results are in Appendix C.

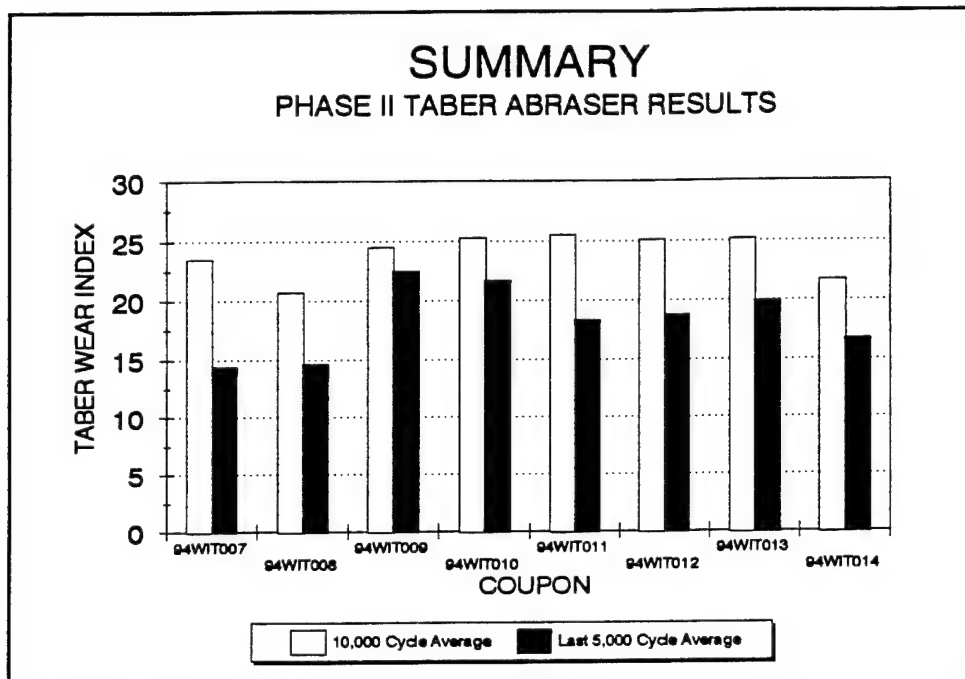


Figure 19. Phase II TABER abramer test results.

5.2.3 Vickers Microhardness and Percent Porosity Data

The microhardness and percent porosity data were collected from mounted and polished cross sections of the sprayed deposits. Photographs of these cross sections are in Appendix D. All cross sections were etched with a 33% nitric acid, 33% hydrofluoric acid, and 34% water etchant.

The average Vickers microhardness number (10 indentations with a 300 gram load), the average percent porosity (20 locations) of mounted and polished cross sections from the metallurgical coupon, and the standard deviation at which the deposits were sprayed are listed in Table 5. The percent porosity was measured with image analysis of the mounted and polished cross section.

Table 5. Phase II Vickers microhardness and percent porosity data.

| Spray Test Number | Standard Deviation | Vickers Microhardness (Average) | Percent Porosity (Average) |
|-------------------|--------------------|------------------------------------|-------------------------------|
| 95-WIT-007 | 1 | 611 | 4.48 |
| 95-WIT-008 | 0.5 | 580 | 2.30 |
| 95-WIT-009 | 3 | 619 | 2.65 |
| 95-WIT-010 | 2 | 635 | 2.73 |
| 95-WIT-011 | 1 | 640 | 2.34 |
| 95-WIT-012 | 0.5 | 690 | 2.12 |
| 95-WIT-013 | 3 | 614 | 3.93 |
| 95-WIT-014 | 2 | 618 | 2.03 |

5.2.4 Statistical Analysis

The data generated during Phase II and III testing was analyzed with a statistical software package called Statistical Analysis Software (SAS) System. SAS is a complex and versatile collection of programming packages that includes data management, analysis, and reporting tools. The power of SAS is that it is an integrated software package so that data handled in the data management component can be used without modification by the analysis and reporting software component. SAS operates on IBM-compatible PCs, minicomputers, or mainframes.

For Phase II testing, an eight-run, random experimental design studying four different spray patterns was selected to determine the effect of spray overlap on coating properties. The response variables analyzed were corrosion resistance, wear resistance, microhardness, and porosity. The analysis also examined the significance of two potential covariates: atmospheric pressure and nozzle deterioration. A covariate is a measurable variable, beyond the control of the experimenter that affects the response variables. Covariates must be accounted for in the model because their effects can overshadow the response of the operating control parameters (track gap or overlap in this case).

For this phase, data from seven of eight runs was analyzed using SAS software. Test 95WIT007 was not included in the analysis since the coating deposit was extremely coarse. Data from corrosion testing was coded on a scale from 1 to 5, with 1 being the worst and 5 being the best.

The statistical analysis for this design was performed as follows: 1) models for corrosion, wear-1 (10,000 cycles), wear-2 (last 5,000 cycles), microhardness, and porosity were fitted using covariates as the only explanatory variables for the responses; 2) using step-wise regression, terms with high p-values (>0.1) were eliminated from the model; 3) after adjusting for covariate effects, the track gap or overlap (σ) parameter was introduced and fitted to each model; and 4) as in step 2, terms in each model were again eliminated using step-wise regression.

Results of the statistical analysis indicate that track gap (σ) was highly significant ($p = 0.0001$) in the corrosion model, moderately significant ($p = 0.05$) in the porosity model, and not significant ($p > 0.10$) in the wear-1, wear-2, and microhardness models. For the covariates: run order (nozzle deterioration) was moderately significant for porosity and wear-1 models; and, atmospheric pressure was moderately significant as an explanatory variable for microhardness.

The fitted models for corrosion and porosity, respectively, are shown below:

$$y_{\text{cor}} = 1.605 - 1.616 (\text{gap}) + 0.914 (\text{gap})^2; \text{ and}$$

$$y_{\text{por}} = 1.129 + 0.138 (\text{ord}) + 0.390 (\text{gap})$$

where:

y_{cor} = response of corrosion (1 = worst and 5 = best);

y_{por} = response of porosity (percent of theoretical density);

gap = track gap (0.5σ , 1σ , etc.); and

ord = nozzle deterioration (number of times nozzle has sprayed).

Increasing the track gap caused higher porosity and reduced corrosion protection; and, the number of spray tests on a nozzle increased the coating deposit porosity. Based on the above models, a track gap of 1σ was selected for Phase III testing.

5.3 PHASE III: CENTRAL COMPOSITE DESIGN

5.3.1 ASTM B117 Salt Fog Corrosion Data

The Phase III corrosion coupons were tested in a salt fog corrosion chamber for 48 hours per ASTM B117-94, Standard Practice for Operating Salt Spray (Fog) Testing Apparatus. The 48-hour exposure was the same duration used in the Boeing Test Series and all phases of this test series, which allowed data from all the qualification tests to be compared.

Photographs of the exposed corrosion coupons are in Appendix E. Figure 20 shows the exposed coupons in the salt fog chamber. Table 6 lists the numerical corrosion protection rating assigned to the samples.

5.3.2 Taber Abraser Wear Data

The sprayed abrasion coupons were tested with a Taber Model 5130 Abraser per Federal Test Method Std. No. 141C, Method 6192.1. The test duration was 10,000 revolutions with 1000 gram load and CS17 abrasive wheels. As with Phase II specimens, the abrasion coupons were first flat ground with a standard magnetic chuck flat grinding system, equipped with a 60 grit aluminum oxide grinding wheel. In addition to removing surface roughness, the flat grinding also produced a surface finish that was similar to that encountered on actual aviation parts that had been hard chromium plated and ground to a finished dimension. The summary on abrasion data is shown in Figure 21. Individual test results are in Appendix F.

Table 6. Phase III corrosion protection rating assigned to samples.

| Spray Test Number | Corrosion Rating |
|-------------------|------------------|
| 95-WIT-020 | 4 |
| 95-WIT-021 | 6 |
| 95-WIT-022 | 8 |
| 95-WIT-023 | 7 |
| 95-WIT-024 | 2 |
| 95-WIT-025 | 1 |
| 95-WIT-026 | 8 |
| 95-WIT-027 | 9 |
| 95-WIT-028 | 5 |
| 95-WIT-029 | 2 |
| 95-WIT-030 | 3 |
| 95-WIT-031 | 8 |
| 95-WIT-032 | 8 |
| 95-WIT-033 | 7 |
| 95-WIT-034 | 8 |
| 95-WIT-035 | 10 |
| 95-WIT-036 | 7 |
| 95-WIT-037 | 9 |
| 95-WIT-038 | 6 |
| 95-WIT-039 | 10 |
| 95-WIT-040 | 10 |
| 95-WIT-041 | * |

*coating peeled during corrosion testing

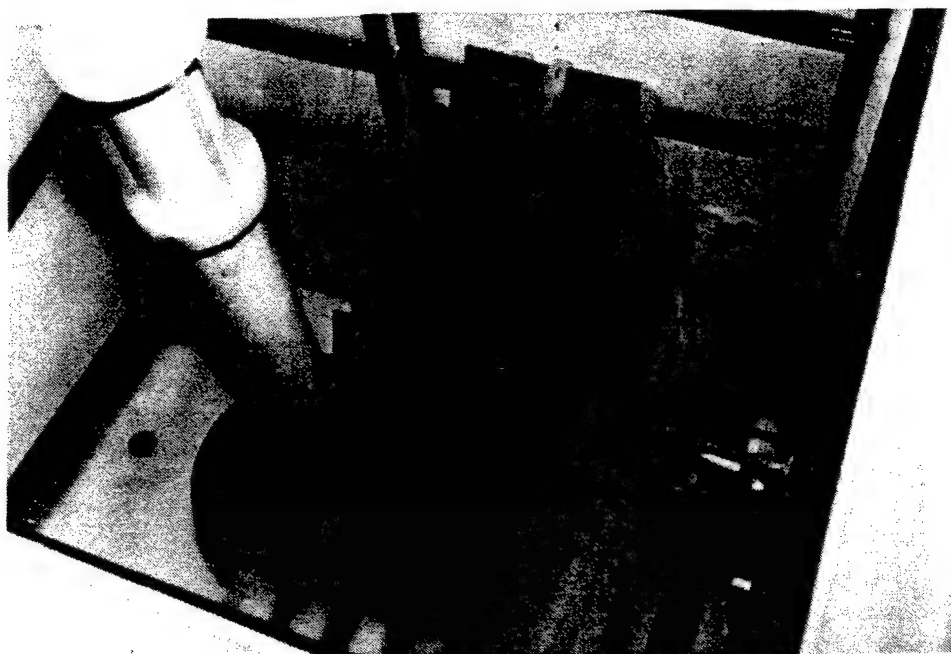


Figure 20. Phase III corrosion coupons in the salt fog chamber.

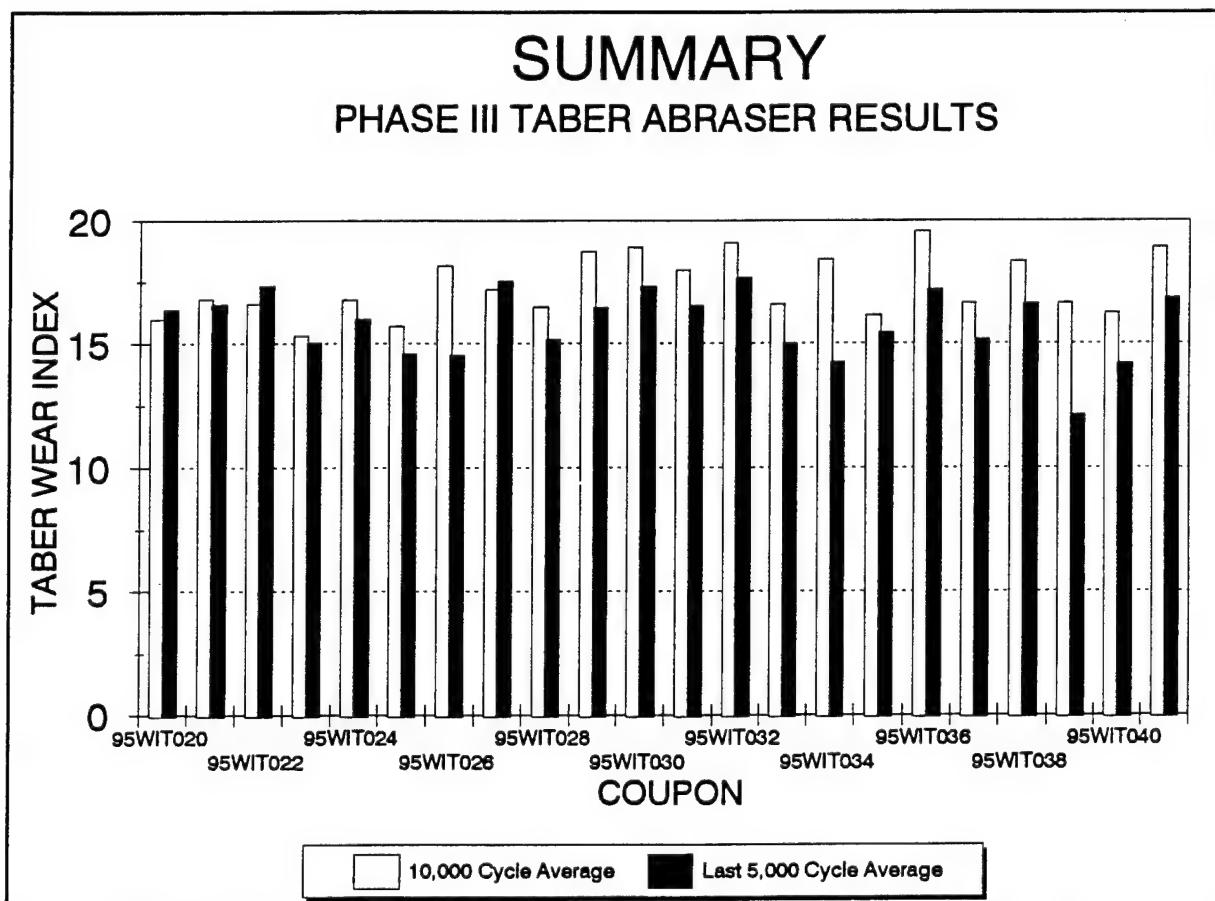


Figure 21. Phase III TABER abraser test results.

5.3.3 Vickers Microhardness and Percent Porosity Data

The microhardness and percent porosity data were collected from mounted and polished cross sections of the sprayed deposits. Photographs of these cross sections are in Appendix G. All cross sections were etched with a 33% nitric acid, 33% hydrofluoric acid, and 34% water etchant.

The average Vickers microhardness number (10 indentations with a 300 gram load), the average percent porosity (20 locations) of mounted and polished cross sections from the metallurgical coupon, the standoff distance, inlet to the nozzle pressure, and the nozzle to tundish pressure differential at which the deposits were sprayed are shown in Table 7. The percent porosity was measured with image analysis of the mounted and polished cross section.

5.3.4 Statistical Analysis

For Phase III testing, a 22-run, central composite design studying three operating parameters (spray distance, nozzle inlet pressure, and nozzle tundish differential pressure) was selected to determine the effects on coating deposit characteristics for corrosion protection, wear resistance, microhardness, and porosity. The analysis also examined the effects of the following covariates:

- feedstock (batch to batch differences);
- thickness of coating;
- atmospheric pressure;
- order (number of spray tests on nozzle);
- (order)² (quadratic effect of the number of spray tests on nozzle).

The spray nozzle was also tested as a blocking variable and was found to be insignificant.

As with Phase II testing, SAS software was used to analyze the results of Phase III testing. Data from corrosion testing was coded on a scale from 1 to 10, with 1 being the worst and 10 being the best. Response surface techniques were utilized to model and analyze data to determine the optimum operating conditions for the range of variables tested. The following second-order model was used to approximate the response surface:

$$y = \beta_0 + \sum_{i=1}^k \beta_i x_i + \sum_{i=1}^k \beta_{ii} x_i^2 + \sum_{\substack{i=1 \\ i < j}}^k \sum_{j=1}^k \beta_{ij} x_i x_j + \epsilon$$

where:

y = response variable (corrosion, wear, microhardness, or porosity);

β = coefficients - estimated by method of least squares with SAS;

x = operating parameter or covariate (inlet pressure, spray distance, or nozzle tundish differential pressure, etc.); and

ϵ = error.

Table 7. Phase III Vickers microhardness and percent porosity data.

| Spray Test Number | Vickers Microhardness (Average) | Percent Porosity | Standoff Distance Inches | Inlet Pressure PSI | Differential Pressure PSI |
|--------------------------|--|-------------------------|---------------------------------|---------------------------|----------------------------------|
| 95-WIT-020 | 519 | 3.46 | 6.0 | 47.0 | 1.00 |
| 95-WIT-021 | 484 | 3.19 | 7.0 | 52.0 | 0.60 |
| 95-WIT-022 | 539 | 3.56 | 6.0 | 47.0 | 1.00 |
| 95-WIT-023 | 593 | 4.05 | 6.0 | 47.0 | 1.00 |
| 95-WIT-024 | 608 | 7.66 | 5.0 | 42.0 | 0.60 |
| 95-WIT-025 | 607 | 2.47 | 5.0 | 42.0 | 1.40 |
| 95-WIT-026 | 587 | 2.58 | 6.0 | 47.0 | 0.33 |
| 95-WIT-027 | 550 | 2.11 | 6.0 | 55.4 | 1.00 |
| 95-WIT-028 | 503 | 6.43 | 7.0 | 52.0 | 1.40 |
| 95-WIT-029 | 561 | 6.22 | 7.0 | 42.0 | 0.60 |
| 95-WIT-030 | 500 | 3.87 | 7.7 | 47.0 | 1.00 |
| 95-WIT-031 | 537 | 2.42 | 6.0 | 47.0 | 1.00 |
| 95-WIT-032 | 559 | 2.73 | 6.0 | 38.6 | 1.00 |
| 95-WIT-033 | 522 | 2.52 | 6.0 | 47.0 | 1.00 |
| 95-WIT-034 | 633 | 2.83 | 6.0 | 47.0 | 1.00 |
| 95-WIT-035 | 577 | 2.92 | 4.3 | 47.0 | 1.00 |
| 95-WIT-036 | 595 | 2.72 | 6.0 | 47.0 | 1.00 |
| 95-WIT-037 | 523 | 2.73 | 6.0 | 47.0 | 1.00 |
| 95-WIT-038 | 593 | 6.09 | 7.0 | 42.0 | 1.40 |
| 95-WIT-039 | 574 | 5.17 | 5.0 | 52.0 | 1.40 |
| 95-WIT-040 | 609 | 4.10 | 5.0 | 52.0 | 0.60 |
| 95-WIT-041 | 580 | 5.65 | 6.0 | 47.0 | 1.67 |

The statistical analysis was performed as follows: 1) models for corrosion, wear-1 (10,000 cycles), wear-2 (last 5,000 cycles), microhardness, and porosity were fitted using covariates as the only explanatory variables for the responses; 2) using step-wise regression, terms with high p-values (>0.1) were eliminated from the model; 3) after adjusting for covariate effects, nozzle inlet pressure, nozzle tundish differential pressure, and spray distance were introduced and fitted to the model; and 4) as in step 2, terms in each model were again eliminated using step-wise regression.

Residual and normal probability plots were then created to check the adequacy of each model to ensure the assumptions of the model were met. The residuals versus the predicted variable (wear, corrosion, microhardness, or porosity coating characteristic) were plotted to determine if there was a dependency between the residuals and one or more of the other variables. If the model is adequate, the residual plots should be structureless, that is, they should contain no obvious patterns—the data should be scattered. However, residual plots without apparent dependency does not prove by itself the adequacy of the model. Therefore; normal probability plots of the residuals were also created to check that the assumptions of the analysis are satisfied. If the points on this plot lie reasonably close to a straight line, the significant effects are accounted for in the model. Residual and corresponding normal probability plots for Phase III models are given in Figures 22 through 31.

Predicted response and standard error contour plots for each of the models are in Appendix H. For each predicted response contour plot, one operating parameter and one covariate parameter are held constant. The response surface was then generated for the remaining two operating parameters. The error for each model was tested and found to be normally and randomly distributed.

Referring to Figure 32, if the desired wear resistance of a coating is a Taber Wear Index (TWI) of 14, operating parameters for inlet pressure and nozzle tundish differential pressure can be selected from the response curve marked with a 14. However, the standard error of the model must also be accounted for in selecting the operating parameters. By overlaying the predicted response and standard error contour plots, the tolerance of the predicted response can be estimated. Referring to Figure 32, the operating parameters that produce the smallest or acceptable error tolerance are selected. The total estimate of error is approximately 2.2 times the value given on the standard error contour plot. For example, the curve for a TWI of 14 intersects a standard error curve of 0.4 at an inlet pressure of 51 psi and a differential pressure of 1.28 psi. The predicted wear is then 14 [$\pm 2.2 \times 0.4 = (0.88)$]. Therefore, we are 95% confident that the coating will have a TWI between 13.12 and 14.88. The contour plots allow responses to be predicted for corrosion and wear resistance, microhardness, and porosity.

5.4 PHASE IV: VALIDATION TESTING

5.4.1 ASTM B117 Salt Fog Corrosion Data

The Phase II corrosion coupons were tested in a salt fog corrosion chamber for 48 hours per ASTM B117-94, Standard Practice for Operating Salt Spray (Fog) Testing Apparatus. The 48-hour exposure was the same duration used in the Boeing Test Series and all phases of this test series, which allowed data from all the qualification tests to be compared.

Photographs of the exposed corrosion coupons are in Appendix I. Figure 33 shows the exposed coupons in the salt fog chamber. Table 8 lists the numerical corrosion protection rating assigned to the samples.

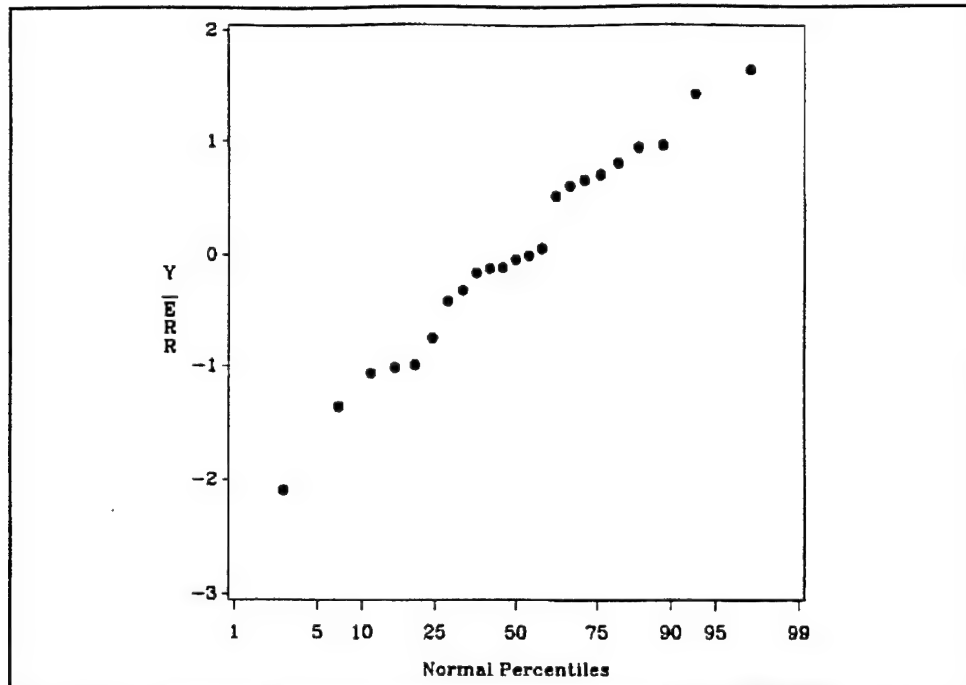


Figure 22. Normal probability plot for the porosity model.

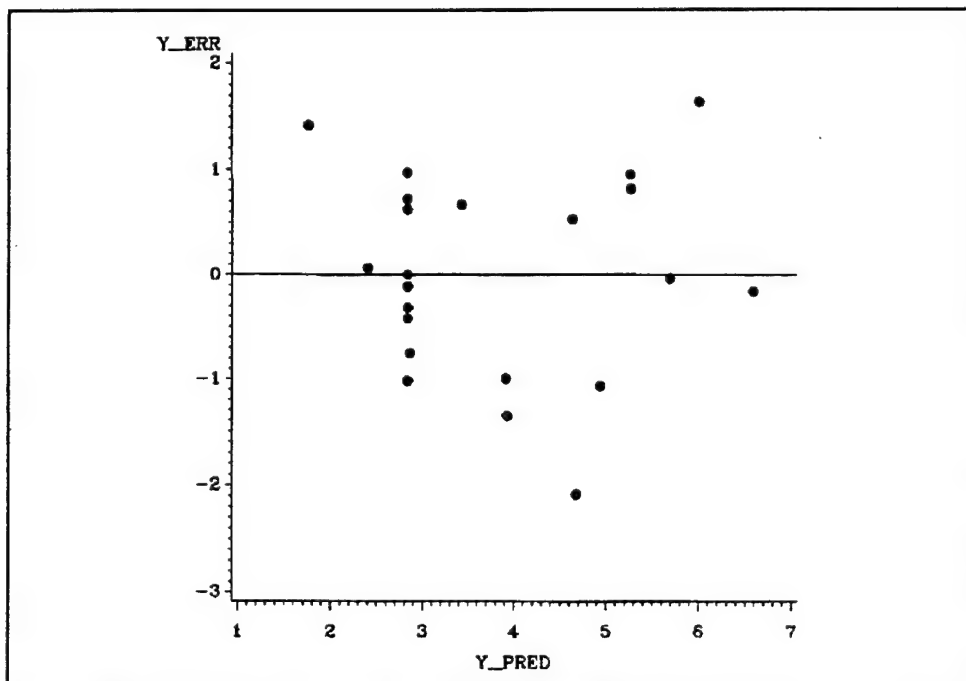


Figure 23. Residual plot for the porosity model.

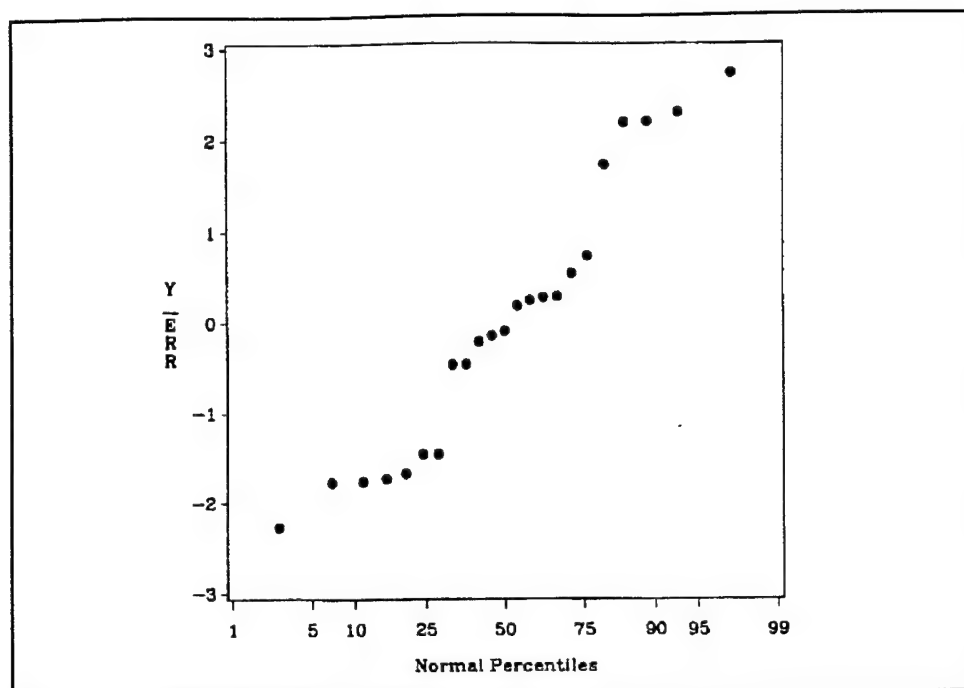


Figure 24. Normal probability plot for the corrosion model.

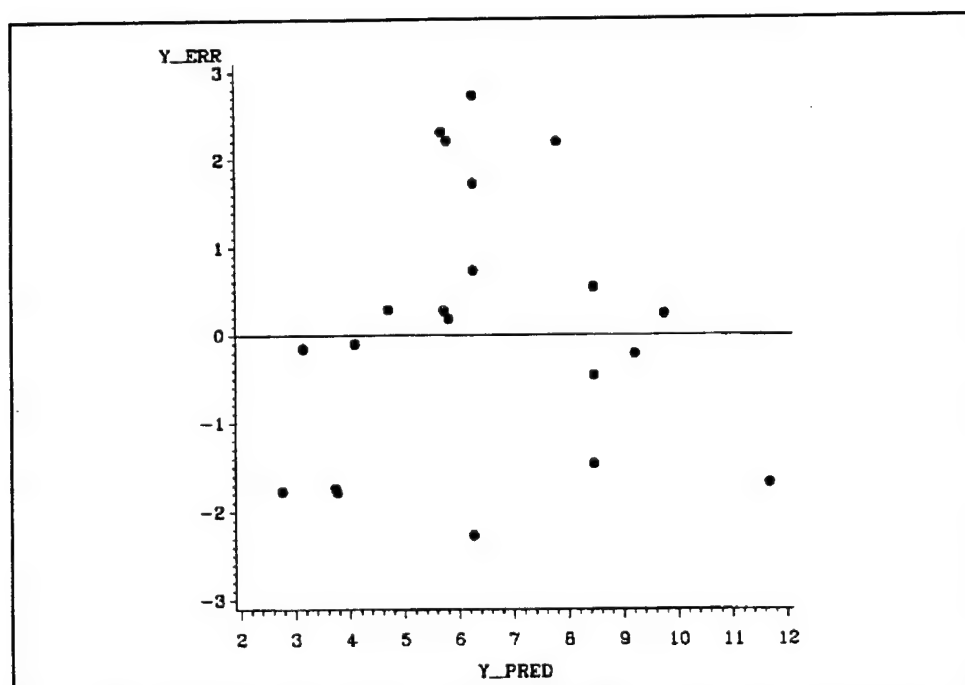


Figure 25. Residual plot for the corrosion model.

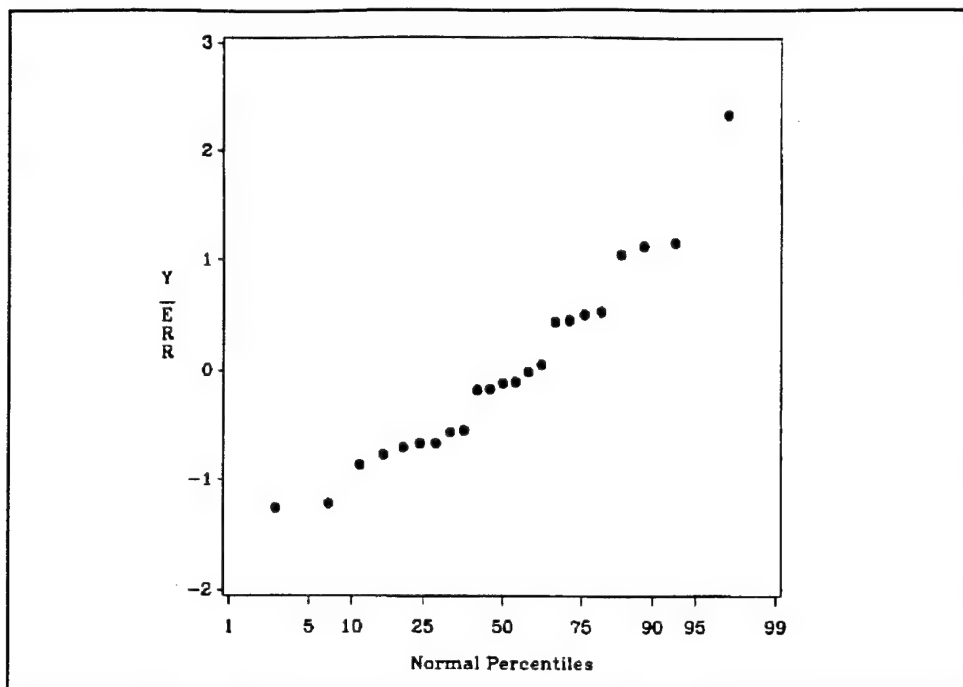


Figure 26. Normal probability plot for the wear-1 model.

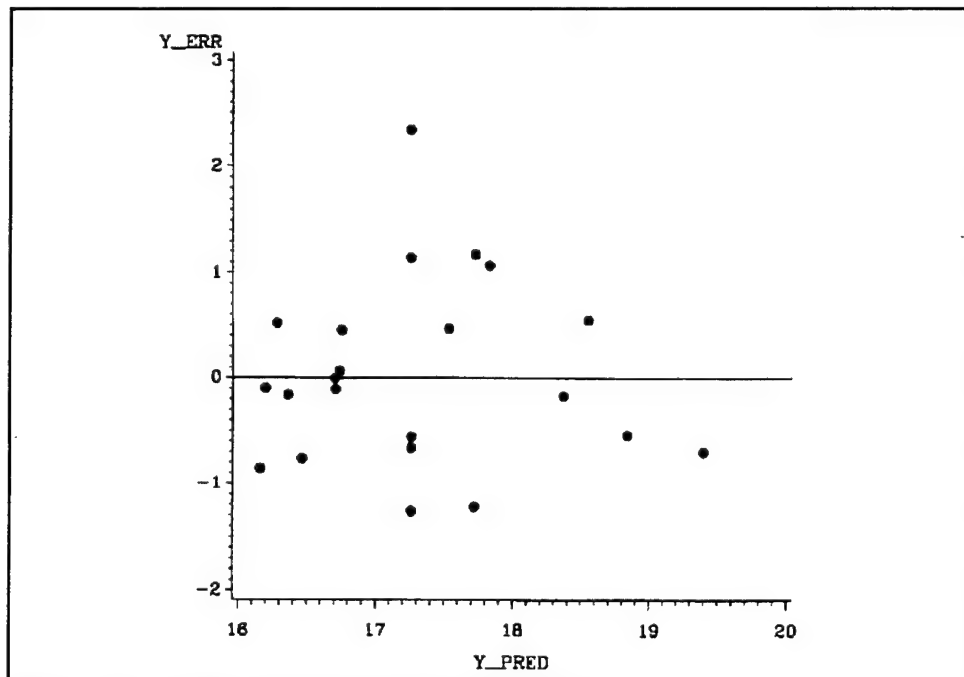


Figure 27. Residual plot for the wear-1 model.

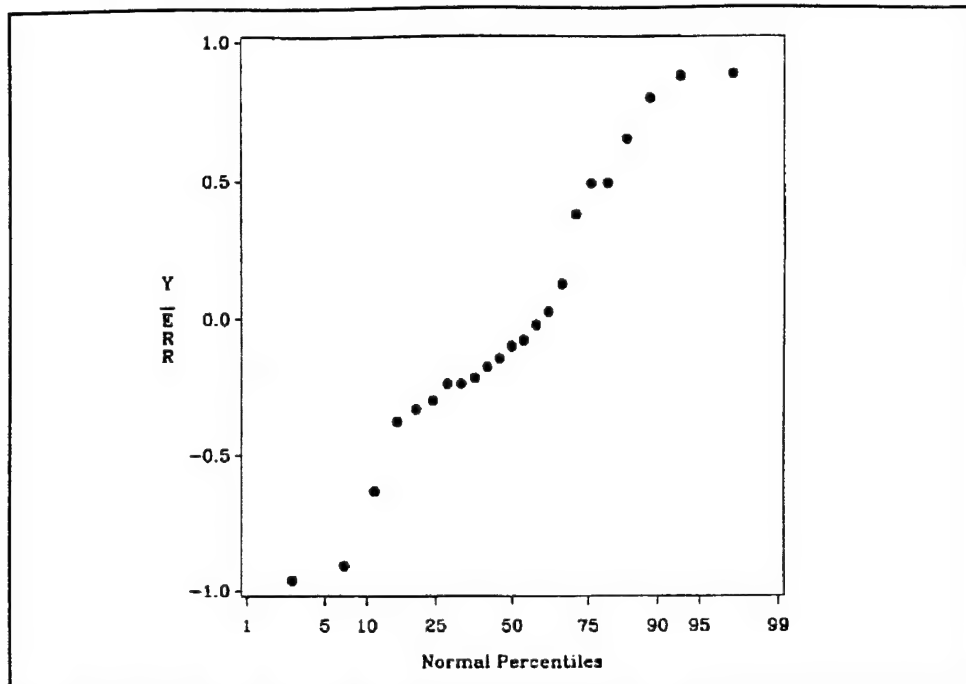


Figure 28. Normal probability plot for the wear-2 model.

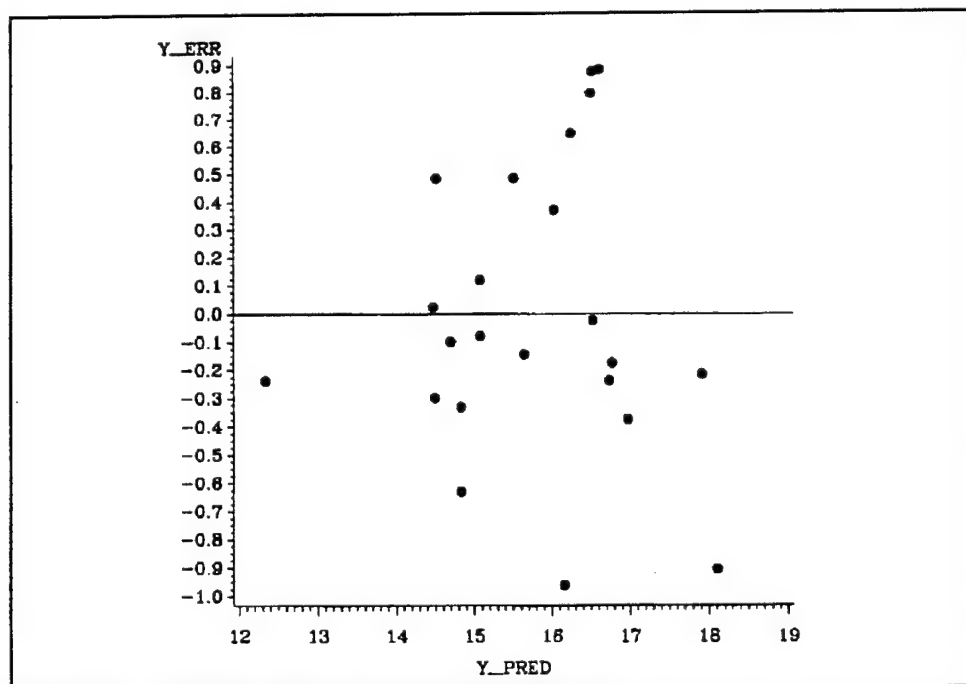


Figure 29. Residual plot for the wear-2 model.

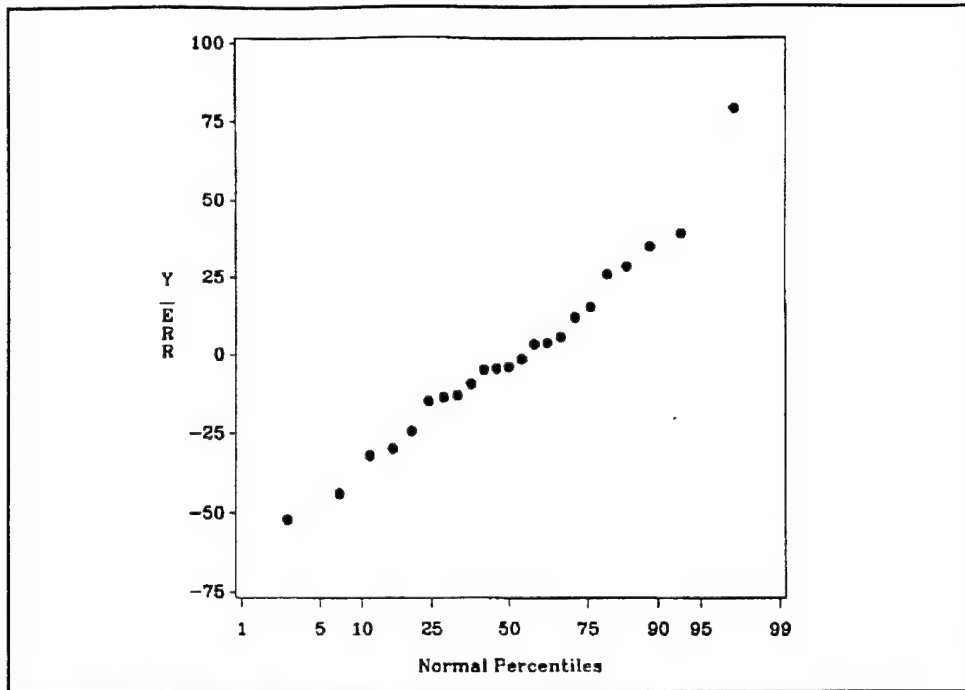


Figure 30. Normal probability plot for the microhardness model.

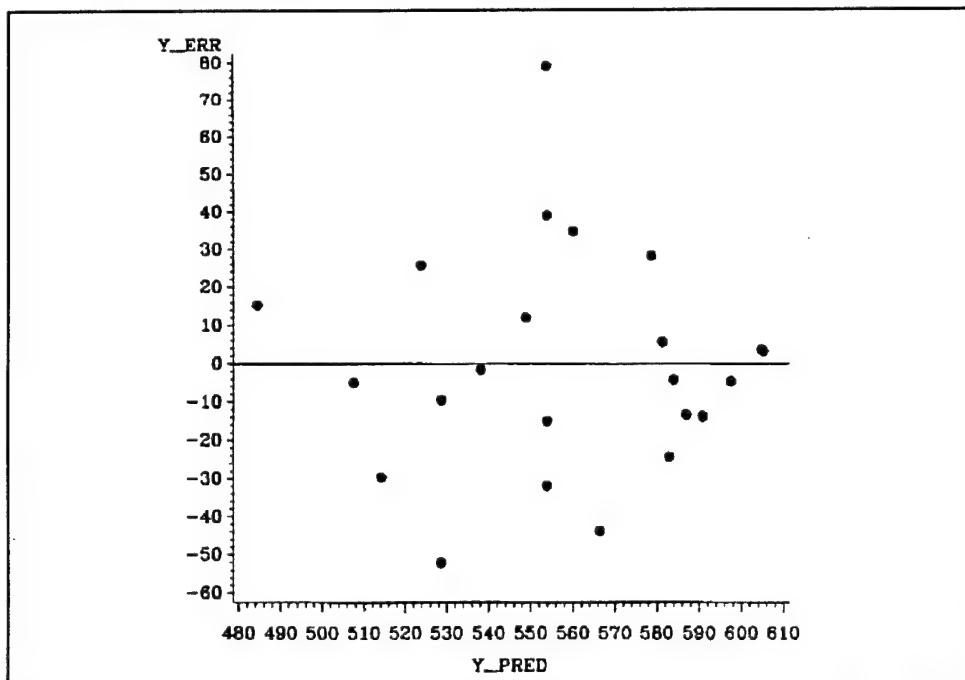


Figure 31. Residual plot for the microhardness model.

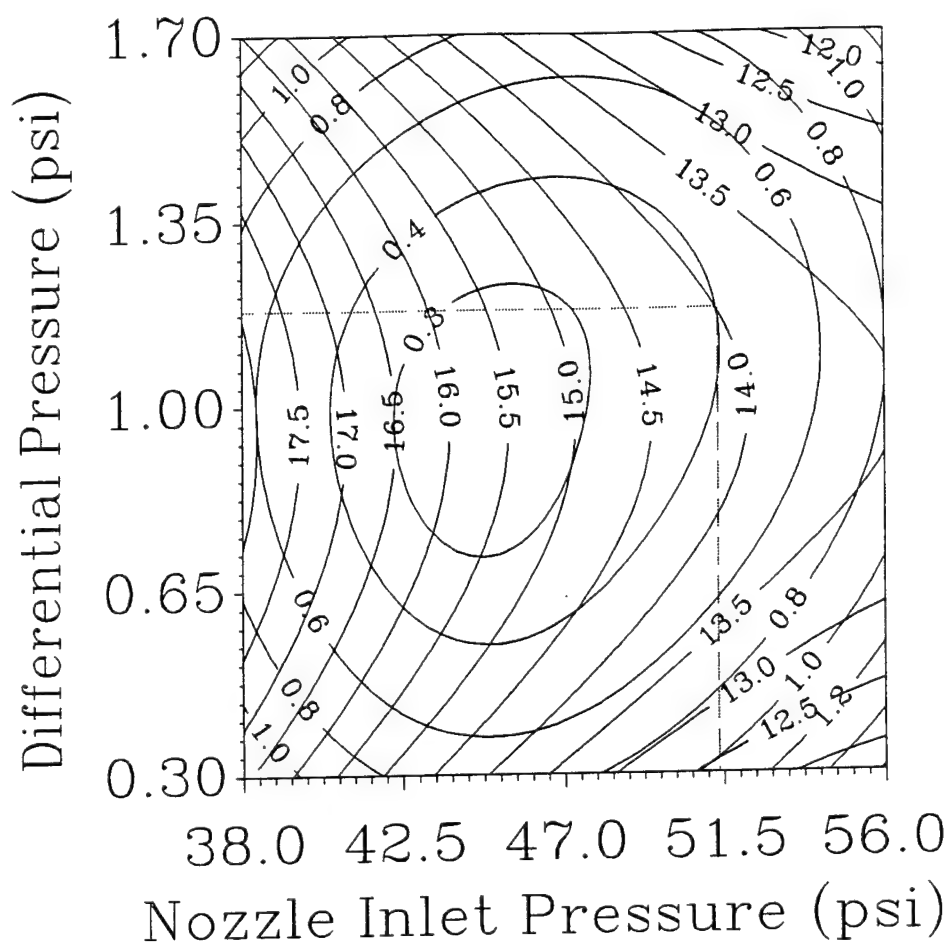


Figure 32. Contour plot of predicted response for Taber wear index wear-2 model with contour plot of predicted standard error overlaid.

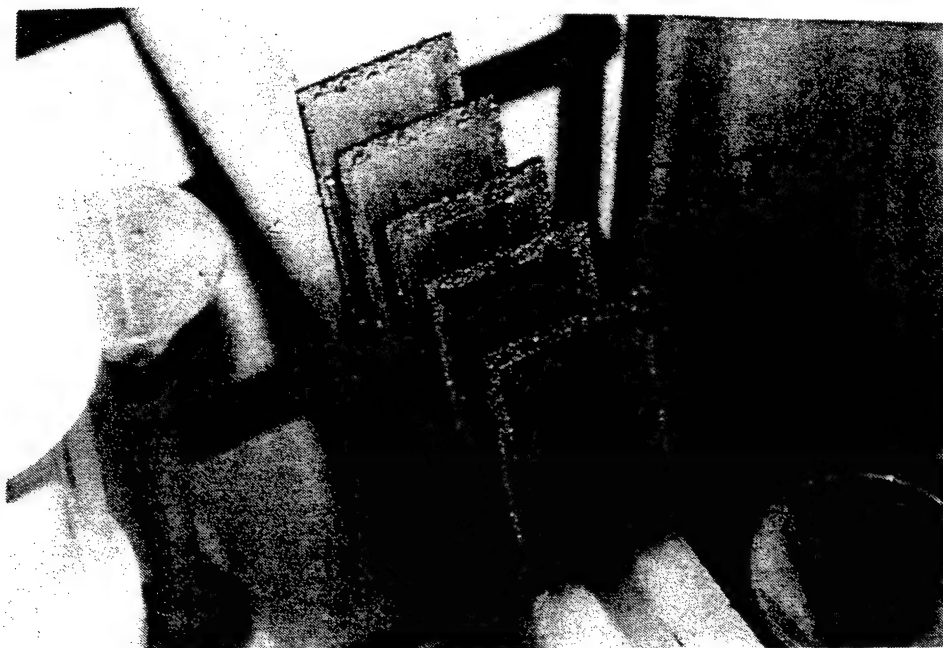


Figure 33. Phase IV corrosion coupons in salt fog chamber.

Table 8. Phase IV corrosion protection rating assigned to samples.

| Spray Test Number | Corrosion Rating |
|-------------------|------------------|
| 95-WIT-042 | 10 |
| 95-WIT-044 | 10 |
| 95-WIT-045 | 10 |
| 95-WIT-046 | 10 |

5.4.2 Taber Abraser Wear Data

The sprayed abrasion coupons were tested with a Taber Model 5130 Abraser per Federal Test Method Std. No. 141C, Method 6192.1. The test duration was 10,000 revolutions with 1000 gram load and CS17 abrasive wheels. As with Phase II and II specimens, the abrasion coupons were first flat ground with a standard magnetic chuck flat grinding system, equipped with a 60 grit aluminum oxide grinding wheel. In addition to removing surface roughness, the flat grinding also produced a surface finish that was similar to that encountered on actual aviation parts that had been hard chromium plated and ground to a finished dimension. The summary for abrasion data is shown in Figure 34. Individual test results are in Appendix J.

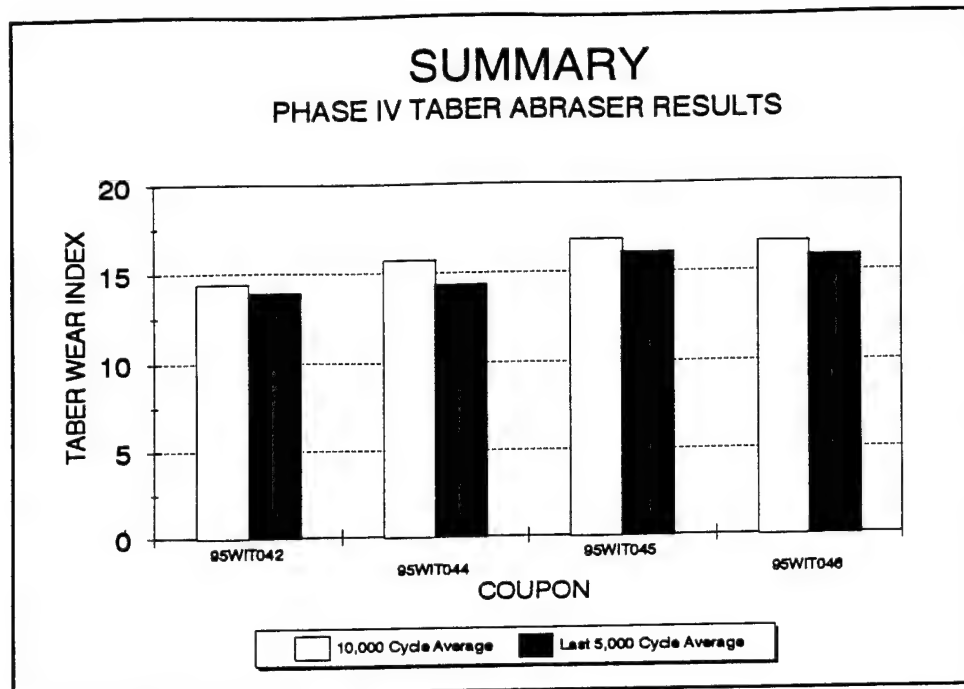


Figure 34. Phase IV Taber abraser results.

5.4.3 Vickers Microhardness and Percent Porosity Data

The microhardness and percent porosity data were collected from mounted and polished cross sections of the sprayed deposits. Photographs of these cross sections are in Appendix K. All cross sections were etched with a 33% nitric acid, 33% hydrofluoric acid, and 34% water etchant.

The average Vickers microhardness number (10 indentations with a 300 gram load) and the average percent porosity (20 locations) of mounted and polished cross sections from the metallurgical coupon are shown in Table 9. The percent porosity was measured with image analysis of the mounted and polished cross section.

Table 9. Phase IV Vickers microhardness and percent porosity data.

| Spray Test Number | Vickers Microhardness | Percent Porosity |
|-------------------|-----------------------|------------------|
| 95-WIT-042 | 633 | 0.53 |
| 95-WIT-044 | 699 | 1.11 |
| 95-WIT-045 | 622 | 0.61 |
| 95-WIT-046 | 653 | 0.91 |

5.4.4 Statistical Analysis

Phase IV testing consisted of a total of four tests. Two tests were run with predicted operating parameter settings for improved corrosion resistance; and two tests were run with predicted operating parameter settings for improved wear resistance (last 5,000 cycles). For each test, coupons for corrosion, wear, and metallurgical testing were sprayed with the PCAP.

Operating parameters selected from the corrosion model were predicted to give a corrosion resistance of 13 ± 4.4 . Results from the corrosion testing show that both coupons optimized for corrosion scored coded values of 10, and that both coupons optimized for wear scored coded values of 10. Therefore, the predicted response for corrosion resistance was reasonably estimated by the corrosion model.

Operating parameters selected from the wear-1 model were predicted to give a wear resistance of 15.25 ± 5.5 . Results from the Taber abraser testing shows that coupons optimized for wear scored a Taber Wear Index of 14.4 and 15.7.; and, that coupons optimized for corrosion resistance scored a Taber Wear Index of 16.8 and 16.6. Therefore, the predicted response for wear resistance appears to be reasonably estimated by the wear-1 (10,000 cycles) model.

6. CONCLUSIONS

6.1 PHASE I: PRELIMINARY TEST

The purpose of the Preliminary Test was to obtain statistical data (standard deviations) on PCAP sprayed deposits that were sprayed at different standoff distances. After several unsuccessful attempts to use computer image analysis to measure cross-sectional heights of the sprayed deposits, a standard toolmakers microscope was used to make direct measurements on the mounted and polished cross sections. The standard deviations were directly incorporated into Phase II testing.

6.2 PHASE II: COMPLETELY RANDOM DESIGN

The purpose of the Completely Random Design testing was to determine the best overlapping condition for successive spray layers. The degree of overlapping was based on the standard deviation width measurements that were calculated in Phase I. Analysis of all the data generated indicated that the 1.0σ overlapping was the optimal condition for maximizing coating corrosion protection and abrasive wear resistance.

6.3 PHASE III: CENTRAL COMPOSITE DESIGN

The purpose of the Central Composite Design was to incorporate the best overlapping condition determined (Phase II testing) into a test design that evaluated the three process control parameters that influenced the coating properties. The basis for selecting these parameters was obtained from experimental designs conducted during the MSE Test Series and from empirical testing during the Boeing and Wright Laboratory Test Series.

The three control parameters chosen were nozzle inlet pressure, nozzle to tundish differential pressure, and standoff distance. The nozzle inlet pressure has a direct effect upon atomization efficiency, particle size, and particle velocity. The nozzle to tundish differential pressure controls the amount of liquid metal that is injected into the throat of the nozzle through an 0.011 inch diameter orifice, and directly influences atomized particle size and velocity. The standoff distance has a direct effect upon the velocity and temperature of liquid particles at impact with the substrate, and the width of the spray plume.

This testing indicated one set operating conditions to maximize resistance to corrosion were a 55 psig nozzle inlet pressure, a 0.90 psig nozzle to tundish differential pressure, and a 5-inch standoff distance. The testing also indicated that one possible set of operating conditions that maximize abrasive wear resistance were a nozzle inlet pressure of 55 psig, a nozzle to tundish differential pressure of 1.60 psig, and a 5-inch standoff distance.

6.4 PHASE IV: VALIDATION TESTING

The purpose of the Validation Testing was to independently test the model developed from the results of Phase III testing. The results from the abrasion and corrosion testing indicate that the work and predictions from the previous three phases were successful in determining that VERSAlloy 50 coating properties can be controlled via the manipulation of PCAP operating parameters. When system

operating parameters were set to produce coatings that maximized corrosion protection or abrasion resistance, the actual sprayed coatings exhibited those characteristics. The ability to predict coating properties from manipulation of operating parameters is fundamental to the successful introduction of PCAP into an industrial setting as a production tool.

7. RECOMMENDATIONS

It is recommended that the next step in developing PCAP as a replacement for hard chromium coatings on aviation hardware be the design and fabrication of a production demonstration system that would be located in an USAF Air Logistic Center or another location that could serve the needs of all branches of the Department of Defense.

Improvements in the adhesion/cohesion strength of PCAP coatings would be a positive benefit in the acceptance of PCAP by production facility personnel. It is recommended that future test series focus upon improving adhesion/cohesion strengths of PCAP coatings.

APPENDIX A

Spray Deposit Profile Data Sheets

WIT TEST SERIES DATA SHEET - PHASE I

SAMPLE: 94WIT02

DATE: 10/24/94

SPRAY DIST: 4.3 inches

| X | Y |
|----------|---------|
| -0.34000 | 0.00000 |
| -0.32075 | 0.00000 |
| -0.32000 | 0.00080 |
| -0.30000 | 0.00250 |
| -0.28000 | 0.00180 |
| -0.26000 | 0.00310 |
| -0.24000 | 0.00525 |
| -0.22000 | 0.00610 |
| -0.20000 | 0.00835 |
| -0.18000 | 0.01105 |
| -0.16000 | 0.01335 |
| -0.14000 | 0.01535 |
| -0.12000 | 0.01675 |
| -0.10000 | 0.01810 |
| -0.08000 | 0.02000 |
| -0.06000 | 0.02060 |
| -0.04000 | 0.02100 |
| -0.02000 | 0.02005 |
| 0.00000 | 0.02185 |
| 0.02000 | 0.02055 |
| 0.04000 | 0.02125 |
| 0.06000 | 0.02030 |
| 0.08000 | 0.02050 |
| 0.10000 | 0.01930 |
| 0.12000 | 0.01900 |
| 0.14000 | 0.01795 |
| 0.16000 | 0.01710 |
| 0.18000 | 0.01615 |
| 0.20000 | 0.01615 |
| 0.22000 | 0.01425 |
| 0.24000 | 0.01225 |
| 0.26000 | 0.01190 |
| 0.28000 | 0.00970 |
| 0.30000 | 0.00820 |
| 0.32000 | 0.00705 |
| 0.34000 | 0.00530 |
| 0.36000 | 0.00550 |
| 0.38000 | 0.00415 |
| 0.40000 | 0.00435 |
| 0.42000 | 0.00155 |
| 0.42075 | 0.00000 |
| 0.44000 | 0.00000 |
| 0.47845 | |

| Weighted (Y) | Mean | Std dev |
|--------------|----------|---------|
| 0.00000 | 0.00000 | 0.00000 |
| 0.00000 | 0.00000 | 0.00000 |
| 0.00167 | -0.00054 | 0.00023 |
| 0.00523 | -0.00157 | 0.00064 |
| 0.00376 | -0.00105 | 0.00041 |
| 0.00648 | -0.00168 | 0.00062 |
| 0.01097 | -0.00263 | 0.00091 |
| 0.01275 | -0.00280 | 0.00092 |
| 0.01745 | -0.00349 | 0.00108 |
| 0.02310 | -0.00416 | 0.00121 |
| 0.02790 | -0.00446 | 0.00122 |
| 0.03208 | -0.00449 | 0.00114 |
| 0.03501 | -0.00420 | 0.00100 |
| 0.03783 | -0.00378 | 0.00084 |
| 0.04180 | -0.00334 | 0.00069 |
| 0.04306 | -0.00258 | 0.00051 |
| 0.04389 | -0.00176 | 0.00035 |
| 0.04191 | -0.00084 | 0.00020 |
| 0.04567 | 0.00000 | 0.00011 |
| 0.04295 | 0.00086 | 0.00004 |
| 0.04441 | 0.00178 | 0.00000 |
| 0.04243 | 0.00255 | 0.00001 |
| 0.04285 | 0.00343 | 0.00004 |
| 0.04034 | 0.00403 | 0.00011 |
| 0.03971 | 0.00477 | 0.00020 |
| 0.03752 | 0.00525 | 0.00031 |
| 0.03574 | 0.00572 | 0.00044 |
| 0.03375 | 0.00608 | 0.00058 |
| 0.03375 | 0.00675 | 0.00077 |
| 0.02978 | 0.00655 | 0.00087 |
| 0.02560 | 0.00614 | 0.00094 |
| 0.02487 | 0.00647 | 0.00111 |
| 0.02027 | 0.00568 | 0.00108 |
| 0.01714 | 0.00514 | 0.00108 |
| 0.01474 | 0.00472 | 0.00108 |
| 0.01108 | 0.00377 | 0.00094 |
| 0.01150 | 0.00414 | 0.00111 |
| 0.00867 | 0.00330 | 0.00095 |
| 0.00909 | 0.00364 | 0.00112 |
| 0.00324 | 0.00136 | 0.00045 |
| 0.00000 | 0.00000 | 0.00000 |
| 0.00000 | 0.00000 | 0.00000 |
| 1.00000 | 0.04871 | 0.15907 |

Standard Deviation = 0.15907

WIT TEST SERIES DATA SHEET - PHASE I

SAMPLE: 94WIT02

DATE: 10/24/94

SPRAY DIST: 5.0 inches

| X | Y |
|----------|---------|
| -0.28000 | 0.00000 |
| -0.27480 | 0.00000 |
| -0.26000 | 0.00130 |
| -0.24000 | 0.00200 |
| -0.22000 | 0.00445 |
| -0.20000 | 0.00615 |
| -0.18000 | 0.00775 |
| -0.16000 | 0.00895 |
| -0.14000 | 0.01135 |
| -0.12000 | 0.01320 |
| -0.10000 | 0.01505 |
| -0.08000 | 0.01685 |
| -0.06000 | 0.01935 |
| -0.04000 | 0.02035 |
| -0.02000 | 0.02090 |
| 0.00000 | 0.02175 |
| 0.02000 | 0.02030 |
| 0.04000 | 0.01985 |
| 0.06000 | 0.01970 |
| 0.08000 | 0.02060 |
| 0.10000 | 0.02070 |
| 0.12000 | 0.01985 |
| 0.14000 | 0.01990 |
| 0.16000 | 0.02090 |
| 0.18000 | 0.01975 |
| 0.20000 | 0.02060 |
| 0.22000 | 0.02005 |
| 0.24000 | 0.02005 |
| 0.26000 | 0.01955 |
| 0.28000 | 0.01900 |
| 0.30000 | 0.01785 |
| 0.32000 | 0.01765 |
| 0.34000 | 0.01580 |
| 0.36000 | 0.01475 |
| 0.38000 | 0.01270 |
| 0.40000 | 0.01130 |
| 0.42000 | 0.00970 |
| 0.44000 | 0.00870 |
| 0.46000 | 0.00635 |
| 0.48000 | 0.00585 |
| 0.50000 | 0.00380 |
| 0.52000 | 0.00285 |
| 0.54000 | 0.00225 |
| 0.54070 | 0.00000 |
| 0.56000 | 0.00000 |
| 0.57975 | |

| Weighted (Y) | Mean | Std dev |
|--------------|----------|---------|
| 0.00000 | 0.00000 | 0.00000 |
| 0.00000 | 0.00000 | 0.00000 |
| 0.00224 | -0.00058 | 0.00035 |
| 0.00345 | -0.00083 | 0.00048 |
| 0.00768 | -0.00169 | 0.00095 |
| 0.01061 | -0.00212 | 0.00117 |
| 0.01337 | -0.00241 | 0.00131 |
| 0.01544 | -0.00247 | 0.00132 |
| 0.01958 | -0.00274 | 0.00146 |
| 0.02277 | -0.00273 | 0.00145 |
| 0.02596 | -0.00260 | 0.00140 |
| 0.02906 | -0.00233 | 0.00131 |
| 0.03338 | -0.00200 | 0.00124 |
| 0.03510 | -0.00140 | 0.00105 |
| 0.03605 | -0.00072 | 0.00084 |
| 0.03752 | 0.00000 | 0.00066 |
| 0.03502 | 0.00070 | 0.00044 |
| 0.03424 | 0.00137 | 0.00029 |
| 0.03398 | 0.00204 | 0.00018 |
| 0.03553 | 0.00284 | 0.00010 |
| 0.03571 | 0.00357 | 0.00004 |
| 0.03424 | 0.00411 | 0.00001 |
| 0.03433 | 0.00481 | 0.00000 |
| 0.03605 | 0.00577 | 0.00003 |
| 0.03407 | 0.00613 | 0.00008 |
| 0.03553 | 0.00711 | 0.00016 |
| 0.03458 | 0.00761 | 0.00026 |
| 0.03458 | 0.00830 | 0.00040 |
| 0.03372 | 0.00877 | 0.00055 |
| 0.03277 | 0.00918 | 0.00071 |
| 0.03079 | 0.00924 | 0.00086 |
| 0.03044 | 0.00974 | 0.00107 |
| 0.02725 | 0.00927 | 0.00117 |
| 0.02544 | 0.00916 | 0.00132 |
| 0.02191 | 0.00832 | 0.00134 |
| 0.01949 | 0.00780 | 0.00139 |
| 0.01673 | 0.00703 | 0.00138 |
| 0.01501 | 0.00660 | 0.00142 |
| 0.01095 | 0.00504 | 0.00117 |
| 0.01009 | 0.00484 | 0.00122 |
| 0.00655 | 0.00328 | 0.00088 |
| 0.00492 | 0.00256 | 0.00074 |
| 0.00388 | 0.00210 | 0.00064 |
| 0.00000 | 0.00000 | 0.00000 |
| 0.00000 | 0.00000 | 0.00000 |
| 1 | 0.13264 | 0.18124 |

Standard Deviation = 0.18124

WIT TEST SERIES DATA SHEET - PHASE I

SAMPLE: 94WIT02

DATE: 10/24/94

SPRAY DIST: 6.0 inches

| X | Y |
|----------|---------|
| -0.66000 | 0.00000 |
| -0.64920 | 0.00000 |
| -0.64000 | 0.00195 |
| -0.62000 | 0.00305 |
| -0.60000 | 0.00395 |
| -0.58000 | 0.00505 |
| -0.56000 | 0.00635 |
| -0.54000 | 0.00735 |
| -0.52000 | 0.00895 |
| -0.50000 | 0.00985 |
| -0.48000 | 0.01175 |
| -0.46000 | 0.01340 |
| -0.44000 | 0.01505 |
| -0.42000 | 0.01580 |
| -0.40000 | 0.01820 |
| -0.38000 | 0.01820 |
| -0.36000 | 0.01925 |
| -0.34000 | 0.01860 |
| -0.32000 | 0.01850 |
| -0.30000 | 0.01875 |
| -0.28000 | 0.01910 |
| -0.26000 | 0.01860 |
| -0.24000 | 0.01805 |
| -0.22000 | 0.01895 |
| -0.20000 | 0.01855 |
| -0.18000 | 0.02005 |
| -0.16000 | 0.01875 |
| -0.14000 | 0.02070 |
| -0.12000 | 0.02065 |
| -0.10000 | 0.01960 |
| -0.08000 | 0.01960 |
| -0.06000 | 0.01970 |
| -0.04000 | 0.02020 |
| -0.02000 | 0.02050 |
| 0.00000 | 0.02100 |
| 0.02000 | 0.02045 |
| 0.04000 | 0.01985 |
| 0.06000 | 0.01775 |
| 0.08000 | 0.01630 |
| 0.10000 | 0.01515 |
| 0.12000 | 0.01480 |
| 0.14000 | 0.01335 |
| 0.16000 | 0.01315 |
| 0.18000 | 0.01100 |
| 0.20000 | 0.00825 |
| 0.22000 | 0.00925 |
| 0.24000 | 0.00665 |
| 0.26000 | 0.00545 |
| 0.28000 | 0.00450 |
| 0.30000 | 0.00455 |
| 0.32000 | 0.00260 |
| 0.34000 | 0.00105 |
| 0.35270 | 0.00000 |
| 0.36000 | 0.00000 |
| 0.69210 | |

| Weighted (Y) | Mean | Std dev |
|--------------|----------|---------|
| 0.00000 | 0.00000 | 0.00000 |
| 0.00000 | 0.00000 | 0.00000 |
| 0.00282 | -0.00180 | 0.00067 |
| 0.00441 | -0.00273 | 0.00096 |
| 0.00571 | -0.00342 | 0.00114 |
| 0.00730 | -0.00423 | 0.00132 |
| 0.00917 | -0.00514 | 0.00151 |
| 0.01062 | -0.00573 | 0.00158 |
| 0.01293 | -0.00672 | 0.00173 |
| 0.01423 | -0.00712 | 0.00170 |
| 0.01698 | -0.00815 | 0.00180 |
| 0.01936 | -0.00891 | 0.00181 |
| 0.02175 | -0.00957 | 0.00178 |
| 0.02283 | -0.00959 | 0.00162 |
| 0.02630 | -0.01052 | 0.00159 |
| 0.02630 | -0.00999 | 0.00134 |
| 0.02781 | -0.01001 | 0.00118 |
| 0.02687 | -0.00914 | 0.00093 |
| 0.02673 | -0.00855 | 0.00074 |
| 0.02709 | -0.00813 | 0.00058 |
| 0.02760 | -0.00773 | 0.00044 |
| 0.02687 | -0.00699 | 0.00030 |
| 0.02608 | -0.00626 | 0.00019 |
| 0.02738 | -0.00602 | 0.00012 |
| 0.02680 | -0.00536 | 0.00006 |
| 0.02897 | -0.00521 | 0.00002 |
| 0.02709 | -0.00433 | 0.00000 |
| 0.02991 | -0.00419 | 0.00001 |
| 0.02984 | -0.00358 | 0.00003 |
| 0.02832 | -0.00283 | 0.00008 |
| 0.02832 | -0.00227 | 0.00016 |
| 0.02846 | -0.00171 | 0.00025 |
| 0.02919 | -0.00117 | 0.00038 |
| 0.02962 | -0.00059 | 0.00053 |
| 0.03034 | 0.00000 | 0.00072 |
| 0.02955 | 0.00059 | 0.00089 |
| 0.02868 | 0.00115 | 0.00108 |
| 0.02565 | 0.00154 | 0.00117 |
| 0.02355 | 0.00188 | 0.00129 |
| 0.02189 | 0.00219 | 0.00141 |
| 0.02138 | 0.00257 | 0.00161 |
| 0.01929 | 0.00270 | 0.00167 |
| 0.01900 | 0.00304 | 0.00187 |
| 0.01589 | 0.00286 | 0.00177 |
| 0.01192 | 0.00238 | 0.00149 |
| 0.01337 | 0.00294 | 0.00187 |
| 0.00961 | 0.00231 | 0.00149 |
| 0.00787 | 0.00205 | 0.00135 |
| 0.00650 | 0.00182 | 0.00122 |
| 0.00657 | 0.00197 | 0.00136 |
| 0.00376 | 0.00120 | 0.00084 |
| 0.00152 | 0.00052 | 0.00037 |
| 0.00000 | 0.00000 | 0.00000 |
| 0.00000 | 0.00000 | 0.00000 |
| -0.15399 | | 0.22370 |

Standard Deviation = 0.22370

WIT TEST SERIES DATA SHEET - PHASE I

SAMPLE: 94WIT02
DATE: 10/24/94
SPRAY DIST 7.0 inches

| X | Y |
|----------|---------|
| -0.62000 | 0.00000 |
| -0.61975 | 0.00000 |
| -0.60000 | 0.00275 |
| -0.58000 | 0.00445 |
| -0.56000 | 0.00490 |
| -0.54000 | 0.00500 |
| -0.52000 | 0.00640 |
| -0.50000 | 0.00855 |
| -0.48000 | 0.00885 |
| -0.46000 | 0.01100 |
| -0.44000 | 0.01080 |
| -0.42000 | 0.01365 |
| -0.40000 | 0.01440 |
| -0.38000 | 0.01575 |
| -0.36000 | 0.01610 |
| -0.34000 | 0.01850 |
| -0.32000 | 0.01840 |
| -0.30000 | 0.01750 |
| -0.28000 | 0.01920 |
| -0.26000 | 0.01975 |
| -0.24000 | 0.02125 |
| -0.22000 | 0.02080 |
| -0.20000 | 0.02085 |
| -0.18000 | 0.02085 |
| -0.16000 | 0.02175 |
| -0.14000 | 0.02020 |
| -0.12000 | 0.02045 |
| -0.10000 | 0.02010 |
| -0.08000 | 0.02025 |
| -0.06000 | 0.01955 |
| -0.04000 | 0.02135 |
| -0.02000 | 0.02105 |
| 0.00000 | 0.02120 |
| 0.02000 | 0.02180 |
| 0.04000 | 0.01975 |
| 0.06000 | 0.01995 |
| 0.08000 | 0.02065 |
| 0.10000 | 0.01955 |
| 0.12000 | 0.01980 |
| 0.14000 | 0.01915 |
| 0.16000 | 0.01875 |
| 0.18000 | 0.01815 |
| 0.20000 | 0.01850 |
| 0.22000 | 0.01710 |
| 0.24000 | 0.01565 |
| 0.26000 | 0.01385 |
| 0.28000 | 0.01195 |
| 0.30000 | 0.01025 |
| 0.32000 | 0.00910 |
| 0.34000 | 0.00745 |
| 0.36000 | 0.00710 |
| 0.38000 | 0.00565 |
| 0.40000 | 0.00450 |
| 0.42000 | 0.00340 |
| 0.44000 | 0.00265 |
| 0.46000 | 0.00190 |
| 0.48000 | 0.00135 |
| 0.50000 | 0.00090 |
| 0.51320 | 0.00000 |
| 0.52000 | 0.00000 |

0.79445

| Weighted (Y) | Mean | Std dev |
|--------------|----------|---------|
| 0.00000 | 0.00000 | 0.00000 |
| 0.00000 | 0.00000 | 0.00000 |
| 0.00346 | -0.00208 | 0.00095 |
| 0.00560 | -0.00325 | 0.00143 |
| 0.00617 | -0.00345 | 0.00145 |
| 0.00629 | -0.00340 | 0.00136 |
| 0.00806 | -0.00419 | 0.00159 |
| 0.01076 | -0.00538 | 0.00194 |
| 0.01114 | -0.00535 | 0.00182 |
| 0.01385 | -0.00637 | 0.00205 |
| 0.01359 | -0.00598 | 0.00181 |
| 0.01718 | -0.00722 | 0.00204 |
| 0.01813 | -0.00725 | 0.00191 |
| 0.01983 | -0.00753 | 0.00184 |
| 0.02027 | -0.00730 | 0.00164 |
| 0.02329 | -0.00792 | 0.00163 |
| 0.02316 | -0.00741 | 0.00139 |
| 0.02203 | -0.00661 | 0.00111 |
| 0.02417 | -0.00677 | 0.00101 |
| 0.02486 | -0.00646 | 0.00085 |
| 0.02675 | -0.00642 | 0.00072 |
| 0.02618 | -0.00576 | 0.00055 |
| 0.02624 | -0.00525 | 0.00041 |
| 0.02624 | -0.00472 | 0.00029 |
| 0.02738 | -0.00438 | 0.00020 |
| 0.02543 | -0.00356 | 0.00011 |
| 0.02574 | -0.00309 | 0.00005 |
| 0.02530 | -0.00253 | 0.00002 |
| 0.02549 | -0.00204 | 0.00000 |
| 0.02461 | -0.00148 | 0.00001 |
| 0.02687 | -0.00107 | 0.00003 |
| 0.02650 | -0.00053 | 0.00008 |
| 0.02669 | 0.00000 | 0.00015 |
| 0.02744 | 0.00055 | 0.00025 |
| 0.02486 | 0.00099 | 0.00033 |
| 0.02511 | 0.00151 | 0.00046 |
| 0.02599 | 0.00208 | 0.00063 |
| 0.02461 | 0.00246 | 0.00076 |
| 0.02492 | 0.00299 | 0.00095 |
| 0.02410 | 0.00337 | 0.00112 |
| 0.02360 | 0.00378 | 0.00131 |
| 0.02285 | 0.00411 | 0.00149 |
| 0.02329 | 0.00466 | 0.00177 |
| 0.02152 | 0.00474 | 0.00188 |
| 0.01970 | 0.00473 | 0.00196 |
| 0.01743 | 0.00453 | 0.00196 |
| 0.01504 | 0.00421 | 0.00190 |
| 0.01290 | 0.00387 | 0.00182 |
| 0.01145 | 0.00367 | 0.00179 |
| 0.00938 | 0.00319 | 0.00162 |
| 0.00894 | 0.00322 | 0.00169 |
| 0.00711 | 0.00270 | 0.00147 |
| 0.00566 | 0.00227 | 0.00128 |
| 0.00428 | 0.00180 | 0.00105 |
| 0.00334 | 0.00147 | 0.00089 |
| 0.00239 | 0.00110 | 0.00069 |
| 0.00170 | 0.00082 | 0.00052 |
| 0.00113 | 0.00057 | 0.00038 |
| 0.00000 | 0.00000 | 0.00000 |
| 0.00000 | 0.00000 | 0.00000 |

1 -0.07538 0.24572

Standard Deviation = 0.24572

WIT TEST SERIES DATA SHEET - PHASE I

SAMPLE: 94WIT02

DATE: 10/24/94

SPRAY DIST: 7.7 inches

| X | Y |
|----------|---------|
| -0.52000 | 0.00000 |
| -0.50430 | 0.00000 |
| -0.50000 | 0.00365 |
| -0.48000 | 0.00565 |
| -0.46000 | 0.00545 |
| -0.44000 | 0.00570 |
| -0.42000 | 0.00690 |
| -0.40000 | 0.00685 |
| -0.38000 | 0.00800 |
| -0.36000 | 0.00855 |
| -0.34000 | 0.00875 |
| -0.32000 | 0.00905 |
| -0.30000 | 0.00990 |
| -0.28000 | 0.01025 |
| -0.26000 | 0.01100 |
| -0.24000 | 0.01190 |
| -0.22000 | 0.01265 |
| -0.20000 | 0.01390 |
| -0.18000 | 0.01530 |
| -0.16000 | 0.01655 |
| -0.14000 | 0.01820 |
| -0.12000 | 0.02000 |
| -0.10000 | 0.02020 |
| -0.08000 | 0.02100 |
| -0.06000 | 0.02075 |
| -0.04000 | 0.02165 |
| -0.02000 | 0.02180 |
| 0.00000 | 0.02085 |
| 0.02000 | 0.02290 |
| 0.04000 | 0.02260 |
| 0.06000 | 0.02155 |
| 0.08000 | 0.02250 |
| 0.10000 | 0.02240 |
| 0.12000 | 0.02165 |
| 0.14000 | 0.02210 |
| 0.16000 | 0.02195 |
| 0.18000 | 0.02175 |
| 0.20000 | 0.02230 |
| 0.22000 | 0.02320 |
| 0.24000 | 0.02250 |
| 0.26000 | 0.02200 |
| 0.28000 | 0.02185 |
| 0.30000 | 0.02225 |
| 0.32000 | 0.02295 |
| 0.34000 | 0.02090 |
| 0.36000 | 0.02100 |
| 0.38000 | 0.01965 |
| 0.40000 | 0.01830 |
| 0.42000 | 0.01815 |
| 0.44000 | 0.01655 |
| 0.46000 | 0.01480 |
| 0.48000 | 0.01360 |
| 0.50000 | 0.01050 |
| 0.52000 | 0.01110 |
| 0.54000 | 0.01115 |
| 0.56000 | 0.01005 |
| 0.58000 | 0.00695 |
| 0.60000 | 0.00845 |
| 0.62000 | 0.00695 |
| 0.64000 | 0.00595 |
| 0.66000 | 0.00795 |
| 0.68000 | 0.00610 |
| 0.70000 | 0.00335 |
| 0.71205 | 0.00000 |
| 0.72000 | 0.00000 |
| 0.92235 | |

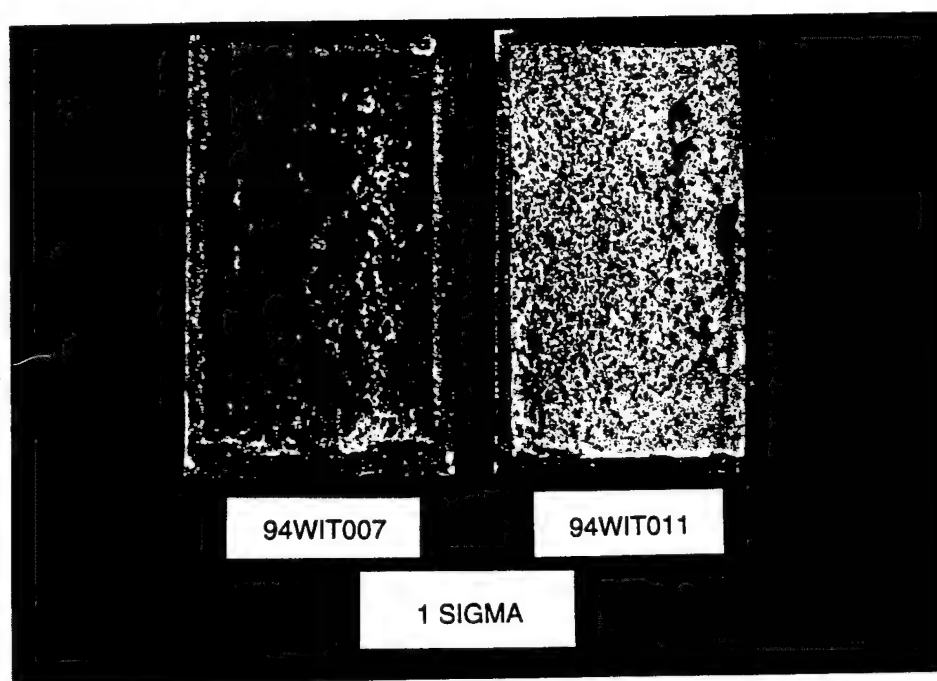
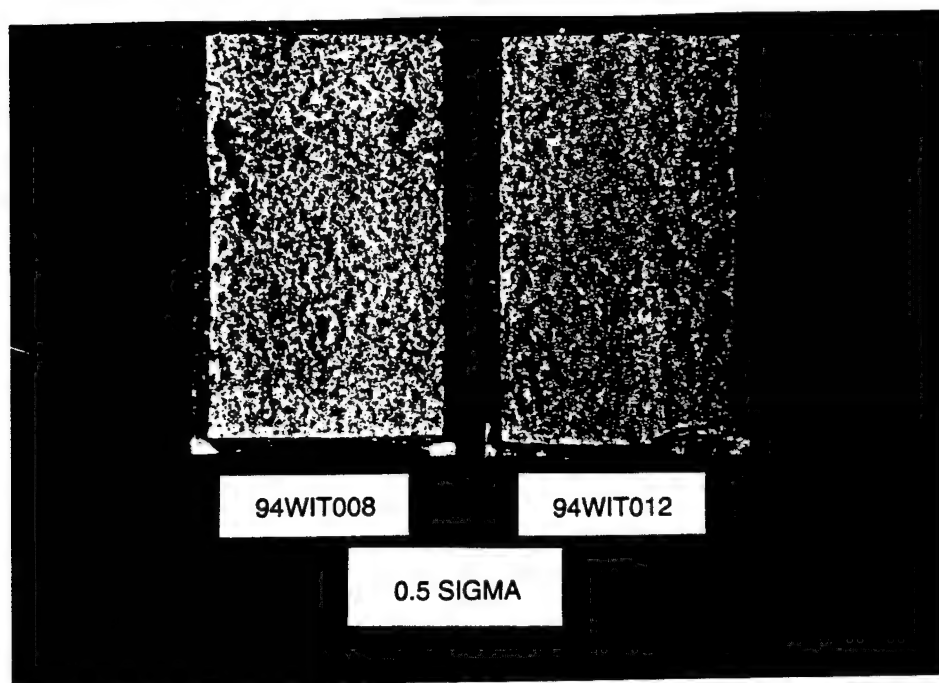
| Weighted (Y) | Mean | Std dev |
|--------------|----------|---------|
| 0.00000 | 0.00000 | 0.00000 |
| 0.00000 | 0.00000 | 0.00000 |
| 0.00396 | -0.00198 | 0.00151 |
| 0.00613 | -0.00294 | 0.00219 |
| 0.00591 | -0.00272 | 0.00198 |
| 0.00618 | -0.00272 | 0.00193 |
| 0.00748 | -0.00314 | 0.00217 |
| 0.00743 | -0.00297 | 0.00199 |
| 0.00867 | -0.00330 | 0.00215 |
| 0.00927 | -0.00334 | 0.00212 |
| 0.00949 | -0.00323 | 0.00199 |
| 0.00981 | -0.00314 | 0.00188 |
| 0.01073 | -0.00322 | 0.00188 |
| 0.01111 | -0.00311 | 0.00178 |
| 0.01193 | -0.00310 | 0.00171 |
| 0.01290 | -0.00310 | 0.00166 |
| 0.01371 | -0.00302 | 0.00157 |
| 0.01507 | -0.00301 | 0.00153 |
| 0.01659 | -0.00299 | 0.00148 |
| 0.01794 | -0.00287 | 0.00139 |
| 0.01973 | -0.00276 | 0.00132 |
| 0.02168 | -0.00260 | 0.00123 |
| 0.02190 | -0.00219 | 0.00104 |
| 0.02277 | -0.00182 | 0.00089 |
| 0.02250 | -0.00135 | 0.00071 |
| 0.02347 | -0.00094 | 0.00059 |
| 0.02364 | -0.00047 | 0.00045 |
| 0.02261 | 0.00000 | 0.00032 |
| 0.02483 | 0.00050 | 0.00024 |
| 0.02450 | 0.00098 | 0.00015 |
| 0.02336 | 0.00140 | 0.00008 |
| 0.02439 | 0.00195 | 0.00004 |
| 0.02429 | 0.00243 | 0.00001 |
| 0.02347 | 0.00282 | 0.00000 |
| 0.02398 | 0.00335 | 0.00001 |
| 0.02380 | 0.00381 | 0.00004 |
| 0.02358 | 0.00424 | 0.00009 |
| 0.02418 | 0.00484 | 0.00016 |
| 0.02515 | 0.00553 | 0.00026 |
| 0.02439 | 0.00585 | 0.00036 |
| 0.02385 | 0.00620 | 0.00048 |
| 0.02369 | 0.00663 | 0.00062 |
| 0.02412 | 0.00724 | 0.00080 |
| 0.02488 | 0.00796 | 0.00101 |
| 0.02266 | 0.00770 | 0.00111 |
| 0.02277 | 0.00820 | 0.00133 |
| 0.02130 | 0.00810 | 0.00146 |
| 0.01984 | 0.00794 | 0.00158 |
| 0.01968 | 0.00826 | 0.00179 |
| 0.01794 | 0.00790 | 0.00186 |
| 0.01605 | 0.00738 | 0.00187 |
| 0.01474 | 0.00708 | 0.00193 |
| 0.01138 | 0.00569 | 0.00166 |
| 0.01203 | 0.00626 | 0.00194 |
| 0.01209 | 0.00653 | 0.00215 |
| 0.01090 | 0.00610 | 0.00213 |
| 0.00754 | 0.00437 | 0.00161 |
| 0.00916 | 0.00550 | 0.00213 |
| 0.00754 | 0.00467 | 0.00190 |
| 0.00645 | 0.00413 | 0.00176 |
| 0.00862 | 0.00569 | 0.00253 |
| 0.00661 | 0.00450 | 0.00209 |
| 0.00363 | 0.00254 | 0.00123 |
| 0.00000 | 0.00000 | 0.00000 |
| 0.00000 | 0.00000 | 0.00000 |

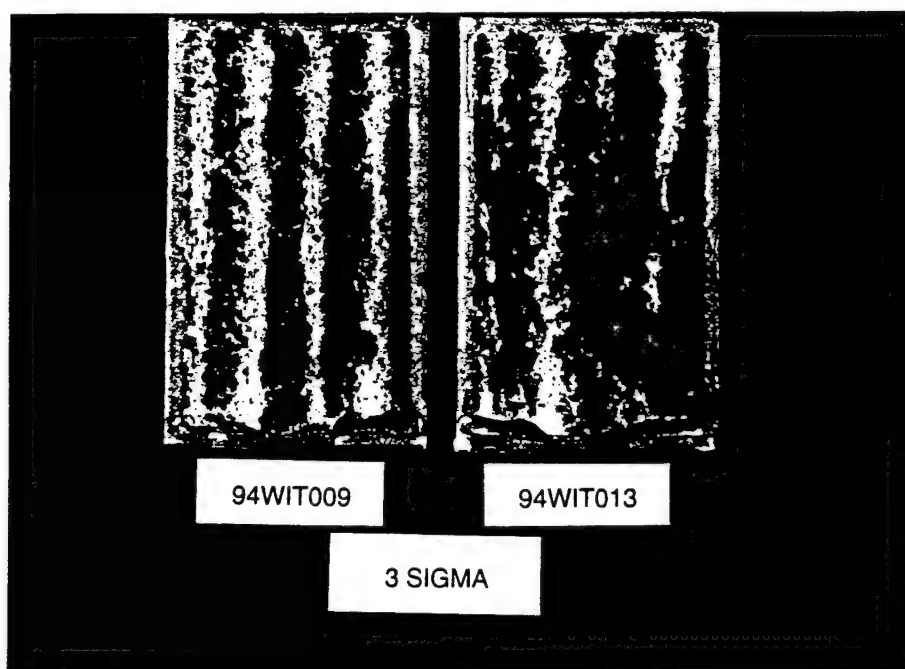
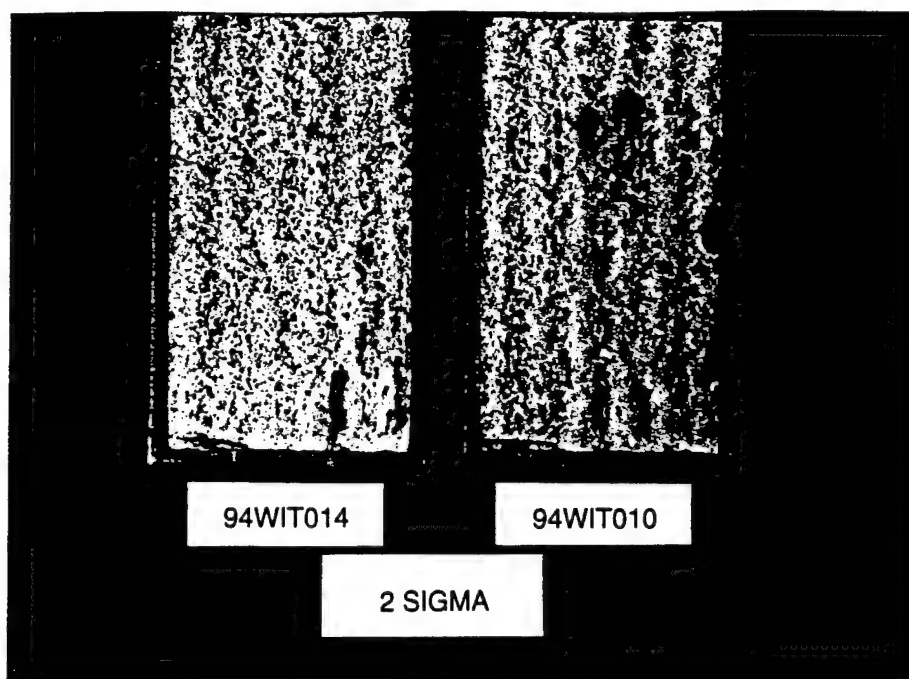
1 0.11824 0.27897

Standard Deviation = 0.27897

APPENDIX B

Phase II Corrosion Test Results



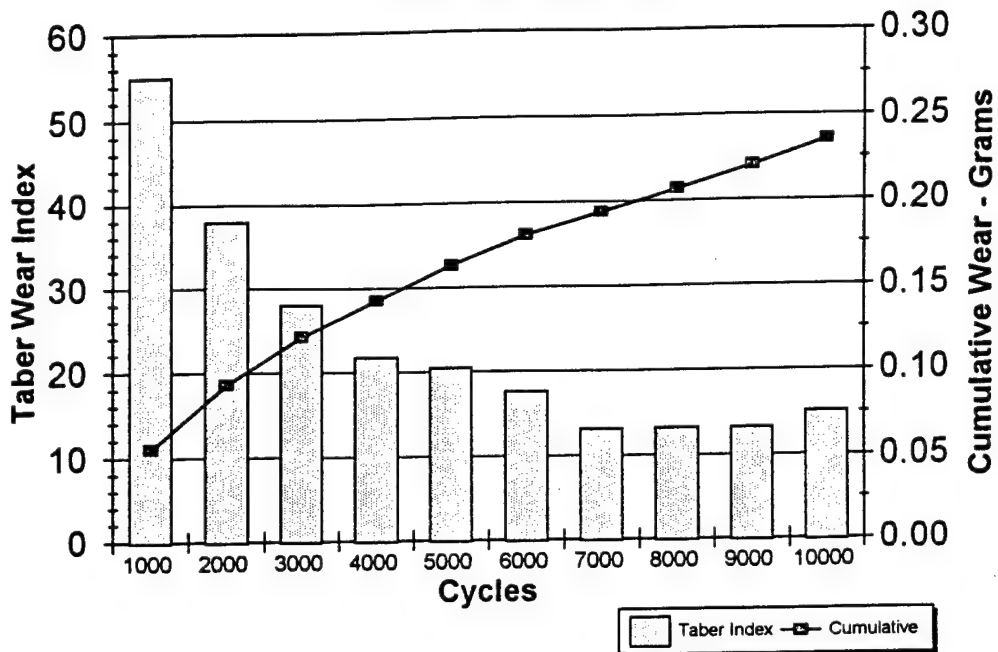


APPENDIX C

Phase II Taber Abraser Wear Test Results

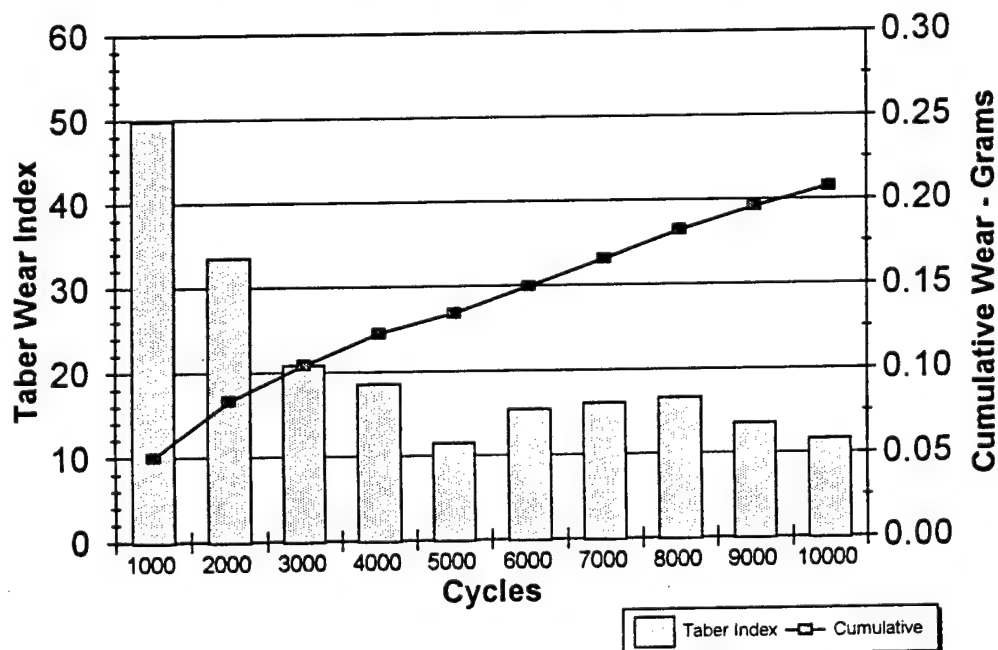
VERSAAlloy 50 Taber Abraser Wear Test

Test No. 94WIT007



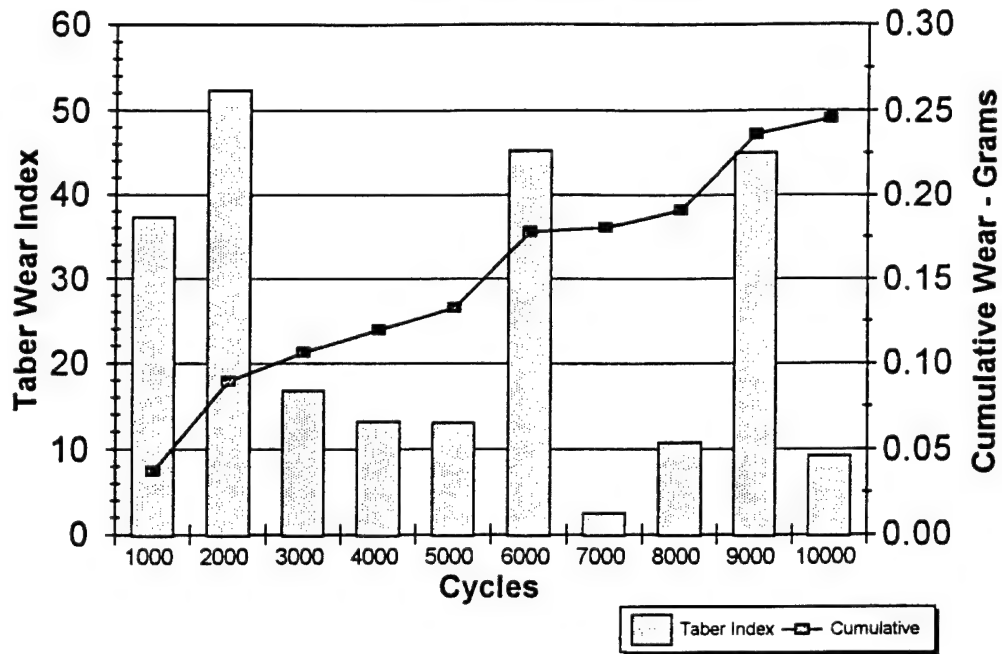
VERSAAlloy 50 Taber Abraser Wear Test

Test No. 94WIT008



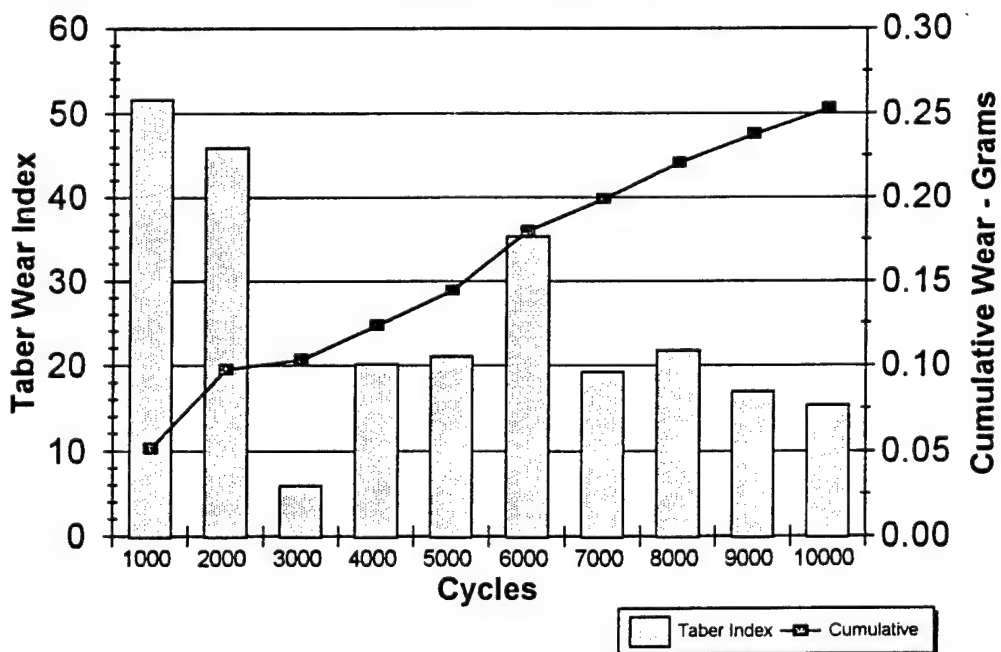
VERSAloy 50 Taber Abraser Wear Test

Test No. 94WIT009



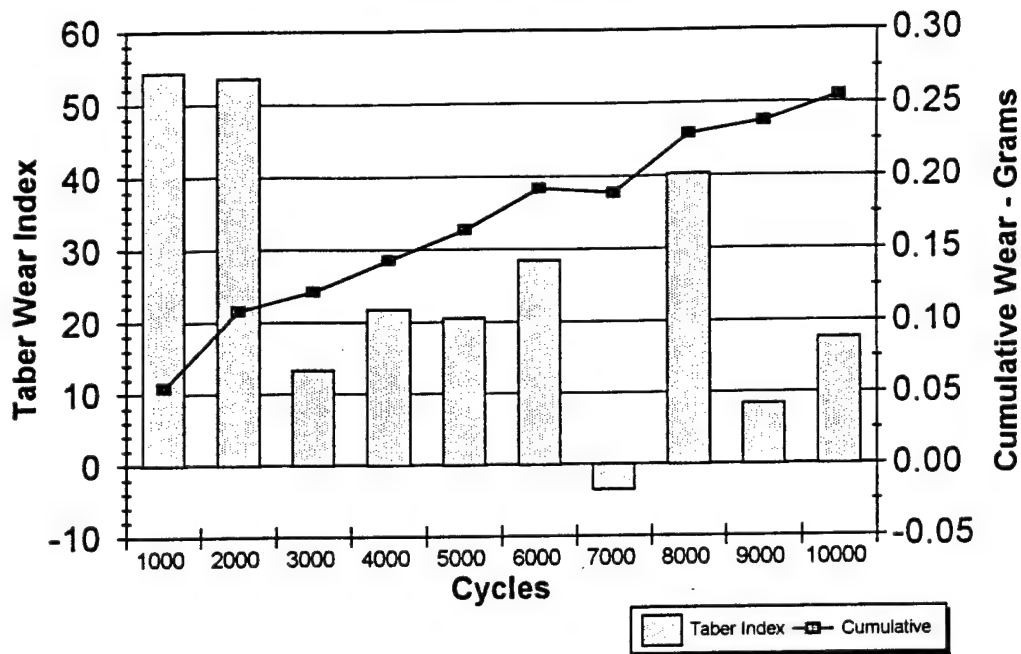
VERSAloy 50 Taber Abraser Wear Test

Test No. 94WIT010



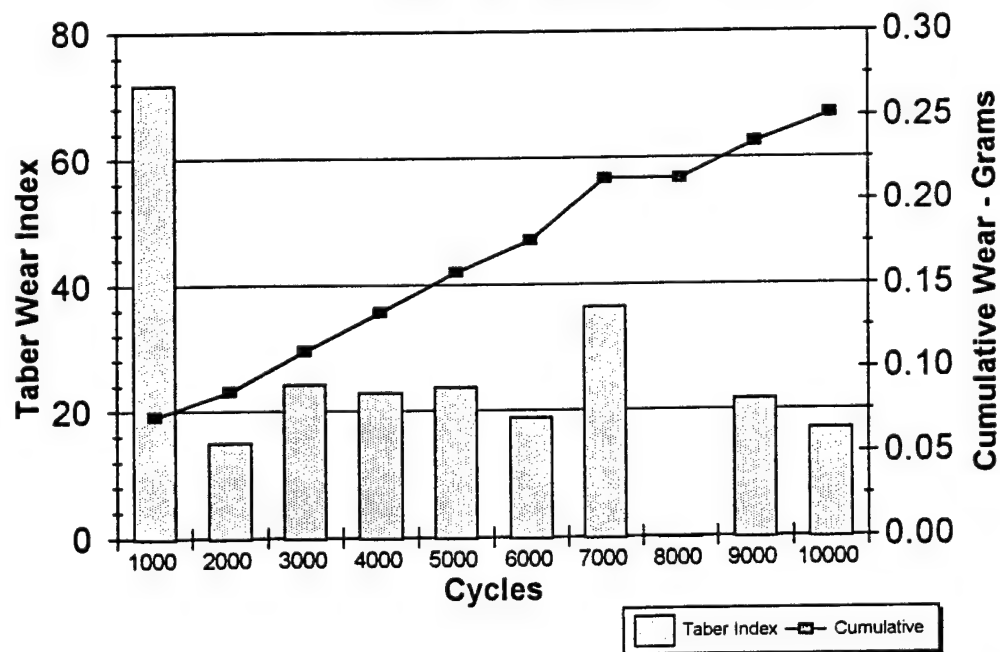
VERSAIloy 50 Taber Abraser Wear Test

Test No. 94WIT011



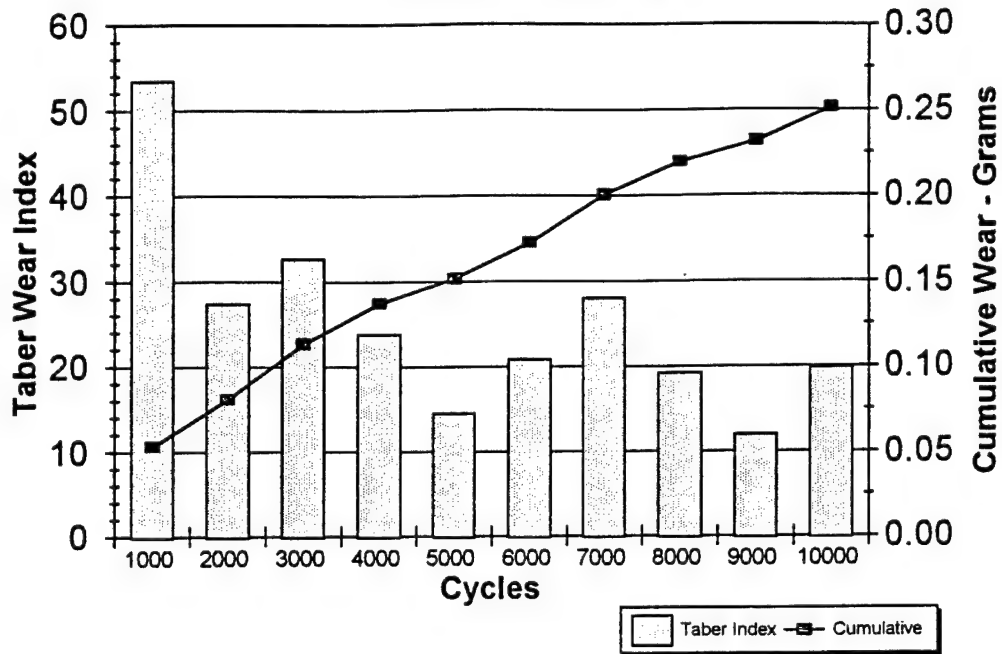
VERSAIloy 50 Taber Abraser Wear Test

Test No. 94WIT012



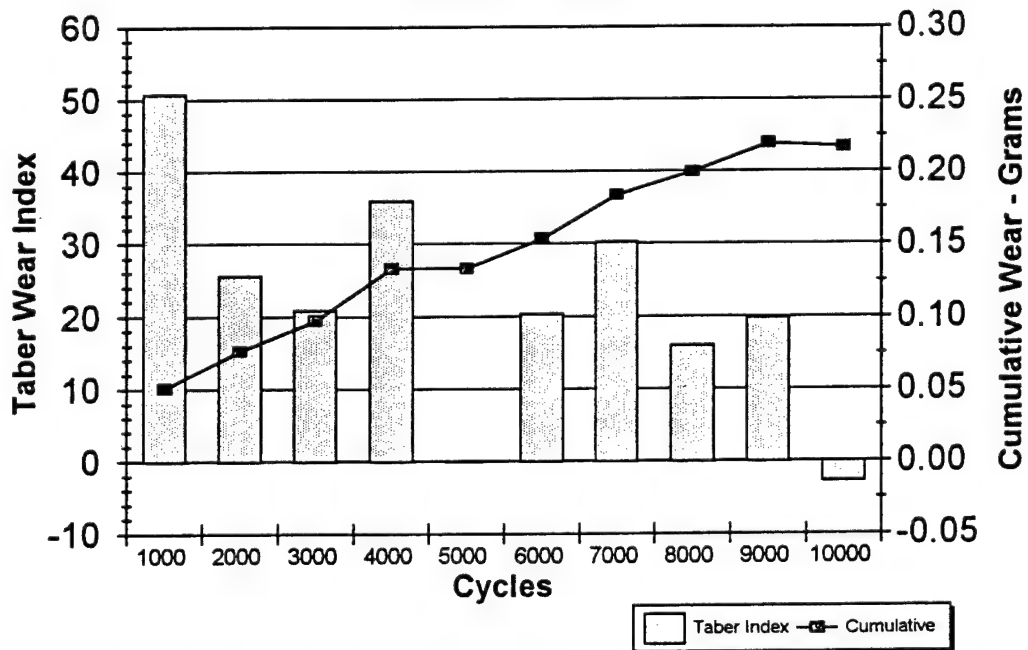
VERSAIloy 50 Taber Abraser Wear Test

Test No. 94WIT013



VERSAIloy 50 Taber Abraser Wear Test

Test No. 94WIT014

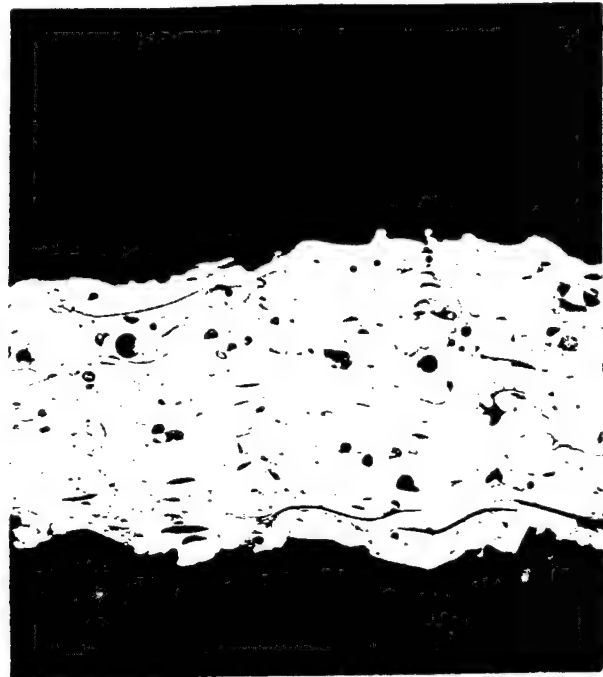


APPENDIX D

Phase II Metallurgical Coupon Microstructures



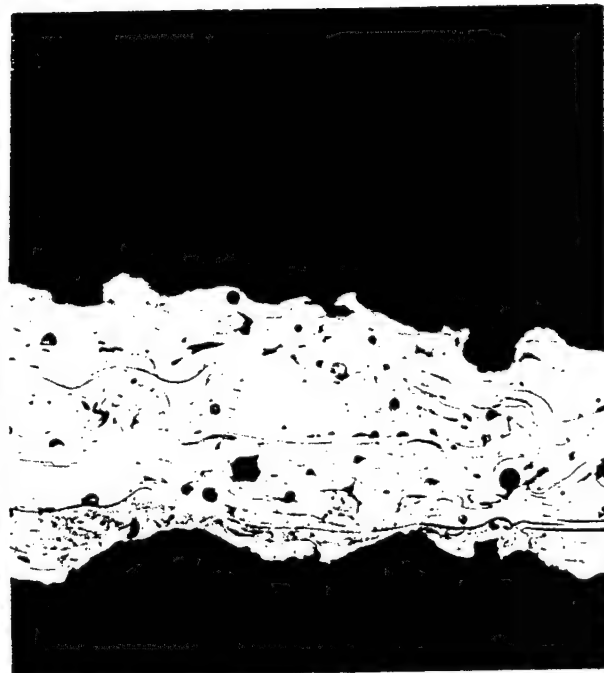
Test 94WIT008 (200x).



Test 94WIT012 (200x).



Test 94WIT007 (200x).



Test 94WIT011 (200x).



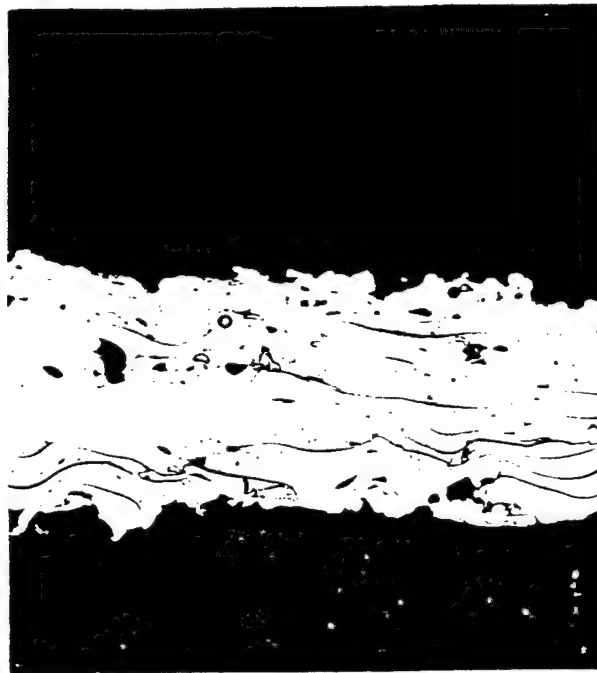
Test 94WIT014 (200x).



Test 94WIT010 (200x).



Test 94WIT009 (200x).

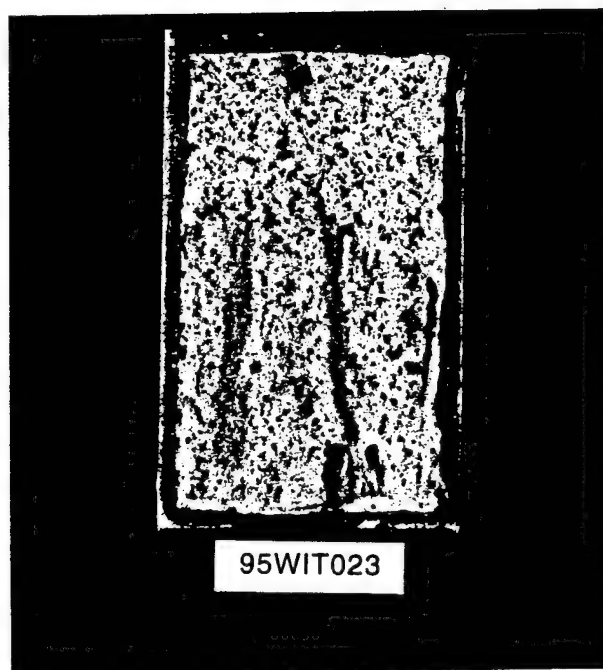
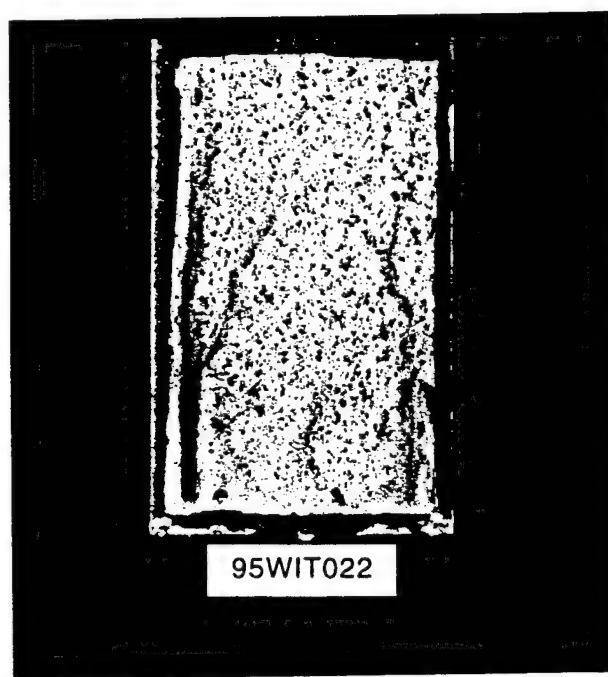
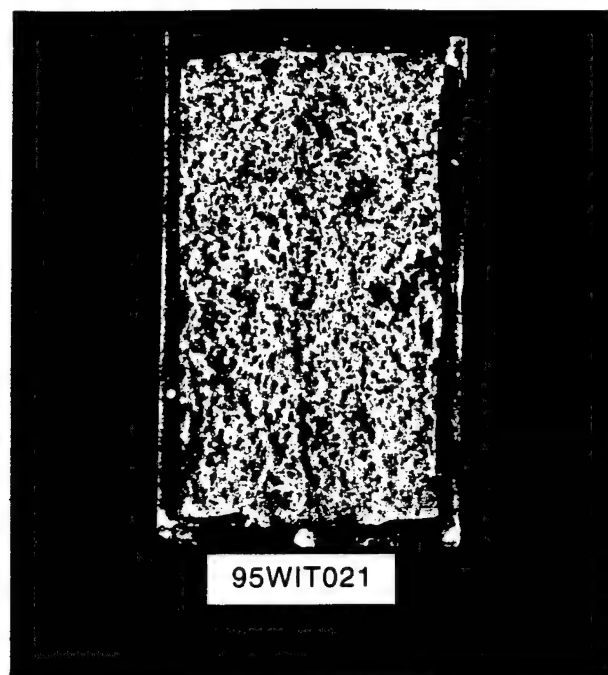
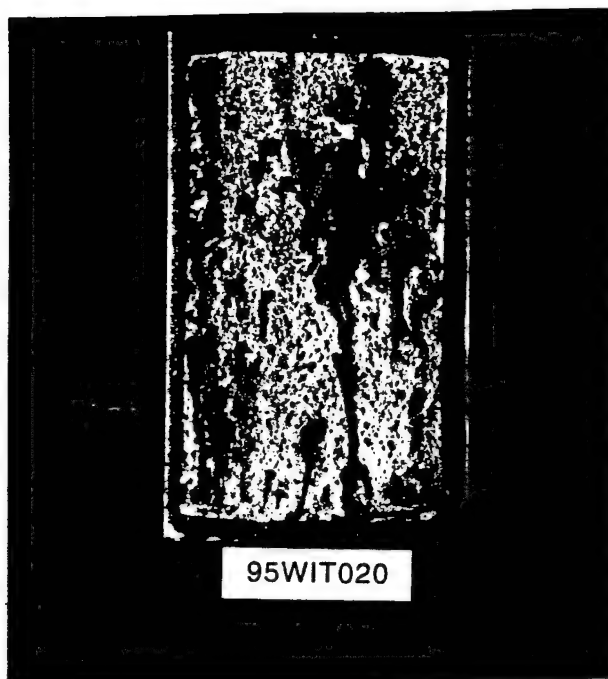


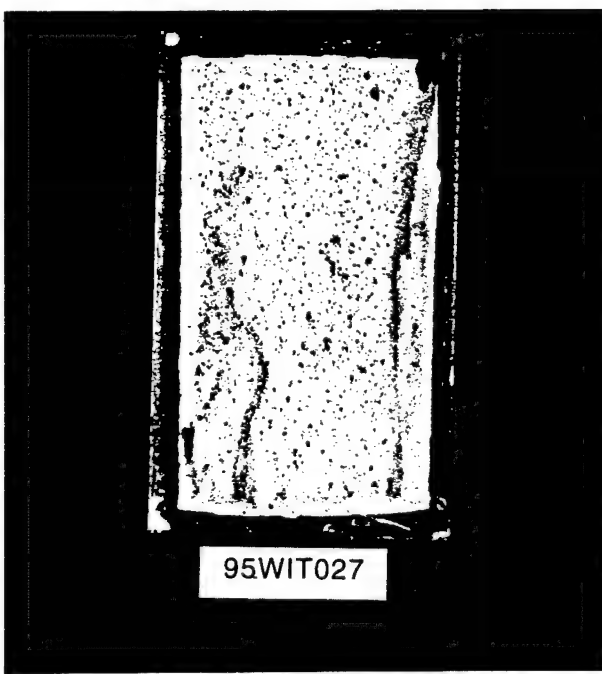
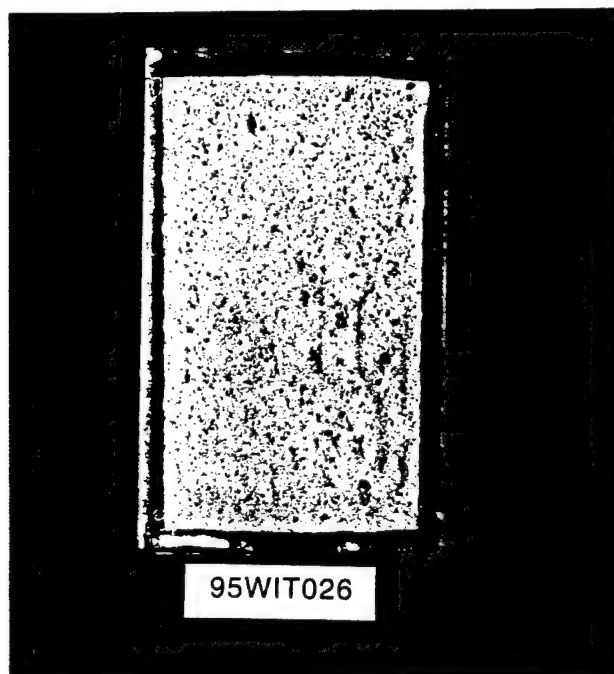
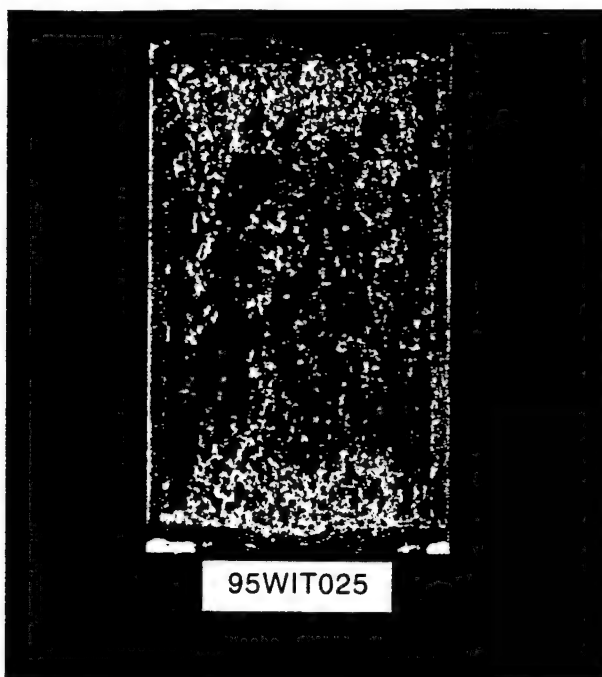
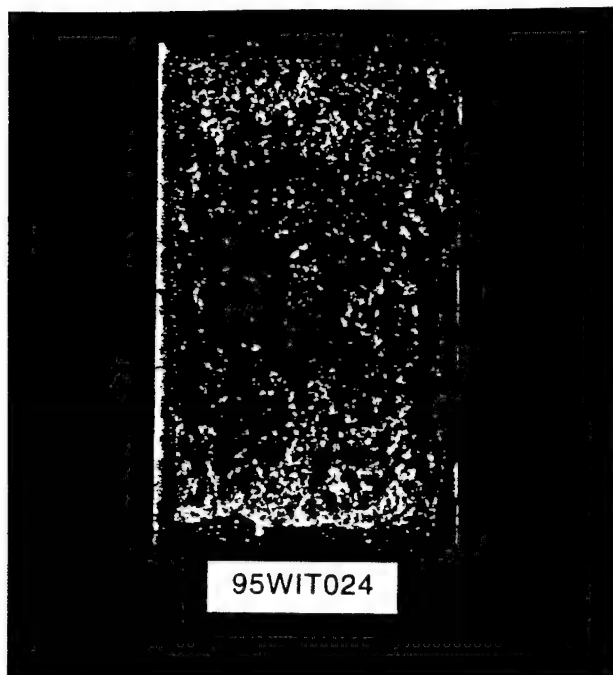
Test 94WIT013 (200x).

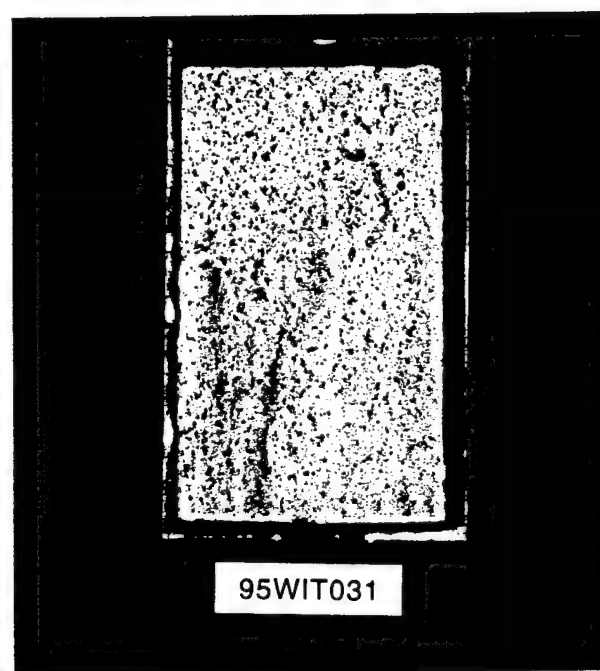
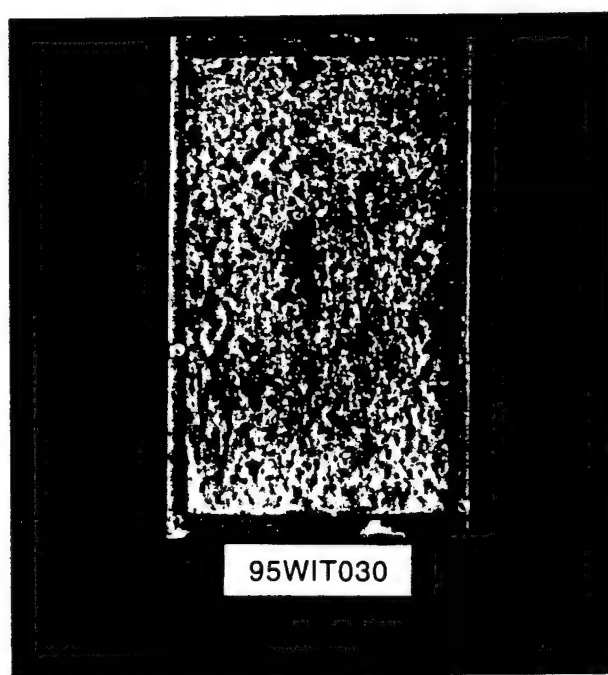
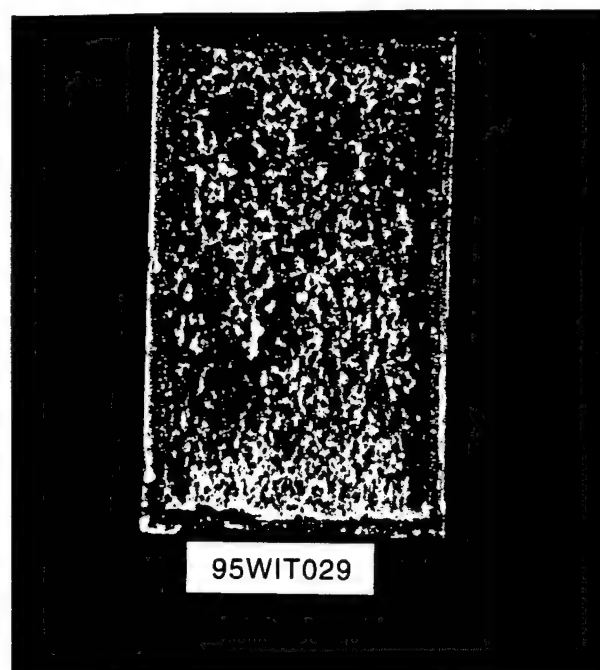
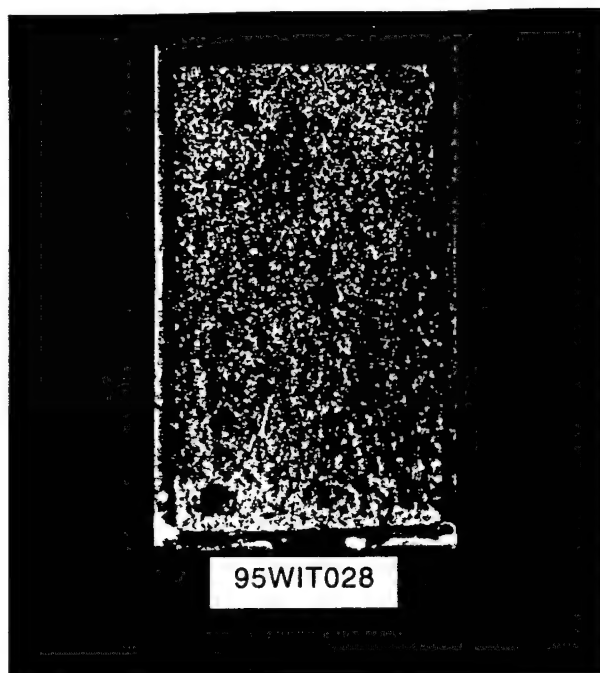
APPENDIX E

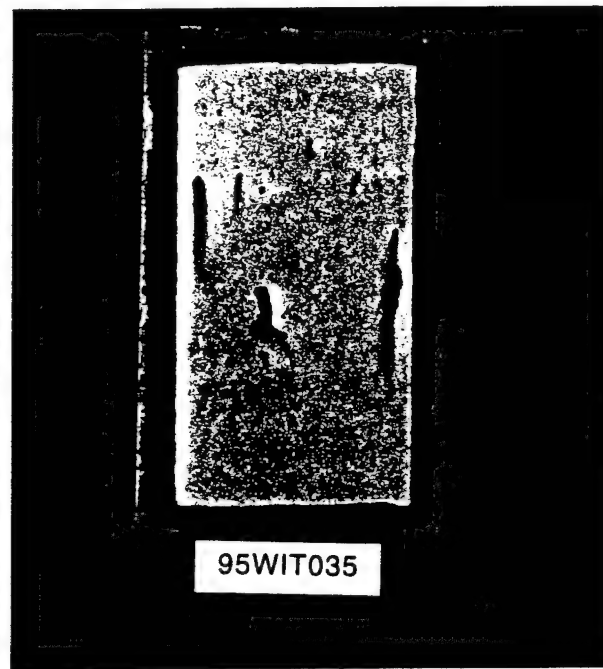
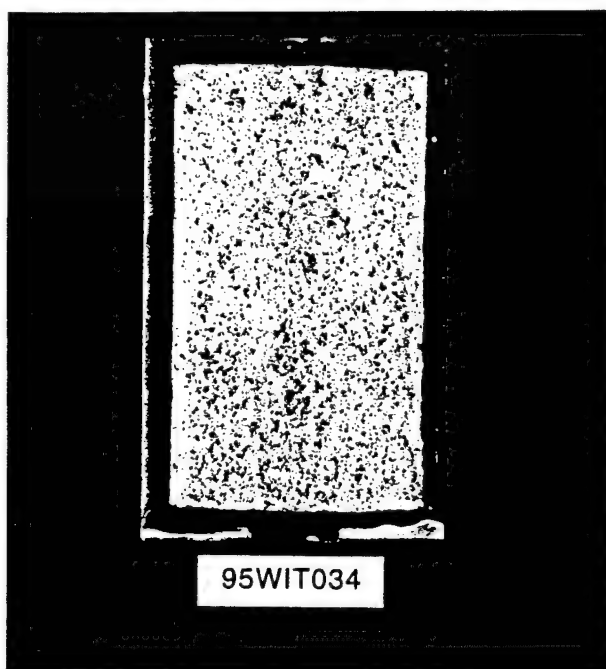
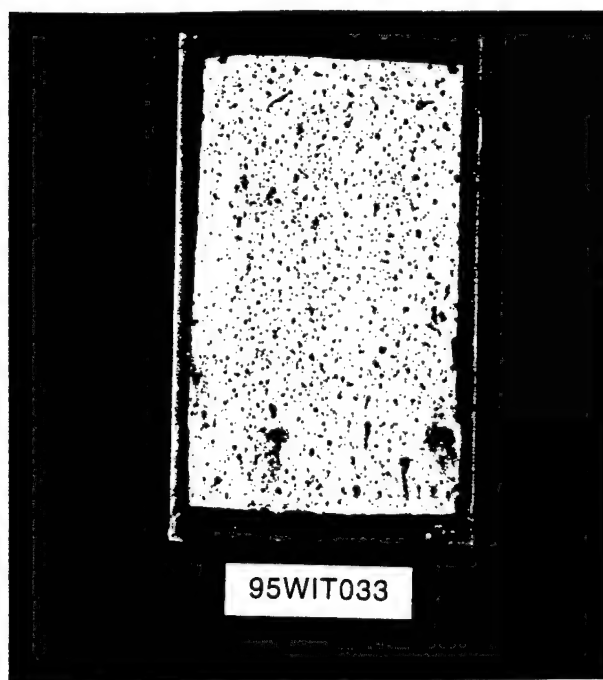
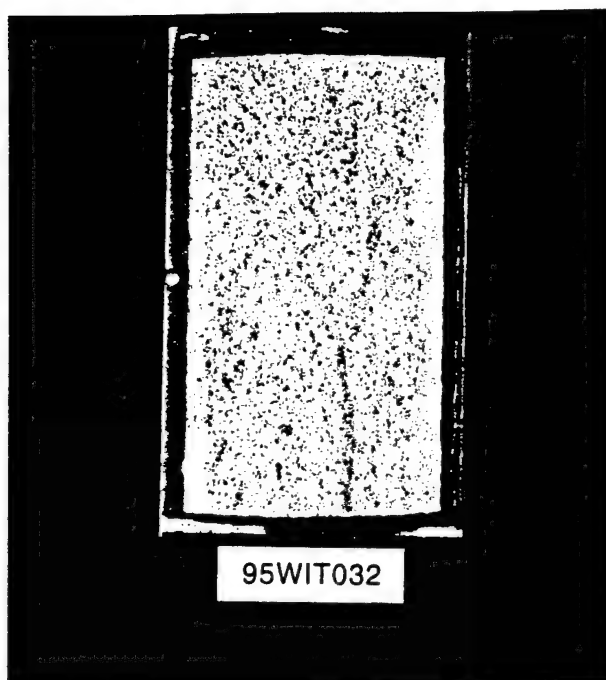
Phase III Corrosion Test Results

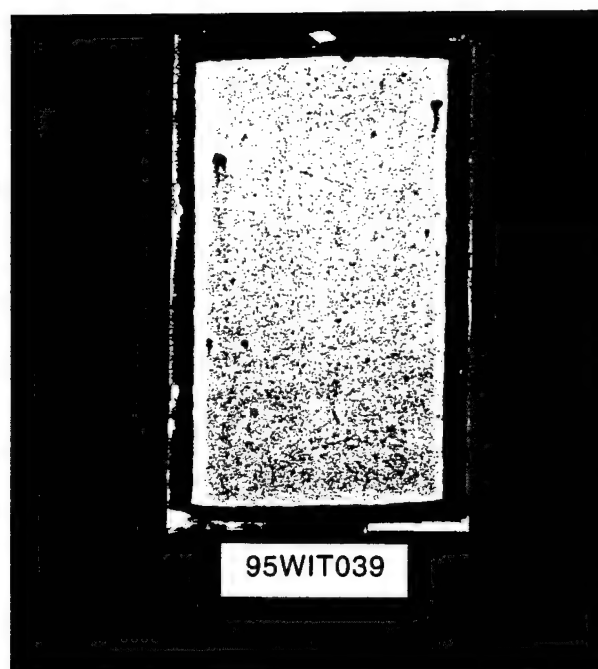
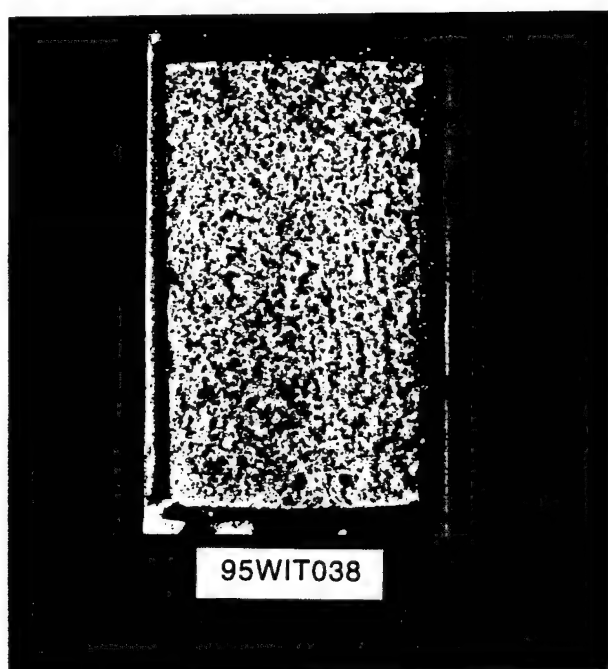
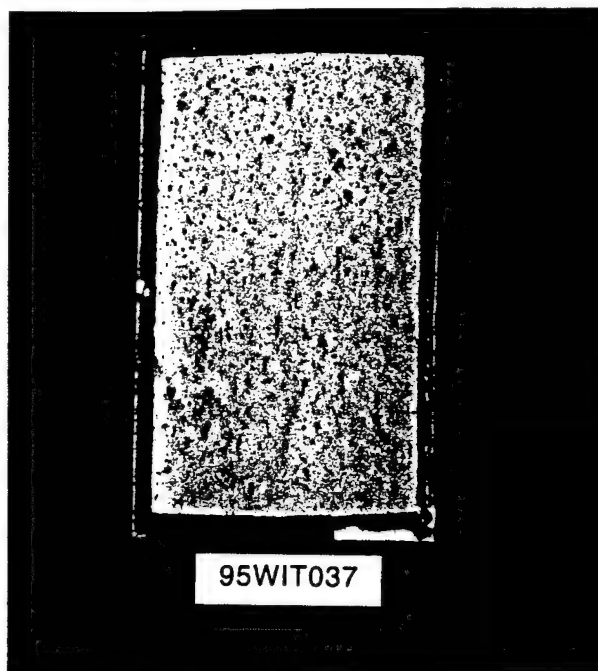
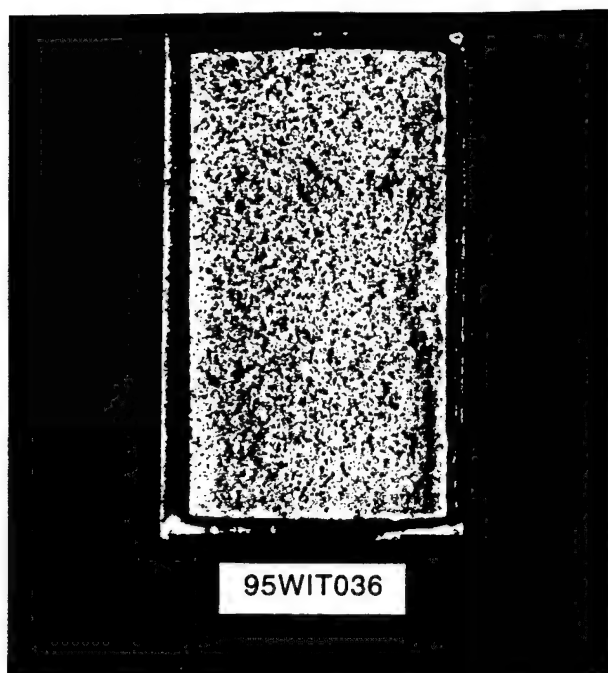
327
(The reverse of this page is blank)

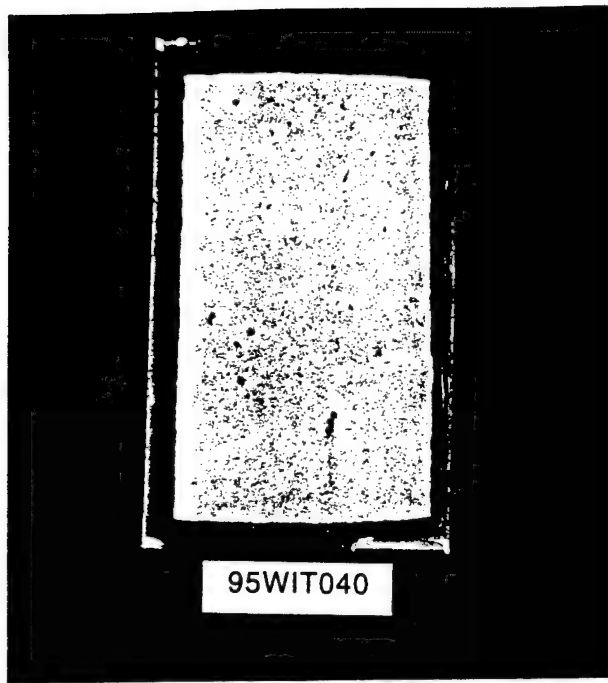










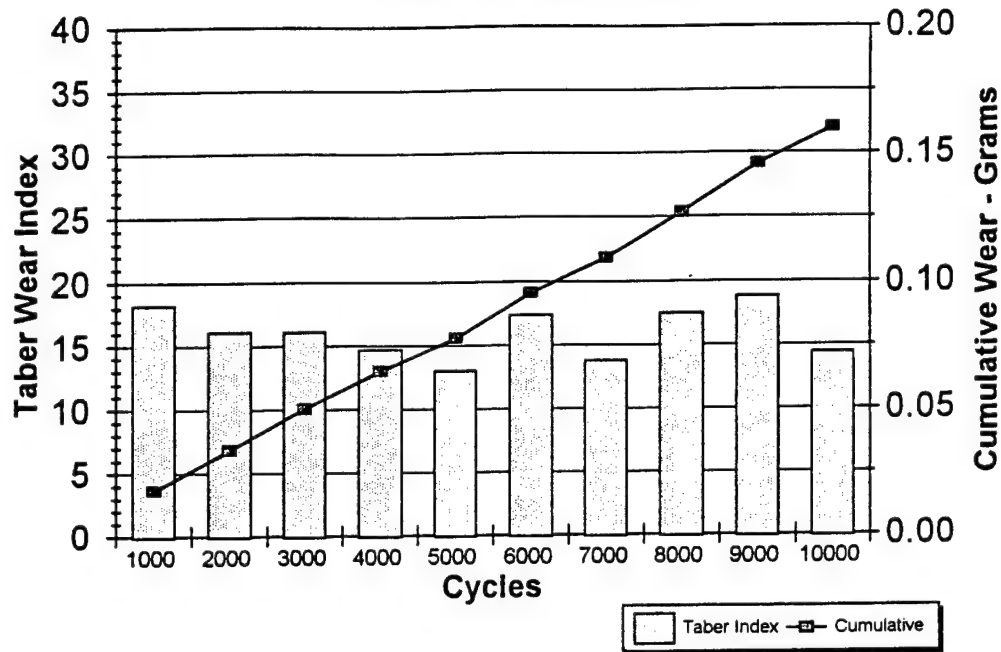


APPENDIX F

Phase III Taber Abraser Wear Test Results

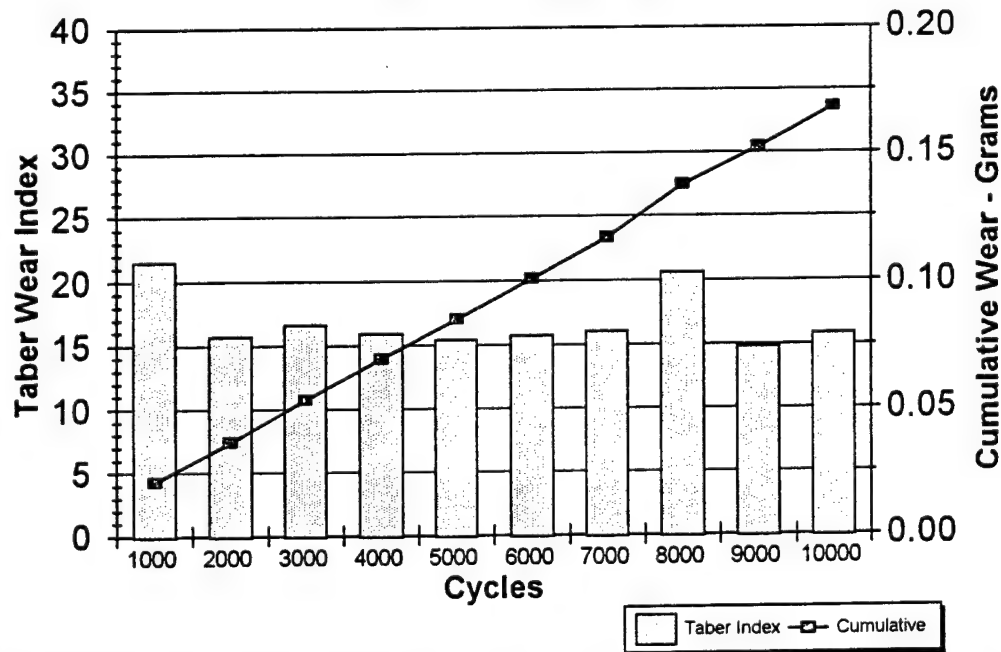
VERSAloy 50 Taber Abraser Wear Test

Test No. 95WIT020



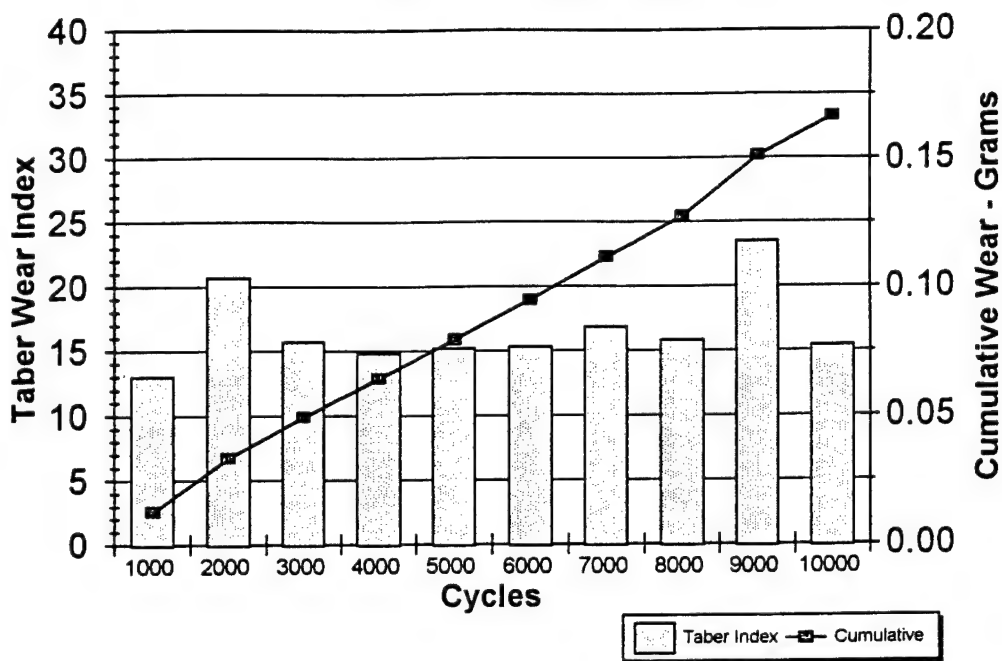
VERSAloy 50 Taber Abraser Wear Test

Test No. 95WIT021



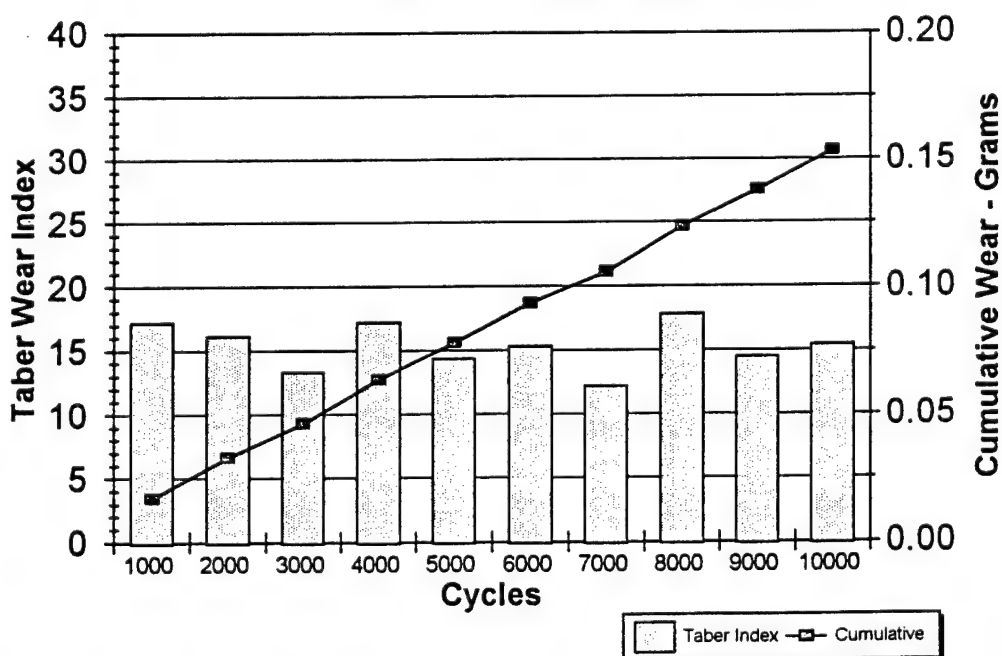
VERSAIloy 50 Taber Abraser Wear Test

Test No. 95WIT022

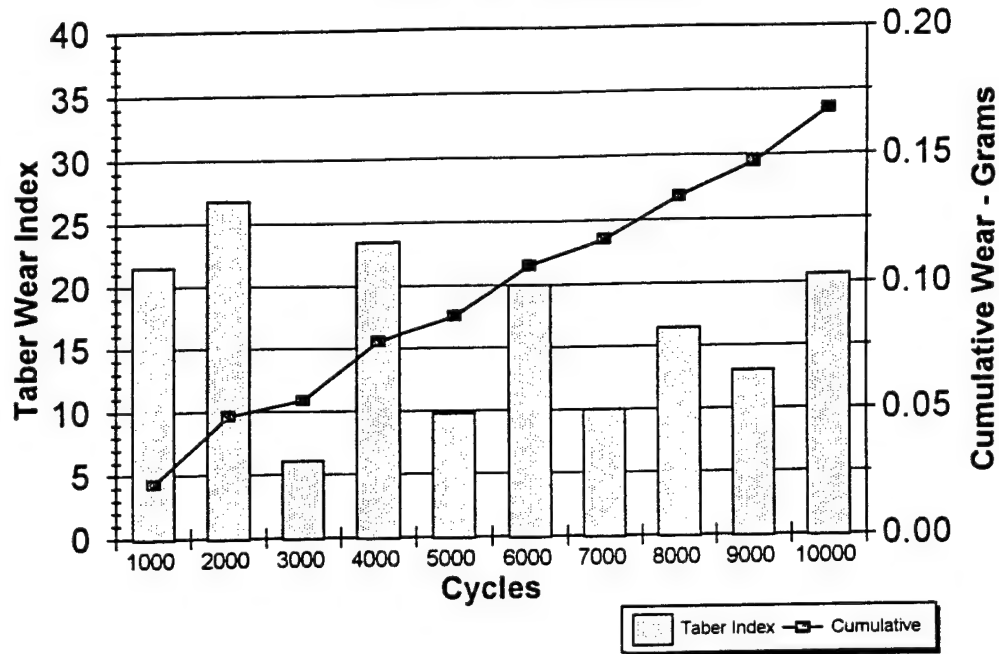


VERSAIloy 50 Taber Abraser Wear Test

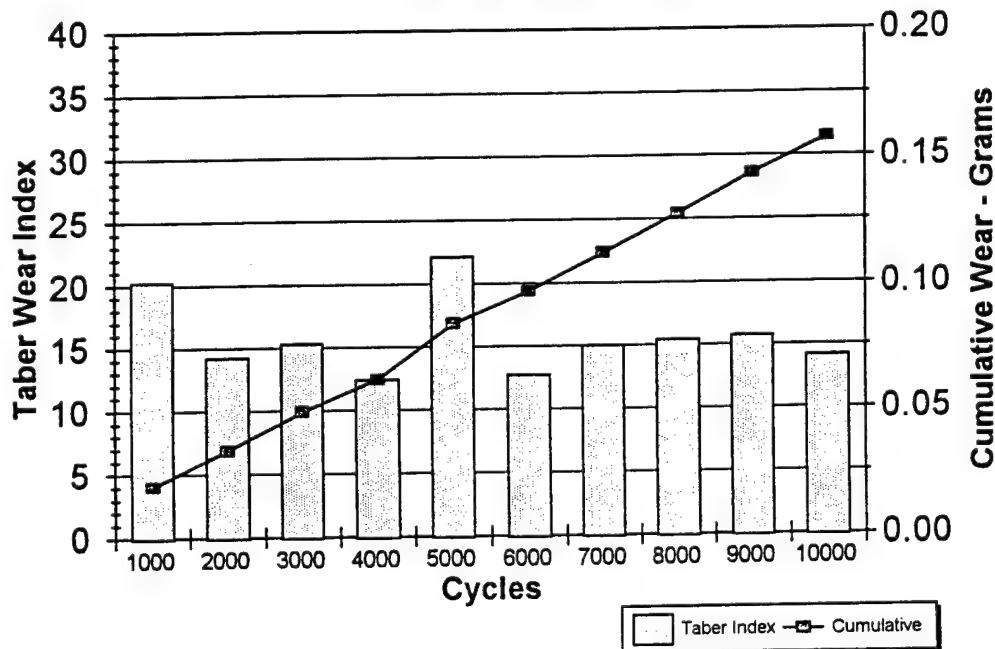
Test No. 95WIT023

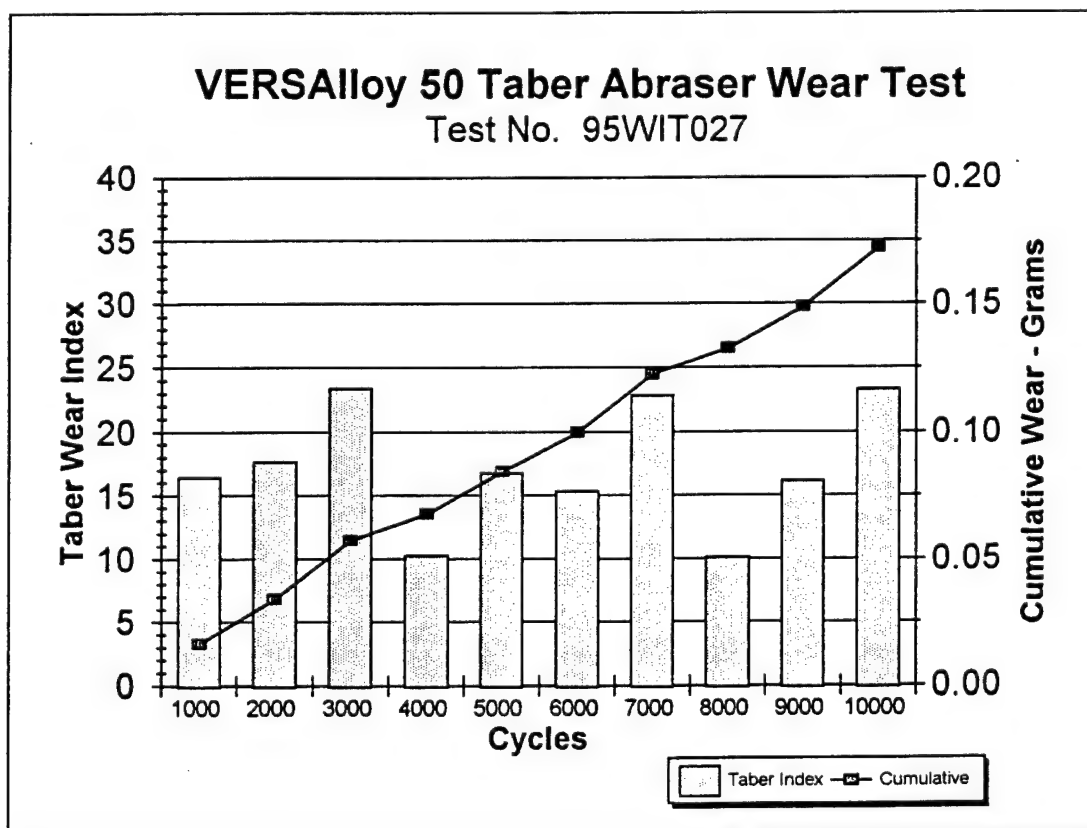
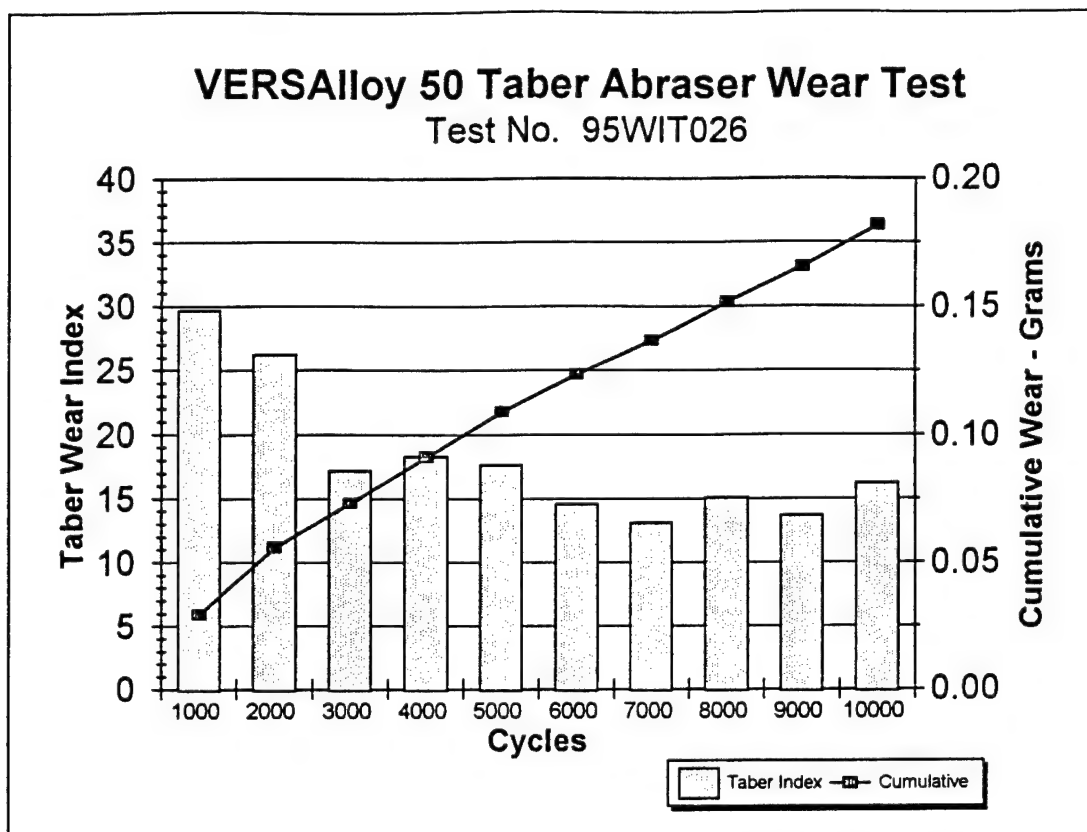


VERSAloy 50 Taber Abraser Wear Test **Test No. 95WIT024**



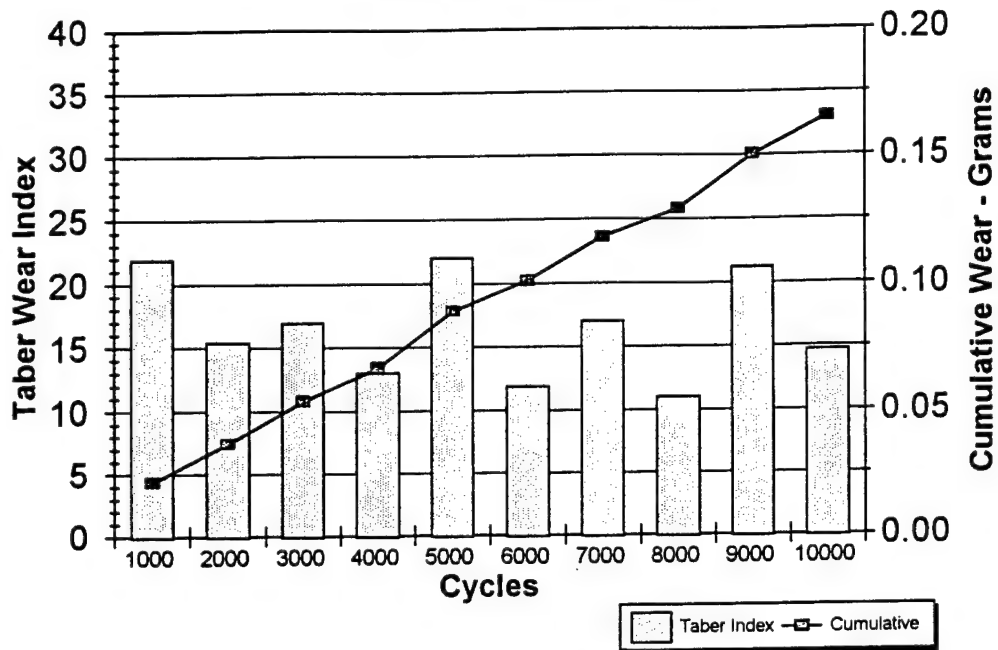
VERSAloy 50 Taber Abraser Wear Test **Test No. 95WIT025**





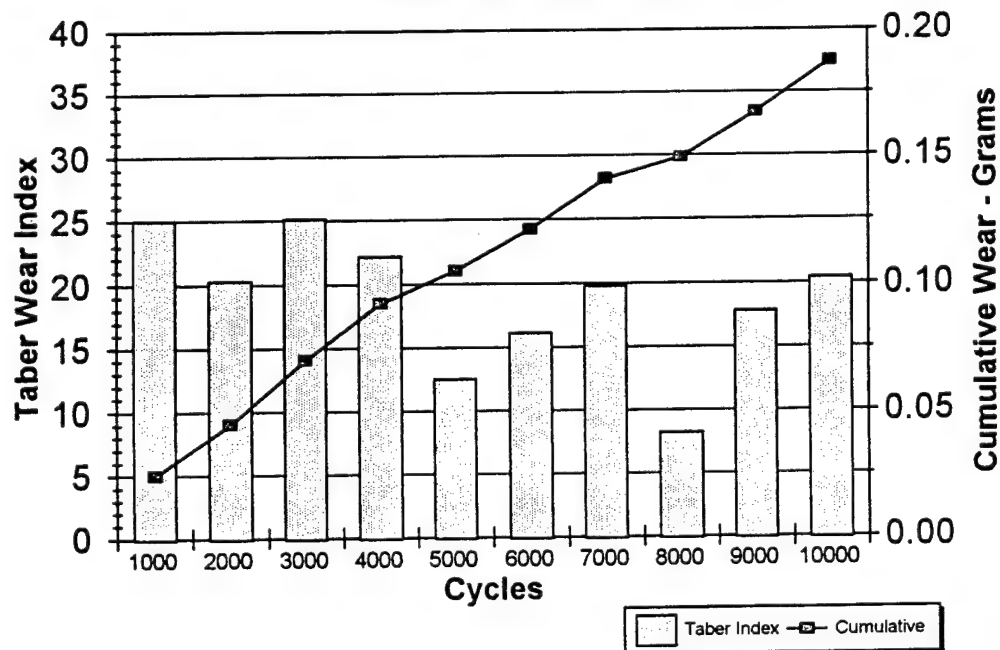
VERSAIloy 50 Taber Abraser Wear Test

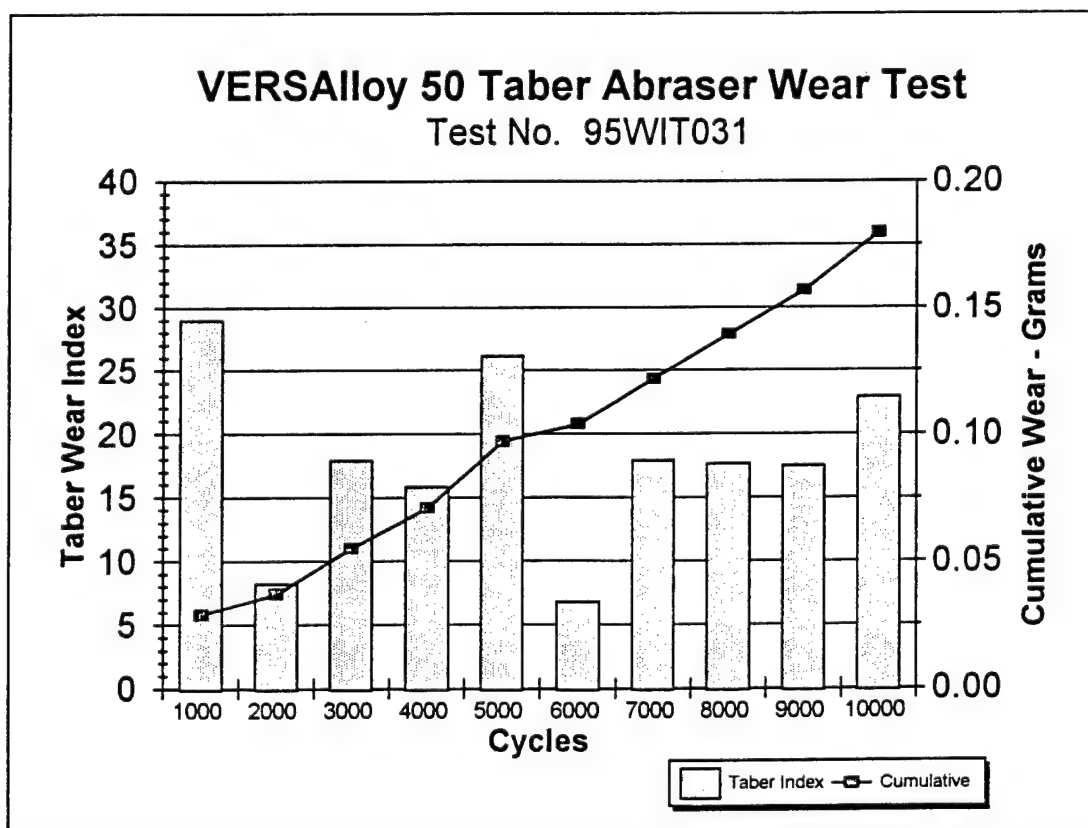
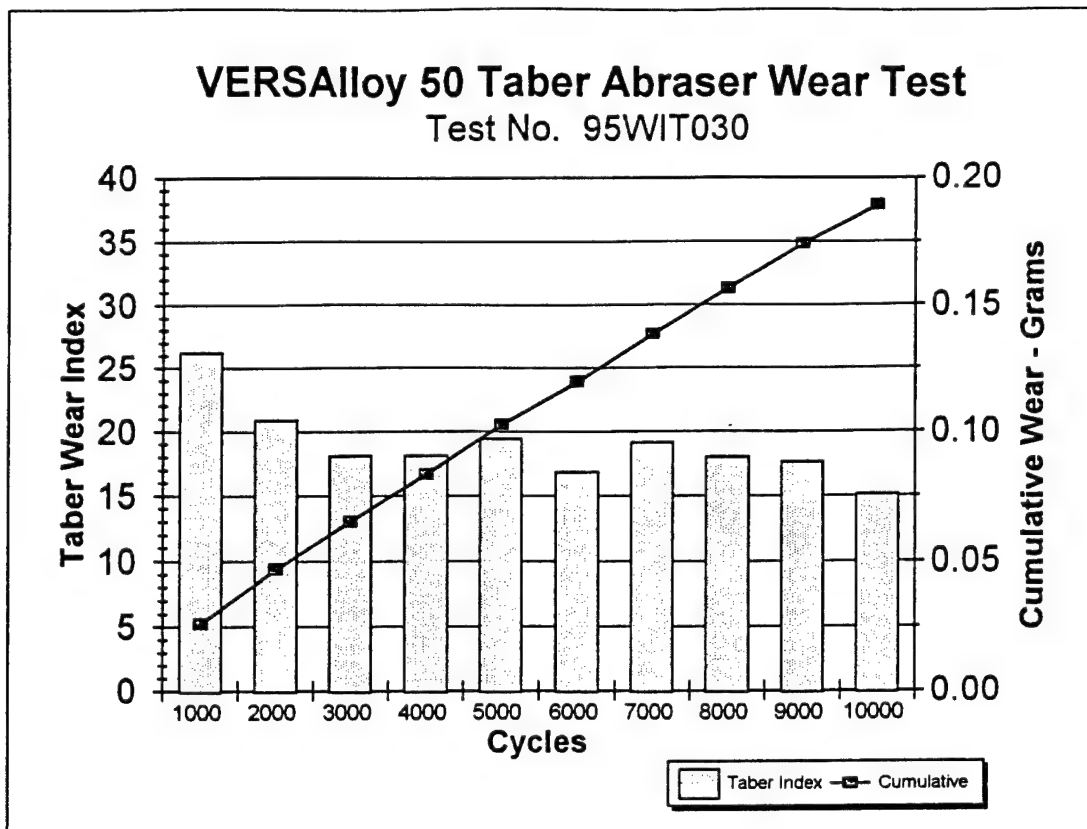
Test No. 95WIT028



VERSAIloy 50 Taber Abraser Wear Test

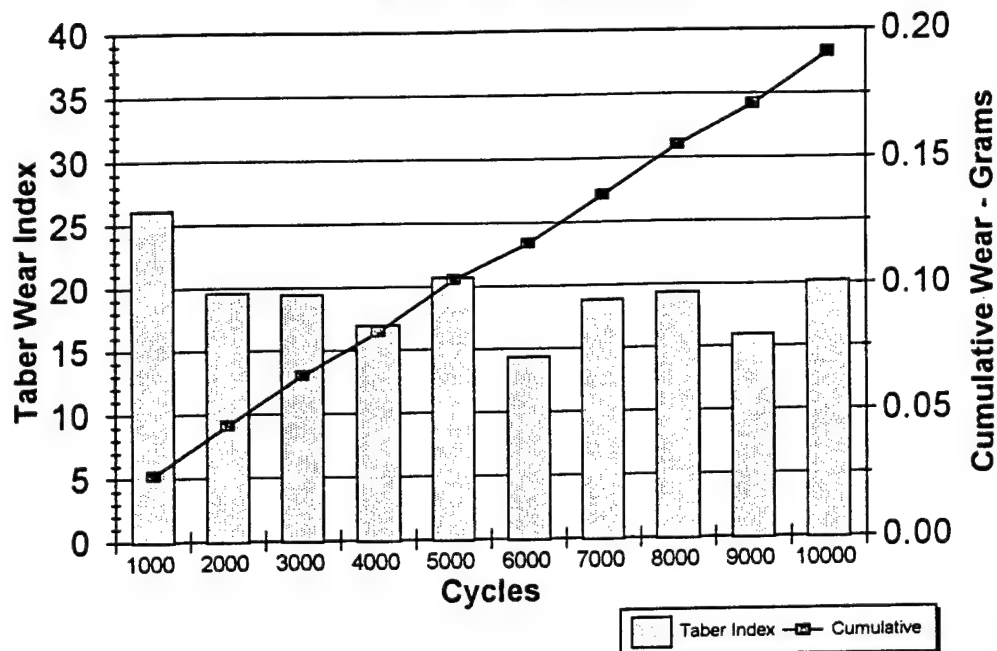
Test No. 95WIT029





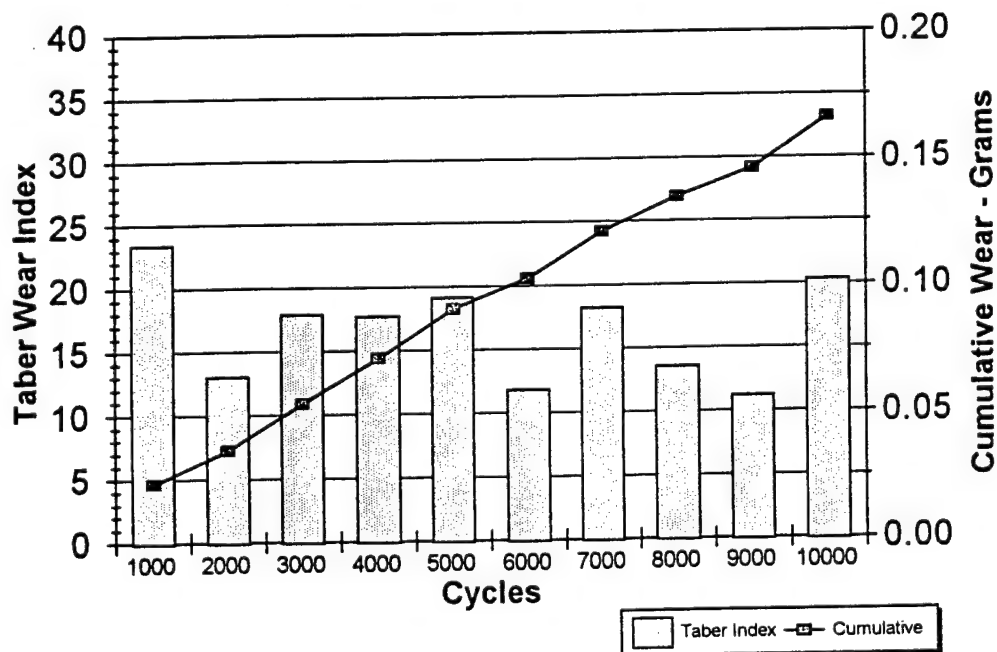
VERSAIloy 50 Taber Abraser Wear Test

Test No. 95WIT032



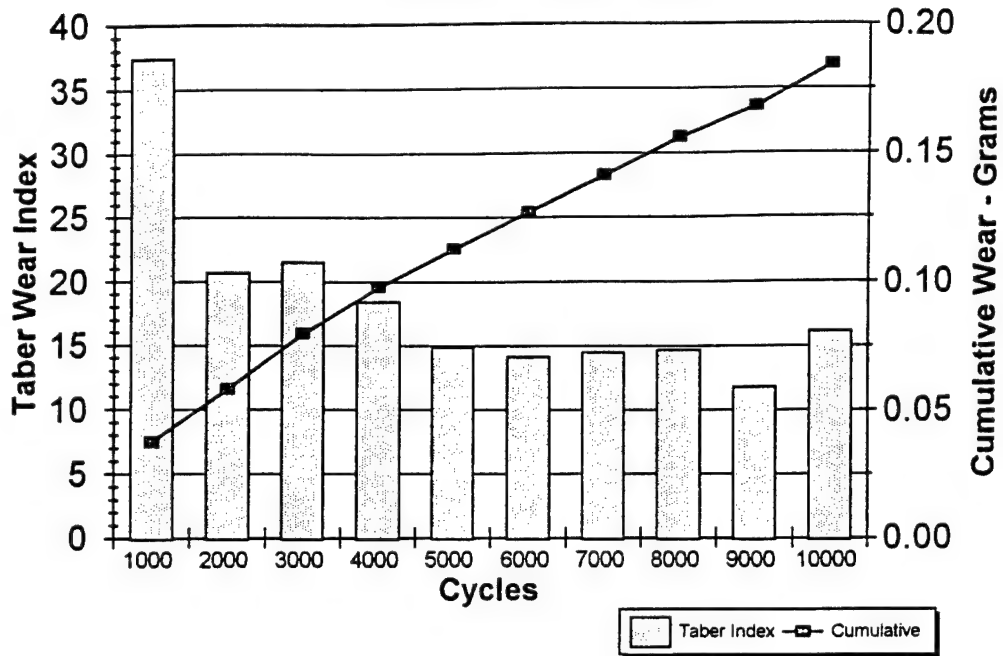
VERSAIloy 50 Taber Abraser Wear Test

Test No. 95WIT033



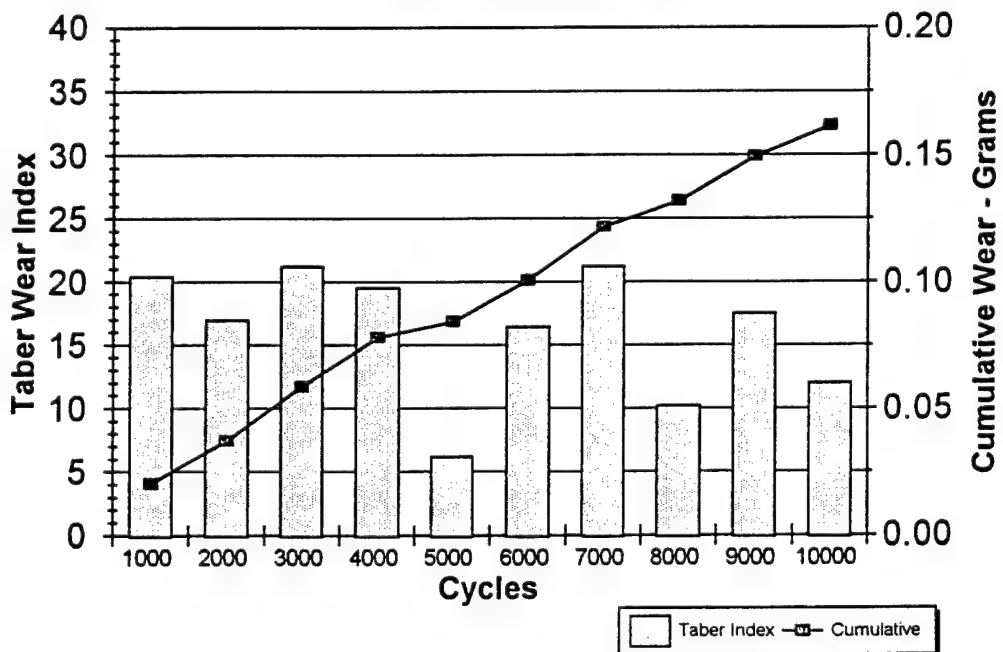
VERSAIloy 50 Taber Abraser Wear Test

Test No. 05WIT034



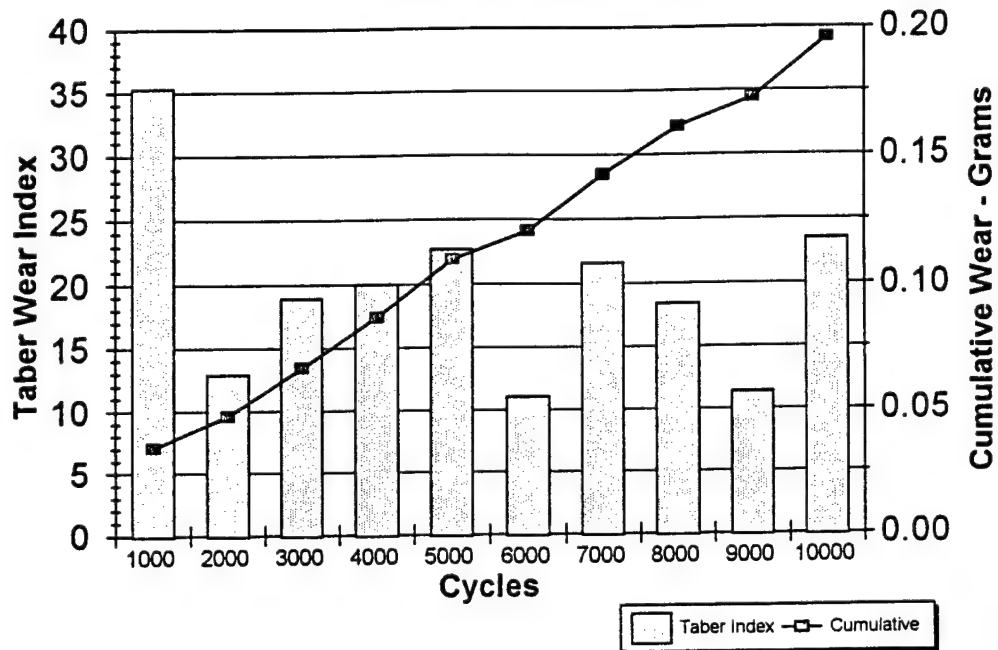
VERSAIloy 50 Taber Abraser Wear Test

Test No.95WIT035



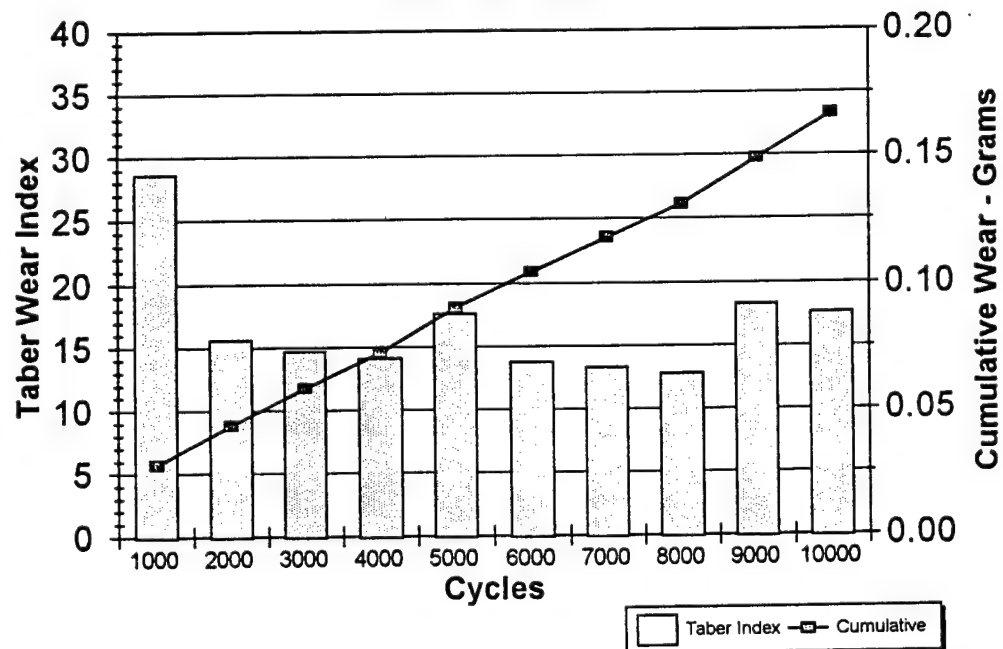
VERSAAlloy 50 Taber Abraser Wear Test

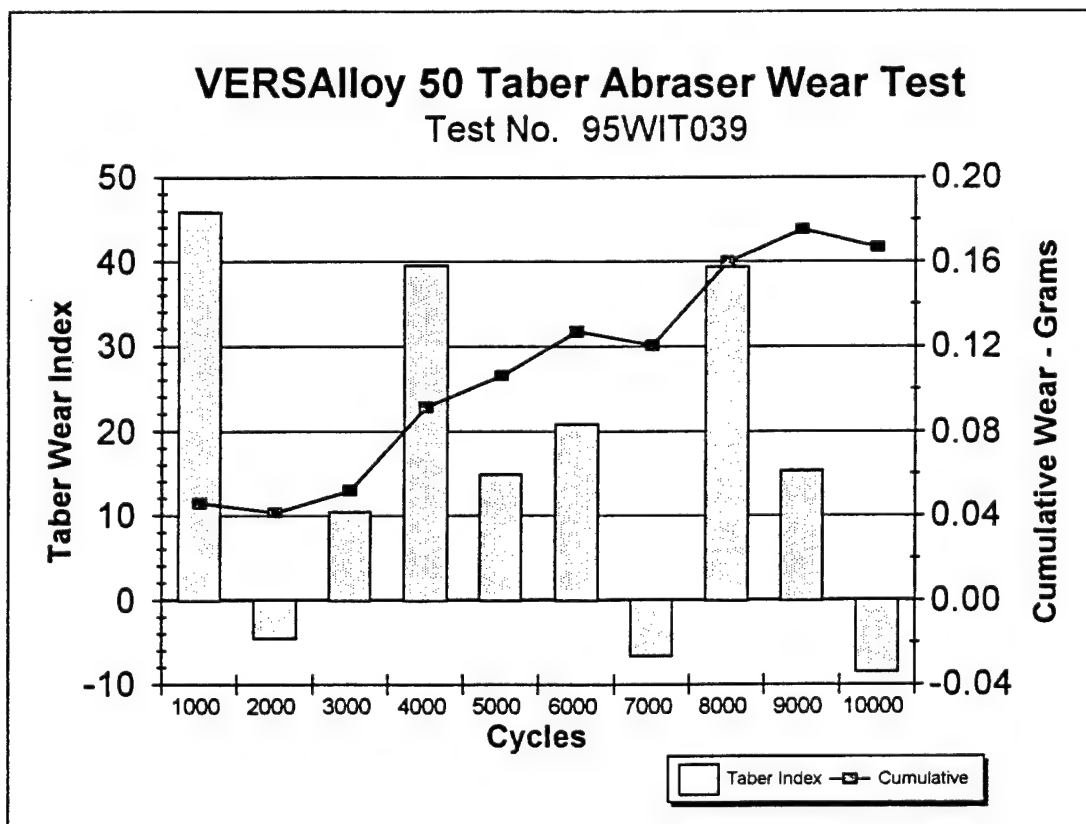
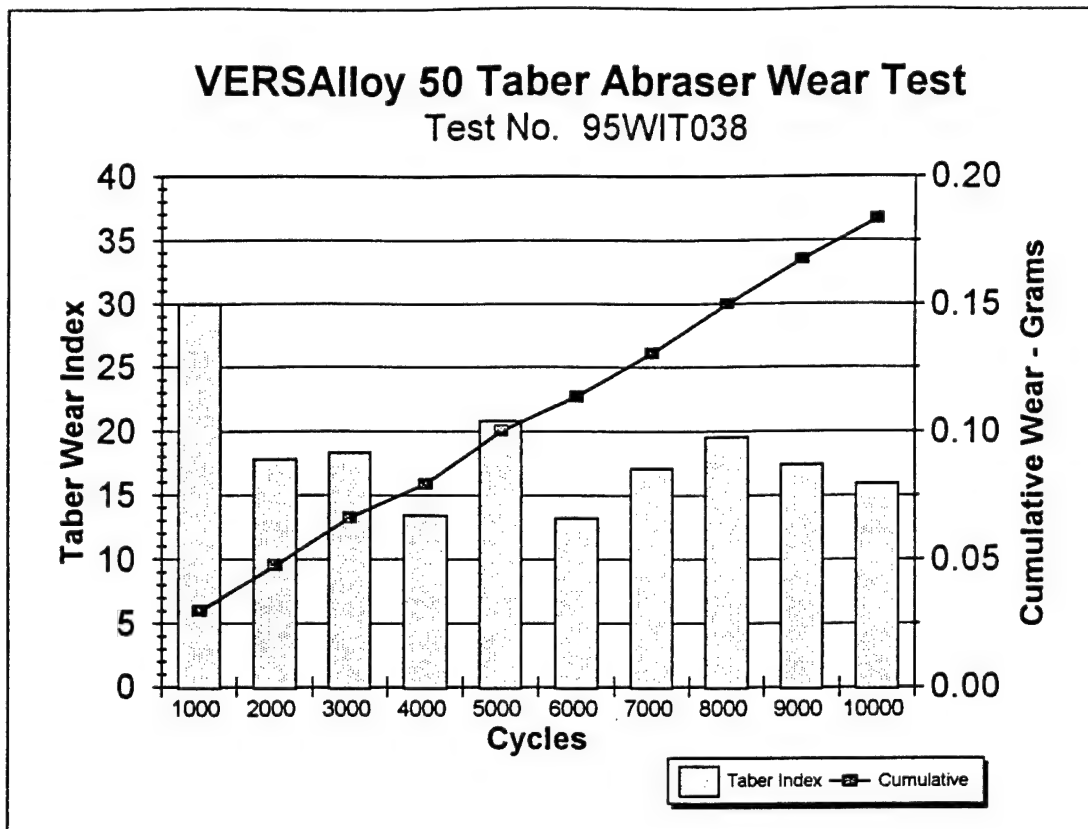
Test No. 95WIT036



VERSAAlloy 50 Taber Abraser Wear Test

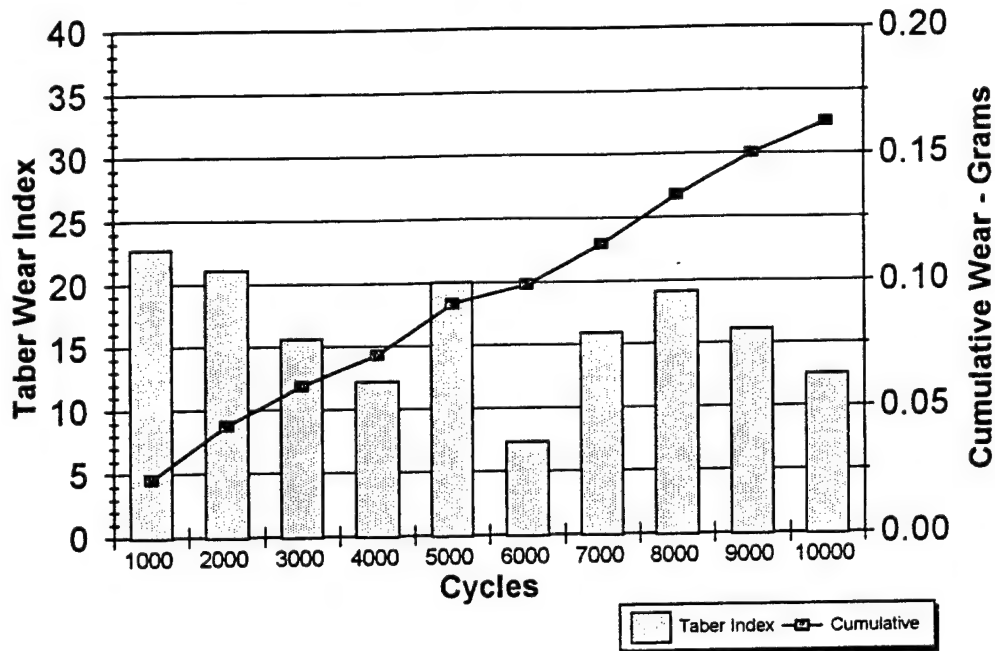
Test No. 95WIT037





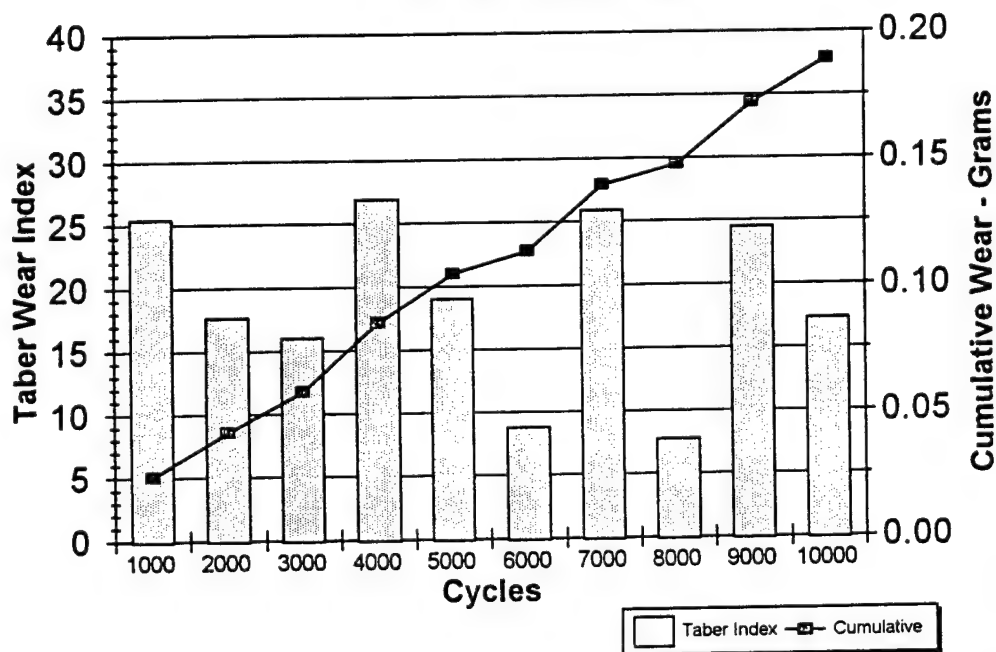
VERSAIloy 50 Taber Abraser Wear Test

Test No. 95WIT040



VERSAIloy 50 Taber Abraser Wear Test

Test No. 95WIT041



APPENDIX G

Phase III Metallurgical Coupon Microstructures



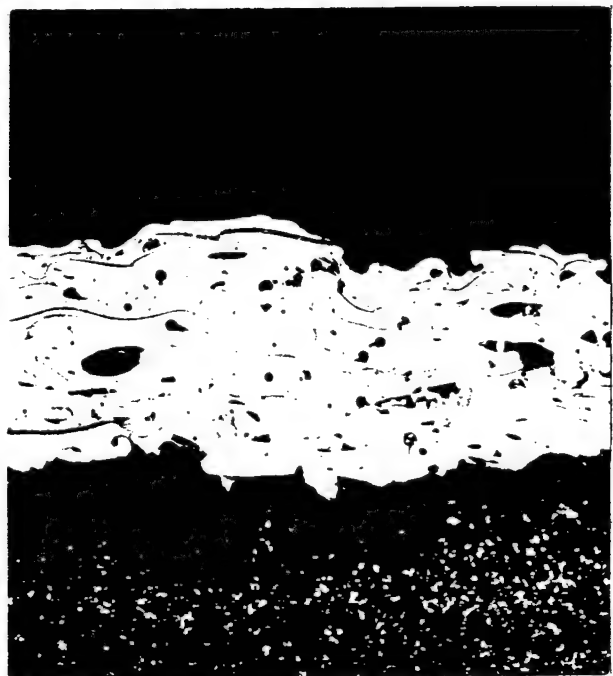
Test 95WIT020 (200x).



Test 95WIT021 (200x).



Test 95WIT022 (200x).



Test 95EIT023 (200x).



Test 95WIT024 (200x).



Test 95WIT025 (200x).



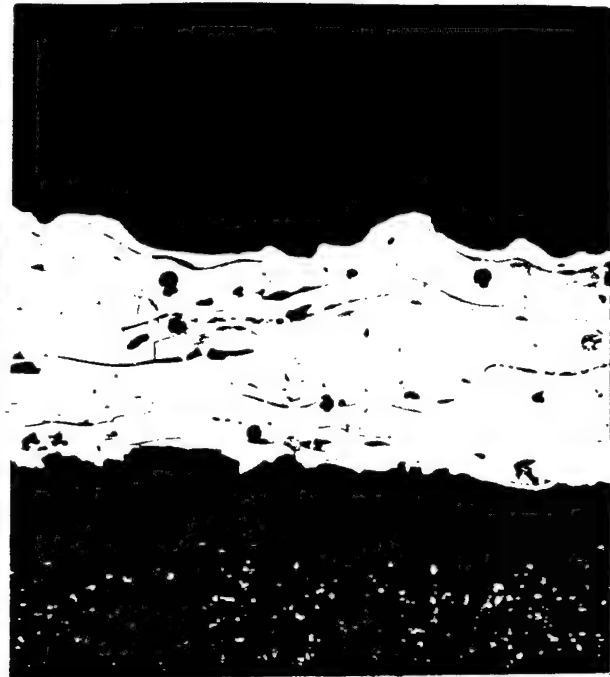
Test 95WIT026 (200x).



Test 95WIT027 (200x).



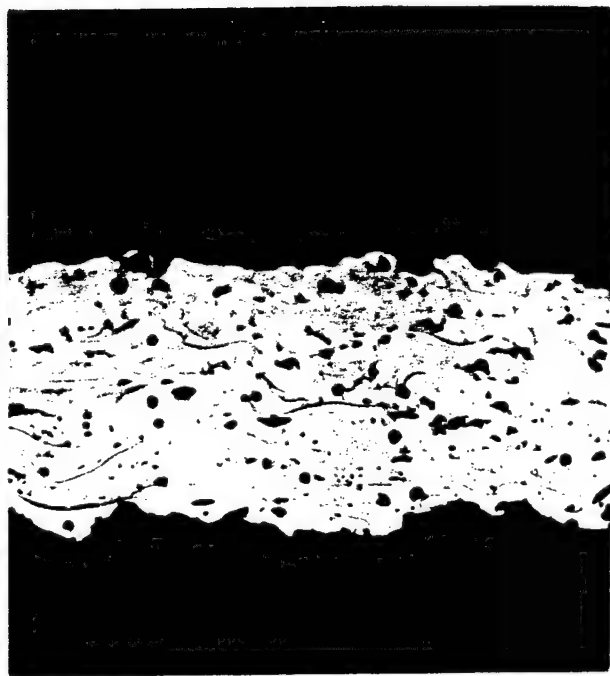
Test 95WIT028 (200x).



Test 95WIT029 (200x).



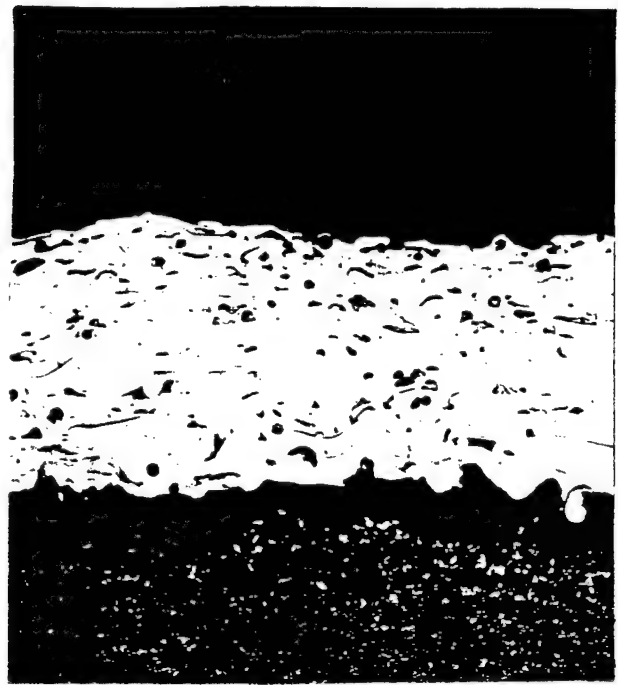
Test 95WIT030 (200x).



Test 95WIT031 (200x).



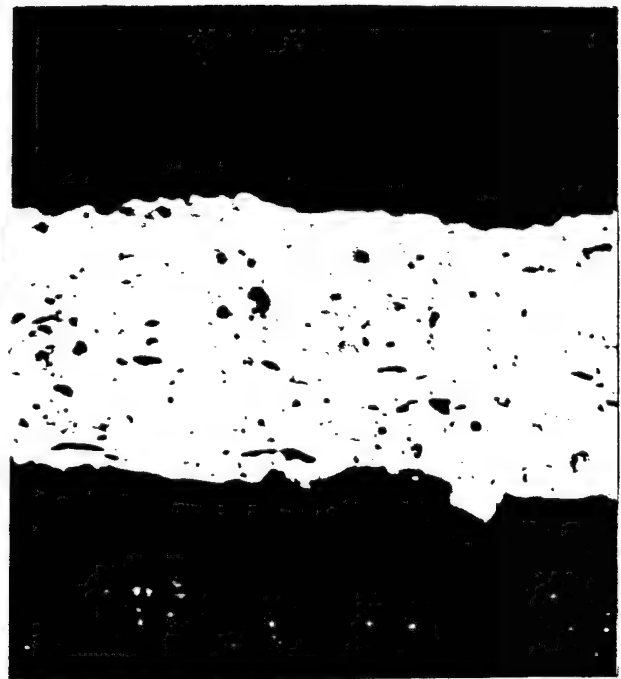
Test 95WIT032 (200x).



Test 95WIT033 (200x).



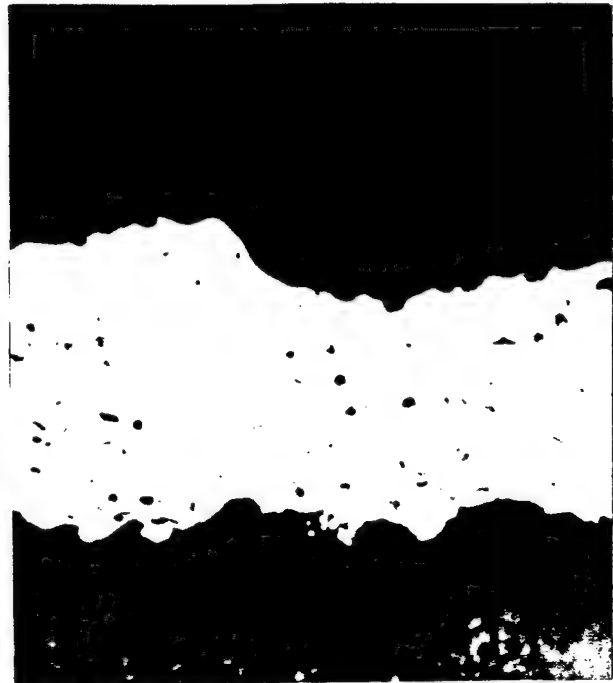
Test 95WIT034 (200x).



Test 95WIT035 (200x).



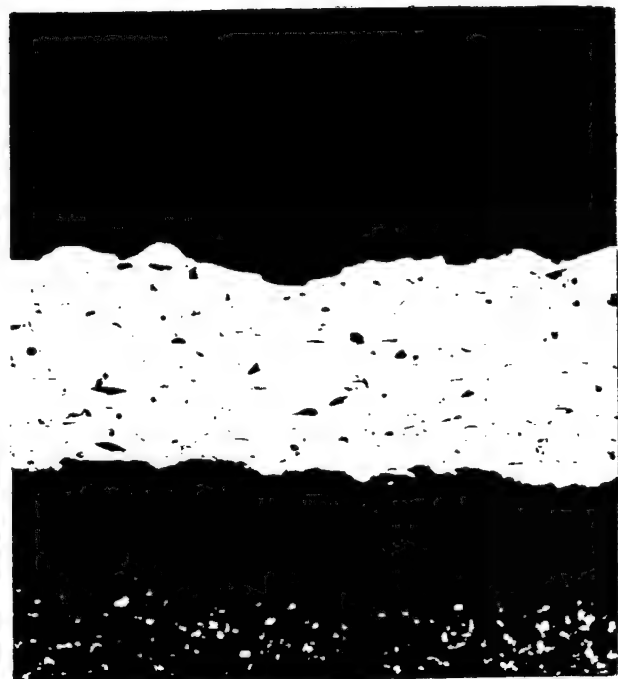
Test 95WIT036 (200x).



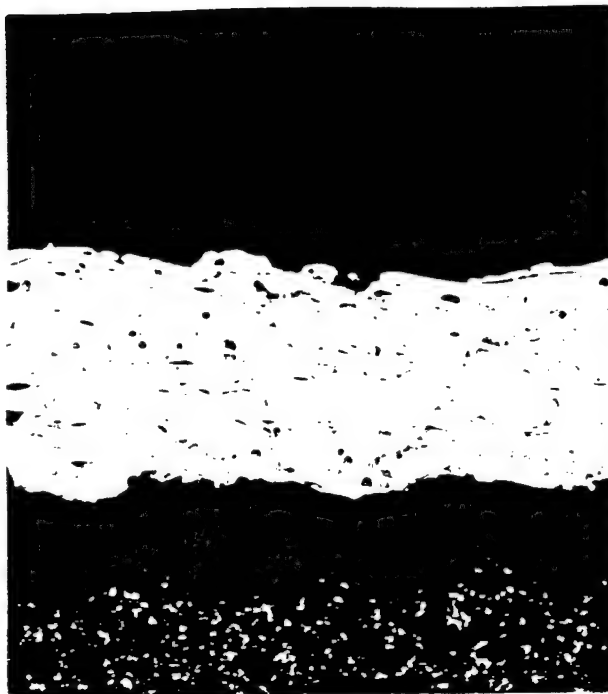
Test 95WIT037 (200x).



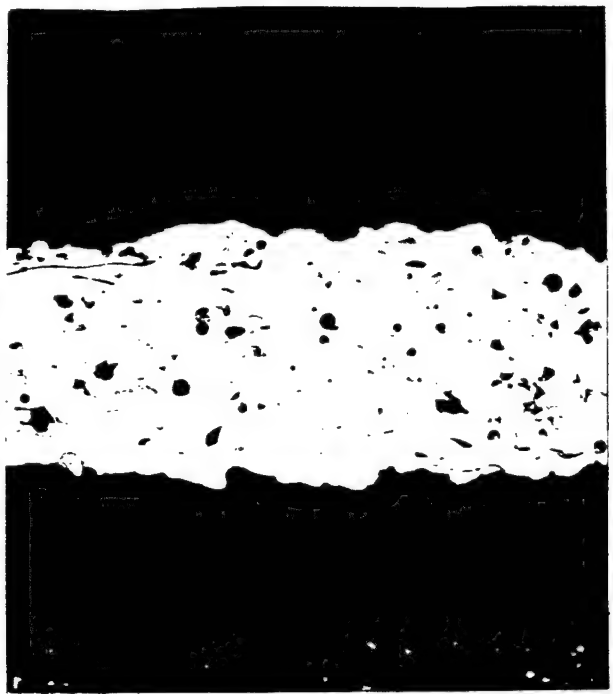
Test 95WIT038 (200x).



Test 95WIT039 (200x).



Test 95WIT040 (200x).

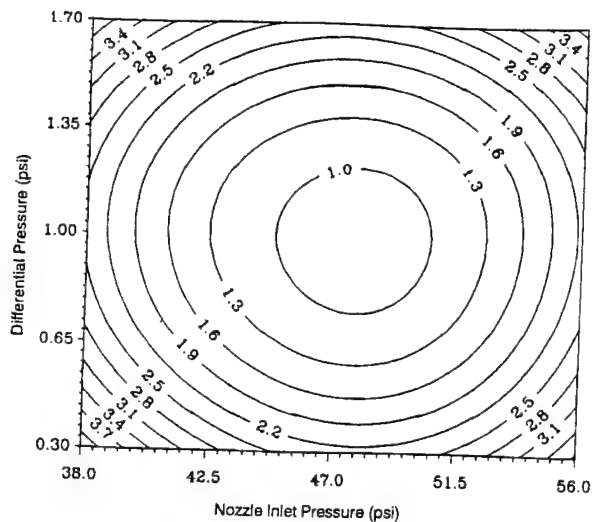


Test 95WIT041 (200x).

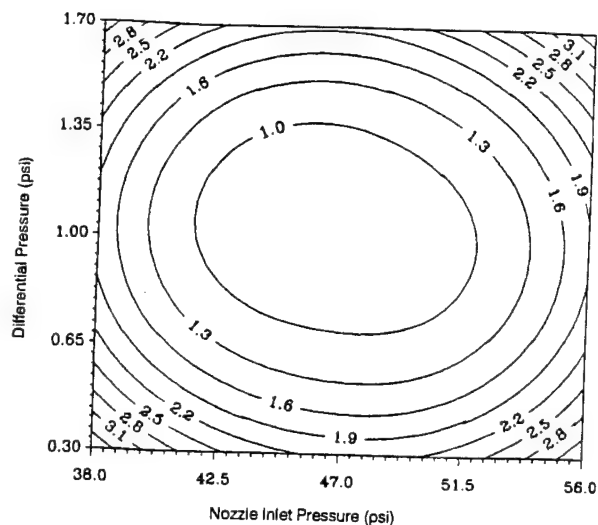
APPENDIX H

Predicted Responses and Standard Error Contour Plots for Phase III Test Results

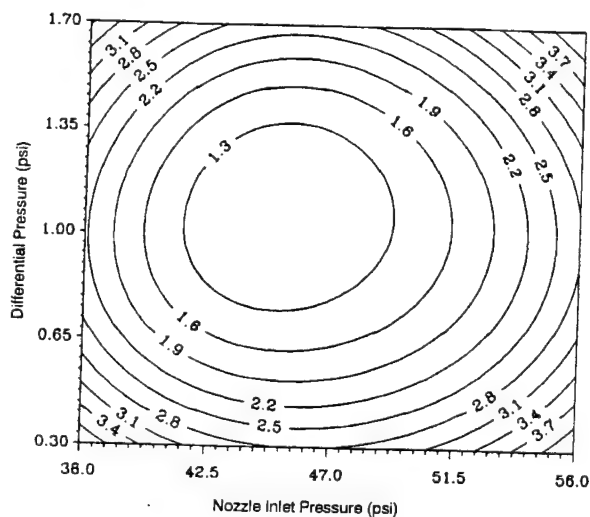
NOTE: The odd pages of this Appendix (plots of predicted error) were originally transparent overlays for the even pages (plots of predicted responses).



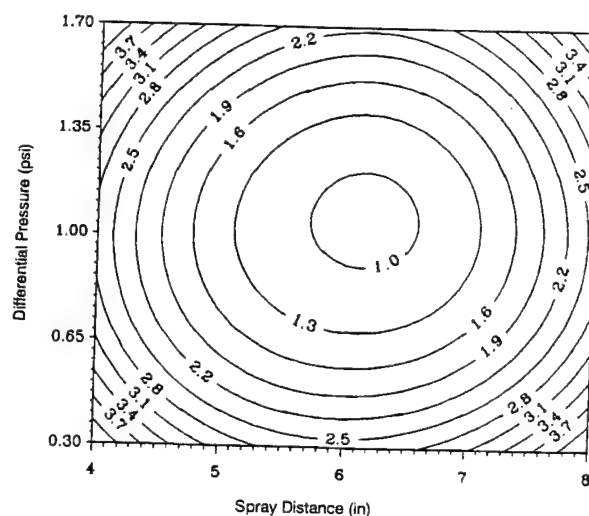
• Contour Plot of predicted standard error for "Corrosion" model. Spray Distance=5 in. and Feedstock=2.



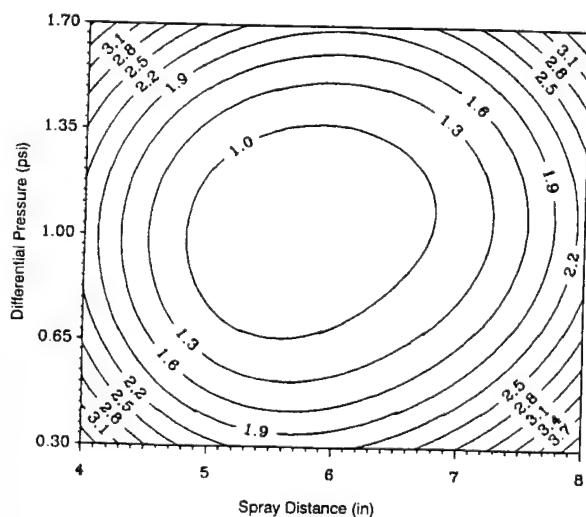
Contour Plot of predicted standard error for "Corrosion" model. Spray Distance=6 in. and Feedstock=2.



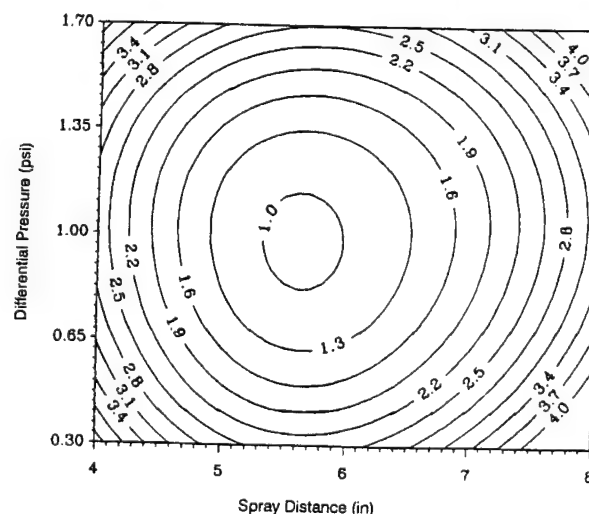
Contour Plot of predicted standard error for "Corrosion" model. Spray Distance=7 in. and Feedstock=2.



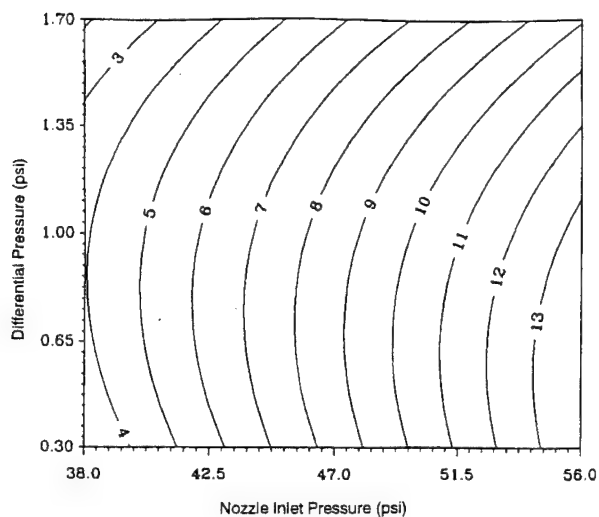
Contour Plot of predicted standard error for "Corrosion" model. Operating Pressure 42.0 psi and Feedstock=2.



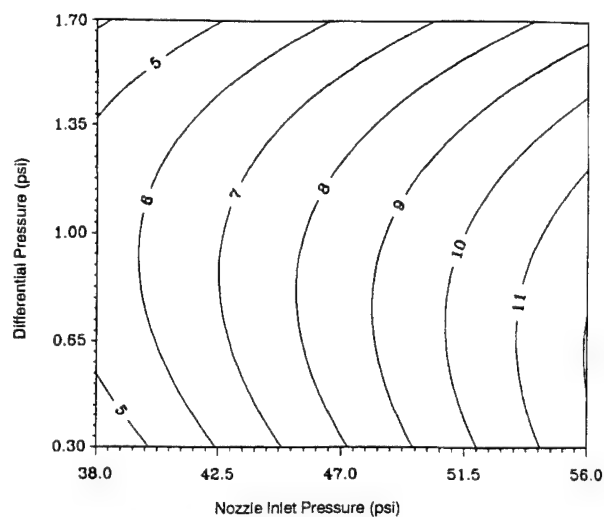
Contour Plot of predicted standard error for "Corrosion" model. Operating Pressure 47.0 psi and Feedstock=2.



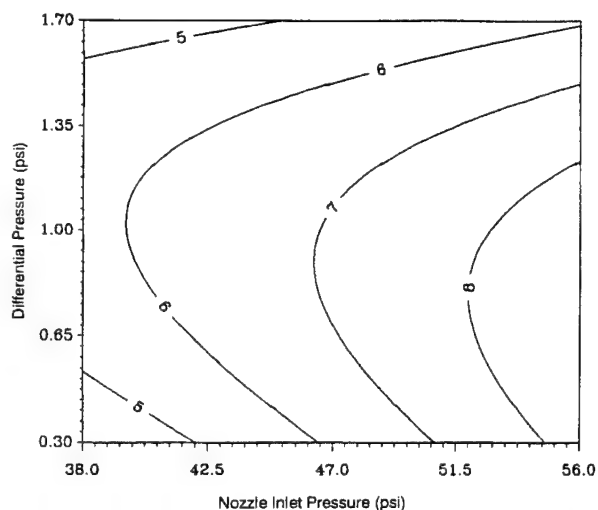
Contour Plot of predicted standard error for "Corrosion" model. Operating Pressure 52.0 psi and Feedstock=2.



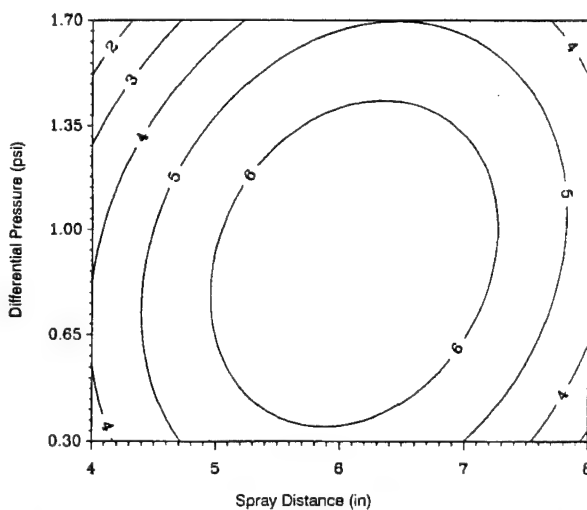
Contour Plot of predicted response for "Corrosion" model.
Spray Distance=5 in. and Feedstock=2.



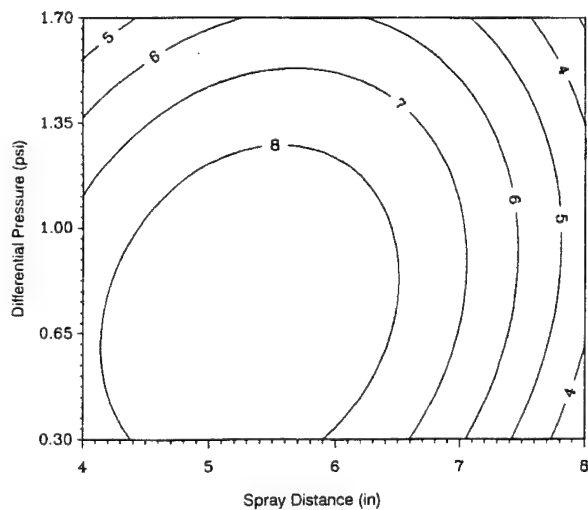
Contour Plot of predicted response for "Corrosion" model.
Spray Distance=6 in. and Feedstock=2.



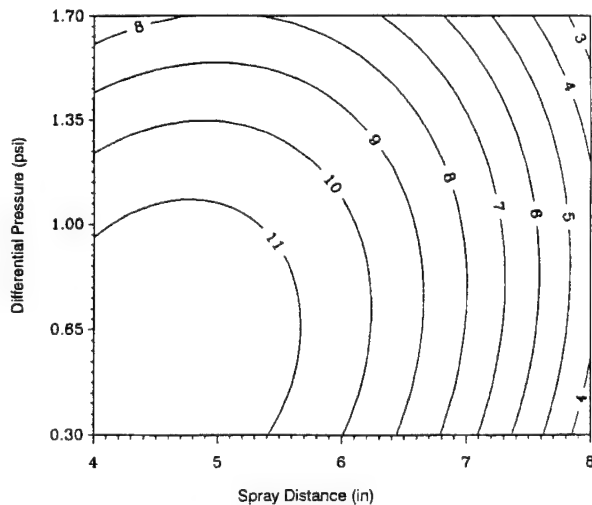
Contour Plot of predicted response for "Corrosion" model.
Spray Distance=7 in. and Feedstock=2.



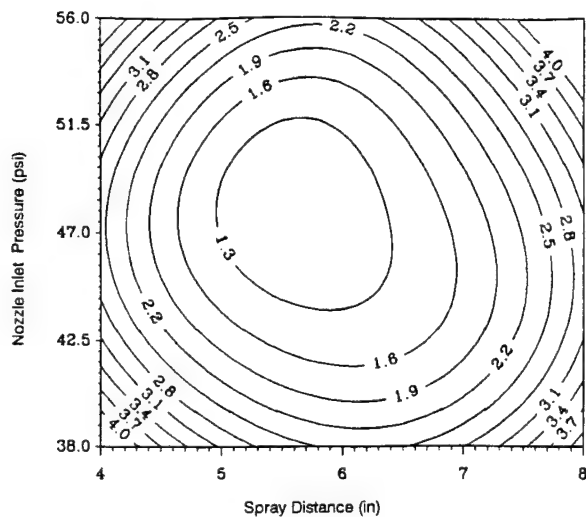
Contour Plot of predicted response for "Corrosion" model.
Operating Pressure 42.0 psi and Feedstock=2.



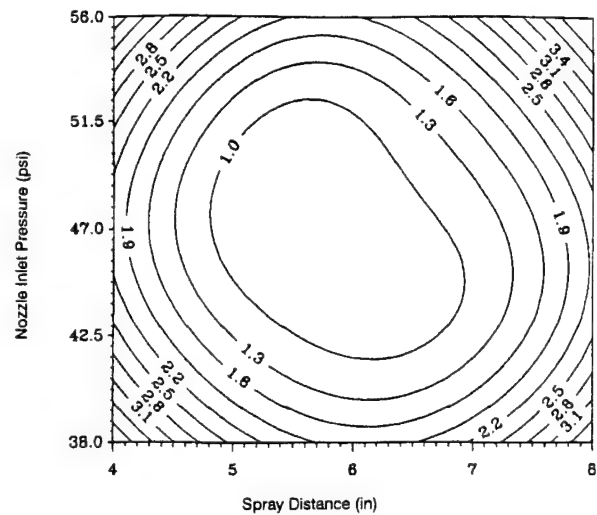
Contour Plot of predicted response for "Corrosion" model.
Operating Pressure 47.0 psi and Feedstock=2.



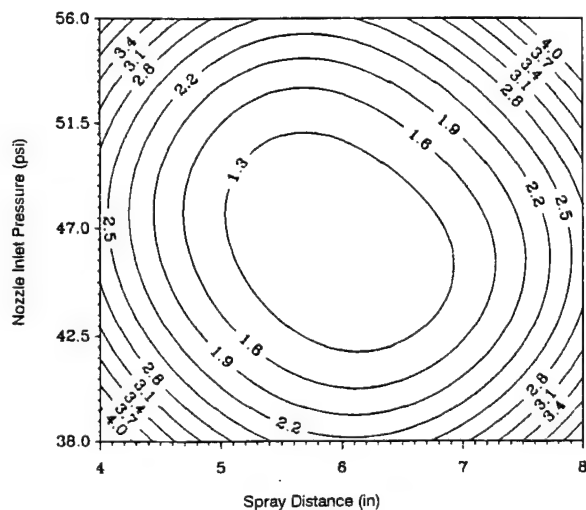
Contour Plot of predicted response for "Corrosion" model.
Operating Pressure 52.0 psi and Feedstock=2.



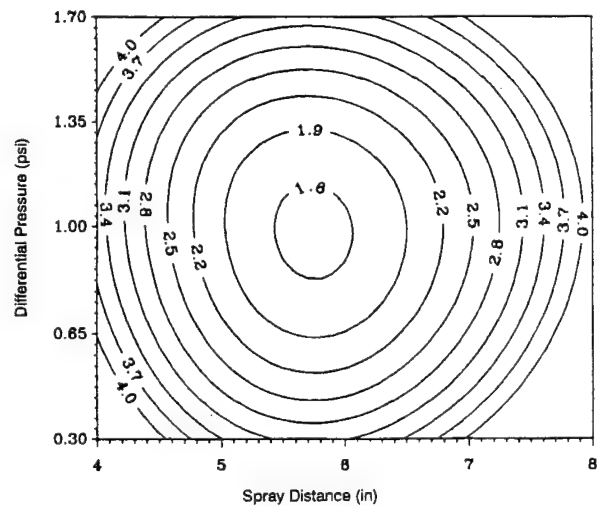
Contour Plot of predicted standard error for "Corrosion" model. Pressure Differential=0.6 psi and Feedstock=2.



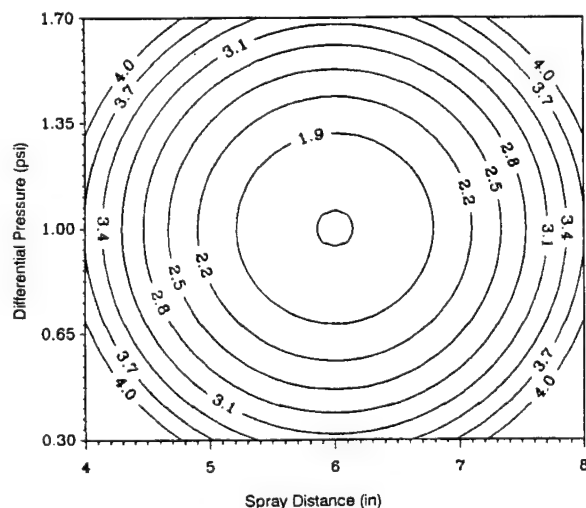
Contour Plot of predicted standard error for "Corrosion" model. Pressure Differential=1.0 psi and Feedstock=2.



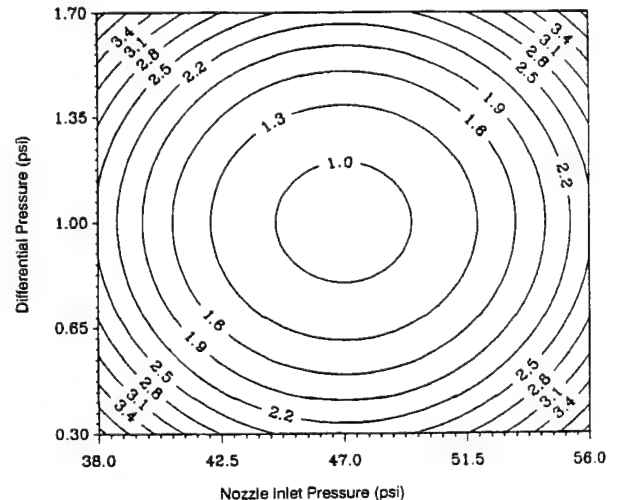
Contour Plot of predicted standard error for "Corrosion" model. Pressure Differential=1.4 psi and Feedstock=2.



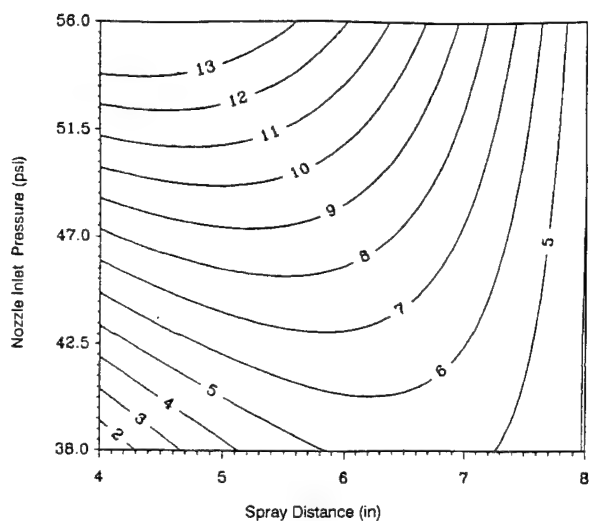
Contour Plot of predicted standard error for "Corrosion" model. Operating Pressure 55.0 psi and Feedstock=2.



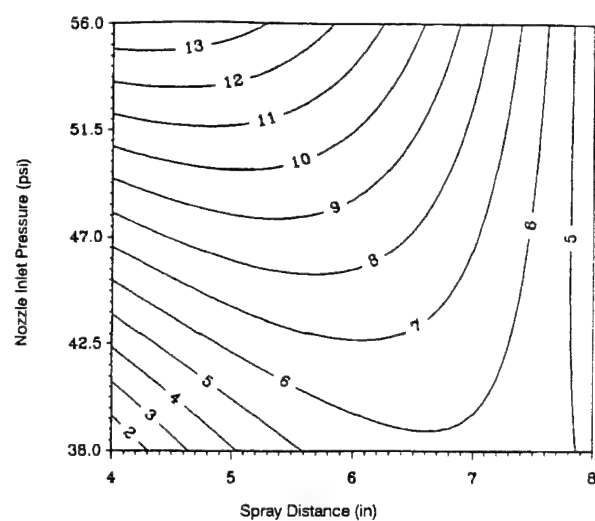
Contour Plot of predicted standard error for "Corrosion" model. Operating Pressure 55.0 psi.



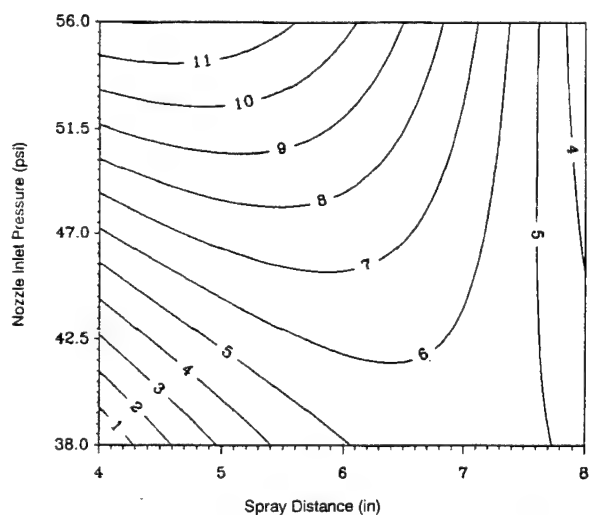
Contour Plot of predicted standard error for "Corrosion" model. Spray Distance=5 in.



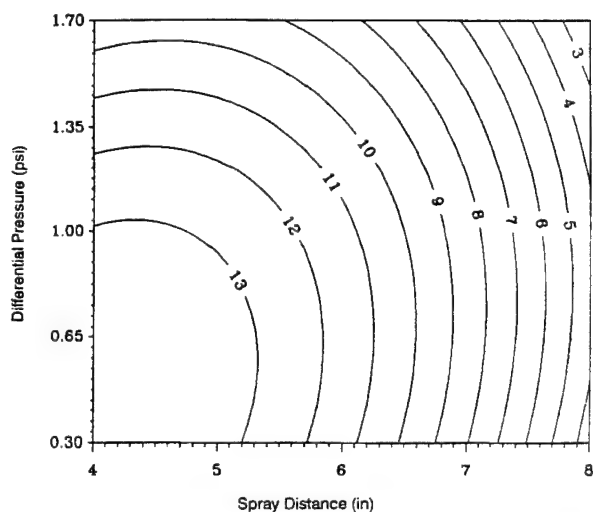
Contour Plot of predicted response for "Corrosion" model.
Pressure Differential=0.6 psi and Feedstock=2.



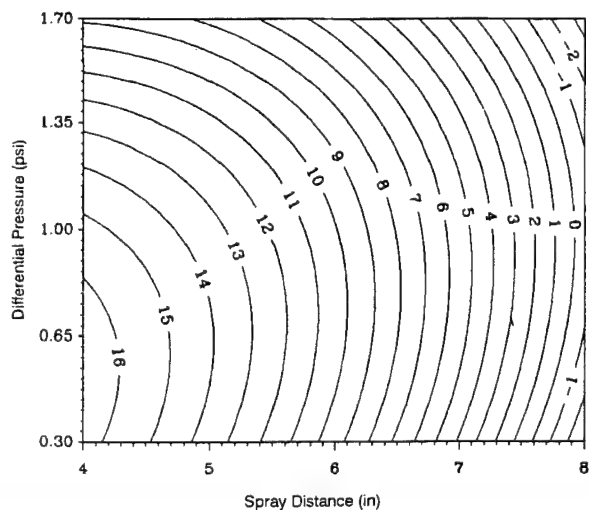
Contour Plot of predicted response for "Corrosion" model.
Pressure Differential=1.0 psi and Feedstock=2.



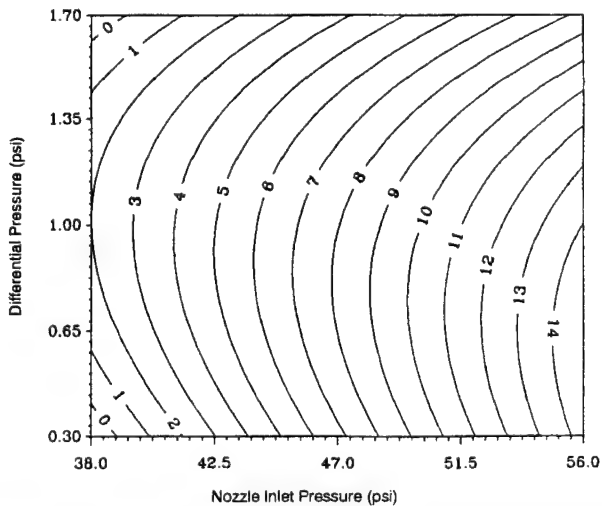
Contour Plot of predicted response for "Corrosion" model.
Pressure Differential=1.4 psi and Feedstock=2.



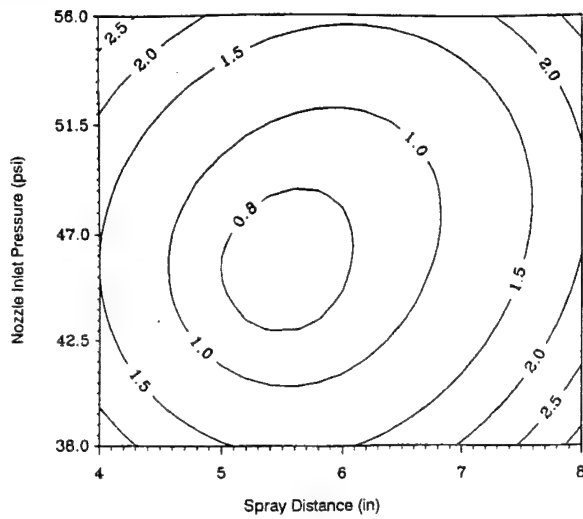
Contour Plot of predicted response for "Corrosion" model.
Operating Pressure 55.0 psi and Feedstock=2.



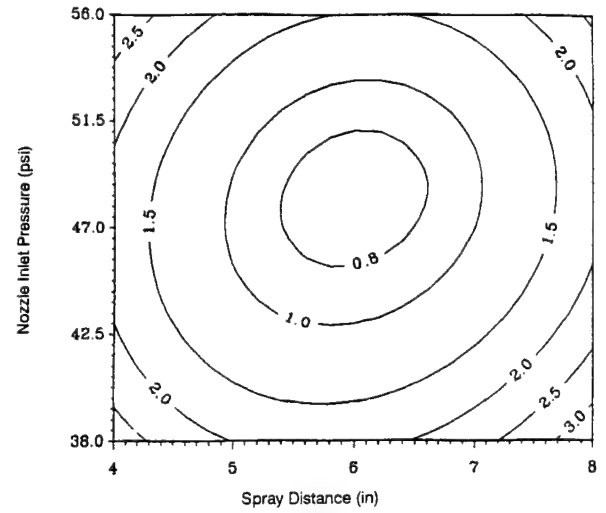
Contour Plot of predicted response for "Corrosion" model.
Operating Pressure 55.0 psi.



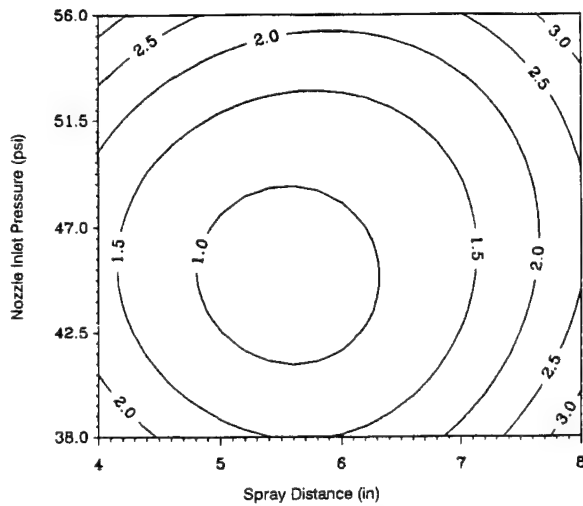
Contour Plot of predicted response for "Corrosion" model.
Spray Distance=5 in.



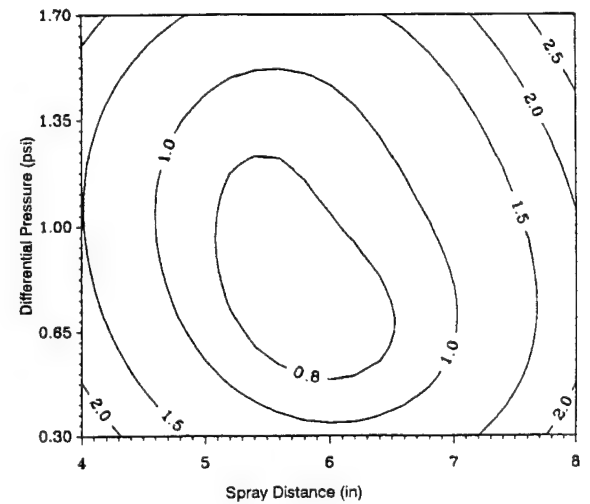
Contour Plot of predicted standard error for "Wear-1" model. Pressure Differential=1.0 psi and Thickness=0.010 in.



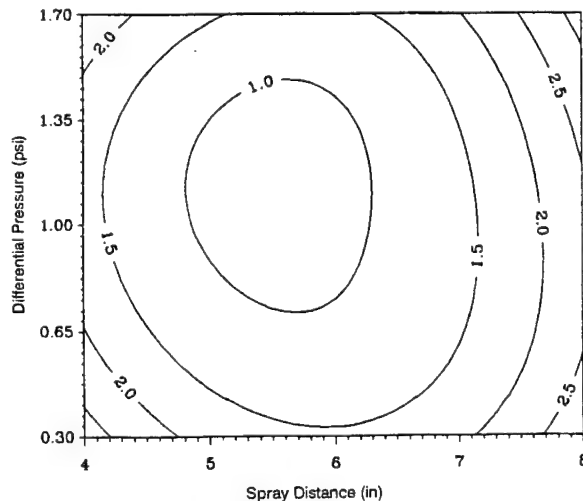
Contour Plot of predicted standard error for "Wear-1" model. Pressure Differential=0.6 psi and thickness=0.010 in.



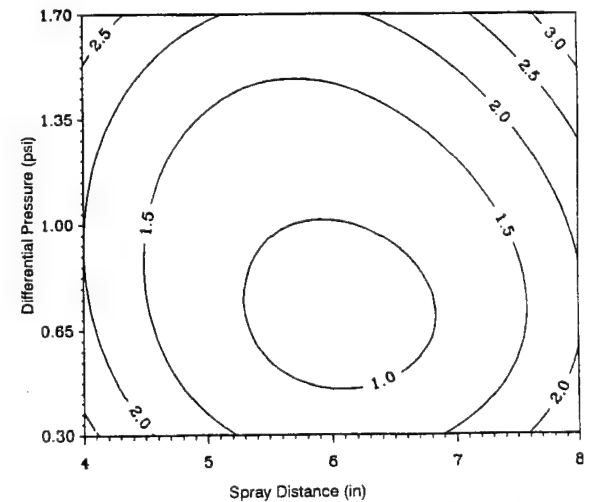
Contour Plot of predicted standard error for "Wear-1" model. Pressure Differential=1.4 psi and thickness=0.010 in.



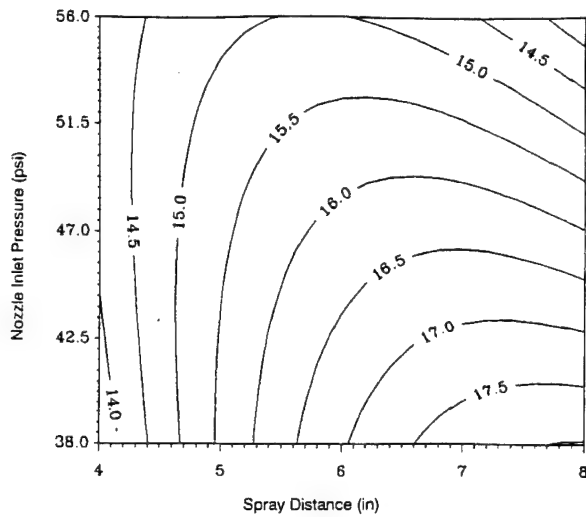
Contour Plot of predicted standard error for "Wear-1" model. Operating Pressure 47.0 psi and thickness=0.010 in.



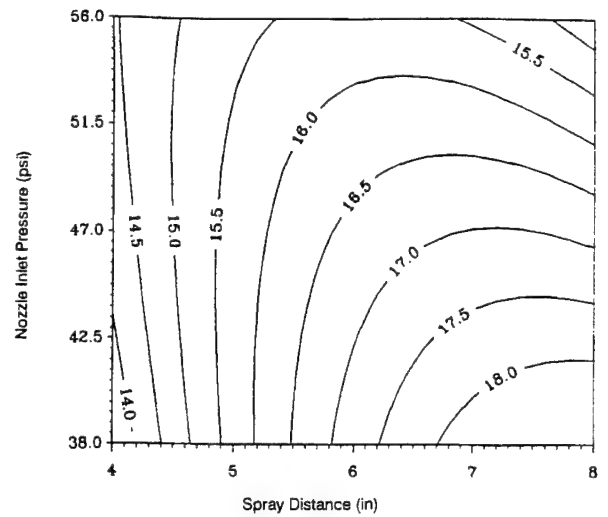
Contour Plot of predicted standard error for "Wear-1" model. Operating Pressure 42.0 psi and thickness=0.010 in.



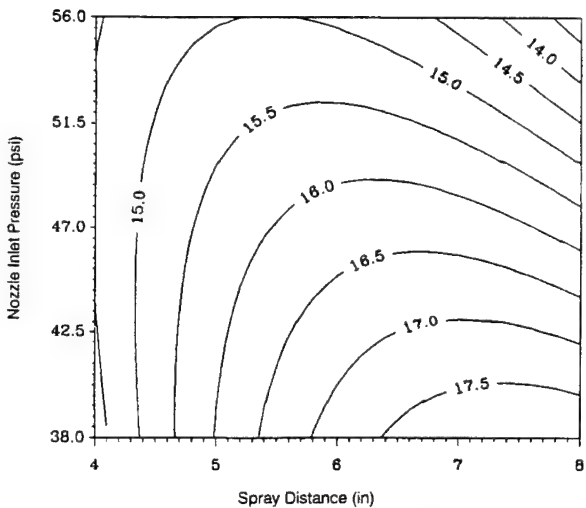
Contour Plot of predicted standard error for "Wear-1" model. Operating Pressure 52.0 psi and Thickness=0.010 in.



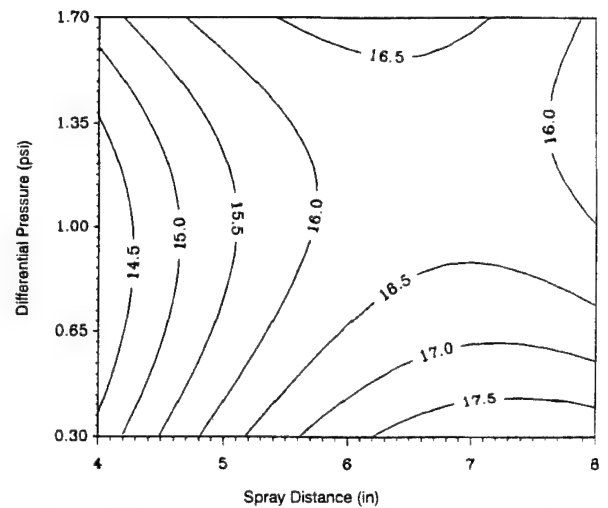
Contour Plot of predicted wear index for "Wear-1" model.
Pressure Differential=1.0 psi and Thickness=0.010 in.



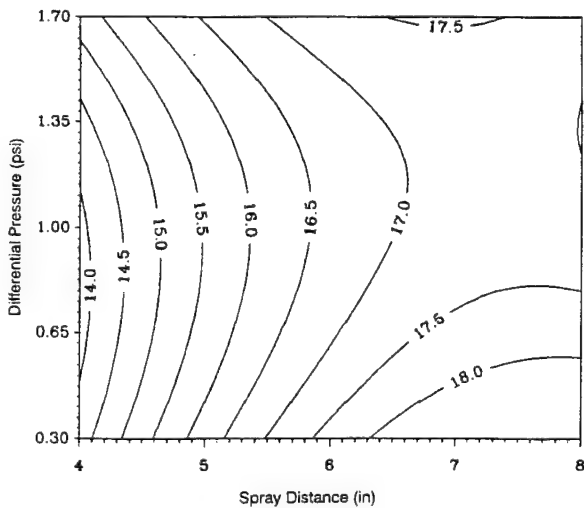
Contour Plot of predicted wear index for "Wear-1" model.
Pressure Differential=0.6 psi and thickness=0.010 in.



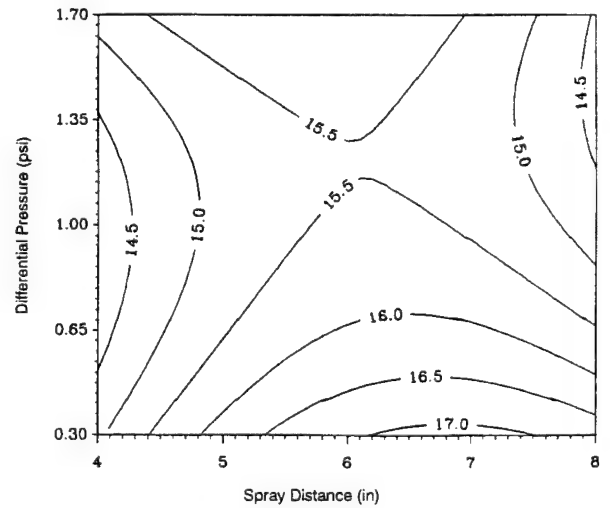
Contour Plot of predicted wear index for "Wear-1" model.
Pressure Differential=1.4 psi and thickness=0.010 in.



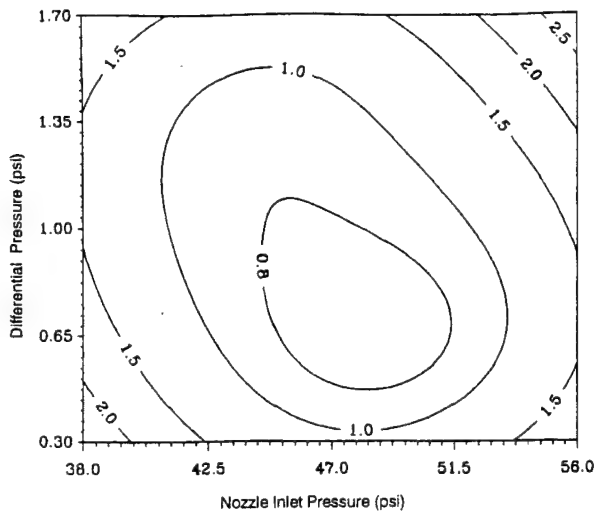
Contour Plot of predicted wear index for "Wear-1" model.
Operating Pressure 47.0 psi and thickness=0.010 in.



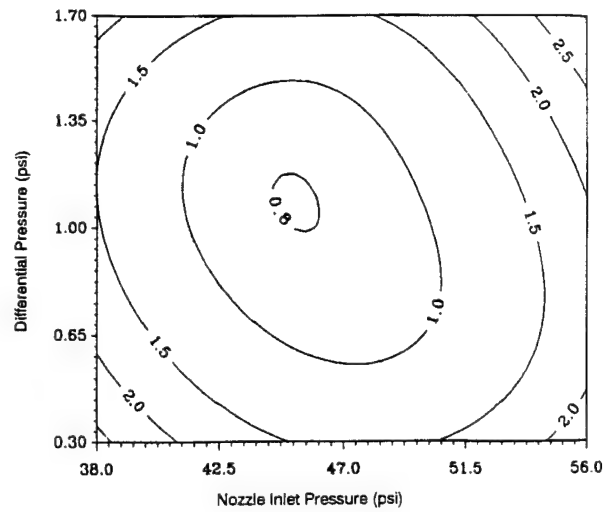
Contour Plot of predicted wear index for "Wear-1" model.
Operating Pressure 42.0 psi and thickness=0.010 in.



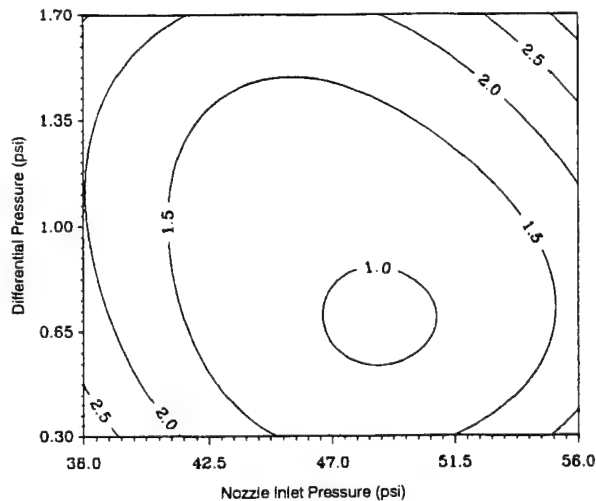
Contour Plot of predicted wear index for "Wear-1" model.
Operating Pressure 52.0 psi and Thickness=0.010 in.



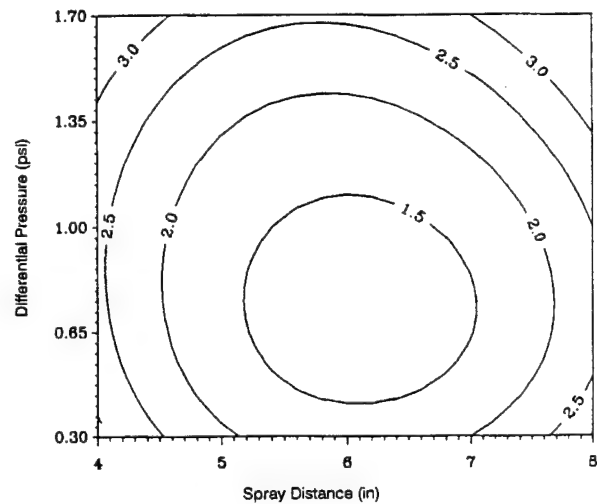
Contour Plot of predicted standard error for "Wear-1" model. Spray Distance=6.0 in. and thickness=0.010 in.



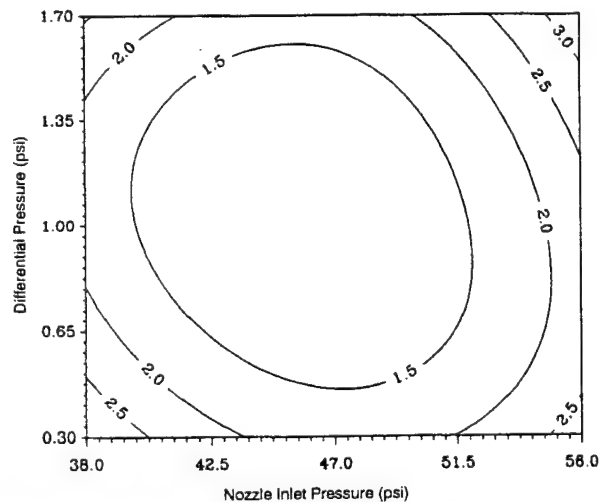
Contour Plot of predicted standard error for "Wear-1" model. Spray Distance=5 in. and thickness=0.010 in.



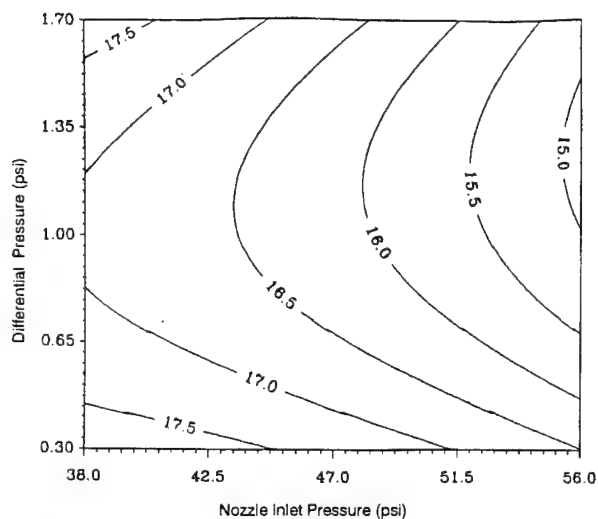
Contour Plot of predicted standard error for "Wear-1" model. Spray Distance=7 in. and thickness=0.010 in.



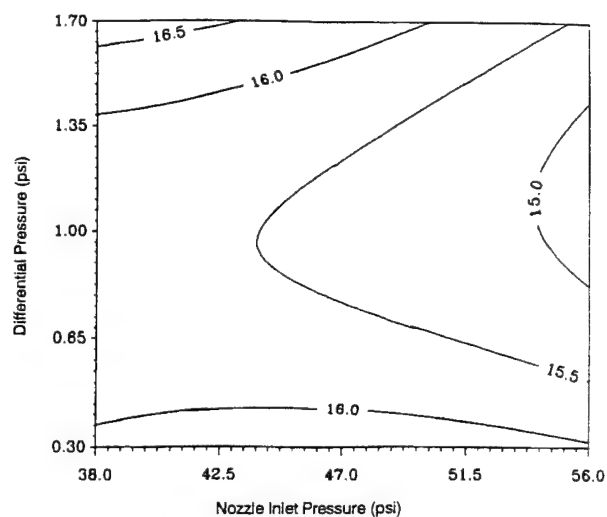
Contour Plot of predicted standard error for "Wear-1" model. Operating Pressure 55.0 psi and thickness=0.010 in.



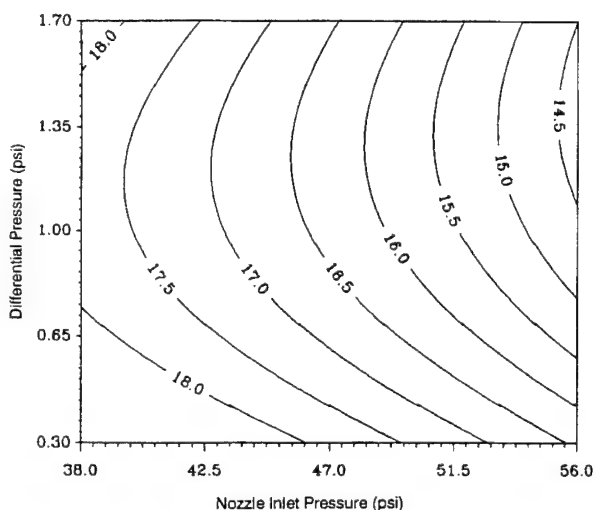
Contour Plot of predicted standard error for "Wear-1" model. Spray Distance=4.5 in. and thickness=0.010 in.



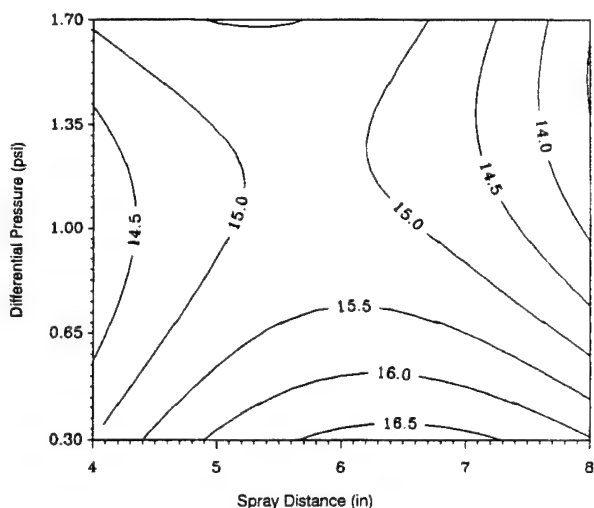
Contour Plot of predicted wear index for "Wear-1" model.
Spray Distance=6.0 in. and thickness=0.010 in.



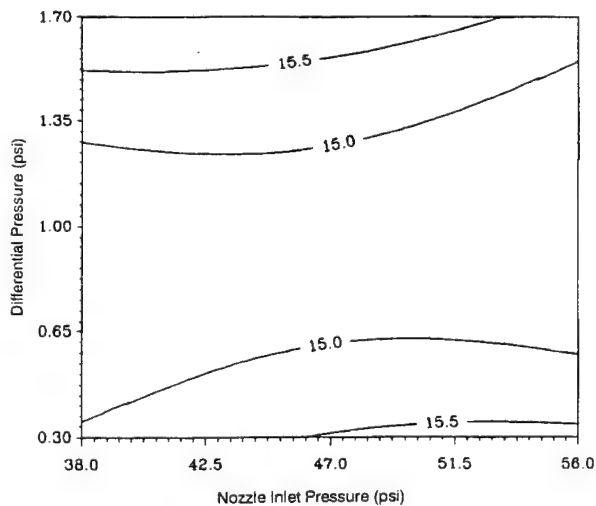
Contour Plot of predicted wear index for "Wear-1" model.
Spray Distance=5 in. and thickness=0.010 in.



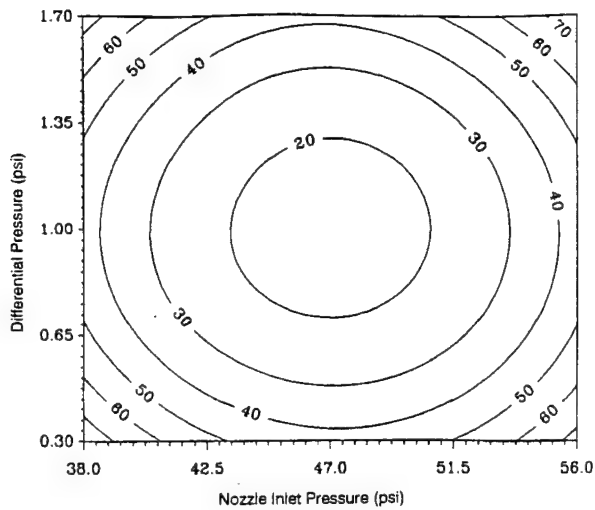
Contour Plot of predicted wear index for "Wear-1" model.
Spray Distance=7 in. and thickness=0.010 in.



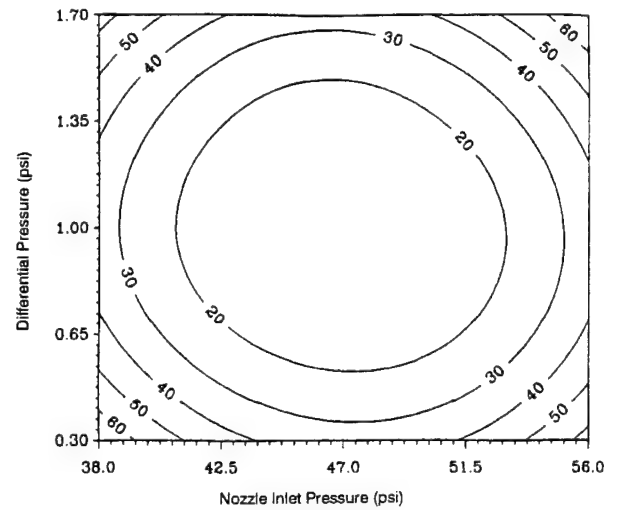
Contour Plot of predicted wear index for "Wear-1" model.
Operating Pressure 55.0 psi and thickness=0.010 in.



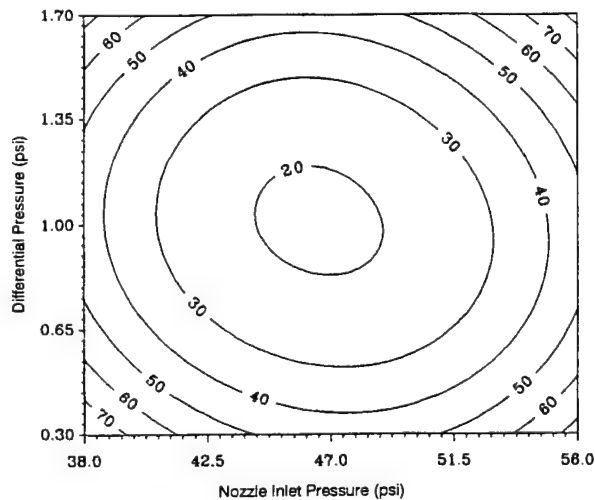
Contour Plot of predicted wear index for "Wear-1" model.
Spray Distance=4.5 in. and thickness=0.010 in.



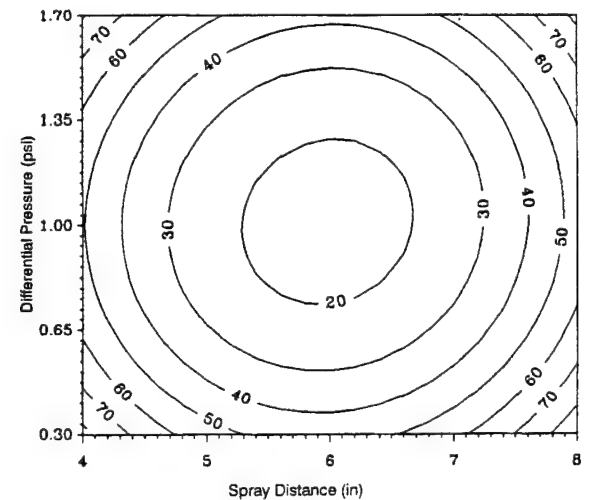
Contour Plot of predicted standard error for "Microhardness" model. Spray Distance=5 in. and atmospheric pressure=11.85 psia.



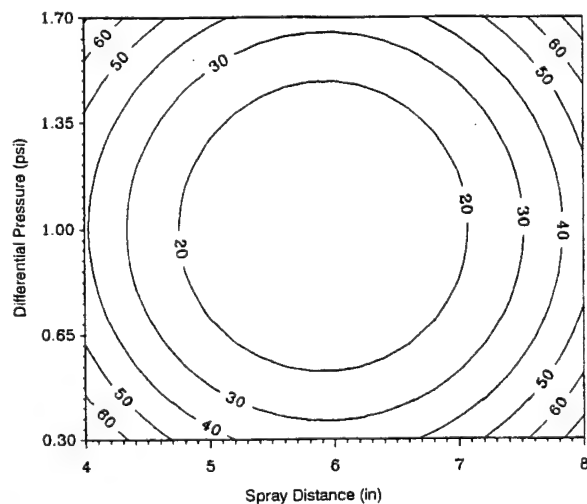
Contour Plot of predicted standard error for "Microhardness" model. Spray Distance=6 in. and atmospheric pressure=11.85 psia.



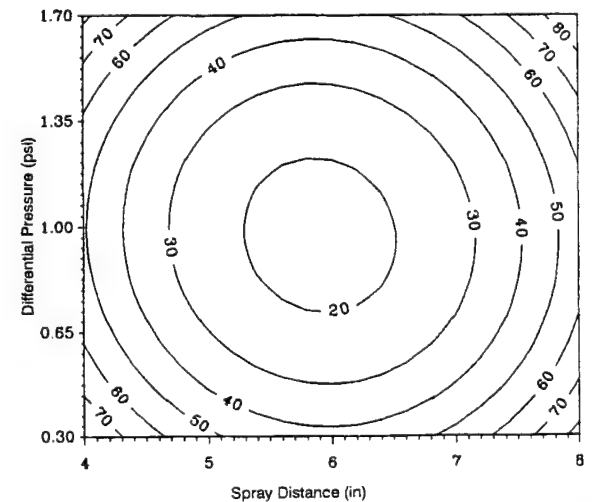
Contour Plot of predicted standard error for "Microhardness" model. Spray Distance=7 in. and atmospheric pressure=11.85 psia.



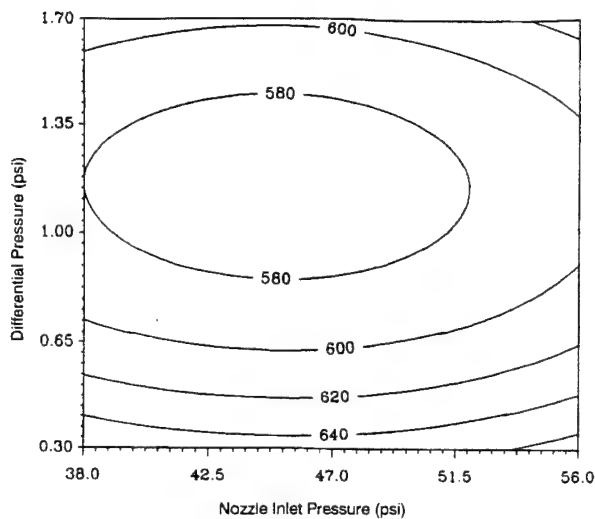
Contour Plot of predicted standard error for "Microhardness" model. Operating Pressure 42.0 psi and atmospheric pressure=11.85 psia.



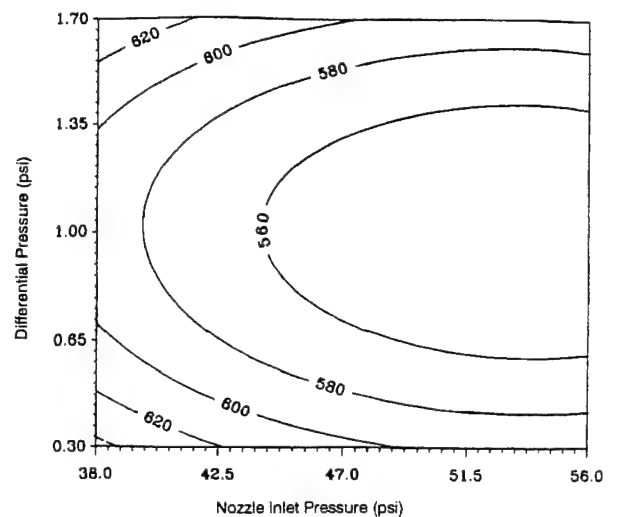
Contour Plot of predicted standard error for "Microhardness" model. Operating Pressure 47.0 psi and atmospheric pressure=11.85 psia.



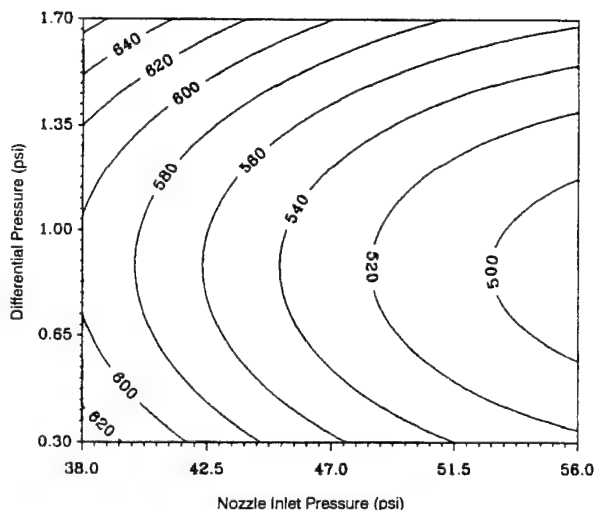
Contour Plot of predicted standard error for "Microhardness" model. Operating Pressure 52.0 psi and atmospheric pressure=11.85 psia.



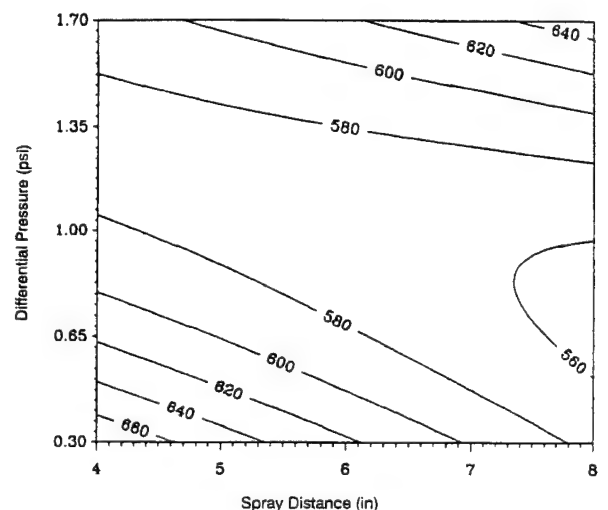
Contour Plot of predicted response for "Microhardness" model. Spray Distance=5 in. and atmospheric pressure=11.85 psia.



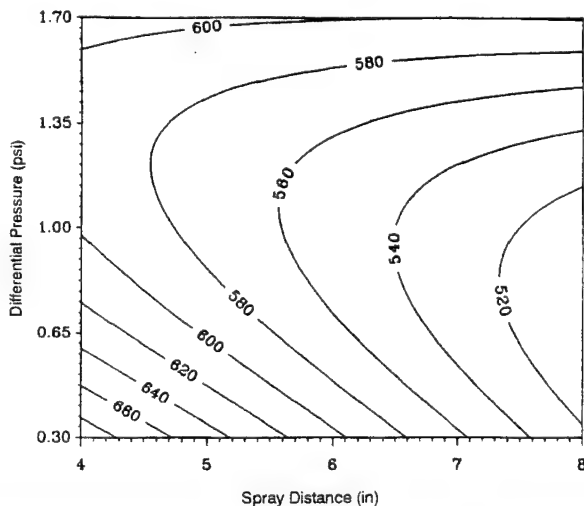
Contour Plot of predicted response for "Microhardness" model. Spray Distance=6 in. and atmospheric pressure=11.85 psia.



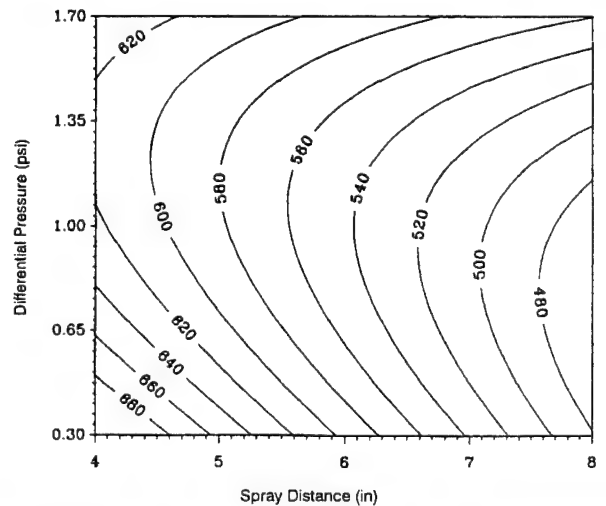
Contour Plot of predicted response for "Microhardness" model. Spray Distance=7 in. and atmospheric pressure=11.85 psia.



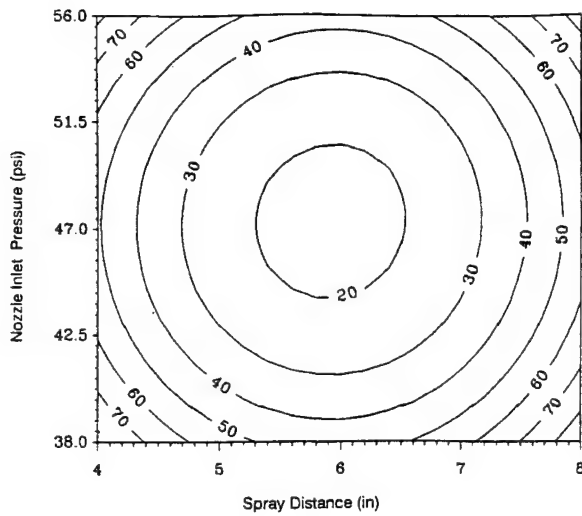
Contour Plot of predicted response for "Microhardness" model. Operating Pressure 42.0 psi and atmospheric pressure=11.85 psia.



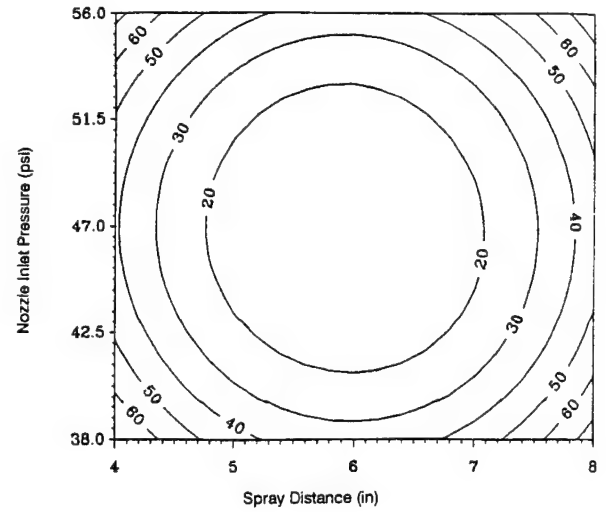
Contour Plot of predicted response for "Microhardness" model. Operating Pressure 47.0 psi and atmospheric pressure=11.85 psia.



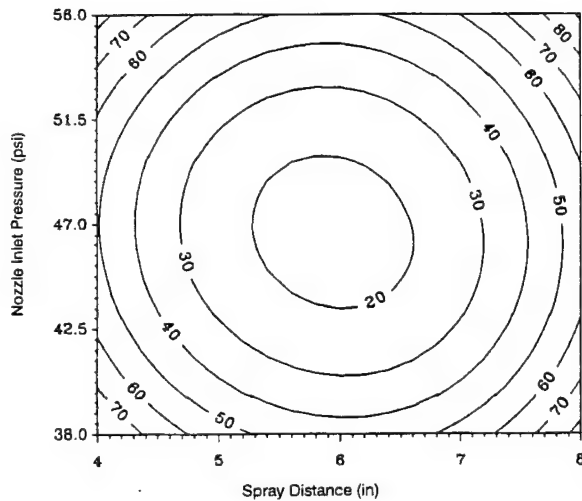
Contour Plot of predicted response for "Microhardness" model. Operating Pressure 52.0 psi and atmospheric pressure=11.85 psia. 368



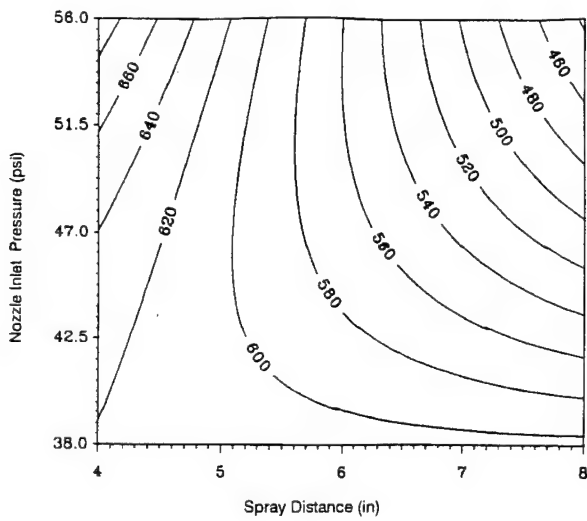
Contour Plot of predicted standard error for "Microhardness" model. Pressure Differential=0.6 psi and atmospheric pressure=11.85 psia.



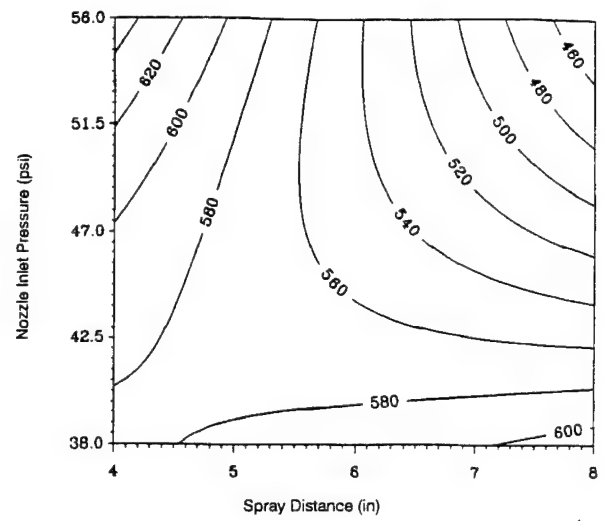
Contour Plot of predicted standard error for "Microhardness" model. Pressure Differential=1.0 psi and atmospheric pressure=11.85 psia.



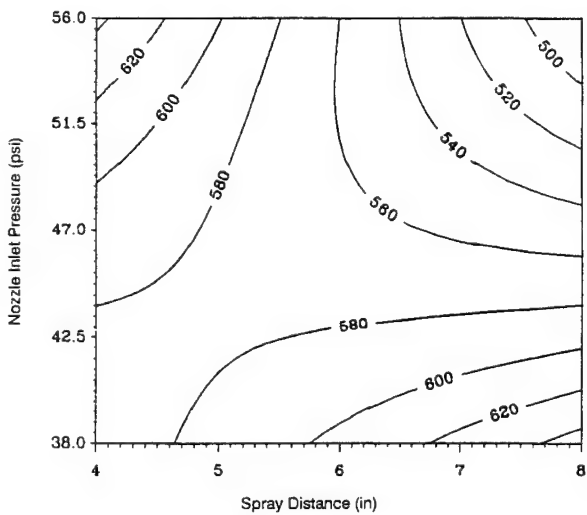
Contour Plot of predicted standard error for "Microhardness" model. Pressure Differential=1.4 psi and atmospheric pressure=11.85 psia.



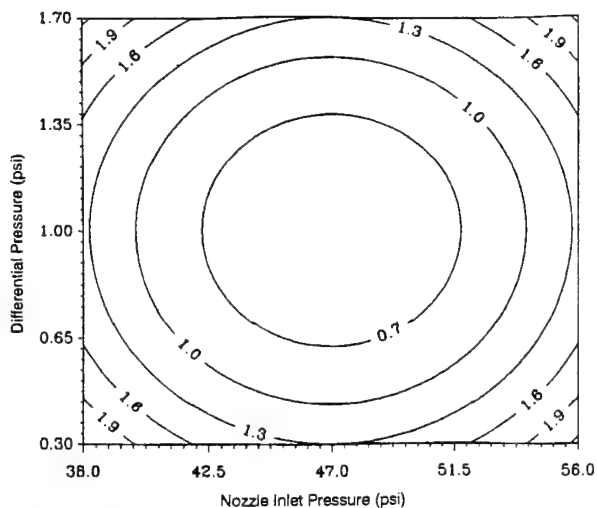
Contour Plot of predicted response for
"Microhardness" model. Pressure Differential=0.6 psi
and atmospheric pressure=11.85 psia.



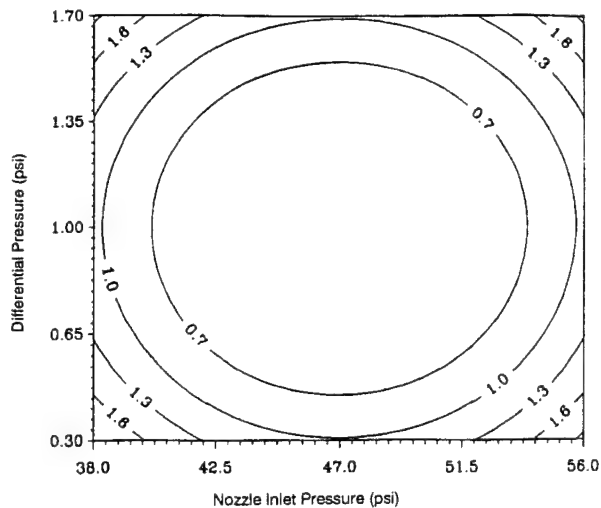
Contour Plot of predicted response for
"Microhardness" model. Pressure Differential=1.0 psi
and atmospheric pressure=11.85 psia.



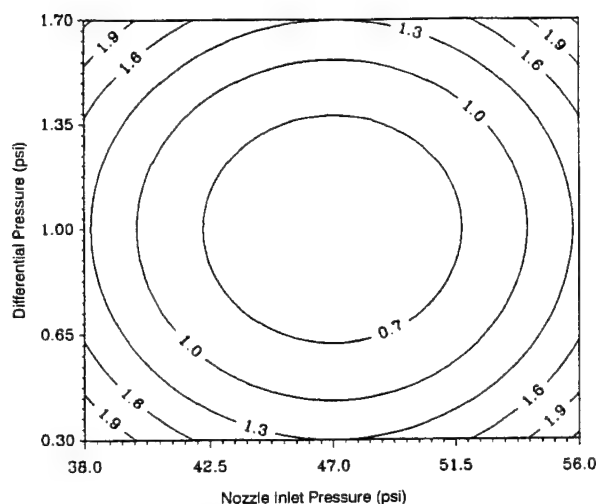
Contour Plot of predicted response for
"Microhardness" model. Pressure Differential=1.4 psi
and atmospheric pressure=11.85 psia.



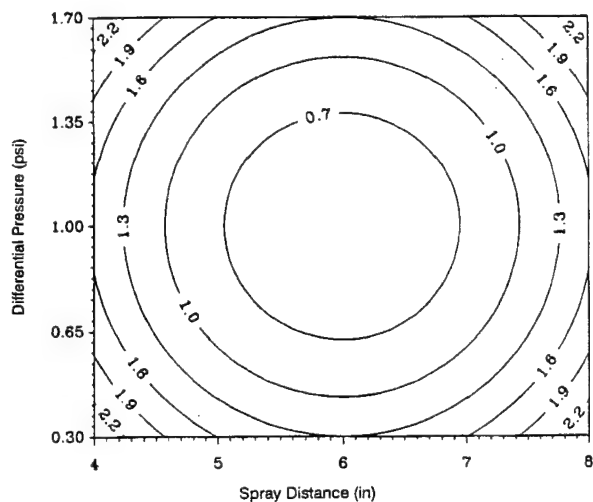
Contour Plot of predicted standard error for "Porosity" model. Spray Distance = 5 in.



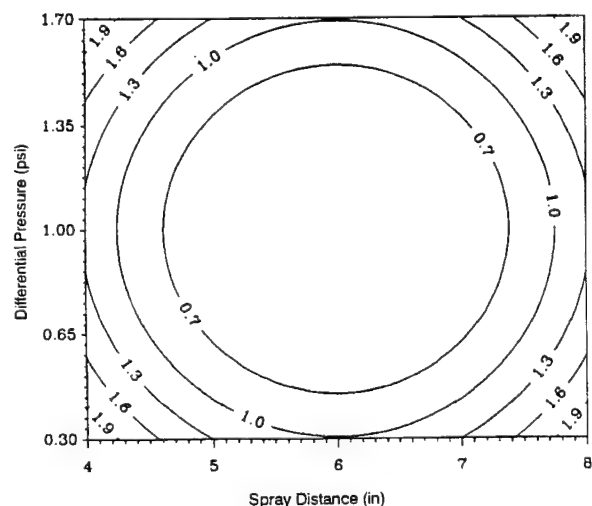
Contour Plot of predicted standard error for "Porosity" model. Spray Distance = 6 in.



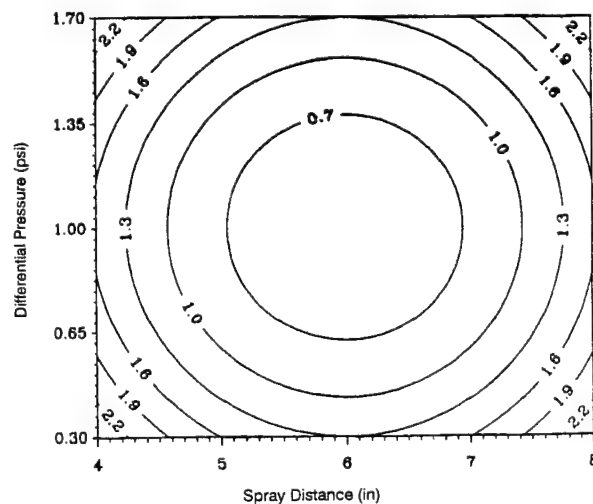
Contour Plot of predicted standard error for "Porosity" model. Spray Distance = 7 in.



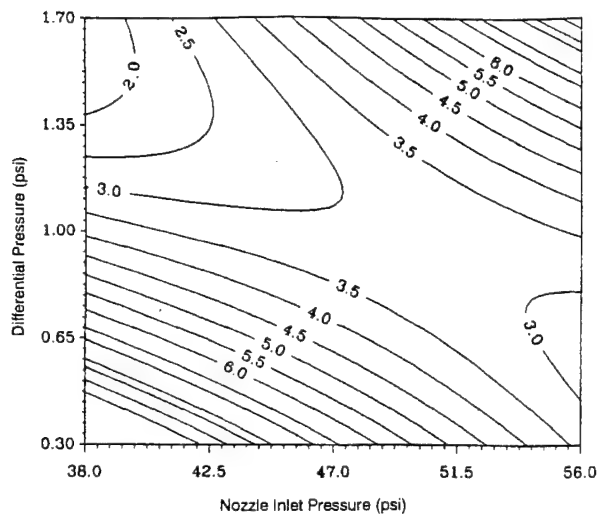
Contour Plot of predicted standard error for "Porosity" model. Operating Pressure 42.0 psi.



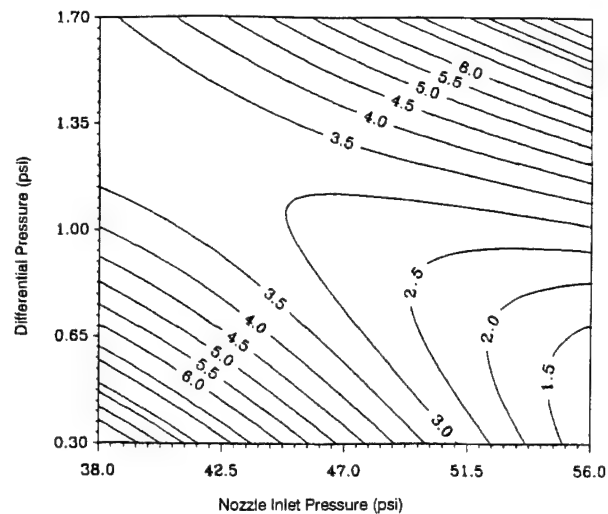
Contour Plot of predicted standard error for "Porosity" model. Operating Pressure 47.0 psi.



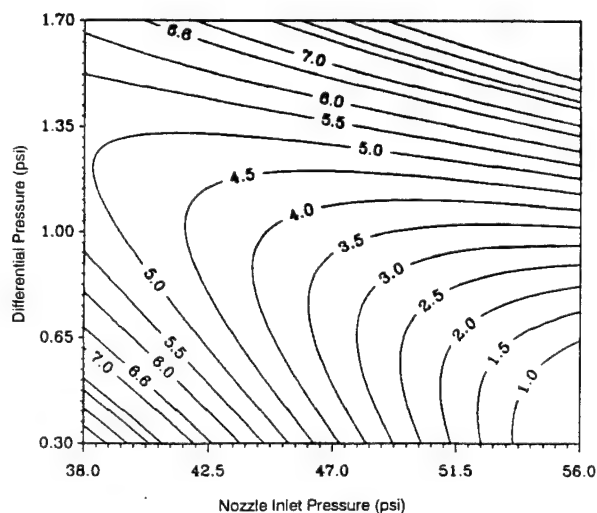
Contour Plot of predicted standard error for "Porosity" model. Operating Pressure 52.0 psi. 37



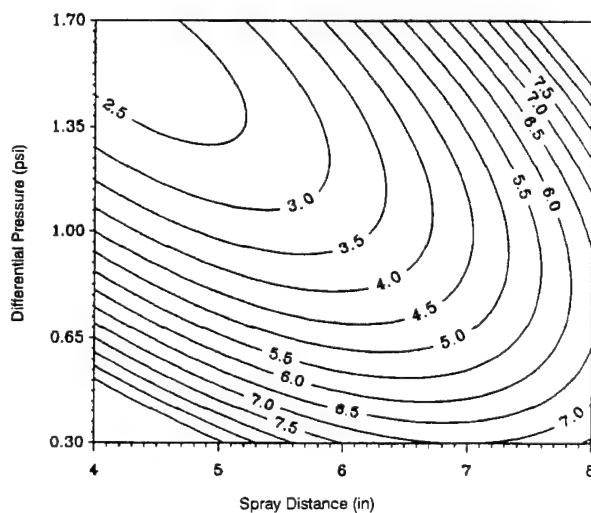
Contour Plot of predicted response for
"Porosity" model. Spray Distance = 5 in.



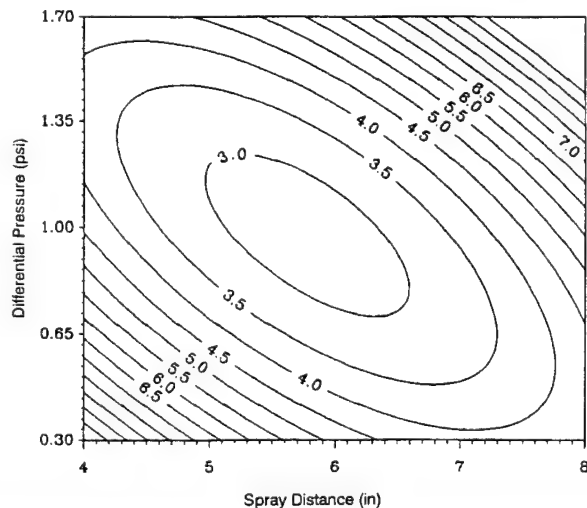
Contour Plot of predicted response for
"Porosity" model. Spray Distance = 6 in.



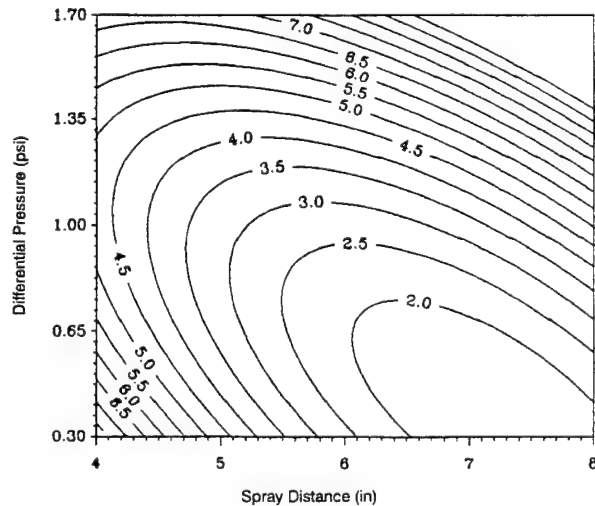
Contour Plot of predicted response for
"Porosity" model. Spray Distance = 7 in.



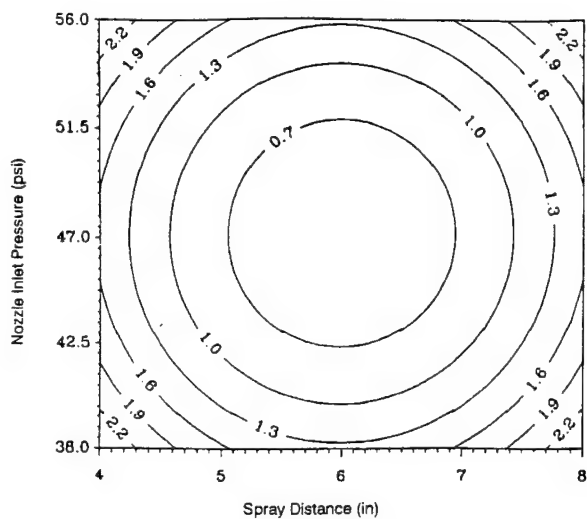
Contour Plot of predicted response for
"Porosity" model. Operating Pressure 42.0 psi.



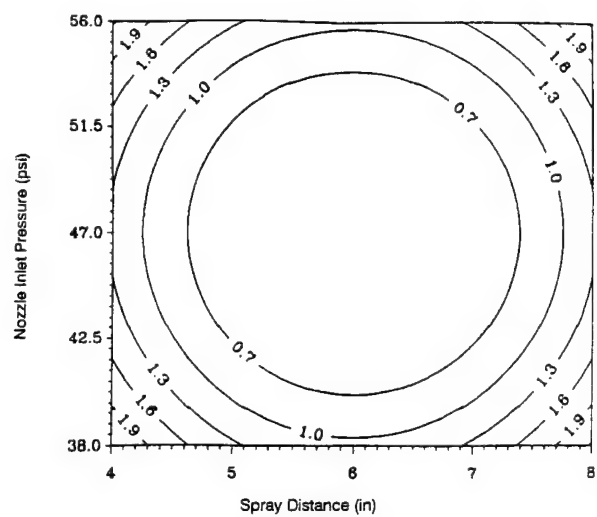
Contour Plot of predicted response for
"Porosity" model. Operating Pressure 47.0 psi.



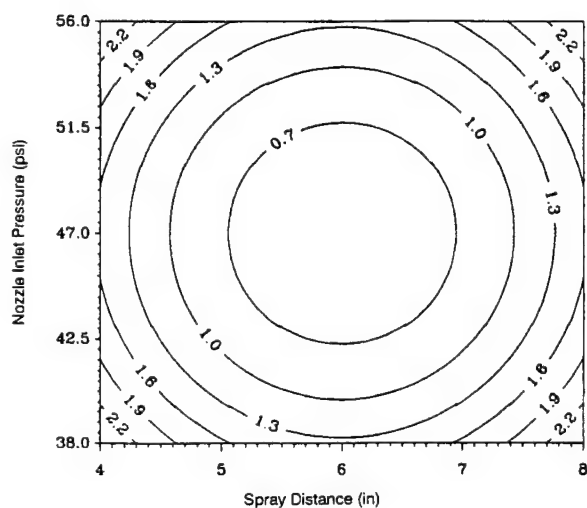
Contour Plot of predicted response for
"Porosity" model. Operating Pressure 52.0 psi.



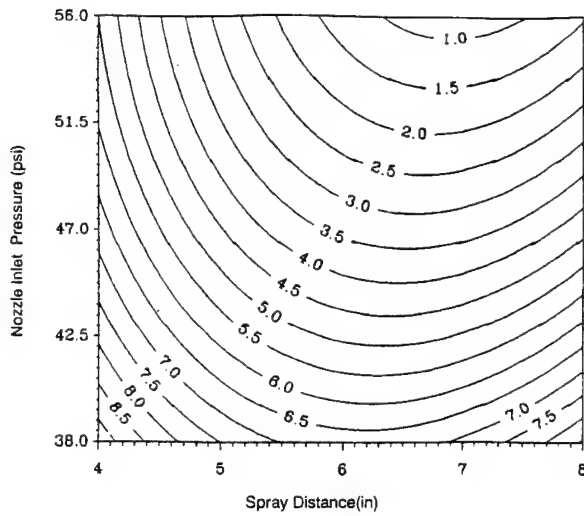
Contour Plot of predicted standard error for "Porosity" model. Pressure Differential=0.6 psi.



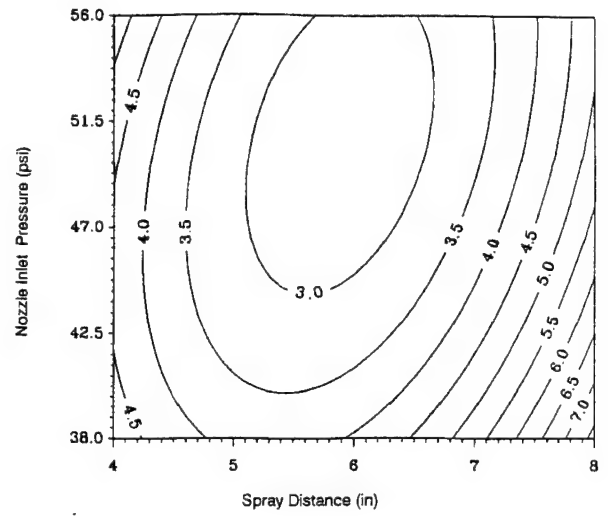
Contour Plot of predicted standard error for "Porosity" model. Pressure Differential=1.0 psi.



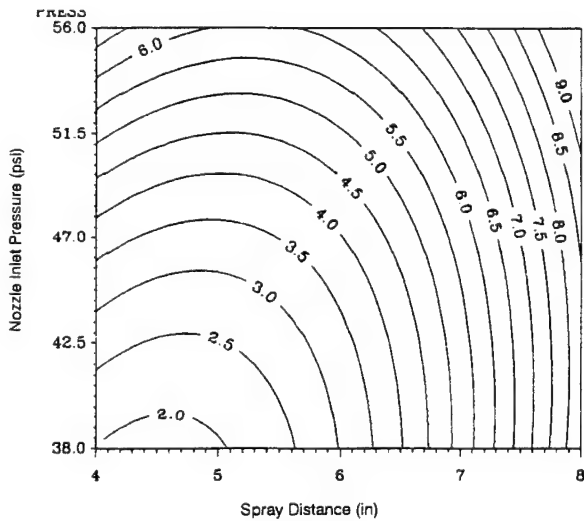
Contour Plot of predicted standard error for "Porosity" model. Pressure Differential=1.4 psi.



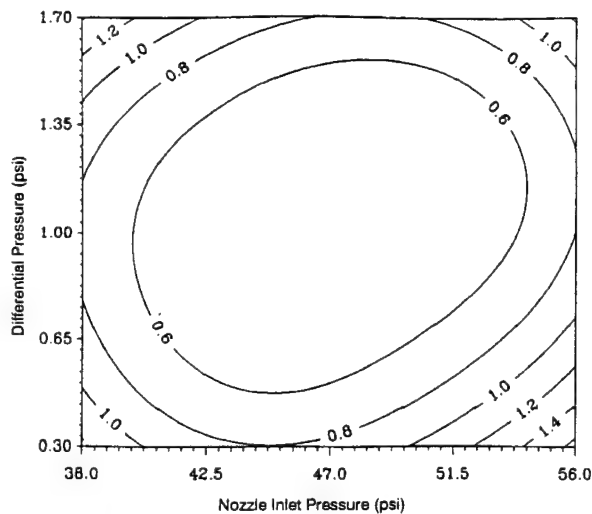
Contour Plot of predicted response for "Porosity" model. Pressure Differential=0.6 psi.



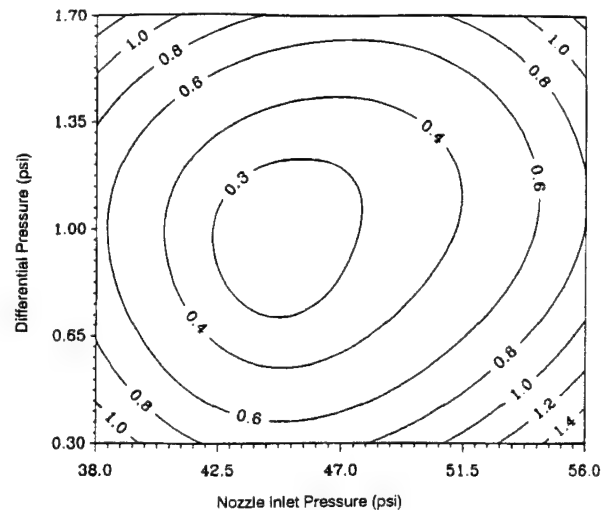
Contour Plot of predicted response for "Porosity" model. Pressure Differential=1.0 psi.



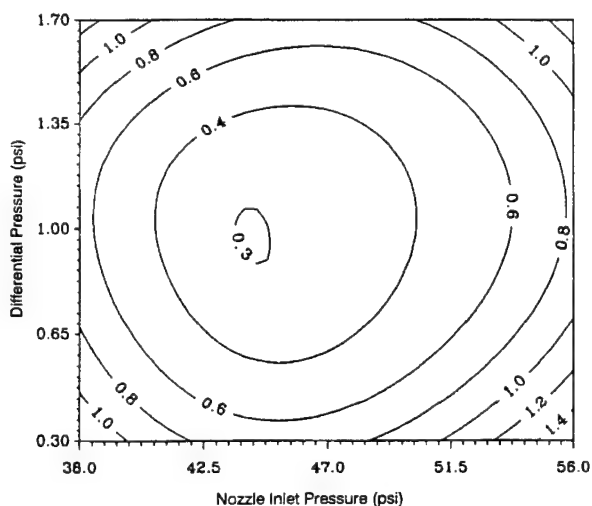
Contour Plot of predicted response for "Porosity" model. Pressure Differential=1.4 psi.



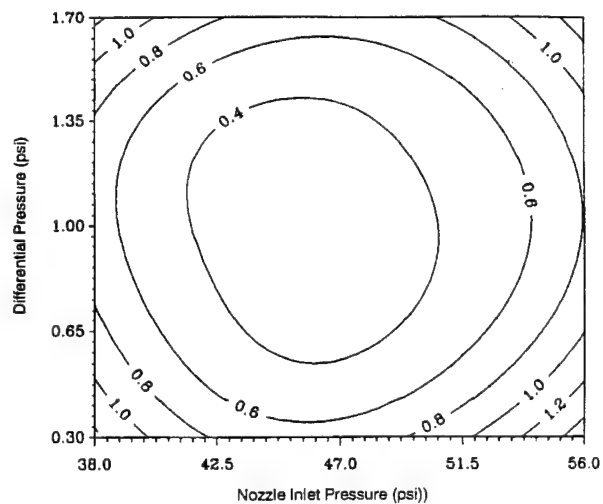
Contour Plot of predicted standard error for "Wear-2" model. Spray Distance=6 in. and order=1.



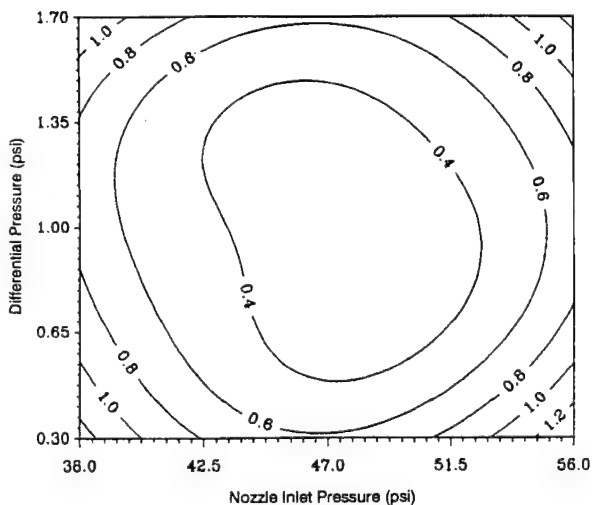
Contour Plot of predicted standard error for "Wear-2" model. Spray Distance=6 in. and order=2.



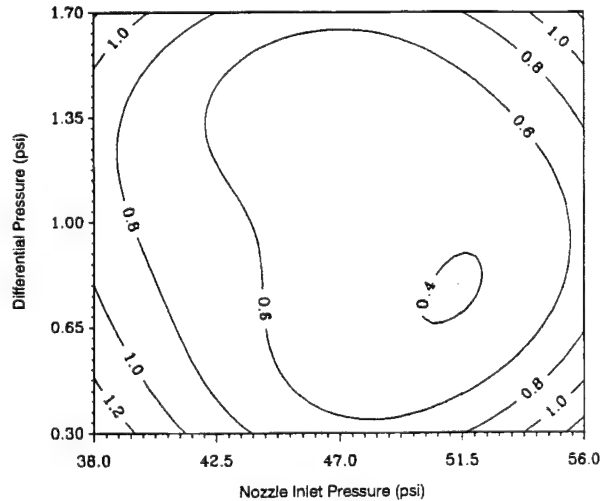
Contour Plot of predicted standard error for "Wear-2" model. Spray Distance=6 in. and order=3.



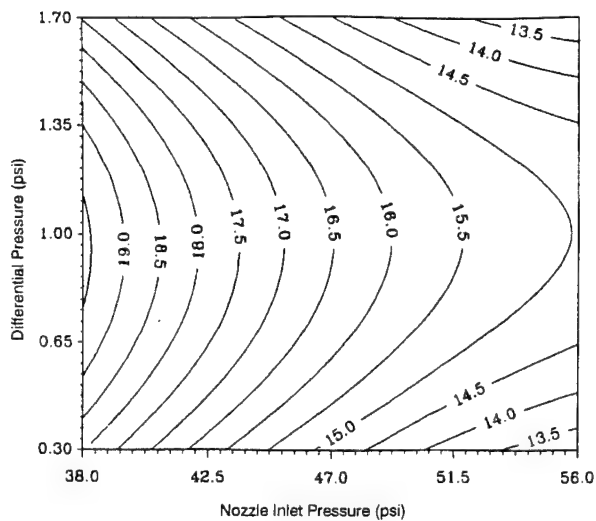
Contour Plot of predicted standard error for "Wear-2" model. Spray Distance=6 in. and order=4.



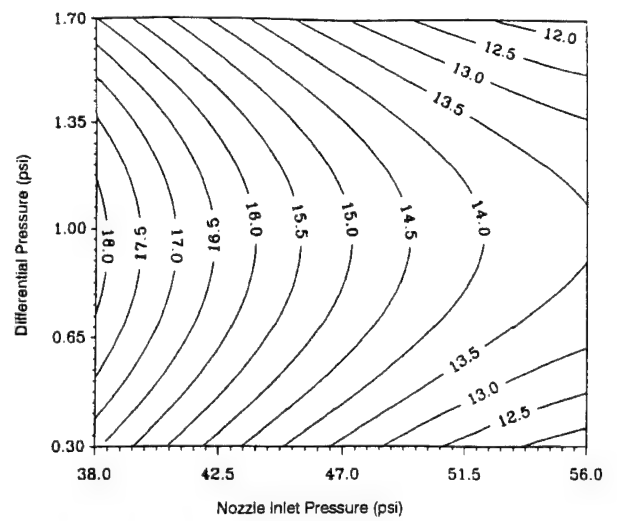
Contour Plot of predicted standard error for "Wear-2" model. Spray Distance=6 in. and order=5.



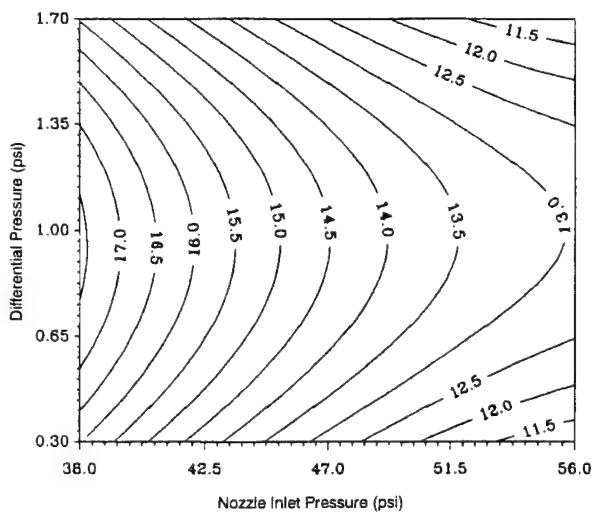
Contour Plot of predicted standard error for "Wear-2" model. Spray Distance=6 in. and order=6.



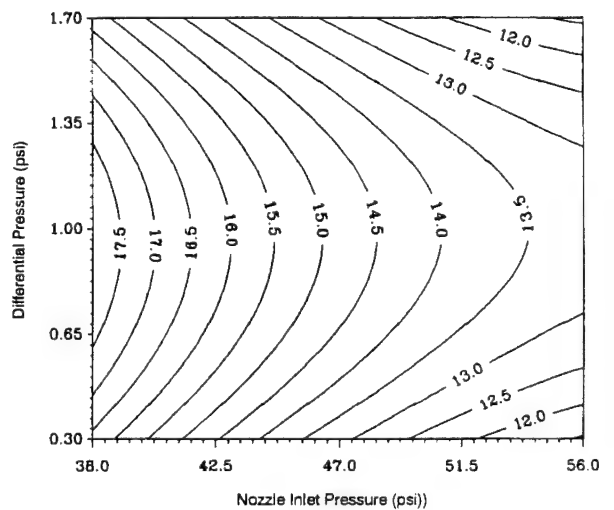
Contour Plot of predicted response for "Wear-2" model. Spray Distance=6 in. and order=1.



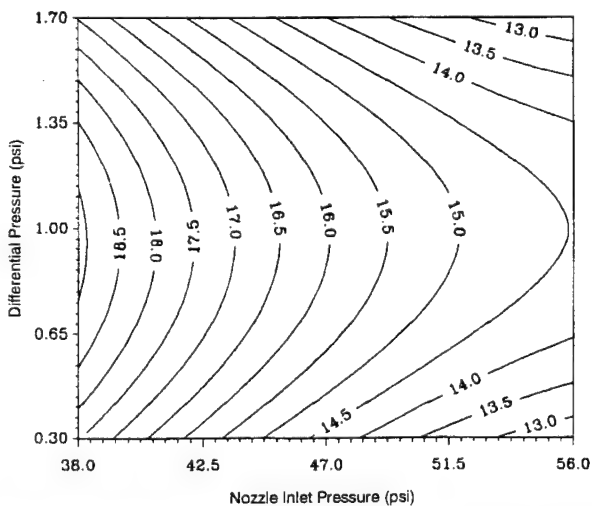
Contour Plot of predicted response for "Wear-2" model. Spray Distance=6 in. and order=2.



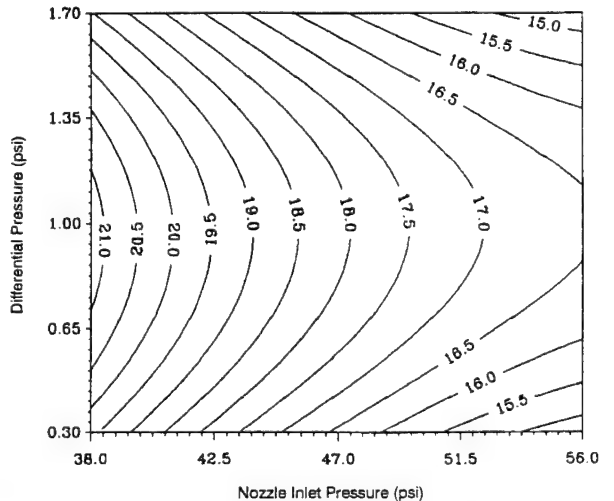
Contour Plot of predicted response for "Wear-2" model. Spray Distance=6 in. and order=3.



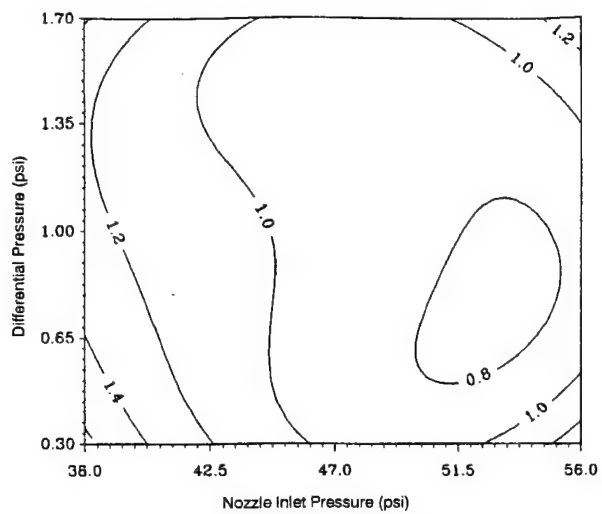
Contour Plot of predicted response for "Wear-2" model. Spray Distance=6 in. and order=4.



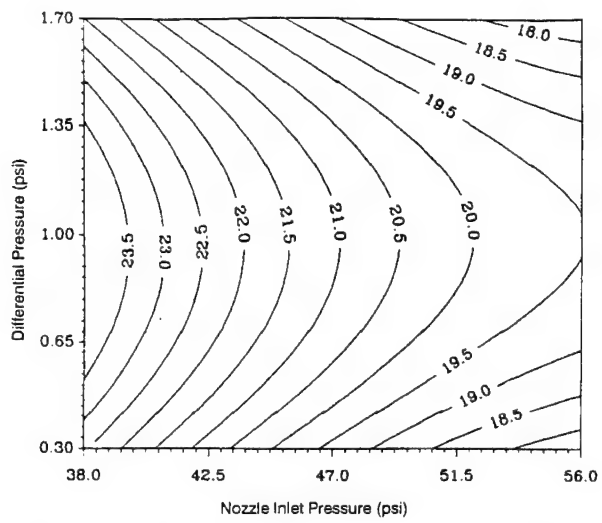
Contour Plot of predicted response for "Wear-2" model. Spray Distance=6 in. and order=5.



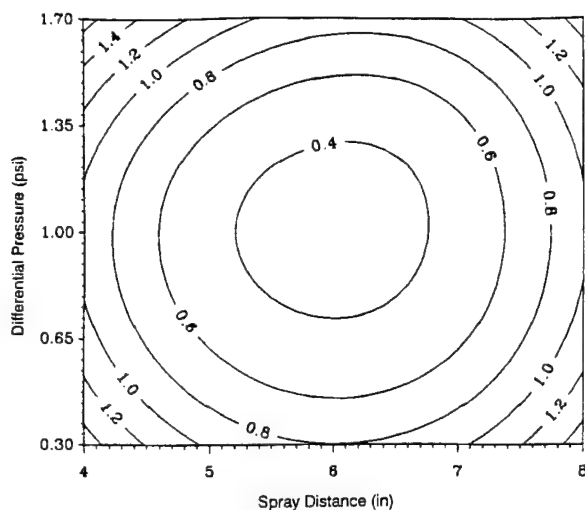
Contour Plot of predicted response for "Wear-2" model. Spray Distance=6 in. and order=6.



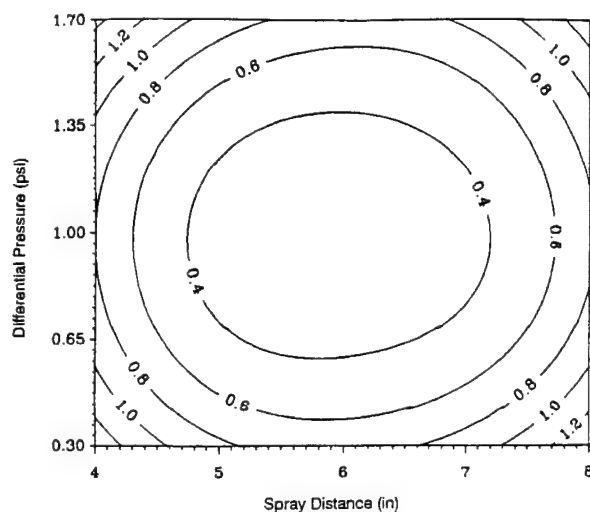
Contour Plot of predicted standard error for "Wear-2" model. Spray Distance=6 in. and order=7.



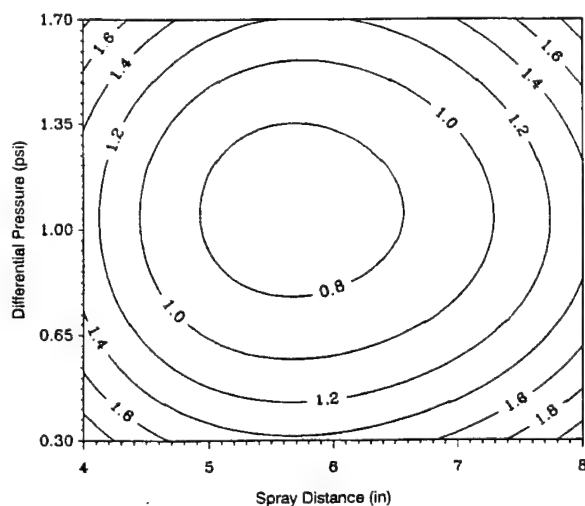
Contour Plot of predicted response for "Wear-2" model. Spray Distance=6 in. and order=7.



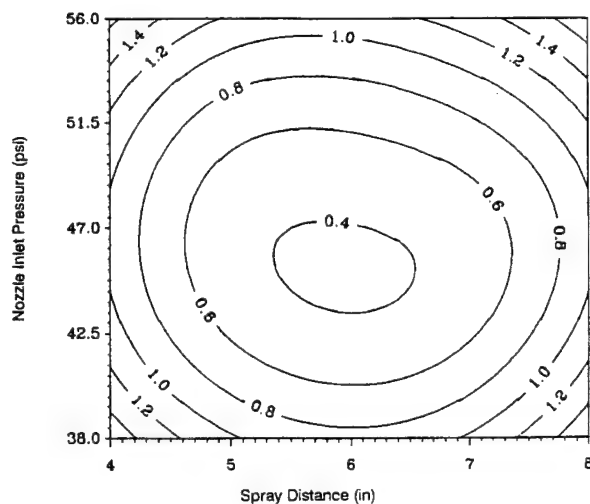
Contour Plot of predicted standard error for "Wear-2" model. Operating Pressure=42.0 psi and order=3.



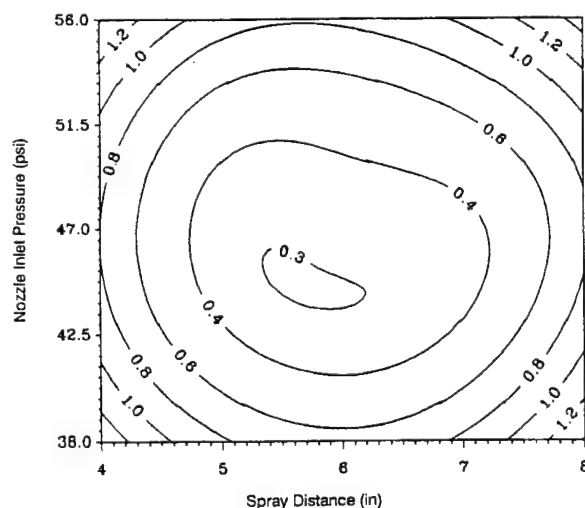
Contour Plot of predicted standard error for "Wear-2" model. Operating Pressure=47.0 psi and order=3.



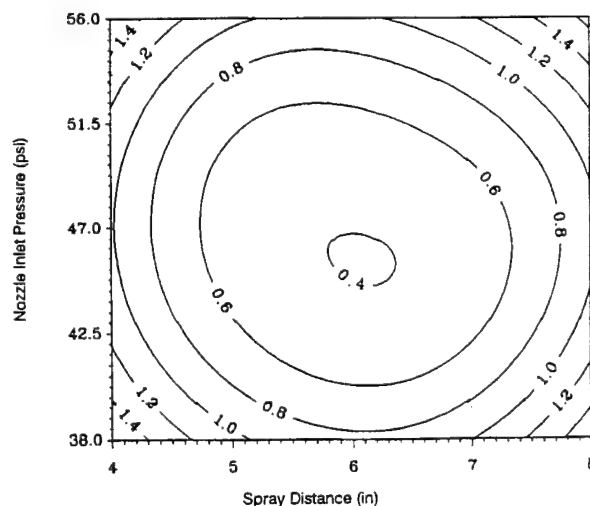
Contour Plot of predicted standard error for "Wear-2" model. Operating Pressure=55.0 psi and order=3.



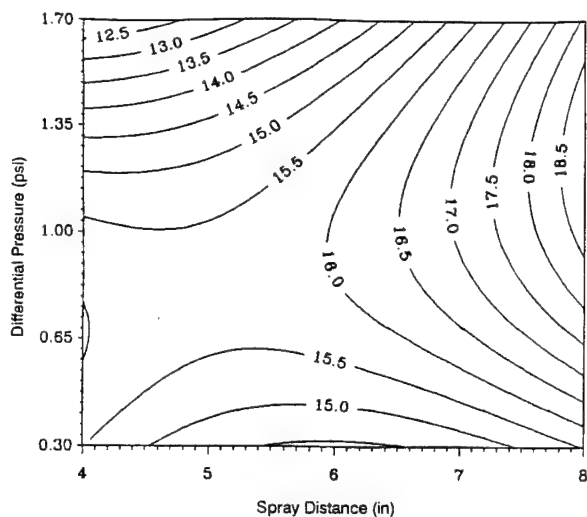
Contour Plot of predicted standard error for "Wear-2" model. Pressure Differential=0.6 psi and order=3.



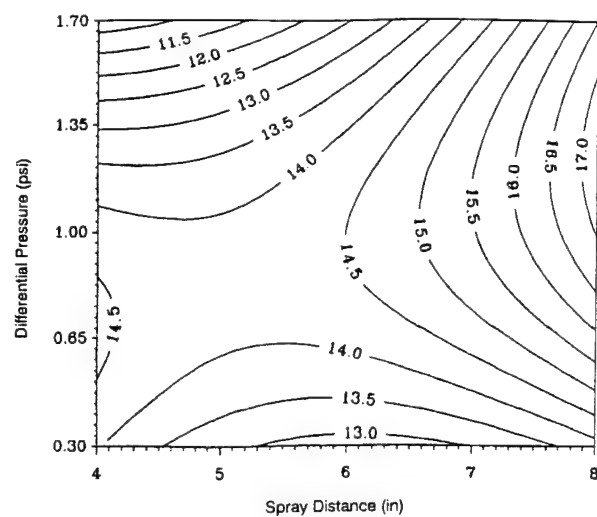
Contour Plot of predicted standard error for "Wear-2" model. Pressure Differential=1.0 psi. and order=3.



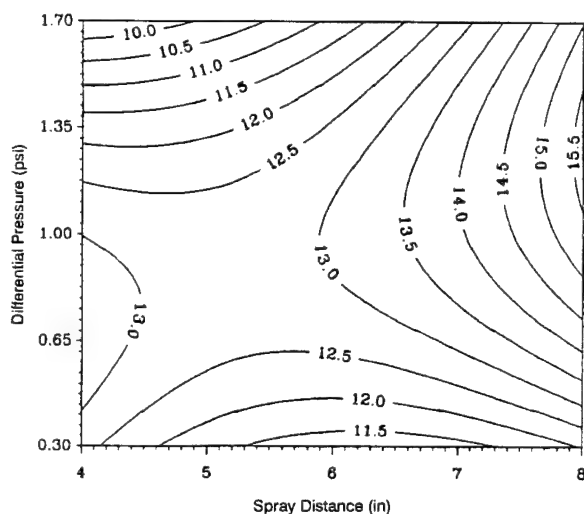
Contour Plot of predicted standard error for "Wear-2" model. Pressure Differential=1.4 psi and order=3.



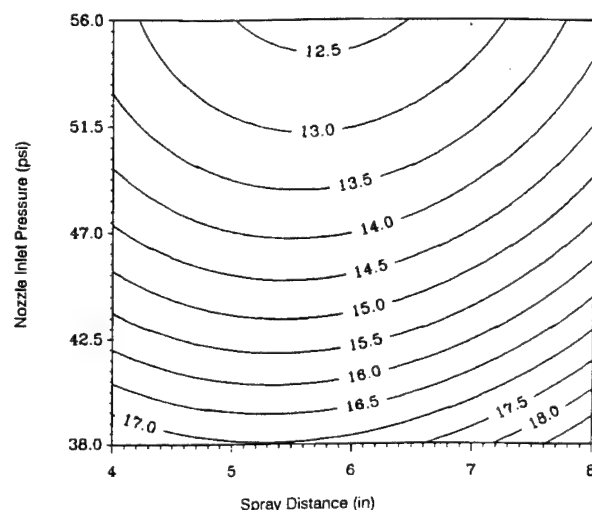
Contour Plot of predicted response for "Wear-2" model. Operating Pressure=42.0 psi and order=3.



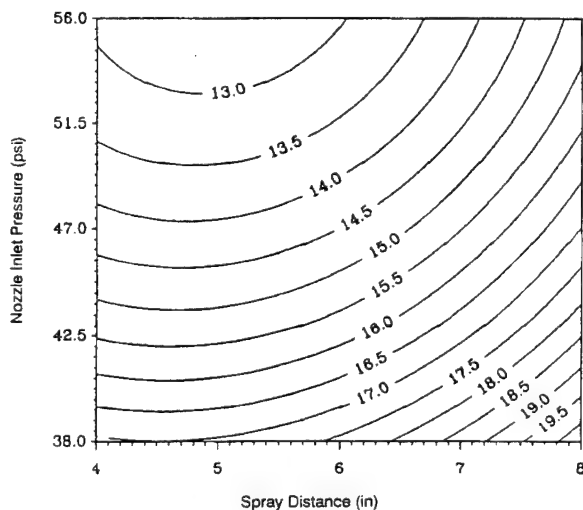
Contour Plot of predicted response for "Wear-2" model. Operating Pressure=47.0 psi and order=3.



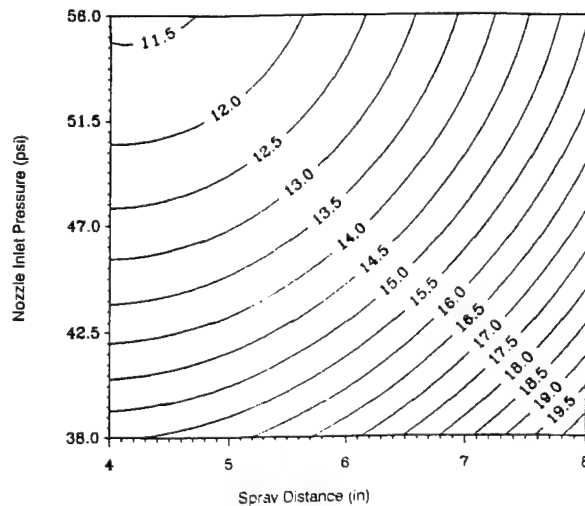
Contour Plot of predicted response for "Wear-2" model. Operating Pressure=55.0 psi and order=3.



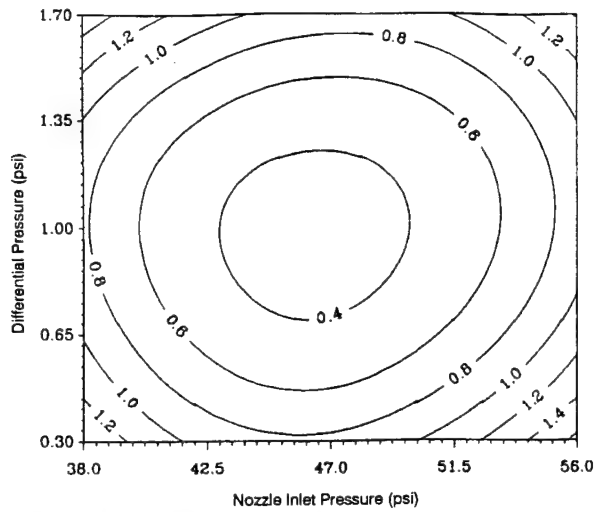
Contour Plot of predicted response for "Wear-2" model. Pressure Differential=0.6 psi and order=3.



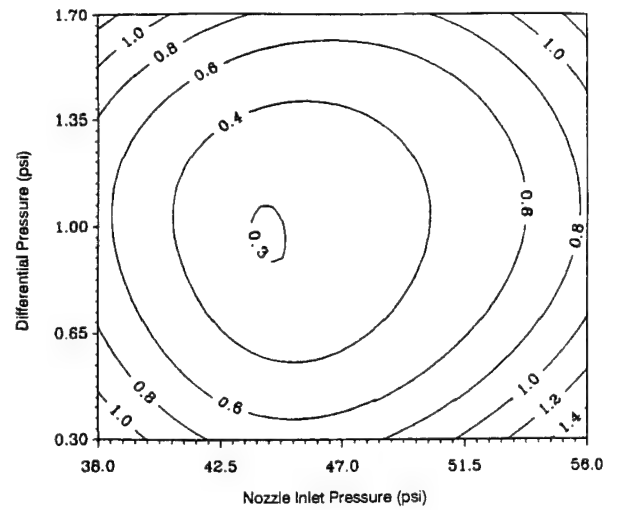
Contour Plot of predicted response for "Wear-2" model. Pressure Differential=1.0 psi and order=3.



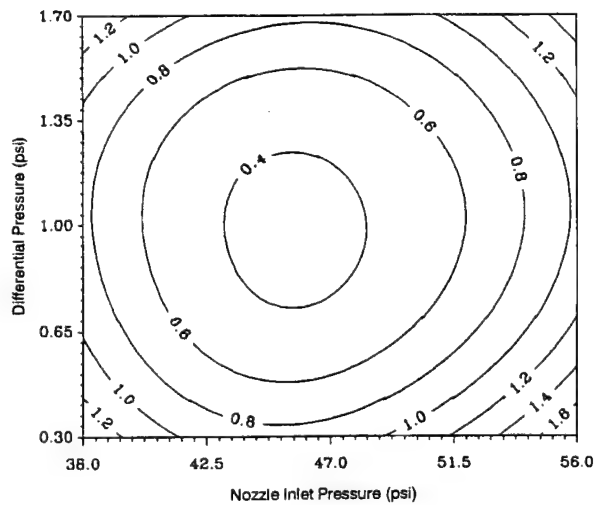
Contour Plot of predicted response for "Wear-2" model. Pressure Differential=1.4 psi and order=3.



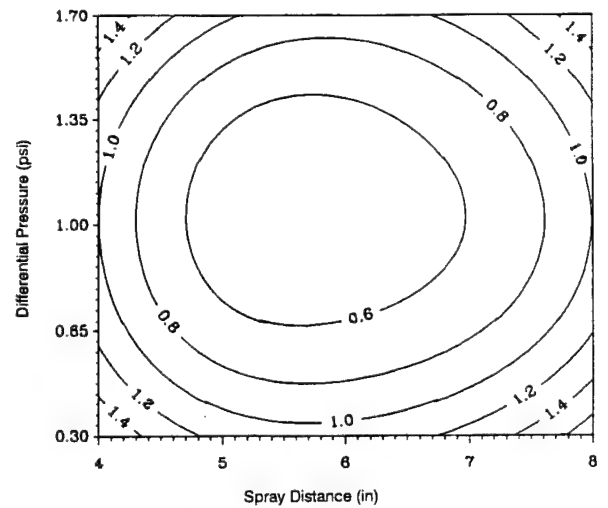
Contour Plot of predicted standard error for "Wear-2" model. Spray Distance=5 in. and order=3.



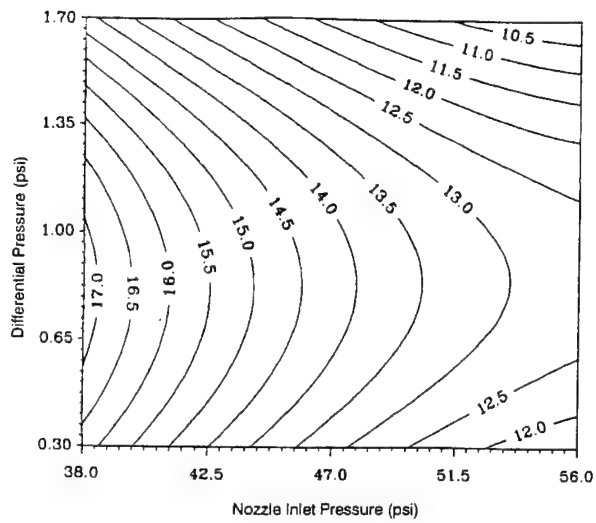
Contour Plot of predicted standard error for "Wear-2" model. Spray Distance=6 in. and order=3.



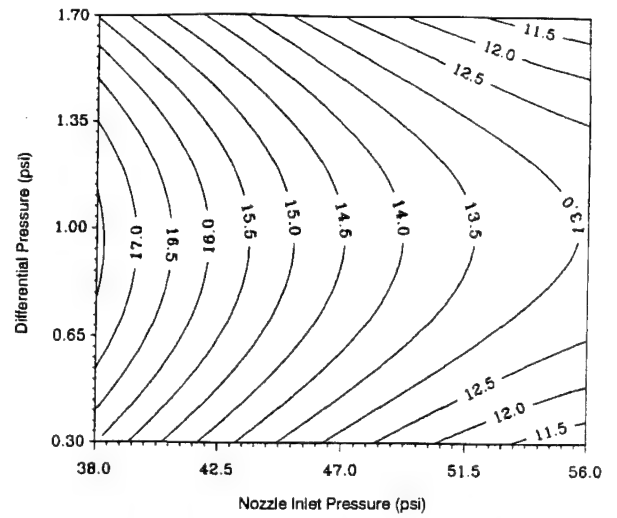
Contour Plot of predicted standard error for "Wear-2" model. Spray Distance=7 in. and order=3.



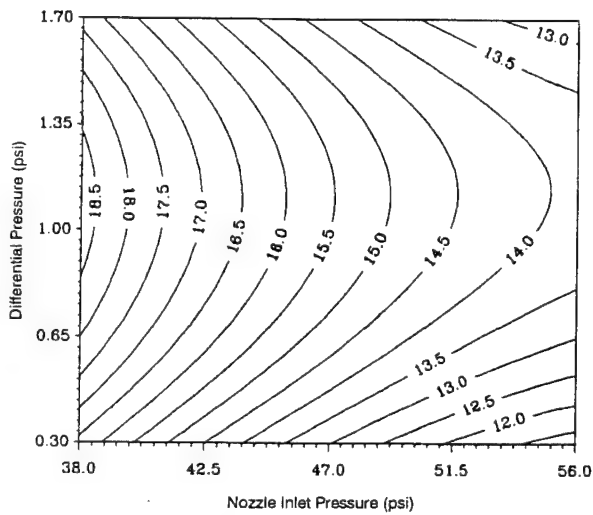
Contour Plot of predicted standard error for "Wear-2" model. Operating Pressure=52.0 psi and order=3.



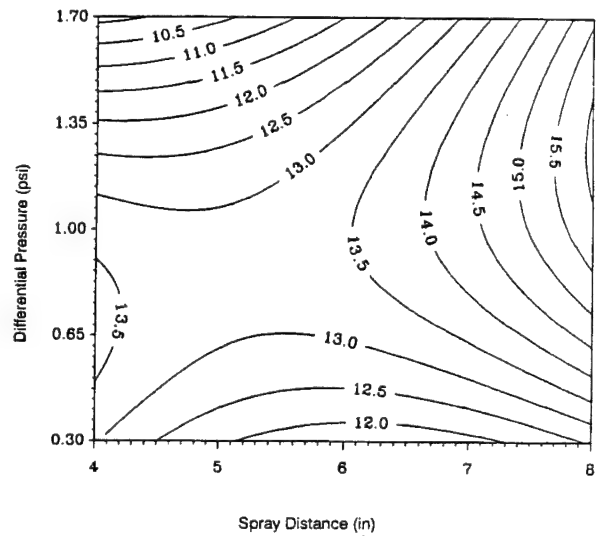
Contour Plot of predicted response for "Wear-2" model. Spray Distance=5 in. and order=3.



Contour Plot of predicted response for "Wear-2" model. Spray Distance=6 in. and order=3.



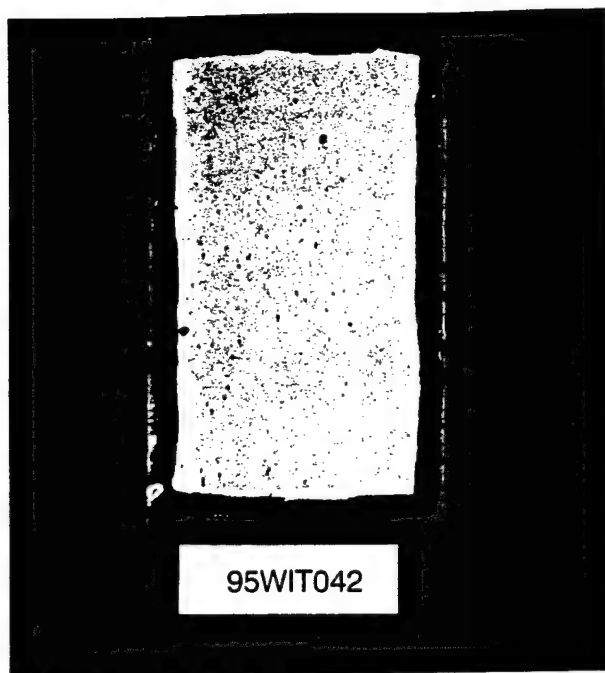
Contour Plot of predicted response for "Wear-2" model. Spray Distance=7 in. and order=3.



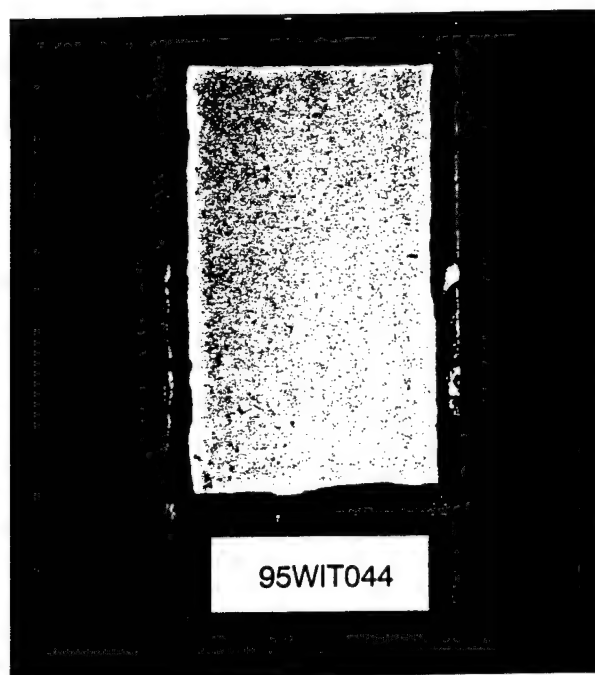
Contour Plot of predicted response for "Wear-2" model. Operating Pressure=52.0 psi and order=3.

APPENDIX I

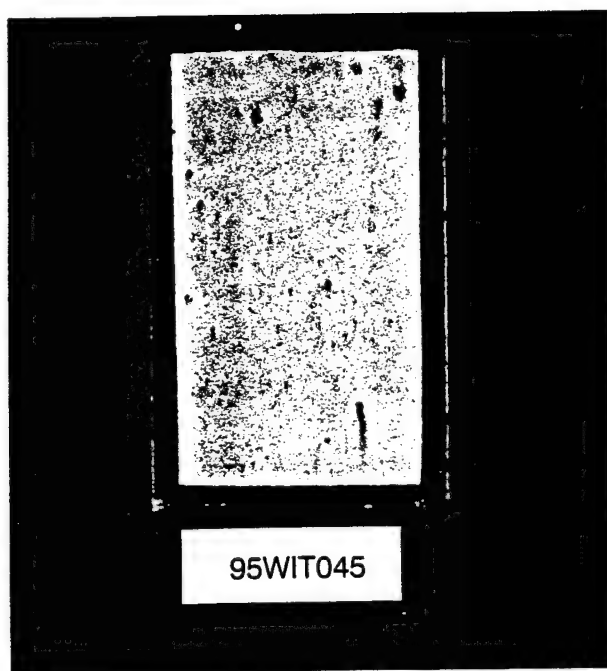
Phase IV Corrosion Test Results



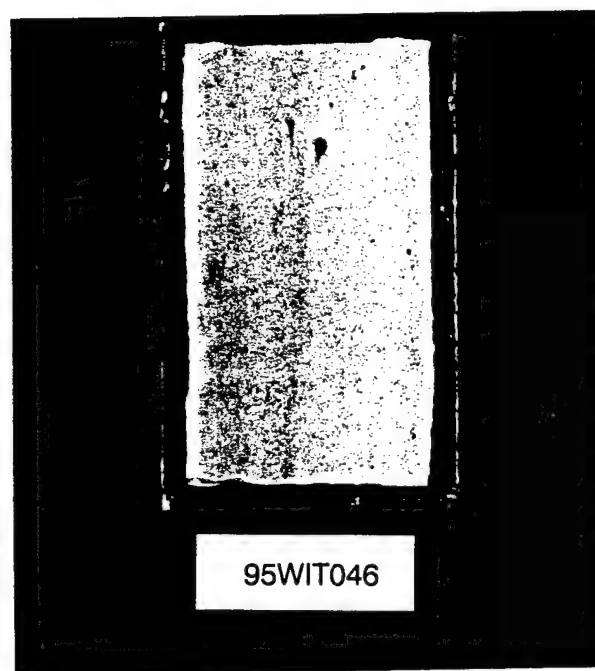
95WIT042



95WIT044



95WIT045



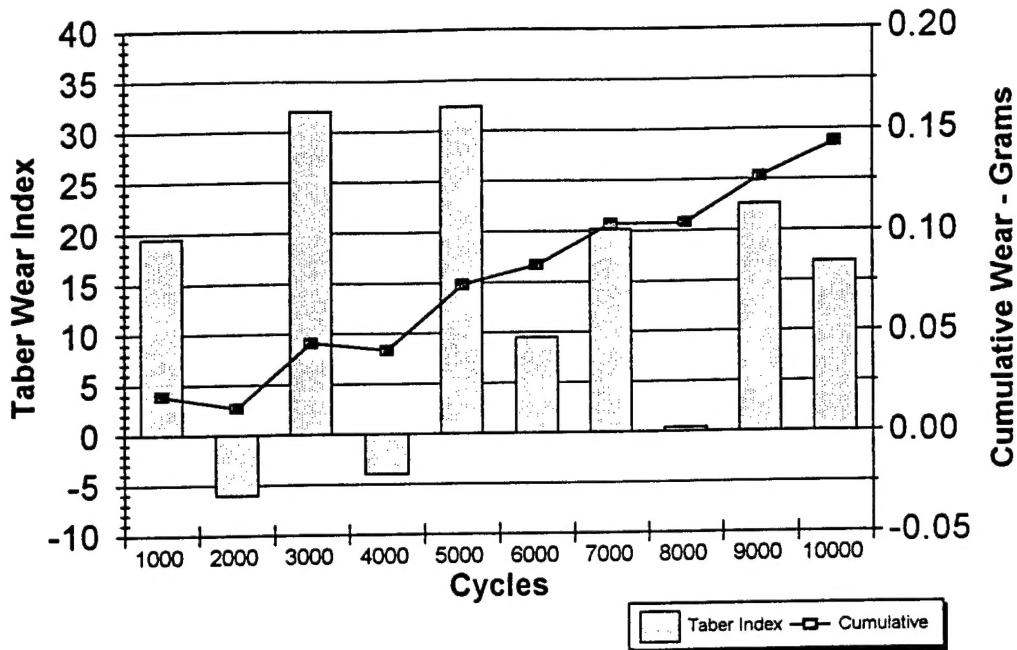
95WIT046

APPENDIX J

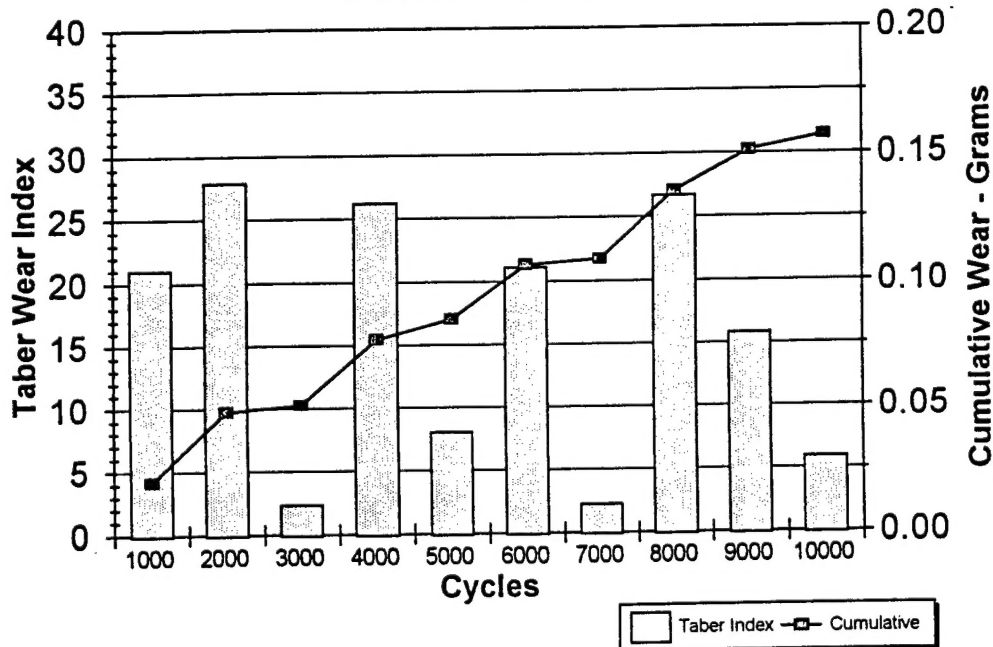
Phase IV Taber Abraser Wear Test Results

387
(The reverse of this page is blank)

VERSAIloy 50 Taber Abraser Wear Test **Test No. 95WIT042**

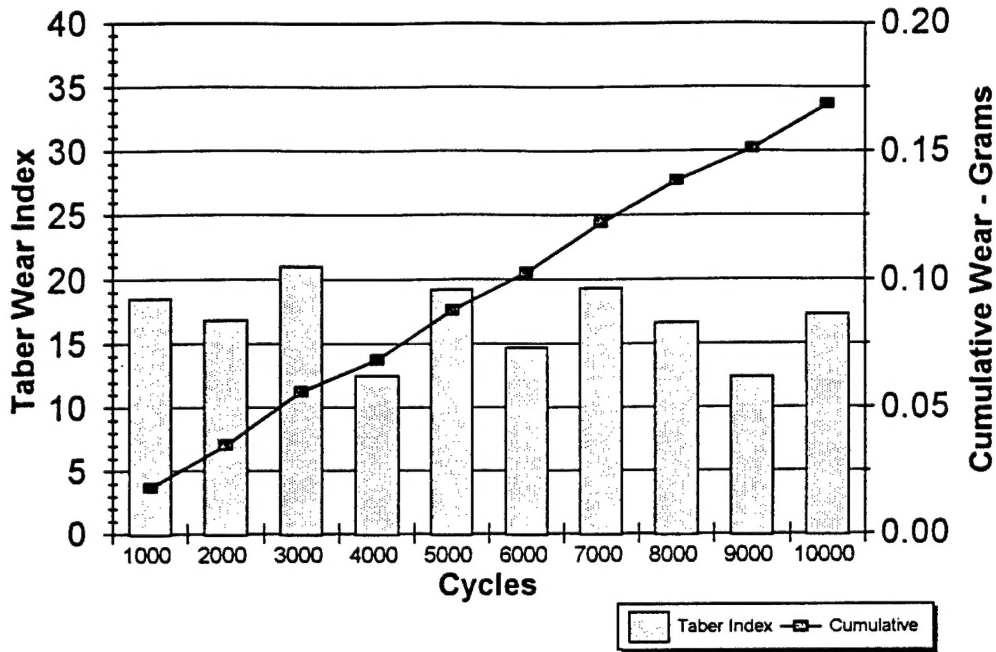


VERSAIloy 50 Taber Abraser Wear Test **Test No. 95WIT044**



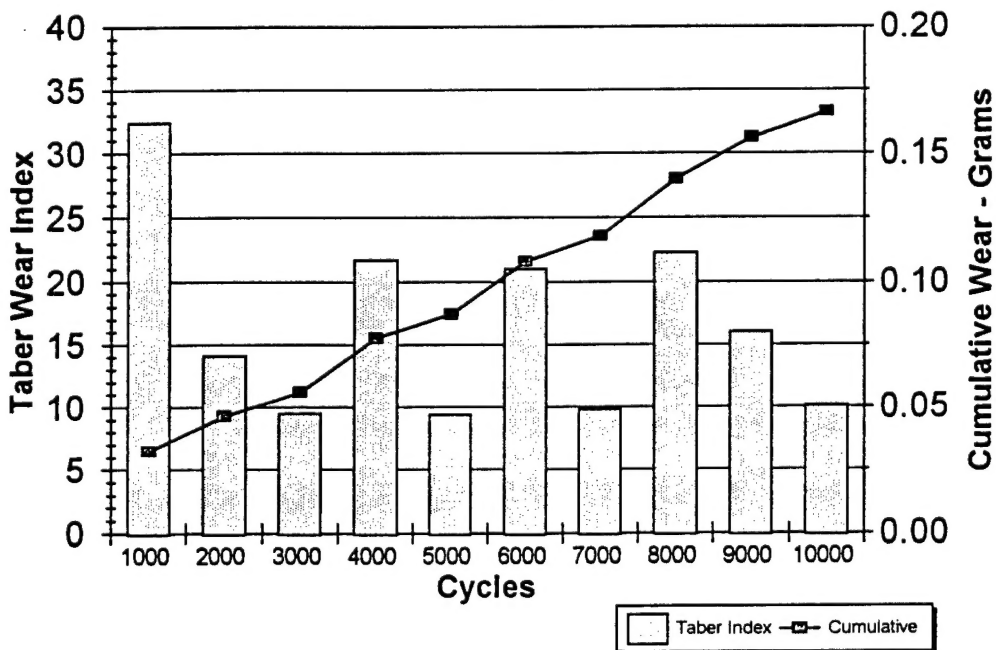
VERSAIloy 50 Taber Abraser Wear Test

Test No. 95WIT045



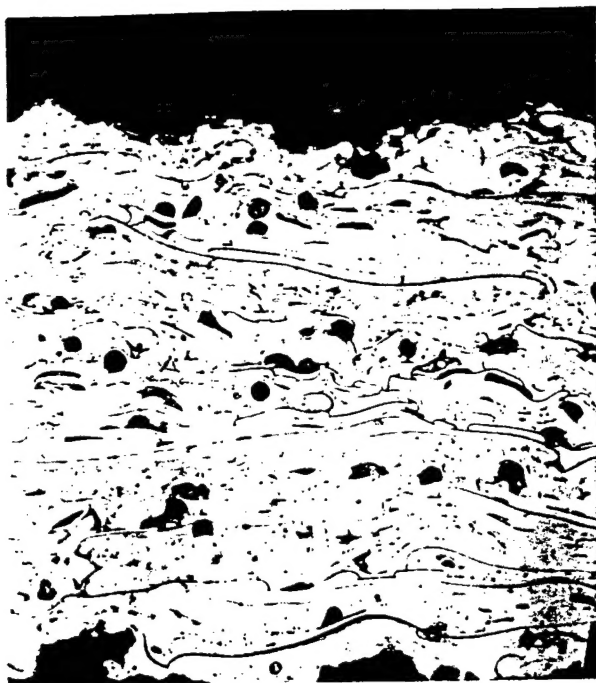
VERSAIloy 50 Taber Abraser Wear Test

Test No. 95WIT046

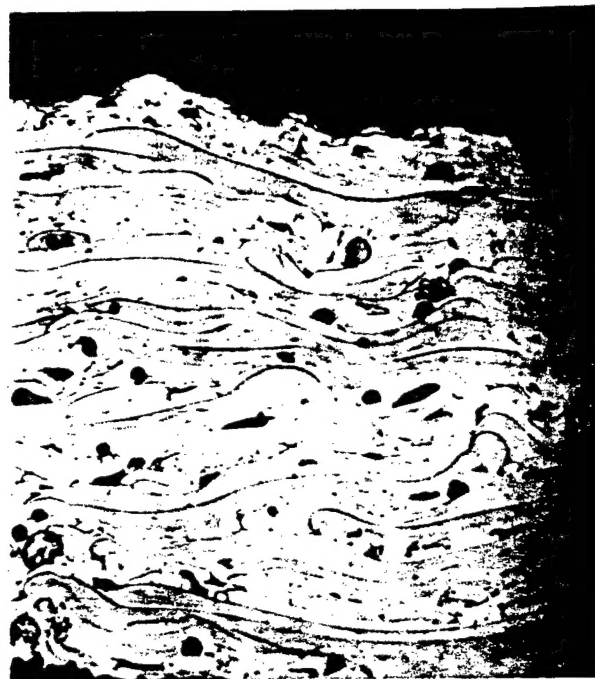


APPENDIX K

Phase IV Metallurgical Coupon Microstructures



Test 94WIT042 (500x).



Test 94WIT044 (500x).



Test 94WIT045 (500x).



Test 94WIT046 (500x).